

The spatial and temporal dynamics of groundwater – river interactions

Studies from the Gippsland Basin, South East Australia

Nicolaas P. Unland Bsc (Hons)

Thesis submitted for the degree of Doctor of Philosophy

School of Geosciences, Monash University

December 2013



© Copyright

by

Nicolaas Unland

2013

Under the Copyright Act 1968, this thesis must be used only under the normal conditions of scholarly fair dealing. In particular no results or conclusions should be extracted from it, nor should it be copied or closely paraphrased in whole or in part without the written consent of the author. Proper written acknowledgement should be made for any assistance obtained from this thesis.

I certify that I have made all reasonable efforts to secure copyright permissions for third-party content included in this thesis and have not knowingly added copyright content to my work without the owner's permission.

Table of Contents

Title page	1
Table of Contents	5
Abstract	12
Declaration	15
Acknowledgements	16
Chapter Declarations	17
Chapter 1	
Introduction, background, aims	23
1.1 Background	23
1.1.1 Water resource management and hydrogeology	23
1.1.2 The Australian setting	25
1.1.3 Groundwater and surface water	26
1.2 Study Area	28
1.2.1 Geology	28
1.2.2 Hydrogeology	30
1.2.3 Hydrology and climate	33
1.3 Scope and research aims	35
1.3.1 Groundwater – surface water fluxes	36
1.3.2 Groundwater-surface water interaction in river banks	37
1.3.3 Groundwater-surface water balances in tidal estuaries	37
1.3.4 Assessing floodplain acid sulphate soils	38
References	39

Chapter 2

Investigating the spatio-temporal variability in groundwater and surface water interactions: a multi-technique approach	43
Abstract	43
2.1 Introduction	44
2.1.1 Study area	47
2.2 Methods	49
2.2.1 River surveys and flow gauging	49
2.2.2 Sampling	51
2.2.3 Sample preparation and analysis	52
2.2.4 Mass balance calculations	53
2.3 Results	55
2.3.1 ^{222}Rn activities	55
2.3.2 River gauging and water elevation	57
2.3.3 Temperature and EC surveys	58
2.3.4 Chloride concentrations	60
2.3.5 Groundwater fluxes	62
2.3.5.1 ^{222}Rn mass balance	62
2.3.5.2 Cl mass balance	64
2.4 Discussion	66
2.4.1 Spatial variability in groundwater discharge to the Tambo River	66
2.4.2 Uncertainty analysis	68
2.4.3 Method comparison	71
2.4.4 Hydrological drivers	74

2.5 Conclusions	76
Acknowledgements	77
References	77
Chapter 3	
Residence times and mixing of water in river banks: implications for recharge and groundwater – surface water exchange	83
Abstract	83
3.1 Introduction	84
3.1.1 Study area	87
3.2 Methods	90
3.3 Results	92
3.3.1 Groundwater elevations and hydraulic conductivities	92
3.3.2 Electrical conductivity	93
3.3.3 Stable isotopes	94
3.3.4 ^3H and ^{14}C	95
3.3.5 Major ions	96
3.4 Discussion	99
3.4.1 Hydrogeochemical processes	99
3.4.2 Aquifer interactions	102
3.4.3 Groundwater residence times and mixing	105
3.4.4 Implications for groundwater – surface water interaction	107
3.5 Conclusions	111
Acknowledgements	112
References	112

Chapter 4

The dynamics of groundwater-surface water exchange in river banks	117
Abstract	117
4.1 Introduction	118
4.2 Methods	120
4.2.1 Study area	120
4.2.2 Analytical procedure	123
4.3 Results	123
4.3.1 Groundwater and surface water elevations	123
4.3.2 Electrical conductivity	127
4.4 Discussion	129
4.4.1 The dynamics of groundwater surface water exchange	129
4.4.2 Numerical modelling	134
4.4.3 Groundwater flux estimates	140
4.5 Conclusions	144
Acknowledgements	145
References	145

Chapter 5

Transient groundwater - surface water interactions in a tidal estuary: a case study from the Tambo River, Eastern Victoria	149
Abstract	149
5.1 Introduction	150
5.1.1 Study area	153

5.2 Methods	154
5.2.1 Continuous monitoring	154
5.2.2 Sampling and analysis	156
5.3 Results	157
5.3.1 Surface section (~50 cm depth)	157
5.3.2 Subsurface section (~200 cm depth)	160
5.3.3 Groundwater	162
5.4 Discussion	163
5.4.1 Modelling groundwater fluxes	163
5.4.2 Uncertainty and sensitivity analysis	168
5.4.3 Tidal dynamics and groundwater-surface water interactions	171
5.5 Conclusions	176
Acknowledgements	178
References	178
Chapter 6	
Assessing the hydrogeochemical impact and distribution of acid sulphate soils, Heart Morass, West Gippsland, Victoria	183
Abstract	183
6.1 Introduction	184
6.2 Methods	187
6.2.1 Field area	187
6.2.2 Field survey	188
6.2.3 Sampling	189
6.2.4 Laboratory analysis	189

6.3 Results	191
6.3.1 Soils	191
6.3.1.1 Low – lying sedgeland	191
6.3.1.2 Floodplain riparian woodland scrub and uplands	193
6.3.2 Hydrochemistry	194
6.3.3 Post-flood conditions	195
6.4 Discussion	197
6.4.1 Pre-flood conditions in the low lying sedgeland	197
6.4.2 Pre-flood conditions in the floodplain riparian woodland and uplands	201
6.4.3 Post-flood conditions	202
6.5 Conclusions	205
Acknowledgements	206
References	206
Chapter 7	
Major findings and concluding remarks	211
7.1 Detailed findings as discussed by chapter	211
7.1.1 Spatial and temporal variability in groundwater and surface water interactions: a multi-technique approach	211
7.1.2 Residence times and mixing of water in river banks	212
7.1.3 Dynamics of river – groundwater exchange in river banks	213
7.1.4 Groundwater – surface water balances in a tidal estuary	213
7.1.5 Hydrogeochemical impact of acid sulphate soils	214

7.2 Implications of research	215
7.3 Further research	216
References	218
Appendix A	219
A multi-tracer approach to quantifying groundwater inflows to an upland river; assessing the influence of variable groundwater chemistry	221
Appendix B	231
Data compiled for thesis (digital copy)	231

Abstract

This thesis evaluates the connectivity and geochemical implications of groundwater-surface water connectivity in the Gippsland Basin. Head gradients, temperature profiles, Cl concentrations and ^{222}Rn activities all indicate higher groundwater fluxes to the Tambo River in areas of increased topographic variation where the potential to form large groundwater-surface water gradients is greater. Groundwater discharge to the Tambo River calculated by Cl mass balance was significantly lower (1.48×10^4 to $1.41 \times 10^3 \text{ m}^3 \text{ day}^{-1}$) than discharge estimated by ^{222}Rn mass balance (5.35×10^5 to $9.56 \times 10^3 \text{ m}^3 \text{ day}^{-1}$) and differential flow gauging (5.41×10^5 to $6.30 \times 10^3 \text{ m}^3 \text{ day}^{-1}$) due to Cl variability in bank waters. Groundwater constituted the lowest proportion of river discharge during times of increased rainfall that followed dry periods, while groundwater constituted the highest proportion of river discharge under baseflow conditions (21.4% of the Tambo in April 2010 and 18.9% of the Nicholson in September 2010).

Groundwater residence times increase towards the Tambo River which implies a gaining river system and not increasing bank storage with proximity to the Tambo River. Major ion concentrations and $\delta^2\text{H}$ and $\delta^{18}\text{O}$ values of bank water also indicate that bank infiltration does not significantly impact groundwater chemistry under baseflow and post-flood conditions, suggesting that the gaining nature of the river may be driving the return of bank storage water back into the Tambo River within days of peak flood conditions. The covariance between ^3H and ^{14}C indicates the leakage and mixing between saline ($\sim 3,000 \text{ }\mu\text{S/cm}$) old ($\sim 17,200$ years) groundwater from a semi-confined aquifer and fresh ($< 500 \text{ }\mu\text{S/cm}$) younger groundwater (< 100 years) near the river where confining layers are less prevalent. The presence of this semi-confined aquifer has also been used to help

explain the absence of bank storage, as rapid pressure propagation into the semi-confined aquifer during flooding will minimise bank infiltration.

Continuous elevation and EC monitoring along the Tambo River bank, indicates that the degree of mixing between the two aquifers and the river varies significantly in response to changing hydrological conditions. Numerical modelling using MODFLOW indicates that saline water moves into the river bank during flooding as hydraulic gradients reverse. This water then returns during flood recession as baseflow hydraulic gradients are re-established. Modelling also indicates that this process will increase groundwater concentrations for up to ~34 days between 20 and 40 meters of the river for flood events as large as 9.7 m in height. For the same flood event, groundwater concentrations within 10 m of the river will only increase for ~15 days as the infiltrating low salinity river water drives groundwater dilution.

Continuous high temporal resolution monitoring of ^{222}Rn activities in the stratified tidal estuary of the Tambo River indicates significant variation in groundwater-surface water interactions over a ~5 day period. In contrast to the limited number of studies in similar areas, ^{222}Rn mass balance indicates that the groundwater fraction varies tidally in the subsurface section of the Tambo River estuary but not in the surface section (the upper 50cm of the water column). The maximum groundwater fraction estimated in the subsurface typically ranged from ~4% to ~8% of total river discharge over individual tidal cycles. While this is partially attributed to varying degrees of mixing between subsurface water and surface water over tidal cycles, the input of groundwater during flow reversal is also likely to affect the groundwater fraction. It is proposed that in a tidal estuary, river water may receive groundwater inputs during both downstream movement at tidal minimum and upstream movement at tidal maximum, resulting in an increased

groundwater fraction during tidal maximums. A reduction in the maximum groundwater fraction in the surface section (from ~11 to ~2%) coincides with increased rainfall in the catchment and a reduction in $\delta^2\text{H}$ values (from -42 to -62‰), suggesting the dilution of groundwater via inputs from rainfall and runoff.

During drought conditions in 2009, low-lying areas of the Heart Morass (0–2 m elevation) were the most affected by acid sulphate soils, with a median soil pH (pHF) of 3.56 to approximately 50 cm depth. Soils below ~100 cm depth in these areas contain pyrite and have reduced inorganic S concentrations of up to 0.85 wt%. Higher areas of the floodplain (2–6 m) do not contain acid sulphate soils, with a median pH of 4.74 to approximately 50 cm depth, an average neutralising capacity of 3.87 kg $\text{H}_2\text{SO}_4/\text{t}$, and no appreciable unoxidised pyrite. In low-lying areas concentrations of Co, Ni, Zn, Mn and Fe in soil increased from <2.0, 4.0, 10, 20 and 2000 mg/kg, respectively, at 56 cm depth to 10, 20, 45, 152 and 15,000 mg/kg at 221 cm depth. In areas of higher elevation, concentrations of Co, Ni, Zn and Fe increased from 6, 11, 21 and 12,500 mg/kg at 44 cm depth to 10, 19, 47 and 19,400 mg/kg at 239 cm depth. These data indicate acidic leaching of metals from the upper soil profile in both low-lying and more elevated areas.

General Declaration

I hereby declare that this thesis contains no material which has been accepted for the award of any other degree or diploma at any university or equivalent institution and that, to the best of my knowledge and belief, this thesis contains no material previously published or written by another person, except where due reference is made in the text of the thesis.

The chapters in this thesis include two original papers published in peer reviewed journals and 3 unpublished papers. The core theme of this thesis is the interaction between groundwater and surface water in the Gippsland Basin. The ideas, development and writing of all the papers in the thesis were the principal responsibility of myself, the candidate, working within the School of Geosciences under the supervision of Prof. Ian Cartwright.

The inclusion of co-authors reflects the fact that the work came from active collaboration between researchers and acknowledges input into team-based research.

In the case of Chapters 2,3,4,5 and 6 my contribution to the work is as follows

Chpt.	Title	Status	Nature and extent of contribution
2	Investigating the spatio-temporal variability in groundwater and surface water interactions: a multi-technique approach	Published	Data collection, analysis and synthesis (85%)
3	Residence times and mixing of water in river banks: implications for recharge and groundwater – surface water exchange	In preparation	Data collection, analysis and synthesis (90%)
4	The dynamics of river – groundwater exchange in river banks	In preparation	Data collection, analysis and synthesis (90%)
5	Transient groundwater - surface water interactions in a tidal estuary: a case study from the Tambo River, Eastern Victoria	In preparation	Data collection, analysis and synthesis (90%)
6	Assessing the hydrogeochemical impact and distribution of acid sulphate soils, Heart Morass, West Gippsland, Victoria	Published	Data collection, analysis and synthesis (90%)

I have renumbered sections of submitted or published papers in order to generate a consistent presentation within the thesis.

Nicolaas Unland, 19 December 2013

Acknowledgements

There are many people who provided me with support during the completion of my thesis, without you all this would not have been possible; my sincere gratitude goes to you all.

Firstly, thank you to Ian Cartwright, my supervisor. Your guidance throughout this research has been invaluable, providing both encouragement to explore research questions independently and technical expertise when necessary. I would also like to thank my co-supervisor Edoardo Daly for his assistance with some of the more technical aspects of the project.

I would also like to thank everyone in our research team who has contributed in some way throughout the course of my PhD. Benjamin Gilfedder, Harald Hofmann, Martin Andersen, Gabriel Rau, Barrie Bolton, Alex Atkinson and Mathew Yu. Your assistance during in field work, experimental setup and scientific discussion has helped shape the research that is presented in this thesis.

A number of technical staff have also provided significant assistance throughout this project. Massimo Raveggi, Rachelle Pierson, Christopher Pierson, Dioni Cendon and Robert Chisari, my thanks goes to you all.

I would also like to thank the National Centre for Groundwater Research and who helped fund this research, as well as everyone involved in the centre who has provided a great support network. It is also important to thank Monash University for their funding and scholarship assistance, without it, this project would not have been possible.

My thanks also goes to everyone from the School of Geosciences at Monash University. Your friendly faces and kind nature have made the last 4 years a pleasure.

I would like to thank my wife Sophie Arnold who has shared in my journey over the last four years, your love, kindness and support have helped me to get through this.

Finally to all of my friends and family, thank you; my parents Olly and Vera Unland, my grandparents Herman Unland, Marion Unland, Kay Donders and Martin Donders, thank you for your support and encouragement over the years. I am the person I am today because of you and this couldn't have happened without you all.

Declaration for Thesis Chapter 2

Declaration by candidate

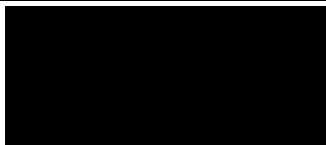
In the case of Chapter 2, the nature and extent of my contribution to the work was the following:

Nature of contribution	Extent of contribution (%)
Collection of data, analysis and interpretation, manuscript production	85%

The following co-authors contributed to the work. If co-authors are students at Monash University, the extent of their contribution in percentage terms must be stated:

Name	Nature of contribution	Extent of contribution (%) for student co-authors only
Ian Cartwright	Supervisory role, review of manuscript	5%
Martin Andersen	Data collection assistance, manuscript review	2.5%
Gabriel Rau	Data collection assistance, manuscript review	2.5%
Jenifer Reed	Data collection assistance	2%
Benjamin Gilfedder	Data collection assistance	1%
Alexander Atkinson	Data collection assistance	1%
Harald Hofmann	Data collection assistance	1%

The undersigned hereby certify that the above declaration correctly reflects the nature and extent of the candidate's and co-authors' contributions to this work*.

Candidate's Signature		Date 22/9/14
-----------------------	---	-----------------

Main Supervisor's Signature		Date 22/9/14
-----------------------------	---	-----------------

*Note: Where the responsible author is not the candidate's main supervisor, the main supervisor should consult with the responsible author to agree on the respective contributions of the authors.

Declaration for Thesis Chapter 3

Declaration by candidate

In the case of Chapter 3, the nature and extent of my contribution to the work was the following:

Nature of contribution	Extent of contribution (%)
Collection of data, analysis and interpretation, manuscript production	90%

The following co-authors contributed to the work. If co-authors are students at Monash University, the extent of their contribution in percentage terms must be stated:

Name	Nature of contribution	Extent of contribution (%) for student co-authors only
Ian Cartwright	Supervisory role, review of manuscript	5%
Dioni Cendón	Data analysis, review of manuscript	3%
Robert Chisari	Laboratory analysis	2%

The undersigned hereby certify that the above declaration correctly reflects the nature and extent of the candidate's and co-authors' contributions to this work*.

Candidate's Signature		Date 22/9/14
-----------------------	---	-----------------

Main Supervisor's Signature		Date 22/9/14
-----------------------------	---	-----------------

*Note: Where the responsible author is not the candidate's main supervisor, the main supervisor should consult with the responsible author to agree on the respective contributions of the authors.

Declaration for Thesis Chapter 4

Declaration by candidate

In the case of Chapter 4, the nature and extent of my contribution to the work was the following:

Nature of contribution	Extent of contribution (%)
Collection of data, analysis and interpretation, manuscript production	90%

The following co-authors contributed to the work. If co-authors are students at Monash University, the extent of their contribution in percentage terms must be stated:

Name	Nature of contribution	Extent of contribution (%) for student co-authors only
Ian Cartwright	Supervisory role, review of manuscript	5%
Edoardo Daly	Supervisory role, review of manuscript	2%
Alexander Atkinson	Data collection assistance	1.5%
Benjamin Gilfedder	Data collection assistance	1.5%

The undersigned hereby certify that the above declaration correctly reflects the nature and extent of the candidate's and co-authors' contributions to this work*.

Candidate's Signature		Date 22/9/14
--------------------------	--	---------------------

Main Supervisor's Signature		Date 22/9/14
-----------------------------------	--	---------------------

*Note: Where the responsible author is not the candidate's main supervisor, the main supervisor should consult with the responsible author to agree on the respective contributions of the authors.

Declaration for Thesis Chapter 5

Declaration by candidate

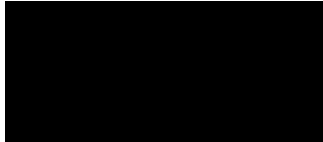
In the case of Chapter 5, the nature and extent of my contribution to the work was the following:

Nature of contribution	Extent of contribution (%)
Collection of data, analysis and interpretation, manuscript production	90%

The following co-authors contributed to the work. If co-authors are students at Monash University, the extent of their contribution in percentage terms must be stated:

Name	Nature of contribution	Extent of contribution (%) for student co-authors only
Ian Cartwright	Supervisory role, review of manuscript	4%
Benjamin Gilfedder	Data collection, review of manuscript	4%
Alexander Atkinson	Data collection assistance	2 %

The undersigned hereby certify that the above declaration correctly reflects the nature and extent of the candidate's and co-authors' contributions to this work*.

Candidate's Signature		Date
		22/9/14

Main Supervisor's Signature		Date
		22/9/14

*Note: Where the responsible author is not the candidate's main supervisor, the main supervisor should consult with the responsible author to agree on the respective contributions of the authors.

Declaration for Thesis Chapter 6

Declaration by candidate

In the case of Chapter 6, the nature and extent of my contribution to the work was the following:

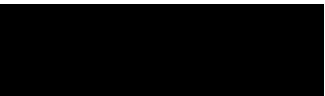
Nature of contribution	Extent of contribution (%)
Collection of data, analysis and interpretation, manuscript production	90%

The following co-authors contributed to the work. If co-authors are students at Monash University, the extent of their contribution in percentage terms must be stated:

Name	Nature of contribution	Extent of contribution (%) for student co-authors only
Helen Taylor	Data collection and analysis	5%
Barrie Bolton	Supervisory role, review of manuscript	2.5%
Ian Cartwright	Supervisory role, review of manuscript	2.5%

The undersigned hereby certify that the above declaration correctly reflects the nature and extent of the candidate's and co-authors' contributions to this work*.

Candidate's Signature		Date 22/9/14
-----------------------	---	-----------------

Main Supervisor's Signature		Date 22/9/14
-----------------------------	---	-----------------

*Note: Where the responsible author is not the candidate's main supervisor, the main supervisor should consult with the responsible author to agree on the respective contributions of the authors.

Chapter 1

Introduction, background and aims

1.1 Background

1.1.1 Water resource management and hydrogeology

Global water resources are becoming increasingly vulnerable as a result of increasing population growth and climate uncertainty (Arnell, 2004). The UN Comprehensive Assessment of the Freshwater Resources of the World estimated that in 1997 around one third of the world's population was living in areas in which water resources were stressed (World Meteorological Organization, 1997). Estimates from this assessment also indicated that this number could as much as double by 2025. It was found that increasing variability in the volume of river discharge, changes in the seasonal availability of water supply (Alcamo et al., 2007), population growth, economic growth, urbanization, agricultural expansion and a range of other socio-economic factors are leading to significant changes in water use and stress. In this context, the effective management of water is continuing to grow in both its scientific and political significance.

While groundwater represents over 98% of Earth's fresh water (Shiklomanov, 2003), it has been historically poorly understood and undervalued by governments, leading to adverse environmental, economic and social consequences (Hiscock, 2005). The earliest accounts of groundwater exploitation come from Persia over 3,000 years ago, where the development of groundwater wells and horizontal tunnels were used to distribute groundwater for irrigation (Young, 2002). It was not until the 17th and 18th centuries that a true understanding of hydrogeology was achieved through investigation of the hydrological

cycle. Increasing water demand during the industrial revolution led to the development of hydrogeology and the production of the first hydrogeological map (Lucas, 1877). Around the same time, work was being done that led to the development of many physical hydrogeological principles used today, including the hydraulics and flow of groundwater through sediment (Darcy, 1856) and the physical properties of aquifers and how they change over time (Meinzer, 1928; Theis, 1935). Following this, the need to characterise water quality for drinking and agriculture led to the study of water chemistry associated with surface and subsurface geology (Piper, 1944; Stiff, 1951). Such studies represent the earliest stages of the field now known as hydrogeochemistry.

As the development of hydrogeology and hydrogeochemistry as sciences has occurred relatively recently in comparison to the exploitation of groundwater, the environmental impact and the long term sustainability of groundwater resources in response to extraction has historically been overlooked. In the United States, large scale groundwater extraction has resulted in the reduction of stream flow and lake levels, reductions in vegetation, land subsidence and the intrusion of sea water into coastal aquifers (Zektser et al., 2005). In China, over extraction and groundwater depletion has led to land subsidence, sea water intrusion and a reduction in groundwater quality through salinization and the infiltration of untreated wastewater (Changming et al., 2001). Furthermore, long term irrigation in China has led to changes in the redox chemistry and biogeochemical reactions that occur in many aquifers, resulting in mobilisation of arsenic in groundwater. In parts of Australia and northern Europe, groundwater extraction from coastal river floodplains has led to the oxidation of sulphidic soils, the production of sulphuric acid and the mobilisation of metals (eg: Johnston et al., 2009, 2010; Österholm and Åström, 2008; Unland et al., 2012). Such outcomes have been the impetus for further research in the field of hydrogeology, hydrogeochemistry and an increase in the social and political awareness of groundwater.

1.1.2 The Australian setting

Australia is the flattest and driest inhabited continent in the world (Potter, 2007), with over 70% of Australia receiving an annual rainfall of less than 350 mm (Bureau of Meteorology, 2013). Most of the interior of Australia is defined as arid (<100 mm rainfall annually) and is characterised by variable, episodic rainfall and recharge. In these areas, groundwater is the only reliable source of water for drinking and irrigation. The importance of groundwater to life in Australia is embodied by early civilisation in Australia, which document the significance of lagoons, springs and unlined wells in many Aboriginal tribes. Aboriginal survival through dry periods in the Australian interior relied on hundreds of springs, and give rise to rich spiritual and cultural beliefs (Commander, 2002). Groundwater dependence in Australia continued through the British settlement, with a number of colonies relying on groundwater as their major water supply. Between 1824 and 1849, attempts to colonise the northern coastline of Australia were made at three different locations. Each of these locations relied on groundwater springs and wells as their primary water source (Department of Land Resource Management, 2013).

Over the last century, groundwater use in Australia has grown. Currently, groundwater accounts for approximately one third of Australia's water consumption (National Water Commission, 2012). In many areas it is the only reliable water source, sustaining townships, farms and mines. Similar to global water resources, Australian water resources have been put under extreme pressure in recent decades in response to drought, climate change and increasing population growth. Increasing groundwater use during such periods has led groundwater over-extraction in a number of areas. Perhaps the most recognised example of this in Australia is the Murray Darling Basin. During 2004-2005 over half of Australia's total water consumption occurred in the Murray Darling Basin (Australian Bureau of Statistics, 2013). Water extraction in the basin diverts around 75% of its average

annual flow, resulting in the closure of the Murray River mouth during periods of low rainfall. Under such rates of extraction, groundwater resources and the agricultural practices that rely on them are unsustainable. Furthermore, groundwater dependant ecosystems through the basin including floodplains, wetlands, estuaries or lakes are likely to be negatively impacted by such flow reductions (Boulton, 2005).

In response to the recognition of water resource vulnerability in Australia, a range of government policies and projects have been implemented. This includes the enforcement of water restrictions, government rebates on water saving products and a push towards the use of water resources less affected by climatic shifts such as desalinated water (Hoang, 2009). Further to this, a number of groundwater focussed research programs have been developed by the Australian Federal Government. This includes the Murray Darling Basin Commission (Authority), which has focussed on determining and maintaining sustainable water use through the Murray Darling Basin. Subsequently, the National Centre for Groundwater Research and Training and the National Groundwater Action Plan have been developed. The research being conducted by these programs will lead to a greater understanding of groundwater processes in Australia, allowing more effective management of Australia's groundwater resources.

1.1.3 Groundwater and surface water

Groundwater and surface water are intrinsically linked throughout the hydrological cycle (Sophocleous, 2002). Many surface water bodies such as rivers, wetlands and lakes lie above the groundwater level. In these settings, surface water will infiltrate into the groundwater system in a process termed groundwater recharge. In contrast, when the elevation of groundwater is greater than that of neighbouring surface water, groundwater may infiltrate into the surface water body in a process termed groundwater discharge. While groundwater and surface water are intimately related, their connectivity has been historically

overlooked by water managers. Failure to account for this can lead to errors in calculating water balances, salt or nutrient loads and the transport of contaminants (Andričević and Cvetković, 1996; Tsur, 1991). This may lead to a range of adverse environmental impacts such as groundwater contamination, salinization, algal blooms, eutrophication and acidification (Santos and Eyre, 2011; Singh, 2011; Su et al., 2011).

In this context, it is important that the interaction between groundwater and surface water is understood conceptually through an understanding of hydrological processes. Furthermore, the scientific methods used to trace and understand such processes need to be refined. While a range of chemical and physical methodologies have been developed to qualitatively and quantitatively determine the flux of water between groundwater and surface water bodies, many give contradictory results, indicating an incomplete conceptual or methodological knowledge. Large discrepancies continue to occur between numerical, physical and chemical methods used for determining the flux of groundwater to streams (Kalbus, 2006). This is largely because across these different sub-disciplines, the way in which different groundwater stores and the connectivity between groundwater and surface water are defined vary considerably (Brunner et al., 2010). For example, numerical hydrologists commonly consider groundwater discharge as any component of a river hydrograph that is not a rapid response to rainfall and runoff. This approach fails to account for intermediate groundwater stores that may vary considerably in chemistry in comparison to regional groundwater. As such, numerical groundwater discharge estimates may vary considerably with chemical groundwater discharge estimates.

In particular, the processes occurring within river banks during bank storage remains poorly researched. While the concept of bank storage is well understood, quantifying the volume of water that infiltrates the banks and the duration of bank return flows is complicated. Furthermore, the impact of bank storage on the age and geochemical nature of

groundwater neighbouring rivers is poorly constrained. As river banks represent the interface between groundwater and surface water, this zone remains ecologically significant through both the biological diversity and the biogeochemical reactions that take place within them (Peyrard, 2011; Woessner, 2000). The dynamics associated with the interface between sea water and terrestrial water in estuaries and coastal lakes present similar challenges. Tidal forcing, chemical and density variations give rise to a number of shallow water habitats and rich biodiversity. The exchange between groundwater and surface water in these areas is poorly understood, as are the chemical changes associated with such exchange. As such, further hydrological, ecological and biogeochemical research is required to understand the chemical and biological dynamics of these systems.

1.2 Study Area

1.2.1 Geology

The majority of research presented in this thesis is focussed on the Tambo River Catchment. This catchment extends from the Eastern Victorian Uplands at its northern margin into the central Gippsland Basin at its southern margin (Fig. 1). The Eastern Victorian Uplands are part of the larger Australian Eastern Highlands. These highlands contain the Australian Alps and the highest peaks in Australia. While the exact geologic evolution of the Australian Eastern Highlands remains a topic of debate, it is largely accepted that the highlands formed through subduction driven uplift during the Silurian and Devonian periods, resulting in the metamorphism of Cambrian seafloor basalts and Ordovician marine sediments (including the turbidite-dominated Pinnack Sandstone) and the formation of schists and gneisses (Birch, 2003; Gray and Foster, 2004).

Explosive volcanism and magmatic intrusions through the Silurian and Devonian periods resulted in the formation of ignimbrites and granites, while subsequent rifting

between Australia and Antarctica resulted in further uplift and episodic basaltic extrusion (Vandenberg, 2010). Subaerial volcanism through these periods yielded rhyolitic lavas, porphyry dykes and sediments that constitute the majority of the Snowy River Volcanics Group. The Eastern Victorian Uplands have remained tectonically active through the Quaternary period, with fault reactivation, uplift and a number of significant earthquakes in the area. These include a magnitude 5.0 earthquake at Mt Baw Baw in 1996 and a magnitude 4.0 earthquake at Corryong in 1998.

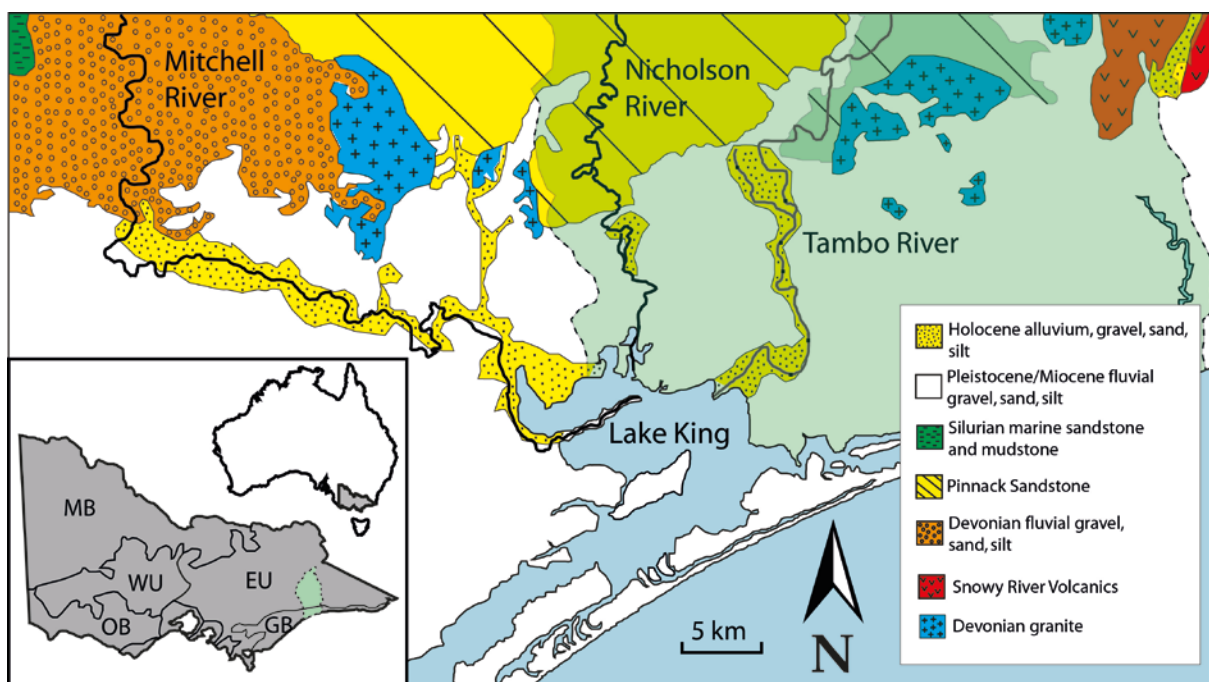


Figure.1. Study area surface geology and location of Tambo River Catchment (green highlight) in relation to major Victorian formations (MB = Murray Basin, OB = Otway Basin, WU = Western Uplands, EU = Eastern Uplands, GB = Gippsland Basin).

Australia-Antarctic rifting during the early Cretaceous period caused further uplift in the Australian Eastern Highlands (Birch, 2003) and also resulted in the opening of the Gippsland Basin. This basin is approximately 400km in length and 80km wide, extending from the onshore Mornington Peninsula at its western extent to the offshore continental shelf at its eastern extent (Fig. 1). The basin boundaries are defined by the Lake Wellington Fault System in the north, the Foster Fault System in the south, the Slewyn Fault in the west and

the Gippsland Rise in the east. Significant subsidence in the system led to the accumulation of up to 14 km of sediment that currently overlies the Palaeozoic formations. Mesozoic deposition was dominated by the formation of the Strzelecki and Latrobe groups. The Strzelecki group consists of fluvial sediments that were deposited during the initial stages of rifting. These sediments range from high energy conglomerates associated with alluvial fan and braided river environments, to sands and muds associated with meandering rivers (Tosolini et al., 1999). Mesozoic formations in the LaTrobe group consist of a mixture of coastal plain, lacustrine and marine sediments. Tertiary deposits include Palaeogene siliclastic sediments and coal measures that extend from the western onshore part of the basin to the foot of the offshore continental slope at its eastern extent. Deposition of carbonate-rich sediments took place through the Neogene and Holocene periods, with the formation of carbonate marls interbedded with clastics throughout high energy outer shelf and canyon-slope offshore environments (Holdgate and Gallagher, 1997; Holdgate, 2003). Marine regression during the late Pliocene and early Pleistocene gave rise to the onshore deposition of the Haunted Hill formation. This formation consists of river fan and alluvial deposits including quartz rich gravels, sands and clays which are generally poorly sorted (Jenkin, 1968). Magnetic surveys show that a variety of river palaeo-channels, meander bends and ox-box lakes underlay the Gippsland shelf and lakes systems (Holdgate, 2003).

1.2.2 Hydrogeology

The Gippsland Basin contains numerous interbedded aquifers. The relationship between these aquifers is illustrated in Fig. 2. The Tambo River Basin is underlain by the Haunted Hill Gravel, Boisdale Formation, Jemmys Point/Tambo River/Lake Wellington Formations, Gippsland Limestone, Lakes Entrance Formation, LaTrobe Valley Group and a Pre-Tertiary basement.

The shallowest units (the Haunted Hill Gravel and Boisdale Formation) are late Tertiary in age and consist of sands and clays with sands becoming more dominant at increasing depth. Quaternary alluvium and Haunted Hill gravel cover most of the Gippsland region, including the Mitchell River valley and Gippsland Lakes area. The Boisdale formation contains an upper clay unit (the Nuntin clay) that consists of brown-grey clay, gravel and fine to coarse sands. This acts as an aquitard in the formation and separates several aquifer horizons from each other (Hocking, 1976). A lower sand unit in the formation (the Wurruk Sand) consists of grey medium to coarse quartz rich sands and is a major aquifer in the central Gippsland area (Wiltshire, 2009). The Boisdale formation increases in thickness to ~200m near the township of Sale and generally yields high volumes of water with a total dissolved solids (TDS) concentration of less than 500 mg/L (Birch, 2003). Water quality in the Haunted hill formation is generally poorer (TDS = 1000-4000 mg/L) and yields from the aquifer are generally low.

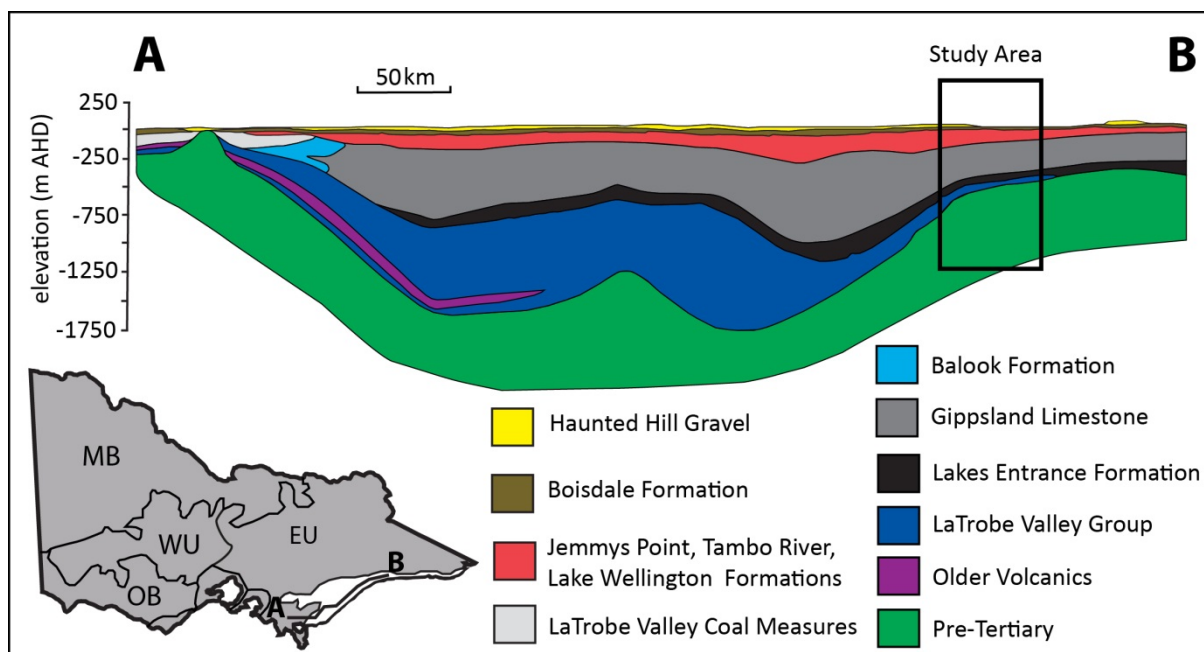


Figure. 2. Aquifer stratigraphy in the Gippsland Basin from A to B after Leonard (1992).

The Gippsland Limestone and Lakes Entrance formations represent periods of major marine transgression throughout the Gippsland Basin (Wiltshire, 2009). The onshore Lakes Entrance Formation is dominated by sands and gravels lower in the sequence and mudstones and marls higher in the sequence. The thickest onshore section of the formation is ~225 m and occurs within the Lake Wellington Depression. The Gippsland Limestone consists of fossiliferous marl and limestone. It overlies the Lake Entrance formation and is up to 500m in thickness within the Lake Wellington and Seaspray Depressions (Hocking, 1976). The water quality and hydraulic conductivity of the limestone are variable, with low water quality and yield where the aquifer is dominated by marl and better water quality where the aquifer is dominated by limestone and shelly sands. The Jemmys Point, Tambo River and Lake Wellington formations overlie the Gippsland Limestone and are generally considered to be aquitards. These formations represent marine transgression from the Oligocene to the Pliocene and consist of calcareous sediments, including shelly and sandy marls, calcareous sands, sands and minor gravels.

The Latrobe Valley Group underlies the Lakes Entrance Formation and is comprised of the Traralgon, Morwell and Yallourn formations. It contains all of the coal bearing sediments and associated volcanics in the onshore part of the Gippsland Basin (Holdgate and Gallagher, 1997). The Traralgon formation is dominated by sands and fine gravels and forms the base of the Latrobe Valley Group. It contains several aquifers interbedded with coal seams that are up to 100 m in thickness. Within the Seaspray Depression, gravel successions up to 150 m in thickness contain a transmissivity of up to 2,000 m²/day (Brumley, 1981). Across the basin where the sands and gravels are saturated, aquifer yields of up to 100 L/s occur. Coal seams within the Traralgon Formation form extensive aquitards and define the upper boundary of the formation. In areas where the upper seam is less established, the boundary between the Traralgon and Morwell formations is less defined, allowing the two

formations to become hydraulically connected. Direct recharge to the Latrobe Valley Group and Traralgon formation predominantly occurs at the Gippsland Basin-Eastern Highland margin where the group outcrops (Wiltshire, 2009). The higher elevation of these recharge areas promote artesian conditions over most of the basin and drive a groundwater flow directions trending from west to east. The Morwell Formation contains several aquifers that increase in thickness to around 200 m in the Lake Wellington Depression and around 400 m in the Latrobe Valley Depression. Aquifers in the Morwell Formation are mostly comprised of inter-seam sediment. These vary from quartz sands and gravels interbedded with clays, to silts, fine sands and volcanic units previously belonging to the Hazelwood Formation (Gloe, 1975). As previously mentioned, the separation between aquifers of the lower Morwell Formation and upper Traralgon Formation is unclear, with similar drawdown responses recorded during dewatering of Traralgon Formation aquifers at the Loy Yang mine site. The Yallourn Formation overlies the Morwell Formation. It is dominated by clay with some fine sands and is overlain by the Yallourn Seam Coal. It does not contain any major aquifers.

The Pre-Tertiary basement throughout the Gippsland area is comprised of similar units as the Eastern Victorian Uplands (section 1.2.1) and is dominated by marine sediments and meta-sediments that are Ordovician in age, as well as Silurian to Devonian volcanics, granites and limestones. While the basement is extensive throughout the region, its low permeability prevents it from providing significant groundwater flow. Minor fractured rock aquifers outcrop in the Highlands and drilling evidence suggests these are likely to underlay the majority of the Gippsland Basin.

1.2.3 Hydrology and Climate

The Tambo River Basin is ~4,200 km² in area and contains the Tambo and Nicholson River. These rivers are perennial and drain roughly southward out of the Eastern Victorian Uplands and through the Gippsland Basin before terminating at Lake King (Unland et al.,

2013). Lake King is part of the saline Gippsland Lakes system that has a permanent entrance to the Tasman Sea through Lakes Entrance (Fig. 1). Tidal forcing through the entrance propagates through the lakes systems and into the lower sections of both the Tambo and Nicholson Rivers, forming saline estuaries that can extend ~15 km upstream under lower flow conditions. Approximately 80% of the catchment is forest and woodland (Department of Agriculture, Fisheries and Forestry, 2006), with cattle grazing of river floodplains dominating the remainder of the catchment.

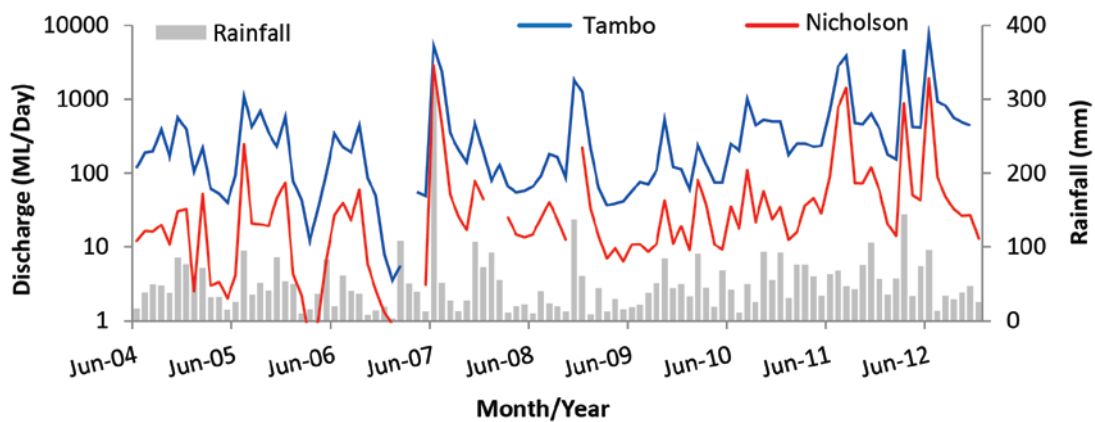


Figure. 3. Monthly rainfall (Bureau of Meteorology, 2013) and average monthly river discharge for the Tambo and Nicholson Rivers (Victorian Water Resources Data Warehouse, 2012), period June 2004 – December 2012.

The catchment receives an annual precipitation of ~705 mm, increasing from 655 mm in the upper catchment to 777 mm in the mid to lower reaches (Bureau of Meteorology, 2013). Rainfall patterns in the catchment indicate slightly above average monthly rainfall in October, November and December. Annual evapotranspiration rates are around 600-700 mm in the upper catchment and 500-600 mm in the lower catchment. Annual river discharge is 522 ML/Day for the Tambo River and 110 ML/Day for the Nicholson River, with generally lower river flows in the drier periods from January and April (Victorian Water Resources Data Warehouse, 2013). The studies presented in this thesis took place between 2009 and late 2012. This period represents the transition from a period of relatively low rainfall and river flow (Tambo River average monthly discharge 2008 to 2009 = 230 ML/Day) to a period in

which successive large rainfall events resulted in increased river discharge and a number of flood events in the Tambo Catchment (average Tambo River discharge 2010 to 2012 = 895 ML/Day).

1.3 Scope and research aims

In general, the overall focus of this thesis is to better understand and trace the movement of water through catchments in order to allow better water management and prediction of potential environmental impacts through anthropogenic influence. The research presented in this thesis addresses many scientific questions in the field of groundwater-surface water research.

Specifically, various tracers of groundwater (both physical and chemical) continue to yield significantly different groundwater flux estimates (e.g. Cook et al., 2012, Unland et al., 2013). This thesis will focus on comparing different groundwater tracers and identify the source of these discrepancies and assess the errors associated with various methods.

Groundwater-surface water exchange at the river bank has been identified as a potential driver of such discrepancies (McCallum et al., 2012). This process, while conceptually well known, remains poorly understood with respect to its impact on groundwater tracers. This will be investigated within this thesis, allowing the age and origin of groundwater near rivers to be established. Further to this, the processes driving such exchange will be studied, allowing quantitative fluxes and potential water quality impacts to be identified. The use of relatively novel groundwater tracing techniques will also be employed to investigate the balance of groundwater and surface water through tidal estuaries. The impact of changing hydrological conditions on the chemical nature of river, groundwater and floodplain environments will be assessed in known acid sulfate soil environments. By conducting this research in the Gippsland Lakes region, the findings of this research will not only further the scientific understanding of groundwater-surface water processes, but will also be directly

applicable to water management in the Gippsland Lakes region. While the studies presented in this thesis are based in south east Australia, this area is typical of many groundwater-surface water systems and as such, the research outcomes presented are applicable to many settings worldwide.

1.3.1 Research objective 1: Groundwater – surface water fluxes

As the study of groundwater-surface water exchange lies at the interface between the fields of surface water hydrology and groundwater hydrogeology, this field of research still poses significant challenges. More specifically, the spatial and temporal dynamics of groundwater and surface water exchange remains poorly understood in a variety of settings (Sophocleous, 2002). Furthermore, numerical, physical and chemical methods continue to yield significantly different groundwater flux estimates (McCallum et al., 2012). One of the major objectives of this thesis is to study the degree to which groundwater and surface water interactions can vary along a river stretch and if such interactions can change significantly over time. This goes beyond defining rivers as either gaining (receiving groundwater) or losing (recharging groundwater) and recognises that river behaviour can vary over space and time. Further to this, a number of physical, chemical and numerical methods will be used to quantify the flux of water between groundwater and surface water reservoirs. By doing this, the strengths and weaknesses of each method may be evaluated and the hydrological framework driving discrepancies between tracers may be identified. This will provide significant scientific information when conducting future groundwater-surface water studies, allowing the optimal tracer (or combination of tracers) to be used within a given setting. Finally, by conducting the study in a location where little work has been done previously, the findings of the study can be directly applied to water management practices in the area.

1.3.2 Research objective 2: Groundwater-surface water interaction in river banks

Conceptually, the interaction between groundwater and surface water at the river bank scale is well understood. During periods of low rainfall, river flow in gaining systems is sustained by groundwater discharge. When rainfall and runoff increase, an increase in river height will result in the infiltration river water into the bank (Brunke and Gonser, 1997; Sophocleous, 2002). As river stage falls, the infiltrated water will return back into the river, compensating for reductions in river flow. Over a given time period, a river can switch between these conditions based on the frequency and duration of rainfall and discharge events in a catchment. While this concept is generally well understood, very few studies have investigated the volumetric exchange between rivers and their banks over time, nor the chemical implication this has for groundwater and surface water chemistry (McCallum et al., 2010). A major focus of the research presented in this thesis is to investigate the exchange between rivers and their banks and how this may vary over time at different locations. The effect of this exchange on groundwater residence times and chemical properties will also be investigated. This has significant implications for calculating groundwater discharge to rivers by chemical baseflow separation, estimating the sustainability of groundwater as a resource, assessing groundwater and surface water quality and determining the fate of any contaminants present within groundwater-surface water systems.

1.3.3 Research objective 3: Groundwater-surface water balances in tidal estuaries

Using chemical tracers to estimate the flux of groundwater to rivers is a method that has been extremely well studied over that past few decades (Cook, 2012). However a lack of river gauging in estuaries and increased salinity can make the use of such methods difficult and therefore less common (Santos et al., 2010). Failure to account for groundwater discharge in the tidal sections of rivers may lead to underestimating nutrient and solute fluxes, as even low volumetric groundwater fluxes may have significant biogeochemical impacts in estuaries

(Santos, 2008). Most studies that do consider groundwater inputs to estuaries do not account for any stratification within the estuary, or any variability's associated tidal cycles. The research presented in this thesis uses relatively novel groundwater tracing methods in order to investigate the variability of groundwater discharge into a stratified estuary over tidal cycles. This includes (1) the effect changing hydraulic gradients between groundwater and surface water during tidal fluctuations in river height (2) density driven partitioning of groundwater above or below the pycnocline and (3) the chemical implications that such processes may have. By conducting this study using a relatively novel technique, any flaws or processes governing its applicability in subsequent studies may be identified. This will lead to further improvements in the methodology and models used to interpret data from such investigations.

1.3.4 Research objective 4: Assessing floodplain acid sulphate soils

In Australia, coastal floodplains are commonly drained for agriculture, reducing the level of local water tables (White et al., 1997). Excess drainage and lower rainfall during drought conditions may expose sulphidic sediments to the atmosphere, leading to oxidation and the production of sulphuric acid. These soils have been widely studied and are termed acid sulphate soils (ASS). Much of the Gippsland Lakes region has been identified as a risk area for the development of coastal acid sulphate soils (Department of Environment and Primary Industries, 2013). Within this thesis, the hydrochemical impact of acid sulphate soils (ASS) in the Heart Morass (a coastal floodplain in the Gippsland Lakes region) is assessed after significant drainage and drought. The areas most affected by ASS are assessed with respect to pH, metal mobilisation, major ion chemistry and sulphur isotope chemistry. These impacts are further assessed after significant flooding in the Heart Morass. Ultimately, this research investigates the source, fate and impact of coastal acid sulphate soils in the Gippsland area, where exchange between rivers and floodplain groundwater may significantly affect redox chemistry.

References

- Alcamo, J., Flörke, M., Märker, M., 2007. Future long-term changes in global water resources driven by socio-economic and climatic changes. *Hydrological Sciences Journal*, 52(2): 247-275.
- Andričević, R., Cvetković, V., 1996. Evaluation of Risk from Contaminants Migrating by Groundwater. *Water Resources Research*, 32(3): 611-621.
- Arnell, N.W., 2004. Climate change and global water resources: SRES emissions and socio-economic scenarios. *Global Environmental Change*, 14(1): 31-52.
- Australian Bureau of Statistics, available at: <http://www.abs.gov.au> (last access 13 January, 2013)
- Birch, W.D., 2003. *The Geology of Victoria*. Geological Society of Australia (Victorian Division), Sydney.
- Boulton, A.J., 2005. Chances and challenges in the conservation of groundwaters and their dependent ecosystems. *Aquatic Conservation: Marine and Freshwater Ecosystems*, 15(4): 319-323.
- Brumley, J.C., Barton, C.M., Holdgate, G.R., Reid, M.A., 1981. *Regional Groundwater Investigation of the Latrobe Valley 1976 – 1981*, State Electricity commission of Victoria & Department of Minerals and Energy, unpubl.
- Brunke, M., Gonser, T.O.M., 1997. The ecological significance of exchange processes between rivers and groundwater. *Freshwater Biology*, 37(1): 1-33.
- Brunner, P., Simmons, C.T., Cook, P.G., Therrien, R., 2010. Modeling Surface Water-Groundwater Interaction with MODFLOW: Some Considerations. *Ground Water*, 48(2): 174-180.
- Bureau of Meteorology: Commonwealth of Australia, available at: <http://www.bom.gov.au> (last access: 28 August 2013), 2013.
- Changming, L., Jingjie, Y., Kendy, E., 2001. Groundwater Exploitation and Its Impact on the Environment in the North China Plain. *Water International*, 26(2): 265-272.
- Commander, D.P., Laws, A. W., Stone, R., 2002. Development of the Canning Bain groundwater resource, International Association of Hyrdologists, Darwin.
- Cook, P.G., 2012. Estimating groundwater discharge to rivers from river chemistry surveys. *Hydrological Processes*: 27(5): 3694–3707.
- Darcy, H., 1856. *Les fontaines publiques de la ville de Dijon.*, Victor Dalmont, Paris.
- Department of Land and Resource Management, 2013, available at: <http://www.lrm.nt.gov.au> (last access 11 January, 2013).
- Department of Agriculture, Fisheries and Forestry, 2006: available at: http://adl.brs.gov.au/water2010/pdf/catchment_223_0_summary.pdf (last access: 19 November 2012).
- Department of Environment and Primary Industries, 2013: available at: <http://vro.dpi.vic.gov.au/dpi/vro/vrosite.nsf/pages/water-gw-quality-quantity> (last access: 5 July 2013).
- Gloe, C.S., 1975. Latrobe Valley Coal Fields in: D.M. Traves, D. King (Eds.), *Economic Geology of Australia and Papua New Guinea. 2. Coal*. Australas. Inst. Min. Metall. Monogr.(6): 645-652.
- Gray, D.R., Foster, D.A., 2004. Tectonic evolution of the Lachlan Orogen, southeast Australia: historical review, data synthesis and modern perspectives. *Australian Journal of Earth Sciences*, 51(6): 773-817.
- Hiscock, K.M., 2005. *Hydrogeology Principles and Practice*. Blackwell Science, Victoria.
- Hoang, M., Bolto, B., Haskard, C., Barron, O., Gray, S., Leslie, G., 2009. *Desalination Australia*, CSIRO.

- Hocking, J.B., 1976. Definition and revision of Tertiary stratigraphic units, onshore Gippsland Basin, Geological Survey of Victoria.
- Holdgate, G., Gallagher, S., 1997. Microfossil paleoenvironments and sequence stratigraphy of Tertiary cool-water carbonates, onshore Gippsland Basin, southeastern Australia. *Special Publication - SEPM (Society for Sedimentary Geology)*, 56: 205-220.
- Holdgate, G.R., Wallace, M. W., Gallagher, Stephen J., Smith, A. J., Keene, J. B., Moore, D., Shafik, S., 2003. Plio-Pleistocene tectonics and eustasy in the Gippsland Basin, Southeast Australia; evidence from magnetic imagery and marine geological data. *Australian Journal of Earth Sciences*, 50(3): 403-426.
- Jenkin, J.J., 1968. The Geomorphology and Upper Cainozoic geology of southeast Gippsland, Victoria.
- Johnston, S.G., Bush, R.T., Sullivan, L.A., Burton, E.D., Smith, D., Martens, M.A., McElnea, A.E., Ahern, C.R., Powell, B., Stephens, L.P., Wilbraham, S.T., VanHeel, S., 2009. Changes in water quality following tidal inundation of coastal lowland acid sulfate soil landscapes. *Estuar. Coast Shelf Sci.* 81, 257–266.
- Johnston, S.G., Burton, E.D., Bush, R.T., Keene, A.F., Sullivan, L.A., Smith, D., McElnea, A.E., Ahern, C.R., Powell, B., 2010. Abundance and fractionation of Al, Fe and trace metals following tidal inundation of a tropical acid sulfate soil. *Appl. Geochem.* 25, 323–335.
- Kalbus, E., Reinstorf, F., Schirmer, M., 2006. Measuring methods for groundwater - surface water interactions: a review. *Hydrol. Earth Syst. Sci.*, 10(6): 873-887.
- Leonard, J.G., 1992. An overview of Victoria's groundwater resources. Background report S3, short term planning guidelines. Drought management plan for Victoria's water resources, Department of Water Resources, Melbourne, Victoria.
- Lucas, J., 1877. Hydrogeological Survey, Stanford, London.
- McCallum, J.L., Cook, P.G., Berhane, D., Rumpf, C., McMahan, G.A., 2012. Quantifying groundwater flows to streams using differential flow gaugings and water chemistry. *Journal of Hydrology*, 416–417(0): 118-132.
- McCallum, J.L., Cook, P.G., Brunner, P., Berhane, D., 2010. Solute dynamics during bank storage flows and implications for chemical base flow separation. *Water Resources Research*, 46(7): W07541.
- Meinzer, O.E., 1928. Compressibility and elasticity of artesian aquifers. *Economic Geology* (23): 263–291.
- National Water Commission, available at: <http://www.nwc.gov.au> (last access 13 January 2013).
- Österholm, P., Åström, M., 2008. Meteorological impacts on the water quality in the Pajuluoma acid sulphate area, W. Finland. *Appl. Geochem.* 23, 1594–1606.
- Peyrard, D., Delmotte, S., Sauvage, S., Namour, Ph, Gerino, M., Vervier, P., Sanchez-Perez, J. M., 2011. Longitudinal transformation of nitrogen and carbon in the hyporheic zone of an N-rich stream: A combined modelling and field study. *Physics and Chemistry of the Earth, Parts A/B/C*, 36(12): 599-611.
- Piper, A.M., 1944. A graphic procedure in the geochemical interpretation of water analyses. , American Geophysical Union, pp. 914–923.
- Potter, E., 2007. *Fresh Water: A new Perspective on Water in Australia*. Melbourne University Publishing Limited, 187 Grattan Street, Carlton, Victoria 3053, Australia.
- Santos, I.R., Burnett, W.C., Chanton, J., Mwashote, B., Suryaputra, I. G. N. A., Dittmar, T., 2008. Nutrient biogeochemistry in a Gulf of Mexico subterranean estuary and groundwater-derived fluxes to the coastal ocean. *Limnology and Oceanography*, 52(2): 805-718.

-
- Santos, I.R., Eyre, B.D., 2011. Radon tracing of groundwater discharge into an Australian estuary surrounded by coastal acid sulphate soils. *Journal of Hydrology*, 396(3–4): 246-257.
- Santos, I.R., Peterson, R.N., Eyre, B.D., Burnett, W.C., 2010. Significant lateral inputs of fresh groundwater into a stratified tropical estuary: Evidence from radon and radium isotopes. *Marine Chemistry*, 121(1–4): 37-48.
- Shiklomanov, I.A., Rodda, J.C., 2003. *World Water Resources at the Beginning of the 21st Century*. Cambridge University Press, Cambridge, UK.
- Singh, A., 2011. Estimating long-term regional groundwater recharge for the evaluation of potential solution alternatives to waterlogging and salinisation. *Journal of Hydrology*, 406(3–4): 245-255.
- Sophocleous, M., 2002. Interactions between groundwater and surface water: the state of the science. *Hydrogeology Journal*, 10(1): 52-67.
- Stiff, H.A., 1951. The interpretation of chemical water analysis by means of patterns. *Journal of Petroleum Technology*(3): 15–17.
- Su, N., Du, J., Moore, W.S., Liu, S., Zhang, J., 2011. An examination of groundwater discharge and the associated nutrient fluxes into the estuaries of eastern Hainan Island, China using ²²⁶Ra. *Science of The Total Environment*, 409(19): 3909-3918.
- Theis, C.V., 1935. The relation between the lowering of the piezometric surface and rate and duration of discharge of a well using groundwater storage, American Geophysical Union, pp. 519–524.
- Tosolini, A.M.P., McLoughlin, S., Drinnan, A.N., 1999. Stratigraphy and fluvial sedimentary facies of the Neocomian lower Strzelecki Group, Gippsland Basin, Victoria. *Australian Journal of Earth Sciences*, 46(6): 951-970.
- Tsur, Y., Graham-Tomaso, T., 1991. The buffer value of groundwater with stochastic surface water supplies. *Journal of Environmental Economics and Management*, 21(3): 201-224.
- Unland, N.P., Cartwright, I., Andersen, M. S., Rau, G. C., Reed, J., Gilfedder, B. S., Atkinson, A. P., Hofmann, H., 2013. Investigating the spatio-temporal variability in groundwater and surface water interactions: a multi-technical approach. *Hydrology and Earth System Sciences Discussions*, 10(3): 3795-3842.
- Unland, N.P., Taylor, H.L., Bolton, B.R., Cartwright, I., 2012. Assessing the hydrogeochemical impact and distribution of acid sulphate soils, Heart Morass, West Gippsland, Victoria. *Applied Geochemistry*, 27(10): 2001-2009.
- Victorian Water Resources Data Warehouse: available at:
<http://www.vicwaterdata.net/vicwaterdata/home.aspx> (last access: 21 November 2013), 2012.
- Vandenberg, A.H.M., 2010. Paleogene basalts prove early uplift of Victoria's Eastern Uplands. *Australian Journal of Earth Sciences*, 57(3): 291-315.
- White, I., Melville, M.D., Wilson, B.P., Sammut, J., 1997. Reducing acidic discharges from coastal wetlands in eastern Australia. *Wetland Ecol. Manag.* 5, 55–72.
- Wiltshire, E., Hulbert, S., Harrison, A., Bolger, P., Foley, G., Pratt, M., 2009. Hydrogeological mapping of southern Victoria, Southern Rural Water, Maffra, Victoria, 3860.
- Woessner, W.W., 2000. Stream and fluvial plain ground water interactions: Rescaling hydrogeologic thought. *Ground Water*, 38(3): 423-429.
- Young, M.E., 2002. Institutional development for sustainable groundwater management – an Arabian perspective. *Geological Society, London, Special Publication*(193): 63-74.
-

Zektser, S., Loáiciga, H.A., Wolf, J.T., 2005. Environmental impacts of groundwater overdraft: selected case studies in the southwestern United States. *Environmental Geology*, 47(3): 396-404.

Chapter 2

Investigating the spatio-temporal variability in groundwater and surface water interactions: a multi-technique approach

N .P. Unland^{1,2}, I. Cartwright^{1,2}, M. S. Andersen^{2,3}, G. C. Rau^{2,3}, J. Reed¹, B. S. Gilfedder^{1,2}, A.P. Atkinson^{1,2}, H. Hofmann^{1,2}

^[1] *School of Geosciences, Monash University, Clayton, Vic. 3800, Australia*

^[2] *National Centre for Groundwater Research and Training, GPO box 2100, Flinders University, Adelaide, SA 5001, Australia*

^[3] *Connected Waters Initiative Research Centre (CWI), School of Civil and Environmental Engineering, University of New South Wales, Sydney NSW 2093, Australia*

Published in Hydrology and Earth Systems Science (10, 3795-3842)

Abstract

The interaction between groundwater and surface water along the Tambo and Nicholson Rivers, southeast Australia, was investigated using ²²²Rn, Cl, differential flow gauging, head gradients, electrical conductivity (EC) and temperature profiles. Head gradients, temperature profiles, Cl concentrations and ²²²Rn activities all indicate higher groundwater fluxes to the Tambo River in areas of increased topographic variation where the potential to form large groundwater-surface water gradients is greater. Groundwater discharge to the Tambo River calculated by Cl mass balance was significantly lower (1.48×10^4 to 1.41×10^3 m³ day⁻¹) than discharge estimated by ²²²Rn mass balance (5.35×10^5 to 9.56×10^3 m³ day⁻¹) and differential flow gauging (5.41×10^5 to 6.30×10^3 m³ day⁻¹) due to bank return waters. While groundwater sampling from the bank of the Tambo River was intended to account for changes in groundwater chemistry associated

with bank infiltration, variations in bank infiltration between sample sites remains unaccounted for, limiting the use of Cl as an effective tracer. Groundwater discharge to both the Tambo and Nicholson Rivers was the highest under high flow conditions in the days to weeks following significant rainfall, indicating that the rivers are well connected to a groundwater system that is responsive to rainfall. Groundwater constituted the lowest proportion of river discharge during times of increased rainfall that followed dry periods, while groundwater constituted the highest proportion of river discharge under baseflow conditions (21.4% of the Tambo in April 2010 and 18.9% of the Nicholson in September 2010).

2.1. Introduction

Constraining the interaction between groundwater and rivers is important for calculating water balances and sustainable levels of water extraction (Tsur and Graham-Tomasi, 1991), maintaining healthy river ecology (Boulton, 1993; Krause et al., 2007; Lambs, 2004), understanding biogeochemical reactions at the groundwater-surface water interface (Peyrard et al., 2011; Sophocleous, 2002; Woessner, 2000) and determining the source and fluxes of nutrients and solutes carried by rivers. In order to estimate groundwater discharge to rivers and to define gaining and losing reaches, a number of physical, chemical and numerical methods have been developed (Kalbus et al., 2006).

Differential flow gauging uses the difference in river discharge at two points along a reach in order to calculate net gains or losses along that stretch (Cey et al., 1998; Harte and Kiah, 2009; McCallum et al., 2012; Ruehl et al., 2006). Discharge is usually measured under baseflow conditions where runoff is negligible, allowing the net groundwater discharge or recharge to be calculated once evaporative losses are accounted for. While gauging stations are usually spaced far apart and often overlook variations at smaller spatial scales, long time series of measurements are commonly available,

allowing for analysis of temporal trends and comparison with other methods (McCallum et al. in press).

As groundwater temperature is commonly higher than that of surface water in winter and lower in summer (Anibas et al., 2009), measurement of temperature in rivers and streambeds can be used to identify the gaining and losing reaches (Anderson, 2005; Andersen and Acworth, 2009, Anibas et al., 2011; Rau et al., 2010; Silliman and Booth, 1993). While quantification of water fluxes using temperature requires detailed subsurface temperature measurements over time, temperature mapping of rivers is a simple and effective method of identifying gaining and losing reaches (Becker et al., 2004). Similarly, if groundwater has a significantly different EC to surface water, changes in river EC can be used to quantify the influx of groundwater (Cartwright et al., 2011; Cey et al., 1998; McCallum et al., 2012). The advantage of along-river temperature/EC surveying is that it allows data to be obtained at a higher spatial resolution than flow gauging or discrete sampling for chemical analysis.

Geochemical tracers including major ions, stable isotopes and radiogenic isotopes have been used to estimate groundwater fluxes in gaining rivers (Cartwright et al., 2011, 2010, 2008; Cook, 2012; Cook et al., 2003, 2006; Durand et al., 1993; Genereux et al., 1993; Genereux and Hemond, 1990; Lamontagne et al., 2005, 2008; Lamontagne and Cook, 2007; Mullinger et al., 2007, 2009; Négrel et al., 2003; Rhode, 1981; Ribolzi et al., 2000; Stellato et al., 2008). The utility of each of these tracers depends on a variety of factors including the difference between the concentration of the tracer in groundwater compared to surface water, its spatial and temporal variability, the accurate characterisation of its sources and sinks, and the potential for it to change by processes such as evaporation, precipitation, radioactive decay, degassing, or biogeochemical reactions. However after such processes are accounted for, chemical tracers are useful in

assessing groundwater fluxes, as runoff does not impact flux estimates and spatial analyses are only limited by sampling frequency.

^{222}Rn is produced by the decay of ^{226}Ra in the ^{238}U to ^{206}Pb decay series. Since ^{226}Ra activities are high in minerals, ^{222}Rn activities in groundwater increase as it achieves secular equilibrium with the ^{226}Ra in minerals over periods of approximately 2-3 weeks (Cook, 2012). After groundwater discharges to a surface water body, degassing and radioactive decay will reduce ^{222}Rn activities resulting in ^{222}Rn activities in surface water that are usually 2 to 3 orders of magnitude lower than those in groundwater (e.g. Cook, 2012; Cook et al., 2006). The use of ^{222}Rn as a groundwater tracer has increased over the last two decades as methods for its measurement in the field have improved (Burnett et al., 2010; Cartwright et al., 2011; Cook et al., 2003; Ellins et al., 1990; Genereux and Hemond, 1990; Gilfedder et al., 2012; Hofmann et al., 2011; Mullinger et al., 2007; Mullinger et al., 2009; Santos and Eyre, 2011). The short half-life (3.82 days) and degassing of ^{222}Rn from surface water makes it a particularly valuable groundwater tracer, as elevated ^{222}Rn activities will only occur close to zones of groundwater discharge.

The effectiveness of ^{222}Rn as a groundwater tracer can be limited by poorly-defined groundwater end members and low surface water concentrations which can lead to high analytical uncertainties. The uncertainties associated with groundwater end members can be reduced by combining groundwater measurements with laboratory experiments in which the ^{222}Rn activity of water in equilibrium with the river sediments is determined (Burnett et al., 2008; Cook et al., 2006; Corbett et al., 1998; Martens et al., 1980; Peterson et al., 2010). Recent studies have also focussed on better quantifying processes such as hyporheic exchange and gas transfer, making the use of ^{222}Rn more reliable (Cook et al., 2006; Lamontagne and Cook, 2007; Mullinger et al., 2007).

This study uses major ion chemistry, differential flow gauging, and ^{222}Rn activities to calculate groundwater fluxes to the Nicholson and Tambo Rivers and assess how groundwater fluxes vary in response to seasonal changes in rainfall and river discharge. These techniques are combined with EC and temperature mapping to evaluate the detailed spatial variability of groundwater discharge. By combining differential flow gauging with chemical mass balance, errors in groundwater estimates due to the presence of losing reaches or runoff during periods of rainfall can be accounted for. By combining these techniques with temperature and EC surveys, the applicability of each technique can be evaluated, and the variability in groundwater-surface water interaction on a fine spatial scale can be investigated. Furthermore, by conducting the study on two rivers in the same catchment, controls on the gaining and losing behaviour of neighbouring rivers can be investigated. Studies that employ multiple techniques for such investigations have been historically less common than research focussed on one or two methods, and can provide additional and more robust information for groundwater-surface water studies (Cox et al., 2007).

2.1.1 Study Area

The Tambo and Nicholson Rivers occur within the Tambo River Basin (Fig. 1), which has a total surface area of $\sim 4,200 \text{ km}^2$. These are perennial rivers that drain southwards from the Eastern Victorian Uplands across the Gippsland Basin to Lake King (a saline coastal lake connected to the Tasman Sea). The lake system is affected by tidal forcing which propagates into the lower sections of both the Nicholson and the Tambo rivers, forming estuarine sections that extend $\sim 15 \text{ km}$ upstream from the lake during low flow conditions. The river sections do not contain significant tributaries and minor creeks were not flowing during the sampling campaigns.

Average annual precipitation in the catchment is ~705 mm, increasing from 655 mm in the upper catchment to 777 mm in the mid-lower reaches. Precipitation is relatively evenly distributed throughout the year, with slightly higher than average monthly rainfall during October to December (Bureau of Meteorology, 2012). Annual evapotranspiration rates decrease from 600 to 700 mm in the upper catchment to 500 to 600 mm in the lower catchment. During the study period, evaporation ranged from $6.7 \times 10^{-3} \text{ m day}^{-1}$ in April 2011 to $3.6 \times 10^{-3} \text{ m day}^{-1}$ during August 2011 (Bureau of Meteorology, 2012). Approximately 80% of the catchment area is covered by forest and woodland, with the remainder dominated by cattle grazing on river floodplains (Department of Agriculture, Fisheries and Forestry, 2006).

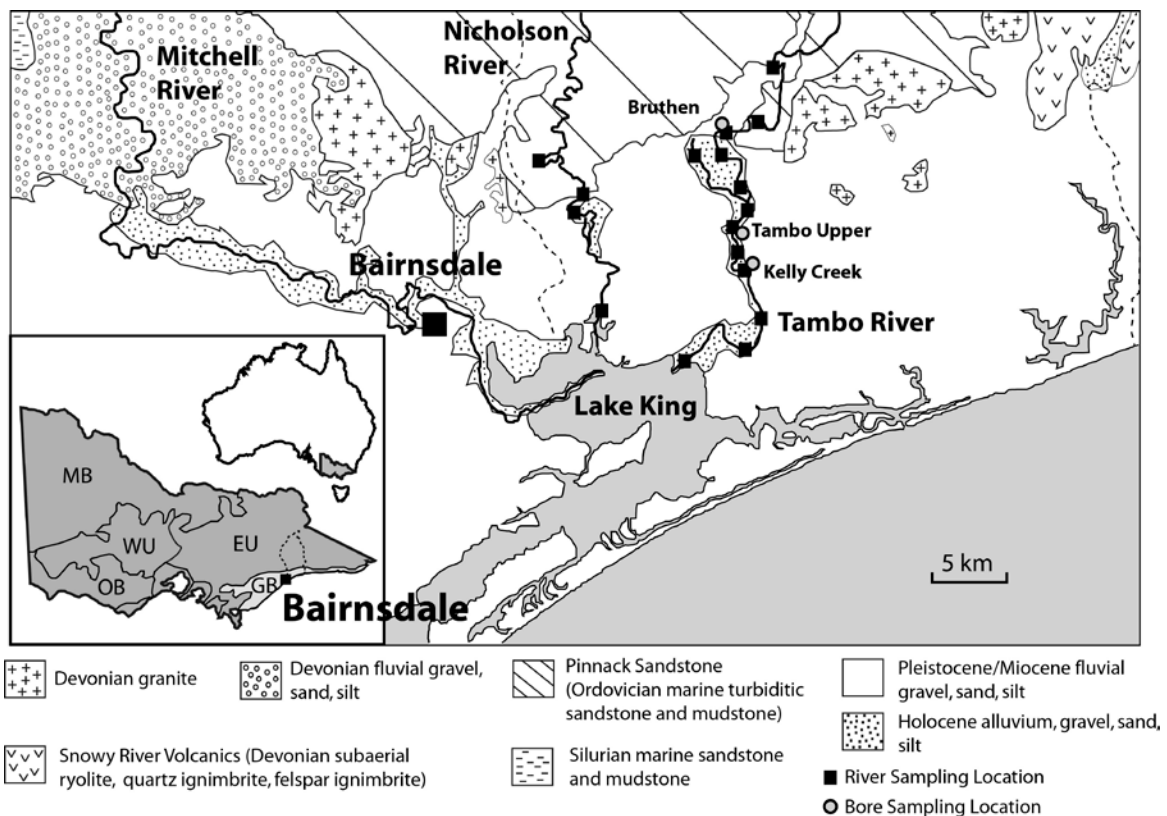


Figure 1. Map of the Tambo River Basin (dashed line) with sampling locations on Tambo and Nicholson Rivers, and local surface geology (modified from Jolly 1997). GB=Gippsland Basin, EU=Eastern Victorian Uplands, WU=Western Victorian Uplands, OB=Otway Basin, MB=Murray Basin.

The geology of the northern region of the Tambo River Basin is dominated by Ordovician gneisses and schists and Silurian-Devonian granites that form a fractured rock aquifer (Chaplin, 1995; Jolly, 1997; Vandenberg and Stewart, 1992). The southern section of the basin is dominated by Tertiary sands and gravels (of the Haunted Hills Gravels and Baxter Sandstone) and Quaternary sands, silts, and calcareous sands of the Shepparton Formation (Fig. 1). Various dune/beach deposits, alluvium and colluvium are locally present with the Tertiary and Quaternary units. While very little is known about the bedrock aquifers in the area, the Tambo and Nicholson rivers flow through an Upper Tertiary aquifer of sands, gravels and clays in the lower catchment. In the study area, the Upper Tertiary aquifer contains groundwater with a total dissolved solids (TDS) content of 500 to 1000 mg L⁻¹. The aquifer overlies Middle and Lower Tertiary aquifers that are dominated by calcareous sands, gravels, coal and basalt that contain groundwater with a TDS of 1000 to 3000 mg L⁻¹.

2.2. Methods

2.2.1 River surveys and flow gauging

River discharge is measured at Sarsfield on the Nicholson River and at Ramrod Creek and Battens Landing at on the Tambo River (Victorian Water Resource Warehouse, 2012). In the absence of runoff, significant tributary inflows or changes in the storage of a river channel, the net groundwater flux to a river (I_N) can be calculated from

$$I_N = Q_d + E - Q_u - P \quad (1)$$

(Lerner et al., 1990), where Q_d is the river discharge at the downstream site, Q_u is the river discharge at a upstream site, E is direct evaporation and P is direct precipitation (all terms have units of m³ day⁻¹).

The groundwater flux to the Tambo River was calculated using Eq. (1) and the difference in river discharge between Battens Landing and Ramrod Creek flow gauging stations. The difference in the timing of discharge events between the two stations was accounted for by time shifting the discharge of data of the Ramrod Creek gauging station so that discharge events matched (McCallum et al., in press). When discharge events did not occur during sampling periods (i.e. baseflow conditions), the Ramrod Creek data was time shifted using the distance between the stations and the river velocity (calculated using the discharge and river width and depth) to calculate the lag time. I_N estimates were based on the discharge data for a period of ~48 hours leading up to and including sampling. Direct evaporation and rainfall were calculated using the surface area of the river and data from the Bairnsdale Airport weather station (Bureau of Meteorology, 2012).

Run-of-the-river continuous surface water EC/temperature surveys were conducted during the February 2010 and March 2012 sampling campaigns using a Schlumberger CTD-Diver and an Aqua TROLL 200 logger with a precision of $\pm 1\%$ (EC) and $\pm 0.1^\circ\text{C}$ (temperature). Elevation and location during the surveys were recorded using a Trimble DGPS with a precision of < 0.02 m. The elevation of bores and the Tambo River adjoining the bores was measured using a Trimble DGPS with a precision of < 0.01 m in February 2011. Elevation of the river in subsequent campaigns was interpolated from river height data at the Battens Landing and Ramrod Creek gauging stations. Groundwater elevations in bores were measured using an electronic water tape during the sampling campaigns. All elevations are reported in metres relative to the Australian Height Datum (AHD). Groundwater-surface water gradients were calculated at Bruthen and Tambo Upper using the measured groundwater elevations of the bore closest to the river and the river. Gradients were only calculated at Kelly Creek during February 2011

as upstream gauging does not account for the tidal nature of the location and could not be used to interpolate river height in subsequent campaigns. River depth and width in upstream reaches was measured in the field using a tape measure. The width of wider downstream reaches was estimated using Google Earth with an uncertainty of < 1.0 m.

2.2.2 Sampling

Investigations were carried out between the upper catchment and the coastal plain of the Tambo and Nicholson Rivers (Fig. 1). Six sampling campaigns were conducted on a ~40 km section of the Tambo River and a ~21 km section of the Nicholson River between April 2010 and March 2012. Surface and groundwater sampling took place over a 1 to 2 day period. Sample locations are designated by distance upstream from Lake King. There are 12 sampling locations on the Tambo River and 5 on the Nicholson River. Sampling in April 2010 was conducted at near base flow conditions, while sampling in September 2010 took place during the recession of a minor discharge event (Fig. 2).

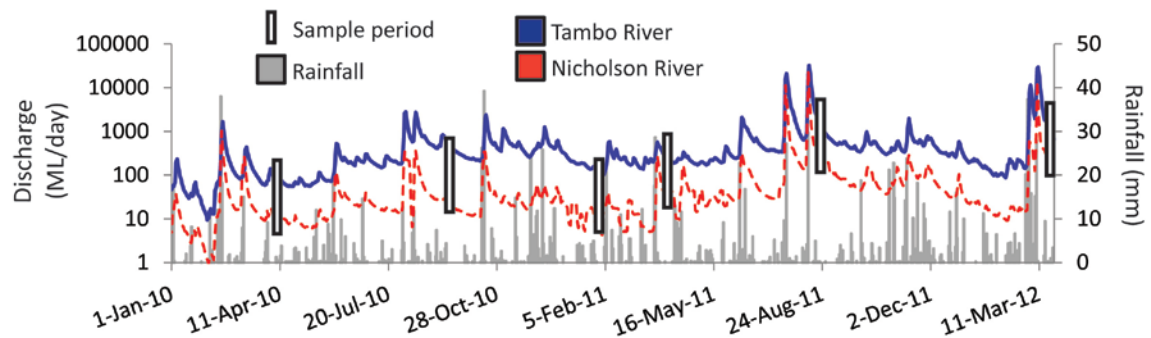


Figure 2. Sampling frequency superimposed on river hydrographs (Tambo River = Battens Landing station 223209, Nicholson River = Sarsfield gauging station 223210) and rainfall in the Tambo Catchment (Bairnsdale Airport, station 85279).

Sampling in February 2011 occurred during a discharge event while the April 2011 campaign was conducted during low flow conditions after a minor discharge event. Sampling campaigns conducted during August 2011 and March 2012 both took place during the recession of major flood events. Groundwater measurement and sampling were conducted in conjunction with river sampling but excluded April 2010 and September

2010 campaigns, as bores were still under construction at these times. Groundwater was sampled at three locations along the Tambo River. Three bores were sampled at Bruthen (28.5km), two at Tambo Upper (20.2km) and 1 at Kelly Creek (13.8km). The bores were installed within 20m of the river at 6 to 7m depth below surface, with screened sections 1 to 1.5m in length. Bores were sampled using an impeller pump set at the screened section and at least 3 bore volumes were pumped before samples were collected.

2.2.3 Sample preparation and analysis

Electrical conductivity (EC) was measured in the field using a calibrated TPS pH/EC meter. Water samples were preserved in the field by refrigeration in air-tight polyethylene bottles. Anion concentrations were measured on samples that were filtered through 0.45 μ cellulose nitrate filters using a Metrohm ion chromatograph at Monash University, Clayton; precision estimated by replicate analysis is $\pm 2\%$. Cation concentrations were measured on filtered samples that were acidified to pH < 2 using twice-distilled 16 M nitric acid by a Varian Vista ICP-AES at the Australian National University or at Monash University, Clayton, using a Thermo Finnigan X series II, quadrupole ICP-MS. Drift during ICP-MS analysis was corrected using internal Sc, Y, In, Bi standards and replicate analyses indicate a precision of $\pm 5\%$. The activity of ^{222}Rn in water samples was measured using a RAD-7 radon-in-air detector by the method outlined in Burnett and Dulaiova (2006) and is reported in Bq m^{-3} . ^{222}Rn was degassed from 500 ml of water for 5 minutes into an air tight loop of a known volume. Total counting times were 2 hrs for surface water and 40 minutes for groundwater. Uncertainties based on 4 replicates are less than 15% for ^{222}Rn activities below 1000 Bq m^{-3} and less than 5% for ^{222}Rn activities above 1000 Bq m^{-3} . Streambed sediments were sampled at Tambo Upper on the Tambo River for ^{222}Rn ingrowth experiments. Four sediment samples of approximately 1.45 kg were allowed to equilibrate with ~500 ml of ^{226}Ra free water for 8

weeks in air tight bottles, before 150 ml of water was sampled for ^{222}Rn analysis using the methods outlined above.

2.2.4 Mass balance calculations

Assuming that both the concentration of ^{222}Rn in the atmosphere and the ingrowth of ^{222}Rn in river water through the decay of ^{226}Ra in suspended sediment are negligible (Cook et al., 2006; Mullinger et al., 2007), the inflow of groundwater along a reach (I in $\text{m}^3 \text{m}^{-1} \text{day}^{-1}$) may be calculated from changes in ^{222}Rn activity in the river c_r (Bq m^{-3}) with distance x (m) by:

$$I = \left(Q \frac{dc_r}{dx} - wEc_r - F_h + kdwc_r + \lambda dwc_r \right) / (c_i - c_r) \quad (2)$$

(Cartwright et al., 2011; Cook et al., 2006), where Q is river discharge ($\text{m}^3 \text{day}^{-1}$), w is stream width (m), E is the evaporation rate (m day^{-1}), F_h is the flux of ^{222}Rn from the hyporheic zone ($\text{Bq m}^{-1} \text{day}^{-1}$), k is the gas transfer constant (day^{-1}), d is river depth (m), λ is the radon decay constant (0.181 day^{-1}) and c_i is the activity of ^{222}Rn in groundwater (Bq m^{-3}). The hyporheic zone can be defined as the part of the surface aquifer adjacent to the river that exchanges water with the river over relatively short distances (centimetres to tens of centimetres) on timescales of seconds to days (Boano et al., 2007; Kasahara and Wondzell, 2003). The net flux of ^{222}Rn from the hyporheic zone can be represented by:

$$F_h = q_h (c_h - c_r) \quad (3)$$

(Cook et al., 2006) where q_h is the volumetric flux of water in and out of the hyporheic zone in $\text{m}^3 \text{day}^{-1}$ (yielding a net flux of $0 \text{ m}^3 \text{day}^{-1}$ to the river) and c_h is the activity of ^{222}Rn in the hyporheic zone (assuming a single well mixed reservoir). While c_h

is simple to measure in the field, calculating q_h has historically been solved by conducting in stream tracer injections and modelling breakthrough curves (Runkel, 1998; Wagner and Harvey, 1997), which can be logistically difficult in large river systems. The flux of ^{222}Rn from the hyporheic zone can alternatively be estimated from river stretches that are not receiving groundwater input where there is little change in ^{222}Rn activity (Cartwright et al., 2011). If $dc_r/dx = 0$ and $I = 0$, F_h may be estimated from Eq. (2) as:

$$F_h = kdwc_r + \lambda dwc_r - wEc_r \quad (4)$$

While the degassing of ^{222}Rn to the atmosphere is controlled by wind driven turbulence in oceans, lakes and estuaries, it has been shown that degassing in upstream rivers is driven by river flow velocity, depth and width (Genereux and Hemond, 1992). As such, gas transfer rates (k) were estimated using the O'Connor and Dobbins (1958) and Negulescu and Rojanski (1969) gas transfer models as modified by Genereux and Hemond (1992) and Mullinger et al. (2007):

$$k = 9.301 \times 10^{-3} \left(\frac{v^{0.5}}{d^{1.5}} \right) \quad (5)$$

and

$$k = 4.87 \times 10^{-4} \left(\frac{v}{d} \right)^{0.85} \quad (6)$$

where d is river depth (m) and v is stream velocity (m day^{-1}) calculated from discharge, depth and width data.

A similar mass balance approach may also be used to estimate groundwater inflows from changes in the concentration of major ions, such as Cl. For a conservative ion such as Cl, mass balance calculations are simplified as decay, degassing and hyporheic flux terms are redundant. Thus Eq. (2) reduces to

$$I = (Q \frac{dCl_r}{dx} - wECl_r)/(Cl_i - Cl_r) \quad (7)$$

where Cl_i and Cl_r are the concentrations of Cl in the groundwater and river, respectively.

2.3. Results

2.3.1 ^{222}Rn activities

Figure 3 shows the ^{222}Rn activities from all sampling campaigns on the Tambo River. These range from 52 to 604 Bq m^{-3} and show significant spatial and temporal variation. Average ^{222}Rn activities were highest for the Tambo River during August 2011 ($380 \pm 62 \text{ Bq m}^{-3}$) and lowest during April 2011 ($160 \pm 50 \text{ Bq m}^{-3}$).

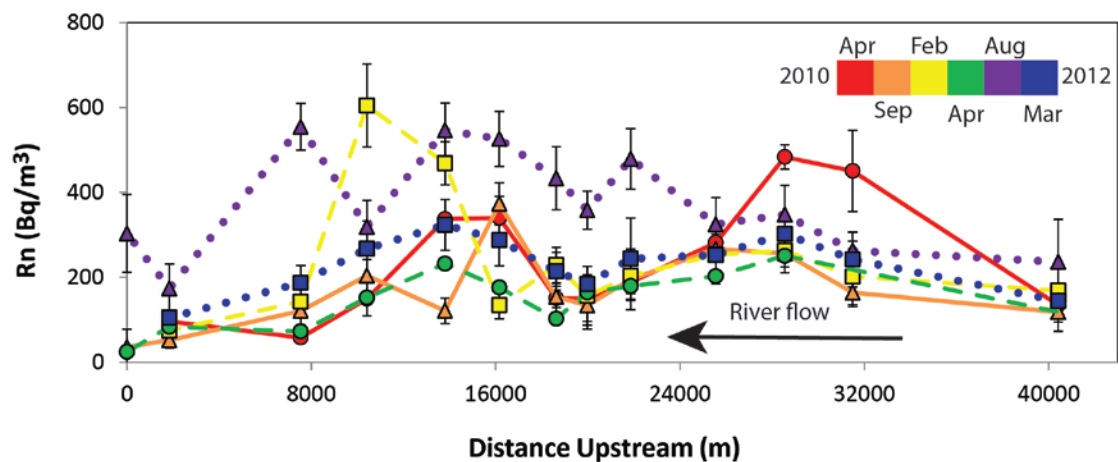


Figure 3. Distribution of ^{222}Rn activities in water sampled from the Tambo River over the study period. Apr 2010 = solid line with circles, Sep 2010 = solid line with triangles, Feb 2011 = dashed line with squares, Apr 2011 = dashed lines with circles, Aug 2011 = dotted line with triangles, Mar 2012 = dotted line with squares.

^{222}Rn activities were generally higher at 28.5, 16.2 and 13.8 km compared to other locations with average activities of 302 ± 51 , 288 ± 51 and 326 ± 37 Bq m^{-3} , respectively. ^{222}Rn activities were generally lower at 20.0 and 1.8 km, with average ^{222}Rn activities of 184 ± 52 Bq m^{-3} and 105 ± 37 Bq m^{-3} , respectively. ^{222}Rn activities in the Nicholson River were generally lower than those in the Tambo River, with 16 of the 27 samples yielding activities below 120 Bq m^{-3} . During April and September 2010, ^{222}Rn activities in the Nicholson River were <100 Bq m^{-3} at all sites except 13.6 km, which had activities of 370 and 734 Bq m^{-3} , respectively (Fig. 4). In February 2011 activities were <200 Bq m^{-3} for all sites except at 3.2 km which had an activity of 856 Bq m^{-3} . Activities varied little during April 2011, with all activities below 120 Bq m^{-3} . In August 2011 and March 2012, activities were <200 Bq m^{-3} at all sites except the uppermost sample point (21.2 km), in which activities were 891 and 292 Bq m^{-3} , respectively.

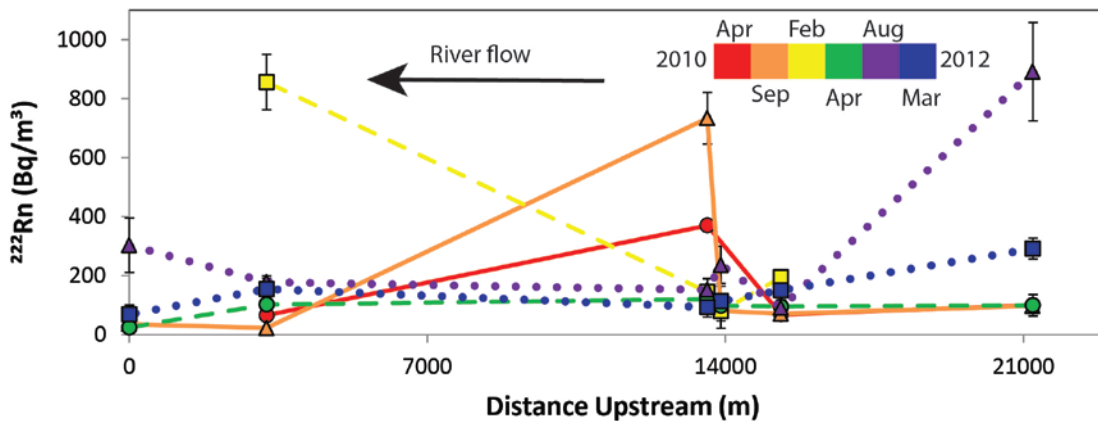


Figure 4. Distribution of ^{222}Rn activities in water sampled from the Nicholson River over the study period. Apr 2010 = solid line with circles, Sep 2010 = solid line with triangles, Feb 2011 = dashed line with squares, Apr 2011 = dashed lines with circles, Aug 2011 = dotted line with triangles, Mar 2012 = dotted line with squares.

Groundwater ^{222}Rn activities at Bruthen ranged from 2,380 to 9,130 Bq m^{-3} , with an average activity of $5,000\pm 2,340$ Bq m^{-3} over the study period. Average activities at this site were generally higher in February and April 2011 ($4,620\pm 2,750$ and $5,160\pm 1,970$ Bq m^{-3}) and lower during August 2011 and March 2012 ($3,100\pm 570$ and $2,150\pm 440$ Bq m^{-3}).

Groundwater activities at Tambo Upper were generally lower than at Bruthen, with average activities at the site ranging from $1,500 \pm 170 \text{ Bq m}^{-3}$ in March 2012 to $2,290 \pm 2,770 \text{ Bq m}^{-3}$ in February 2011. Activities at this site were also highly variable ranging from 330 to $4,240 \text{ Bq m}^{-3}$ over the study period. Groundwater activities at Kelly Creek were the highest of any site, with an average activity of $8,740 \pm 3,550 \text{ Bq m}^{-3}$, ranging from $13,480 \text{ Bq m}^{-3}$ in August 2011 to $5,220 \text{ Bq m}^{-3}$ in March 2012. The activity of ^{222}Rn in water equilibrated with streambed sediments ranged from 1,900 to $3,740 \text{ Bq m}^{-3}$, with an average activity of $2,640 \pm 880 \text{ Bq m}^{-3}$ (Table 1). This is within the range of the average ^{222}Rn activities of groundwater at Bruthen and Tambo Upper (2,320 to $4,600 \text{ Bq m}^{-3}$).

Sample	^{222}Rn	Test 1	Test 2	Test 3	Test 4	Average	Std. Deviation 1σ
1	Bq m^{-3}	2,540	2,980	3,300	3,010	2,960	310
2	Bq m^{-3}	1,230	2,230	2,600	1,850	1,980	590
3	Bq m^{-3}	1,430	2,140	1,930	2,090	1,900	320
4	Bq m^{-3}	3,170	3,830	3,970	3,990	3,740	390

Table 1. Activity of water equilibrated with streambed sediments in four samples.

2.3.2 River gauging and water elevation

The parameters used to calculate net groundwater fluxes I_N using Eq. (1) are listed in Table 2. The discharge of the Tambo River at the Battens Landing station varied by up to two orders of magnitude during the study, ranging from $6.6 \times 10^4 \text{ m}^3 \text{ day}^{-1}$ in April 2010 to $7.9 \times 10^6 \text{ m}^3 \text{ day}^{-1}$ in August 2011. Direct rainfall to the river for the 48 hr period leading up to and including sampling/analysis ranged from 0 to $4,093 \text{ m}^3 \text{ day}^{-1}$. Direct evaporative losses for the same periods were on a similar order of magnitude as rainfall, ranging from 636 to $1,974 \text{ m}^3 \text{ day}^{-1}$ and averaging $1,190 \text{ m}^3 \text{ day}^{-1}$.

River elevation during the February 2011 survey decreased from 6.66 m to -0.15 m between 31.5 km and 18.1 km with a slope of $\sim 0.46 \text{ m km}^{-1}$. River slope increased to

1.1 m km⁻¹ between 30.5 km and 30.0 km and to 0.79 m km⁻¹ between 29.5 km and 29.2 km, but decreased to 0.2 m km⁻¹ between 24.7 km and 23.7 km before levelling out to -0.01±0.06 m downstream of 18.1 km. Groundwater elevations neighbouring the Tambo River were the highest in August 2011 ranging from 8.86 m at Bruthen to 3.63 m at Kelly Creek. Elevations were the lowest in April 2011 ranging from 7.51 m at Bruthen to 3.15 m at Kelly Creek. Hydraulic gradients at Bruthen were towards the Tambo River (positive) in all campaigns except August 2011. Hydraulic gradients ranged from -0.018 (August 2011) to 0.112 (March 2012), with an average gradient of 0.027±0.019 (Fig. 5d). Hydraulic gradients at Tambo Upper were towards the river during all campaigns, ranging from 0.001 in August 2011 to 0.075 March 2012, with an average gradient of 0.033±0.013. The hydraulic gradient at Kelly Creek in February was 0.013.

Parameter	Apr-10	Sep-10	Feb-11	Apr-11	Aug-11	Mar-12
Q _u (m ³ day ⁻¹)	60,473	305,115	152,516	188,493	7,328,592	1,249,945
Q _d (m ³ day ⁻¹)	65,978	354,034	178,316	201,032	7,869,027	1,393,043
P (m ³ day ⁻¹)	238	0	4,093	3,378	119	40
E (m ³ day ⁻¹)	1,033	1073	1,974	636	636	1,788
I (m ³ day ⁻¹)	6,300	49,992	2,3681	9,797	540,952	144,846

Table 2. Parameters used for calculating the net groundwater flux (I_N) by differential flow gauging using eqn. 1.

2.3.3 Temperature and EC surveys

Results from the temperature/EC surveys on the Tambo River are illustrated in Fig. 5. The temperature of river water in February increased from 21.6 °C at 31.5 km to 25.0 °C at 7.7 km (Fig. 5b). Groundwater temperatures near the Tambo River at this time were ~15.5 °C at Bruthen, increasing to ~16.5 °C at Kelly Creek. Temperature increase was generally gradual in the Tambo River between 31.5 km and 15.6 km (~0.11 °C km⁻¹). River temperature however remained constant at ~20.0 °C between 29.9 km and 28.7 km. Temperature also remained constant at ~23.2 °C between 20.5 and 18.9 km, and declined

from 22.8 °C to 22.5 °C between 24.8 km and 24.0 km. Higher rates of temperature increase occurred between 26.6 km and 25.8 km (~ 0.5 °C km⁻¹) and between 21.5 and 21.4 km (~ 7 °C km⁻¹). Downstream of 15.6 km the River became estuarine and temperatures more variable, ranging from 23 °C to 25 °C with a drop in temperature of >1.0 °C between 13.2 km and 11.8 km. River EC values in February ranged from 112 to 9,270 $\mu\text{S cm}^{-1}$ with a sharp increase from 120 to 645 $\mu\text{S cm}^{-1}$ between 16 and 15 km, indicating the mixing of fresh water with estuarine water. EC's changed very little between 31.5 and 15 km (from 114 to 150 $\mu\text{S cm}^{-1}$) and increased variably to $>9,270$ $\mu\text{S cm}^{-1}$ downstream of 15 km. Groundwater EC during February 2011 ranged from 145 to 260 $\mu\text{S cm}^{-1}$ at Bruthen, from 2,200 to 2,400 $\mu\text{S cm}^{-1}$ at Tambo Upper and was 7,080 $\mu\text{S cm}^{-1}$ at Kelly Creek.

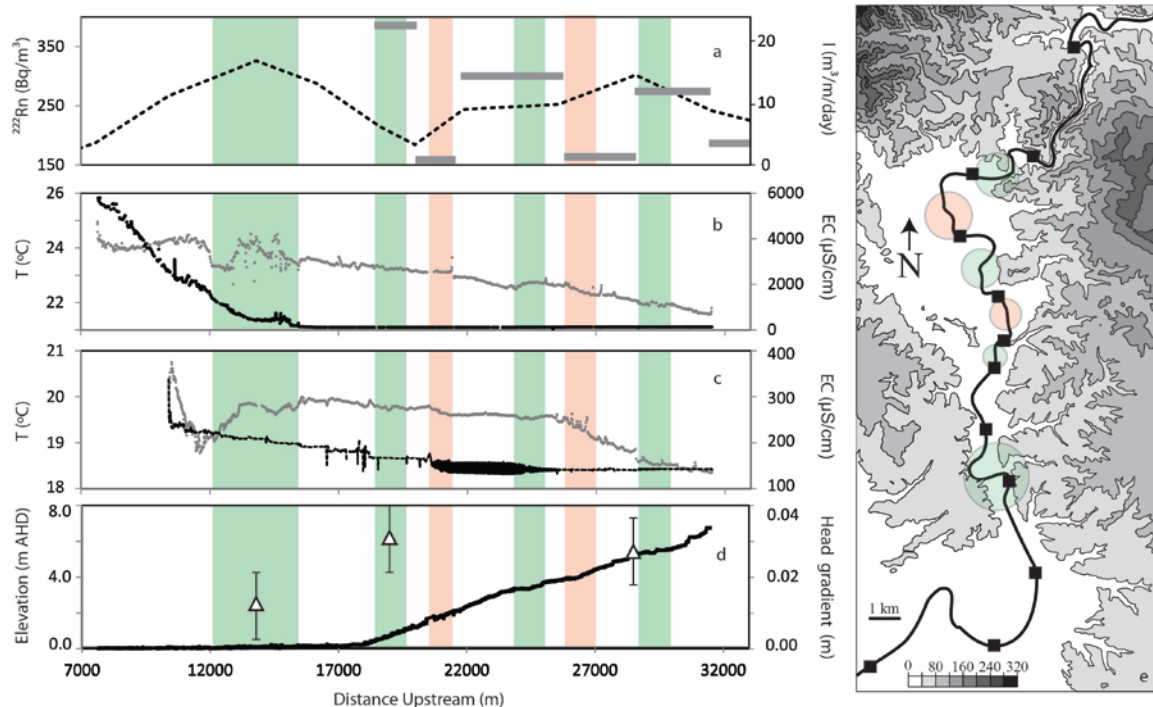


Figure 5. Inferred zones of increased groundwater discharge (green shading) and decreased groundwater discharge (red shading) on the Tambo River as indicated by; (a) Average ^{222}Rn activities (dashed line) and average groundwater fluxes by ^{222}Rn mass balance (grey bars), temperature (grey dots) and EC (black dots) profiles from February 2011 (b) and March 2012 (c), average groundwater – surface water gradients (triangles) surface water elevation (black line) (d), and local topography (e).

Surface and groundwater temperatures were less variable in March 2012, with groundwater increasing from ~15.3 °C at Bruthen to ~15.5 °C at Kelly Creek and river water ranging from 18.4 °C to 20.1 °C. River temperature remained at ~18.5 °C between 30.1 km and 29.2 km (Fig. 5c) before increasing irregularly to 19.6 °C between 29.2 and 25.5 km. Temperatures then declined to 19.4 °C between 25.5 and 24.3 km before stabilizing at 19.5±0.1 °C between 24.3 km and 21.1 km.

River temperature then increased to 19.8 °C between 21.1 km and 20.3 before stabilizing at 19.8±0.1 °C between 20.3 and 15.8 km. Downstream of 15.8 km temperature increased variably as the river became estuarine, with an initial drop in temperature from 19.8 to 18.8 °C between 13.7 and 11.7 km. River EC during March 2012 ranged from 141 to 195 $\mu\text{S cm}^{-1}$ between 40.4 and 20.1 km before increasing variably to 338 $\mu\text{S cm}^{-1}$ downstream of 16 km. Groundwater EC in March 2012 ranged from 140 to 290 $\mu\text{S cm}^{-1}$ at Bruthen, from 1,650 to 1,850 $\mu\text{S cm}^{-1}$ at Tambo Upper and was 3,410 $\mu\text{S cm}^{-1}$ at Kelly Creek.

2.3.4 Chloride concentrations

Cl concentrations in the Tambo River follow a similar trend to EC values from EC/temperature surveys (Fig. 6), with lower Cl concentrations increasing gradually in the upstream reaches (between 40.4 and 20.0) km and more significant increases between 20.0 km and Lake King as the river becomes estuarine. Upstream Cl concentrations were the lowest in April 2011 and the highest in April 2010, with concentration ranges of 3.58 to 4.14 mg L^{-1} and 13.43 to 18.94 mg L^{-1} , respectively. The interface between fresh upstream water and saline lake water varied considerably in the Tambo River.

Under low flow conditions in April 2010, Cl concentrations increased from 25.5 to 10,700 mg L^{-1} between 18.6 and 16.2 km, but under high flow conditions in August 2011, Cl concentrations were 33.0 mg L^{-1} at 7.5 km and 4,030 mg L^{-1} at Lake King.

Similar trends were observed on the Nicholson River, with Cl concentrations increasing from 15.1 to 4,950 mg L⁻¹ between 21.2 and 15.3 km in April 2010, and from 53.2 to 4,030 mg L⁻¹ between 3.2 km and Lake King in August 2011 (Fig. 7). Upstream Cl concentrations in the Nicholson River were also lower in April 2011 and higher during April 2010, with minimum Cl concentrations of 6.43 and 15.14 mg L⁻¹, respectively.

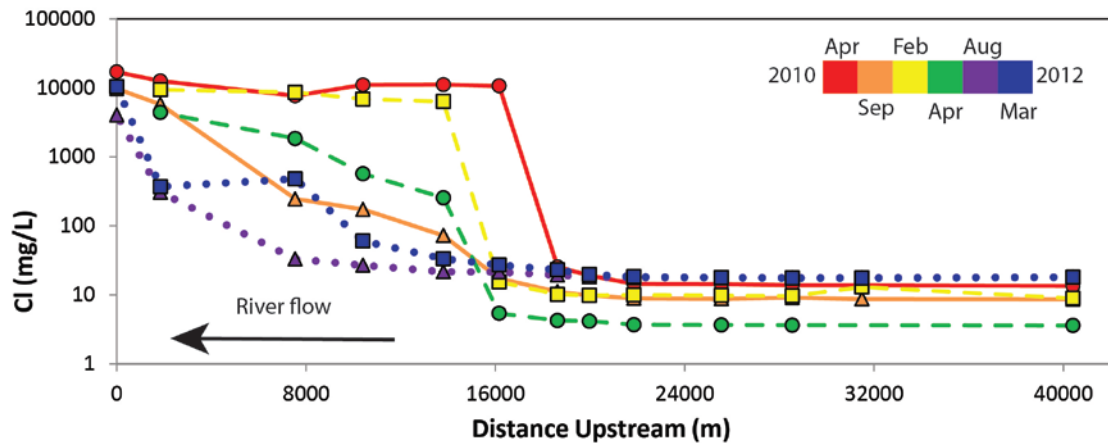


Figure 6. Distribution of Cl concentrations in water sampled from the Tambo River over the study period. Apr 2010 = solid line with circles, Sep 2010 = solid line with triangles, Feb 2011 = dashed line with squares, Apr 2011 = dashed lines with circles, Aug 2011 = dotted line with triangles, Mar 2012 = dotted line with squares.

Cl concentrations in groundwater at Bruthen were the highest during March 2012, with a range of 17.8 to 23.4 mg L⁻¹. Average Cl concentrations at this location were the lowest during April 2011, with a range of 6.75 to 10.3 mg L⁻¹. Concentrations at Tambo Upper were significantly higher than Bruthen, with concentrations ranging between 385 mg L⁻¹ and 599 mg L⁻¹ over the study period. Concentrations at Tambo Upper were generally higher in February 2011 (563±11.7 mg L⁻¹) and lower in March 2012 (464±112 mg L⁻¹). Concentrations at Kelly Creek were higher than at Tambo Upper, ranging from 474 mg L⁻¹ in April 2011 to 598 mg L⁻¹ in March 2012.

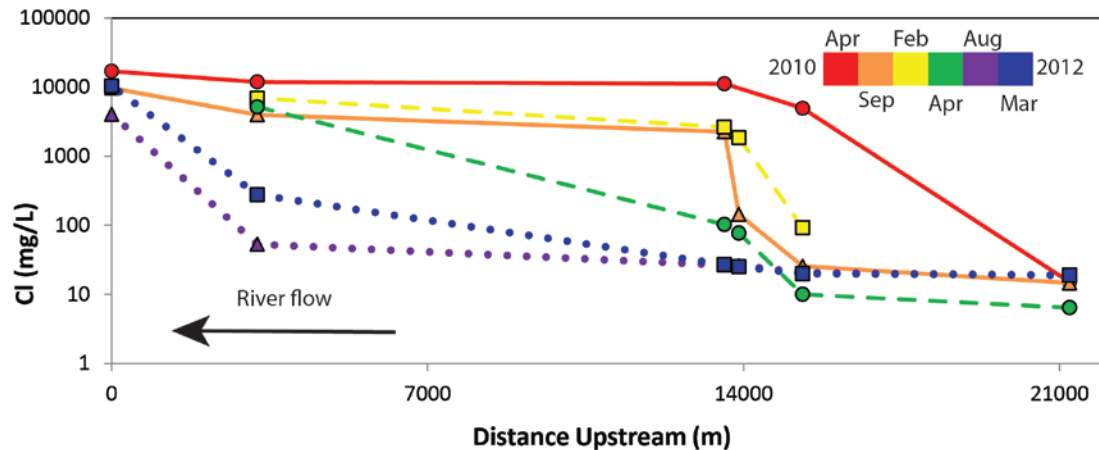


Figure 7. Distribution of Cl concentrations in water sampled from the Nicholson River over the study period. Apr 2010 = solid line with circles, Sep 2010 = solid line with triangles, Feb 2011 = dashed line with squares, Apr 2011 = dashed lines with circles, Aug 2011 = dotted line with triangles, Mar 2012 = dotted line with squares.

2.3.5 Groundwater fluxes

2.3.5.1 ^{222}Rn mass balance

Groundwater fluxes were calculated using Eq. (2). River discharge (Q) for the Tambo River was based on interpolation between discharge at the Ramrod Creek (40.4 km) and Battens Landing (20 km) flow gauging stations, while Q for the Nicholson River uses the discharge at the Sarsfield gauging station at 15.3 km. As flow gauging did not occur in the river estuaries where river discharge will vary tidally, groundwater fluxes were not calculated where EC data indicates estuarine conditions. Calculations are based on the average ^{222}Rn activity of groundwater (C_i) measured in each sampling round at Bruthen and Tambo Upper (total = 5 bores). Groundwater from these bores are located in the upstream reaches for which groundwater fluxes have been calculated and has ^{222}Rn activities that are within $2,000 \text{ Bq m}^{-3}$ of the average of the sediment ingrowth experiments (Table. 1).

Groundwater fluxes for a given reach are calculated using the average depth, width and gas transfer velocities for that reach. The flux of ^{222}Rn from the hyporheic zone (F_h) of the Tambo River is estimated using Eq. (4). Groundwater fluxes (I) of $0 \text{ m}^3 \text{ m}^{-1}$

day^{-1} were calculated by Cl and ^{222}Rn mass balance between 21.9 km and 20.0 km in February 2011 (Figs 8 and 9). At that time there is little change in ^{222}Rn activities along this stretch of river (i.e., $dc_r/dx \sim 0$). Using $k = 1.16 \text{ day}^{-1}$, $E = 5 \times 10^{-3} \text{ m day}^{-1}$ (Bureau of Meteorology, 2012) and $C_r = 150 \text{ Bq m}^{-3}$ yields $F_h = 5,440 \text{ Bq m}^{-1}\text{day}^{-1}$. A similar calculation was made for the Nicholson River for April 2011. Cl and ^{222}Rn mass balance for the stretch between 13.6 and 3.2 km yielded $I = 0 \text{ m}^3 \text{ m}^{-1}\text{day}^{-1}$ and again there is little change in ^{222}Rn activities. For $k = 0.1 \text{ m day}^{-1}$, $E = 5 \times 10^{-3} \text{ m day}^{-1}$ and $C_r = 102 \text{ Bq m}^{-3}$, $F_h = 7,610 \text{ Bq m}^{-1}\text{day}^{-1}$. The river morphology and stream bed sediment of these sections are representative of the Tambo and Nicholson Rivers and likely to accurately represent F_h to the rivers. It is possible however that F_h will vary over time and location as a function of river slope and I . The uncertainties associated F_h are discussed further in section 4.2.

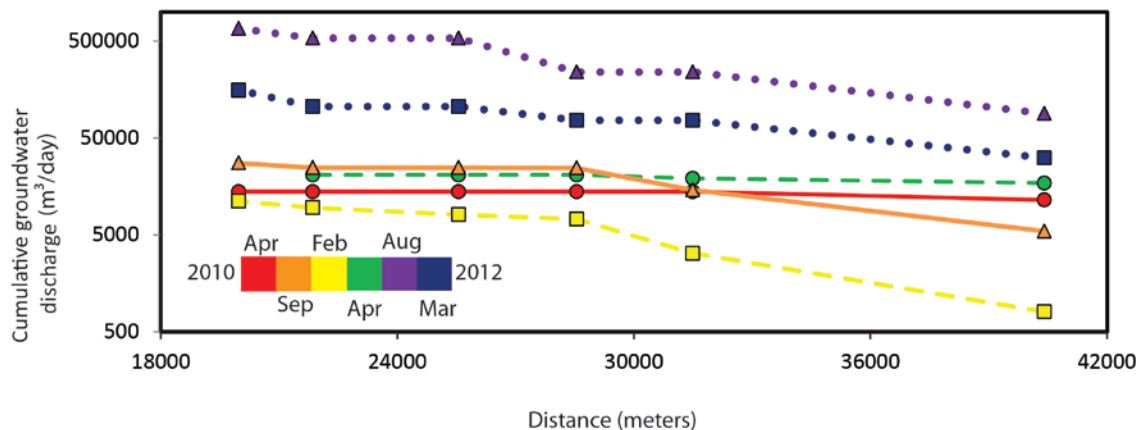


Figure 8. Cumulative groundwater discharge to the Tambo River from ^{222}Rn mass balance. Apr 2010 = solid line with circles, Sep 2010 = solid line with triangles, Feb 2011 = dashed line with squares, Apr 2011 = dashed lines with circles, Aug 2011 = dotted line with triangles, Mar 2012 = dotted line with squares.

Total groundwater discharge between 40.4 and 18.6 km on the Tambo River ranged from $9,660$ to $24,700 \text{ m}^3 \text{ day}^{-1}$ between April 2010 and April 2011 (Fig. 8). This reflects between 21.4 and 10.5% of river discharge under low flow conditions (April 2010 and 2011, respectively), and between 6.83 and 7.44% of river discharge under intermediate flow conditions (September 2010 and February 2011, respectively). Under higher flow conditions during August 2011 and March 2012, groundwater discharge

ranged from 535,000 to 105,000 m³ day⁻¹ (Fig. 8), representing 12.7 and 8.2 % of river discharge, respectively. Groundwater fluxes were generally higher between 31.5 and 28.5 km in comparison to other reaches. Between April 2010 and April 2011 fluxes to this section ranged from 0 to 3.3 m³ m⁻¹day⁻¹, increasing to 50.1 and 15.3 m³ m⁻¹day⁻¹ during August 2011 and March 2012, respectively. Groundwater fluxes were generally lower between 21.9 and 20.0 km, with fluxes of 0 m³ m⁻¹day⁻¹ during all periods except February 2011 (0.78 m³ m⁻¹day⁻¹).

Groundwater fluxes were not calculated for the Nicholson River during April 2010 and February 2011 due to tidal forcing in the upper reaches. Total groundwater discharge to the Nicholson River was lower than the Tambo River, ranging from 88.4 m³ day⁻¹ in April 2011 to 32,900 m³ day⁻¹ in August 2012. Similar to the Tambo River, groundwater reflected a higher proportion of river discharge under low flow conditions in September 2010 (18.9%), a lower proportion of river discharge under intermediate flow conditions in April 2011 (<1%) and an intermediate proportion of river discharge under high flow conditions in August 2011 and March 2012 (10.9 and 14.9 %, respectively).

2.3.5.2 Cl mass balance

Groundwater fluxes were estimated from Cl concentrations using Eq. (7). Groundwater fluxes were only calculated for the upstream reaches in which estuarine water did not impact Cl concentrations. Cl mass balance calculations for the Tambo River are based on the average Cl concentrations of groundwater from Bruthen and Tambo Upper, which ranged from 228 to 253 mg L⁻¹. For the Nicholson River, Cl mass balance was conducted between 21.2 km and 13.5 km for all periods except August 2011. Groundwater sampling near the Nicholson River was not possible; however, the regional groundwater near the Nicholson River has similar total dissolved solids (TDS) concentrations to groundwater at Tambo Upper (Department of Environment and Primary

Industries, 2013). Furthermore Cl is the dominant anion in groundwater in this region and its concentration varies regularly with TDS (Water Resources Data Warehouse, 2012). Thus, the Cl concentrations from Tambo Upper have been used to calculate the fluxes along the Nicholson River.

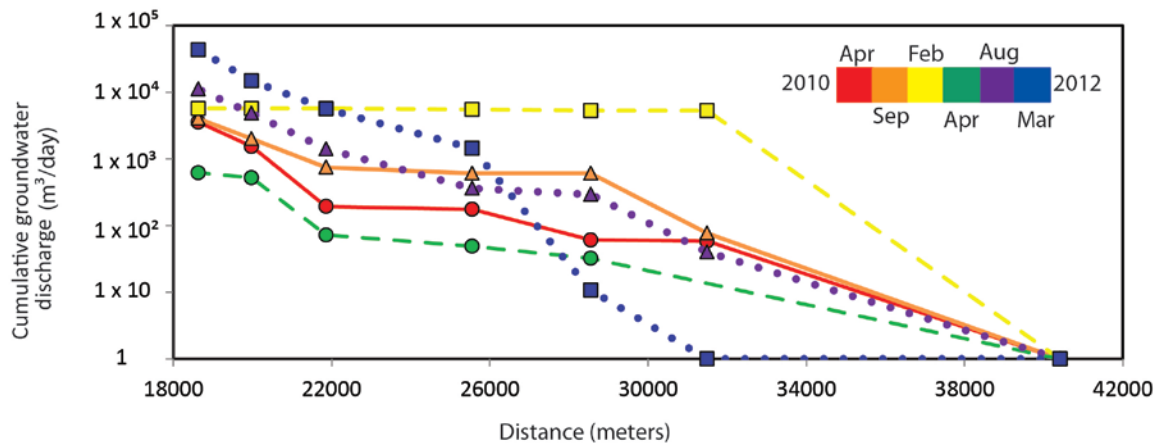


Figure 9. Cumulative groundwater discharge to the Tambo River from Cl mass balance. Apr 2010 = solid line with circles, Sep 2010 = solid line with triangles, Feb 2011 = dashed line with squares, Apr 2011 = dashed lines with circles, Aug 2011 = dotted line with triangles, Mar 2012 = dotted line with squares.

Groundwater fluxes to the Tambo River from Cl mass balance range from 0 to $4.85 \text{ m}^3 \text{ m}^{-1} \text{ day}^{-1}$. Fluxes were generally higher between 21.9 and 20.0 km with an average flux of $1.17 \pm 1.82 \text{ m}^3 \text{ m}^{-1} \text{ day}^{-1}$. Total groundwater discharge by was the highest in March 2012 ($14,800 \text{ m}^3 \text{ day}^{-1}$) and the lowest in April 2011 ($522 \text{ m}^3 \text{ day}^{-1}$) (Fig. 9).

Groundwater constituted the highest proportion of river discharge in April 2010 (2.4%) and the lowest under intermediate flow conditions in September 2010 (0.61%).

Groundwater discharge to the Nicholson River was higher during August 2011 ($38,300 \text{ m}^3 \text{ day}^{-1}$) and September 2011 ($20,900 \text{ m}^3 \text{ day}^{-1}$), and lower during September 2010 ($4,810 \text{ m}^3 \text{ day}^{-1}$) and March 2012 ($3,960 \text{ m}^3 \text{ day}^{-1}$). Groundwater discharge represented the highest proportion of river flow under low flow conditions during September 2010 at 29.4%, compared to high flow conditions in August 2011 and March 2012 in which groundwater constituted less than 7% of total river discharge.

2.4. Discussion

This section focuses on combining chemical and physical methods in order to characterise the distribution of gaining and losing reaches along the Tambo and Nicholson Rivers. The impact of changing meteorological and hydrological conditions as drivers of groundwater fluxes is also investigated. Finally the discrepancies, strengths and weaknesses of different tracer methods are discussed.

2.4.1 Spatial variability of groundwater discharge to the Tambo River

As groundwater temperatures near the Tambo River were lower than river temperatures during the temperature surveys, decreases in river temperature are likely to indicate increased groundwater discharge, while increased river temperature is likely to indicate reduced groundwater discharge (e.g. Becker et al., 2004). Temperature along the Tambo River in both surveys increased steadily between 31.5 and 27.0 km except for a zone at ~29 km where water temperature did not increase (Fig. 5), suggesting increased groundwater discharge. Average ^{222}Rn activities at 28.5 km are the second highest ($302 \pm 100 \text{ Bq m}^{-3}$) of any location on the Tambo River yielding an average groundwater flux of $12.1 \text{ m}^3 \text{ m}^{-1} \text{ day}^{-1}$. Furthermore, groundwater-surface water gradients nearby at Bruthen were towards the river (6.1×10^{-3} to 0.112) during all periods except August 2011, supporting the gaining nature of this stretch. River elevation through this stretch is 5 to 10 m while land areas within 200 m of the river are over 80 m in elevation (Fig. 5e). Such areas of increased topography will likely result in steep hydraulic gradients towards the river (Sophocleous, 2002) and may account for the higher groundwater fluxes.

A decrease in groundwater discharge between 27.0 and 25.5 km is indicated by a general decline in ^{222}Rn activities (Fig. 3) and an average groundwater flux of $0.89 \text{ m}^3 \text{ m}^{-1} \text{ day}^{-1}$ (Fig. 5a). This is supported by an increase in temperature from 22.3 to 22.7°C between 26.8 and 25.8 km in February 2011, and from 19.1 to 19.6°C between 26.8 and

25.4 km in March 2012. This stretch of river flows through extensive floodplains that extend for >2 km from the river (Fig. 5e). Given the subdued topography, it is likely that groundwater head gradients are lower which will reduce groundwater influxes. A similar trend is observed between ~21 km and ~19 km where river temperatures increased from 22.9 to 23.6°C in February 2011, and from 19.5 to 19.8°C in March 2012, suggesting reduced groundwater discharge (Fig. 5b,c). This is again supported by ^{222}Rn mass balance, which gives an average groundwater flux between 21.9 and 20.2 km of $0.13 \text{ m}^3 \text{ m}^{-1} \text{ day}^{-1}$. This is also an area of low topographic variation, with likely lower head gradients (Fig. 5e).

In contrast to these sections, increased topography near the Tambo River at ~25 km correlates with decreased river temperature during both in February 2011 (0.3 °C) and March 2012 (0.2 °C), suggesting increased groundwater discharge. The average groundwater flux from ^{222}Rn mass balance between 25.5 and 21.5 km is also relatively high at $14.8 \text{ m}^3 \text{ m}^{-1} \text{ day}^{-1}$. Similarly, the river section between ~20 km and 19 km is characterised by relatively stable river temperatures and an average groundwater flux of $23.5 \text{ m}^3 \text{ m}^{-1} \text{ day}^{-1}$ (between 20 and 18.6 km). These observations support local topographic variation as a driver of groundwater discharge, with reduced groundwater discharge in regions of wider floodplains and increased groundwater discharge in areas of greater topographic variation (Fig. 5e).

Between ~16 and 6.5 km, EC values increased to $>23,000 \mu\text{S cm}^{-1}$ in February 2011 and $>300 \mu\text{S cm}^{-1}$ in March 2012, indicating the transition into an estuarine setting. In this zone, mixing with warmer lake water (25 to 30 °C, Arnott and McKinnon, 1985) is expected to cause an increase in river temperature; however river temperature declines between 13.5 and 11.5 km, suggesting a zone of increased groundwater discharge. Nevertheless, mixing between lake water and river water through the estuarine fringe is

not always systematic (e.g. MacKay and Schumann, 1990; Nunes Vaz et al., 1989; Stacey et al., 2008), and the decline in river temperature may be an artefact of measuring different water types as they mix variably through the estuarine fringe. While river discharge is not constrained through this reach preventing mass balance calculations, the average ^{222}Rn activities through this zone are the highest of any location on the Tambo River, supporting an increase in groundwater discharge. At 13.8 km the Tambo River is immediately adjacent to a cliff >40 m in elevation. This may again facilitate high groundwater gradients toward the river resulting in higher groundwater inputs.

While ^{222}Rn activities at 13.8 km were the highest of any sample location on the Tambo River, they were also highly variable (between 135 and 526 Bq m⁻³). This variability may reflect the transient nature of the interface between river water and lake water as they mix under tidally driven flow conditions. Furthermore, changing river flow in estuaries over tidal cycles may affect the balance of ^{222}Rn at the estuarine fringe (Santos et al., 2010). Constraining such balances requires further work and is beyond the scope of this paper. While the tidal nature of the lower river sections prevents mass balance calculations, a decline in ^{222}Rn activities through these reaches suggests reduced groundwater fluxes in the lower estuaries. Lower topographic variation through these sections (Fig. 5e) will again provide lower potential for the formation of high groundwater gradients. This is consistent with topographic variation as a driver of groundwater discharge to the Tambo River as asserted above.

2.4.2 Uncertainty analysis

The impact of uncertainties in k on groundwater discharge estimates using ^{222}Rn mass balance calculations was investigated by comparing alternate k values from Eq. (5) and Eq. (6). The Negulescu and Rojanski model generally yields higher k values (and

hence results in higher calculated groundwater fluxes) than the O'Connor and Dobbins model, although this is reversed at low velocities and shallow depths (Fig. 10).

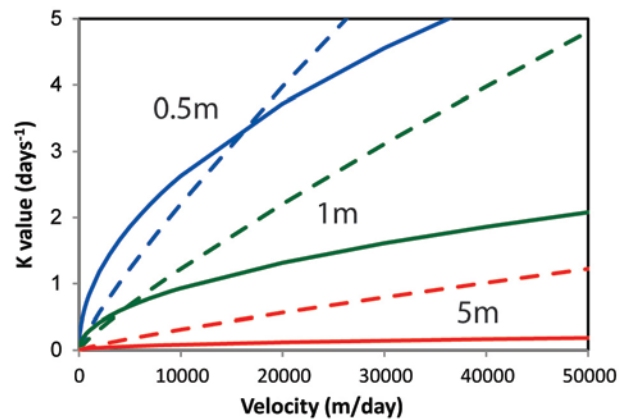


Figure 10. K values from O'Connor and Dobbins (solid lines) and Negulescu and Rohanski (dashed lines) models at 0.5m (blue), 1m (green) and 5m depth (red) with increasing river velocities.

This is demonstrated by the cumulative groundwater discharge estimates to the Tambo River, which were higher using Eq. (5) under low flow conditions during April 2010 and February 2011, but lower during higher flow conditions from other sampling periods. Systematic trends in k values under changing flow conditions are less apparent on the Nicholson River, as river velocity is less variable and changes in river width and depth downstream have a greater impact on the the k values. The difference in the cumulative groundwater discharge to the Nicholson River calculated using Eq. (5) and (6) ranged from 3.1 to 44% with an average difference of $20 \pm 17\%$. For the Tambo River these differences ranged from 2.5 to 48% with an average difference of $30 \pm 16\%$. The variability in k is recognised as a source of error in ^{222}Rn mass balance calculations, however it has very little impact the distribution of gaining reaches or seasonal trends in groundwater discharge identified by ^{222}Rn mass balance (Fig. 11).

For both the Tambo and Nicholson Rivers, F_h estimates were made when dc/dx was 0 (within 1 SD of the equipment precision). As the activity of ^{222}Rn in the Tambo and Nicholson Rivers is relatively low, failure to account for F_h will result in overestimations during groundwater flux calculations. On average, failure to account for F_h on the

Tambo River resulted in a 104% increase in groundwater discharge. Excluding April 2011, failure to account for F_h on the Nicholson River results in an average increase in the estimated groundwater discharge by 45%. As ^{222}Rn activities in the Nicholson are particularly low ($<120 \text{ Bq m}^{-3}$) at all locations during April 2011, failure to account for F_h at this time results in nearly a 630% increase in the groundwater discharge estimate. This illustrates the need to account for F_h in streams with lower ^{222}Rn activities where the dc_r/dx term in Eq. (2) is small (c.f., Cook et al., 2006).

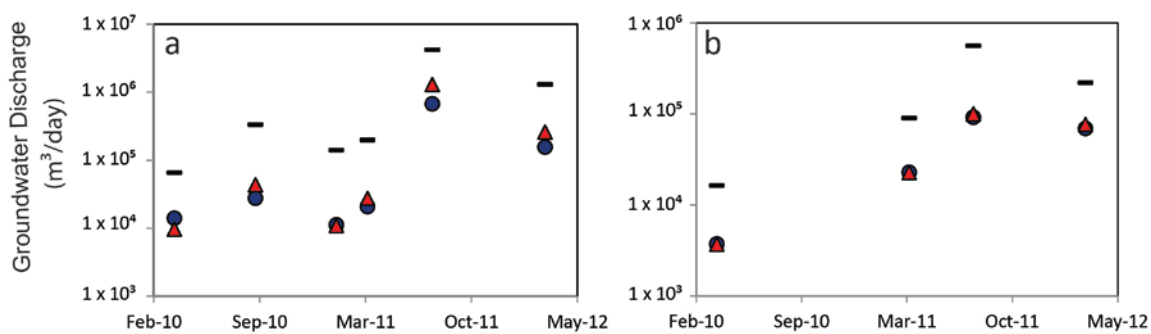


Figure 11. Temporal variations in river discharge (black lines) and groundwater discharge to the Tambo River (a) and Nicholson River (b) given by ^{222}Rn mass balance using O'Connor and Dobbins (blue circles) and Negulescu and Rojanski (red triangles) models of gas transfer.

The variability of C_i represents the greatest source of uncertainty in ^{222}Rn mass balance calculations as C_i values varied by up to 3 orders of magnitude at different locations. As $C_i \gg C_r$ during all sampling periods, a 50% change in C_i will result in an approximate 50% change in I . The sensitivity of the model to C_i is demonstrated by calculating I at one standard deviation from the average C_i values used during mass balance calculations. For example, during February 2011 when C_i was the most varied ($4,600 \pm 2,750 \text{ Bq m}^{-3}$), groundwater discharge to the Tambo River will range from 5,860 to $25,800 \text{ m}^3 \text{ day}^{-1}$ based on C_i values one standard deviation from the mean. This demonstrates the need to accurately assign groundwater end member values. The variability of ^{222}Rn activity in groundwater remains a source of uncertainty when

conducting groundwater studies, and further research in characterising such variability both spatially and temporally would be useful to subsequent studies.

The sensitivity of the Cl mass balance model to Cl_i on the Tambo River was tested by assuming the Cl_i end member was a mixture between groundwater from Bruthen and Tambo Upper, and then varying the weighting between each location. Using Tambo Upper concentrations as the end member reduced groundwater discharge estimates for the stretch by between 39% and 40% during individual sampling periods. Estimates using the Bruthen concentrations as the end member increased estimates by 2 to 4 orders of magnitude during September 2010, February 2011, April 2011 and March 2012 and reduced estimates to 0 during April 2010 and August 2011 periods. Cl_i again represents the greatest source of uncertainty in mass balance calculations given that values vary by up to 3 orders of magnitude between Bruthen and Tambo Upper. Furthermore, C_i is generally similar to C_r in upstream reaches, making Cl mass balance calculations very sensitive to variations in C_i , as opposed to ^{222}Rn mass balance calculations where $C_i \gg C_r$. This again highlights the need for accurate characterisation of groundwater end members.

2.4.3 Method comparison

While similar temporal trends in groundwater discharge to the Tambo River (i.e. increased groundwater discharge under high flow conditions) were identified by differential flow gauging, Cl mass balance and ^{222}Rn mass balance, estimates from Cl mass balance were generally 1 to 2 orders of magnitude lower than those from ^{222}Rn mass balance or differential flow gauging (Fig. 12). It is likely that some discrepancies between the tracer methods results from uncertainties in groundwater end member characterisation, and the sensitivity of the mass balance models to this parameter. It has been shown that interaction between groundwater and surface water near rivers is likely

to increase the variability of groundwater chemistry near rivers, making accurate characterisation of the groundwater end member difficult (Lambs, 2004; McCallum, 2010). For example, infiltration of river water into the banks at high river discharges may result in near-river groundwater having lower Cl concentrations than the regional groundwater. This would result in the fluxes from Cl mass balance being too low (McCallum, 2012). Bank infiltration will vary as a function of river morphology, aquifer characteristics and changing flow conditions (Chen and Chen, 2003; Chen et al., 2006; Lambs, 2004; McCallum et al., 2010; Woessner, 2000) and is difficult to characterise accurately. While this study sampled near-river groundwater, it is possible that the near-river groundwater along the Tambo River has variable Cl concentrations, resulting in a level of uncertainty in the characterisation of groundwater end members.

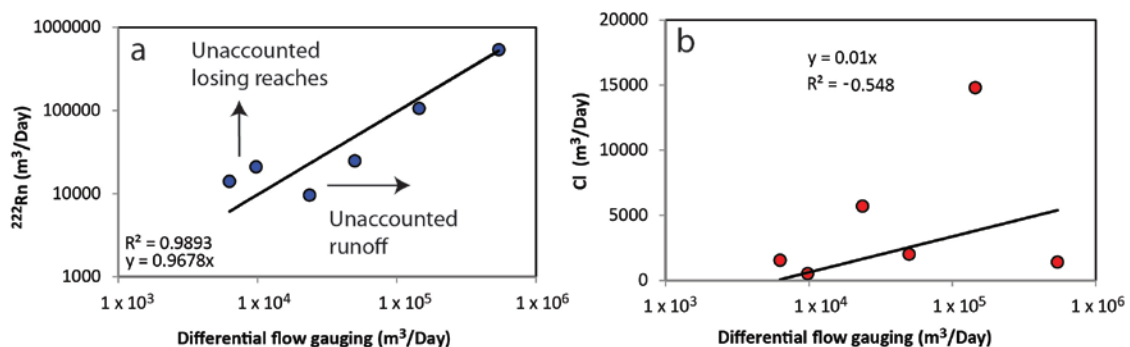


Figure 12. Groundwater discharge to the Tambo River by differential flow gauging (x axis) versus groundwater discharge given by ²²²Rn mass balance (a) and Cl mass balance (b).

Discrepancies between the Cl and ²²²Rn mass balances may also reflect the discharge of relatively young groundwater that has been stored for a period of weeks, either as recently infiltrated rainfall, bank return flow or parafluvial flow (McCallum et al., 2010; Woessner, 2000). Chemically, such groundwater would have low Cl concentrations but elevated ²²²Rn activities through ingrowth (Cartwright et al., 2011). Cook (2012) makes the point that variations in groundwater Cl concentrations will be greater than ²²²Rn activities as a function of such processes. Under these conditions,

groundwater estimates from ^{222}Rn mass balance will more closely reflect the total volume of groundwater entering the river, whereas Cl mass balance will more closely reflect the volume of regional groundwater entering the river. This may account for the agreement between groundwater inflows from differential flow gauging and ^{222}Rn mass balance but the poor agreement between differential flow gauging and Cl mass balance (Fig. 12).

While there is a strong correlation between groundwater discharge estimates from ^{222}Rn mass balance and differential flow gauging, estimates from ^{222}Rn mass balance are greater than those from differential flow gauging during April 2010 and April 2011 (Fig. 12). As ^{222}Rn mass balance will account for the total groundwater discharge, compared to differential flow gauging which accounts for the net groundwater discharge (inflow-outflow), this discrepancy may result from the presence of losing reaches. Sampling during April 2010 and April 2011 occurred after dry periods when the water table was low and losing reaches are more likely to develop (Fig. 13a). In contrast, groundwater discharge estimates during February 2011 given by differential flow gauging were greater than ^{222}Rn mass balance. This discrepancy is likely to reflect unaccounted runoff during increased rainfall in the catchment in the days leading up to sampling (Fig. 13b).

In contrast to the Tambo River, Cl and ^{222}Rn mass balance give groundwater discharge estimates generally on the same order of magnitude for the Nicholson River, with discharge by Cl mass balance ranging from 654 to 38,300 $\text{m}^3 \text{day}^{-1}$ and discharge by ^{222}Rn mass balance ranging from 88.4 to 61,100 $\text{m}^3 \text{day}^{-1}$. While groundwater near the Tambo River was used to characterise groundwater entering the Nicholson River, these results suggest that the groundwater end members used for mass balance calculations on the Nicholson River reasonably characterise the groundwater entering the Nicholson River. It also implies that groundwater-surface water interaction along the Nicholson

River is less variable than the Tambo River. Under such conditions, uncertainties associated with groundwater characterisation will be reduced.

These results not only highlight the importance of accurately characterising groundwater chemistry for mass balance calculations, but also emphasize the need for groundwater characterisation both regionally and at a high spatial resolution proximal to river systems. This is because near river groundwater (which is the water that enters rivers) may have a different and more variable chemistry than regional groundwater.

2.4.4 Hydrological drivers

Groundwater discharge to both the Tambo and Nicholson Rivers increased with river discharge. Sampling during high flow periods occurred in the days to weeks following peak flow conditions and is likely to reflect a period in which river discharge is receding while groundwater levels remain high from recharge. Under these conditions high groundwater gradients can form, resulting in increased groundwater discharge (Fig. 13c,f). These results indicate that during high rainfall periods, groundwater levels in the Tambo Catchment can increase quickly enough to maintain a groundwater fraction of ~10% in the Nicholson and Tambo Rivers around 1 week after flooding (e.g. Cey et al., 1998). This indicates that the sand-rich Tertiary and Quaternary aquifers of the region are responsive to rainfall.

While the total groundwater discharge to the Tambo and Nicholson Rivers was highest under high flow conditions, groundwater constituted the highest proportion of river flow under low flow conditions (Fig. 13a,d). For the Tambo River this occurred during April 2010, with groundwater discharge by ^{222}Rn mass balance representing 21.4% of total river flow. For the Nicholson River, this occurred during September 2010, with groundwater discharge by ^{222}Rn mass balance constituting 18.9% of river flow. Conversely, groundwater constituted the lowest proportion of river flow under

intermediate flow conditions. This occurred during February 2011 on the Tambo River, with groundwater discharge by ^{222}Rn mass balance constituting 6.8% of river discharge. For the Nicholson River this occurred during April 2011, with groundwater discharge by ^{222}Rn mass balance constituting <1% of river discharge. Both of these sampling campaigns took place during a time of increased rainfall (~35mm of rainfall in the 4 days leading up to sampling) that followed an extended dry period. As such, it is likely that these periods represent conditions in which the water table was still low while river levels were increasing due to runoff, which would result in reduced groundwater discharge (Fig. 13 b,e).

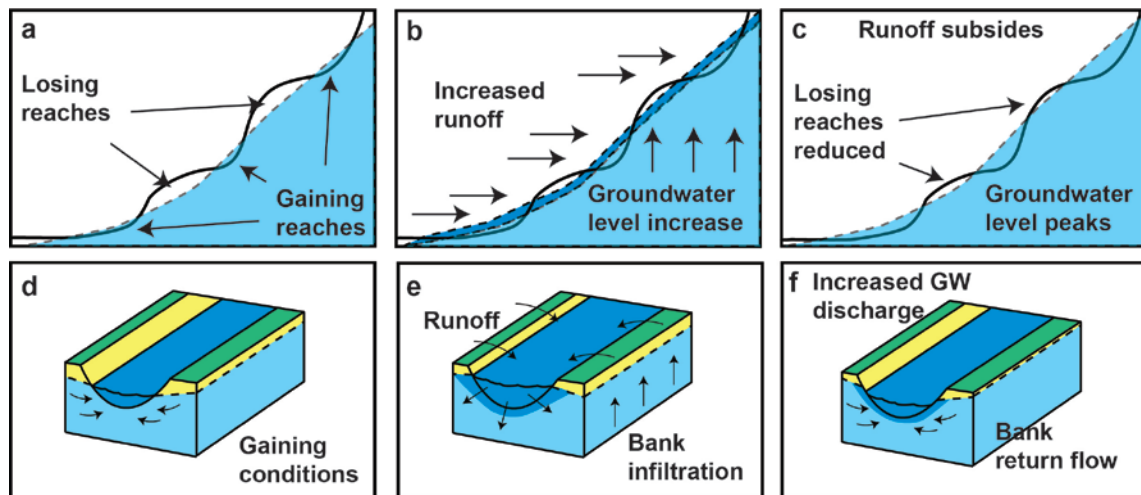


Figure 13. Schematic representation of the Tambo River profile (solid line), water table (dashed line/light blue shading) and runoff (dark blue shading) under baseflow conditions (a), high flow conditions (b) receding conditions (c). River cross sections shown in (d), (e), (f) for baseflow, high flow and recession, respectively.

This study shows that while two rivers within the same aquifer system may vary considerably with respect to discharge volumes, groundwater may still represent a similar proportion of the total river discharge in each case. Further to this, when two rivers occur in the same aquifer system, they are likely to respond similarly under changing rainfall and flow conditions; with relatively low volumes of groundwater providing a high proportion of river discharge under base flow conditions, rainfall and runoff providing a higher proportion of river discharge during increased rainfall following dry periods, and

higher volumes of groundwater representing an intermediate proportion of river flow in the weeks following extensive rainfall in the catchment. This suggests that the lower discharge volumes associated with the Nicholson River are likely to represent the smaller catchment area from which its flow is derived, as opposed to differences in groundwater-surface water interaction.

2.5 Conclusions

By combining the use of chemical and physical tracer methods on the Tambo River, increased groundwater influxes were identified near areas of increased topographic variation, where the potential for higher groundwater-surface water gradient formation is increased. The highest volume of groundwater discharge occurred in the days to weeks following heavy rainfall, when river levels were receding and groundwater levels remained high. Groundwater formed the highest proportion of river discharge under baseflow conditions, while rainfall and runoff formed a higher proportion of river flow during periods of increased rainfall that followed from dry periods in the catchment. Discrepancies between ^{222}Rn and Cl mass balance suggest that spatially variable bank exchange processes can amplify the heterogeneity of Cl in groundwater neighbouring rivers, while the equilibration between ^{222}Rn in aquifer sediments with groundwater can reduce the heterogeneity of ^{222}Rn in groundwater. Under these circumstances, extensive spatial groundwater sampling is required to accurately characterise the groundwater Cl end member. The impact of water exchange between rivers and groundwater on tracers at the bank scale is a process that is still poorly defined, and further investigation into these processes may prove particularly useful in the interpretation of tracer data during future groundwater-surface water studies.

Acknowledgements

We would like to thank Massimo Raveggi and Rachelle Pierson for their help with major ion analyses. Funding for this research was provided by the National Centre for Groundwater Research and Training, and Australian Government initiative, supported by the Australian Research Council and the National Water Commission.

References

- Anderson, M. P.: Heat as a ground water tracer, *Ground Water*, 43, 951–968, 2005.
- Andersen, M. S. and Acworth, R. I.: Stream-aquifer interactions in the Maules Creek catchment, Namoi Valley, New South Wales, Australia, *Hydrogeol. J.*, 17, 2005–2021, 2009.
- Anibas, C., Fleckenstein, J. H., Volze, N., Bius, K., Verhoeven, R., Meire, P., and Batelaan, O.: Transient or steady-state? Using vertical temperature profiles to quantify groundwater– surface water exchange, *Hydrol. Process.*, 23, 2165–2177, 2009.
- Anibas, C., Buis, K., Verhoeven, R., Meire, P., and Batelaan, O.: A simple thermal mapping method for seasonal spatial patterns of groundwater–surface water interaction, *J. Hydrol.*, 397, 93–104, 2011.
- Arnott, G. H. and McKinnon, A. D.: Distribution and abundance of eggs of the anchovy, in relation to temperature and salinity in the Gippsland Lakes, *Mar. Freshwater Res.*, 36, 433–439, 1985.
- Becker, M. W., Georgian, T., Ambrose, H., Siniscalchi, J., and Fredrick, K.: Estimating flow and flux of ground water discharge using water temperature and velocity, *J. Hydrol.*, 296, 221–233, 2004.
- Boano, F., Revelli, R., and Ridolfi, L.: Bedform-induced hyporheic exchange with unsteady flows, *Adv. Water Resour.*, 30, 148–156, 2007.
- Boulton, A.: Stream ecology and surface-hyporheic hydrologic exchange: implications, techniques and limitations, *Mar. Freshwater Res.*, 44, 553–564, 1993.
- Bureau of Meteorology: Commonwealth of Australia, available at: <http://www.bom.gov.au> (last access: 11 January 2013), 2012.
- Burnett, W. C. and Dulaiova, H.: Radon as a tracer of submarine groundwater discharge into a boat basin in Donnalucata, Sicily, *Cont. Shelf Res.*, 26, 862–873, 2006.
- Burnett, W. C., Peterson, R., Moore, W. S., and de Oliveira, J.: Radon and radium isotopes as tracers of submarine groundwater discharge – results from the Ubatuba, Brazil SGD assessment intercomparison, *Estuar. Coast. Shelf S.*, 76, 501–511, 2008.
- Burnett, W. C., Peterson, R., Santons, I. R., Hicks, R. W.: Use of automated radon measurements for rapid assessment of groundwater flow into Florida streams, *J. Hydrol.*, 380, 298–304, 2010.

- Cartwright, I., Weaver, T. R., and Tweed, S. O.: Integrating physical hydrogeology, hydrochemistry, and environmental isotopes to constrain regional groundwater flow: Southern Riverine Province, Murray Basin, Australia, in: International Association of Hydrogeologists Special Publication 11, Groundwater Flow Understanding from Local to Regional Scale, edited by: Carrillo, R. J. J. and Ortega, G. M. A., Taylor and Francis, London, UK, 10–134, 2008.
- Cartwright, I., Weaver, T. R., Simmons, C. T., Fifield, L. K., Lawrence, C. R., and Chisari, R.: Physical hydrogeology and environmental isotopes to constrain the age, origins, and stability of a low-salinity groundwater lens formed by periodic river recharge: Murray Basin, Australia, *J. Hydrol.*, 380, 203–221, 2010.
- Cartwright, I., Hofmann, H., Sirianos, M. A., Weaver, T. R., and Simmons, C. T.: Geochemical and ^{222}Rn constraints on baseflow to the Murray River, Australia, and timescales for the decay of low-salinity groundwater lenses, *J. Hydrol.*, 405, 333–343, 2011.
- Cey, E. E., Rudolph, D. L., and Parkin, G. W., Aravena, R.: Quantifying groundwater discharge to a small perennial stream in southern Ontario, Canada, *J. Hydrol.*, 210, 21–37, 1998.
- Chaplin, H. J.: Eastern Victoria Water Table Aquifers, Groundwater Beneficial Use Map Series, Department of Conservation and Natural Resources, available at: <http://www.water.vic.gov.au/> (last access: 20 March 2013), 1995.
- Chen, X., and Chen, X.: Stream water infiltration, bank storage, and storage zone changes due to stream-stage fluctuations, *J. Hydrol.*, 280, 246–264, 2003.
- Chen, X., Chen, D. Y., and Chen, X.: Simulation of baseflow accounting for the effect of bank storage and its implication in baseflow separation, *J. Hydrol.*, 327, 539–549, 2006.
- Corbett, D. R., Burnett, W. C., Cable, P. H., and Clark, S. B.: A multiple approach to the determination of radon fluxes from sediments, *J. Radioanal. Nucl. Ch.*, 236, 247–252, 1998.
- Cook, P. G.: Estimating groundwater discharge to rivers from river chemistry surveys, *Hydrol. Process.*, online first, doi:10.1002/hyp.9493, 2012.
- Cook, P. G., Favreau, G., Dighton, J. C., and Tickell, S.: Determining natural groundwater influx to a tropical river using radon, chlorofluorocarbons and ionic environmental tracers, *J. Hydrol.*, 277, 74–88, 2003.
- Cook, P. G., Lamontagne, S., Berhane, D., and Clark, J. F.: Quantifying groundwater discharge to Cockburn River, southeastern Australia, using dissolved gas tracers Rn-222 and SF_6 , *Water Resour. Res.*, 42, W10411, doi:10.1029/2006WR004921, 2006.
- Cox, M. H., Su, G. W., and Constantz, J.: Heat, Chloride, and Specific Conductance as Ground Water Tracers near Streams, *Ground Water*, 45, 187–195, 2007.
- Department of Agriculture, Fisheries and Forestry: available at: http://adl.brs.gov.au/water2010/pdf/catchment_223_0_summary.pdf (last access: 19 November 2012), 2006.
- Department of Environment and Primary Industries: available at: <http://vro.dpi.vic.gov.au/dpi/vro/vrosite.nsf/pages/water-gw-quality-quantity> (last access: 5 July 2013), 2013.
- Durand, P., Neal, M., and Neal, C.: Variations in stable oxygen isotope and solute concentrations in small submediterranean montane streams, *J. Hydrol.*, 144, 283–290, 1993.

- Ellins, K. K., Roman-Mas, A., and Lee, R.: Using ^{222}Rn to examine groundwater/surface discharge interaction in the Rio Grande de Manati, Puerto Rico, *J. Hydrol.*, 115, 319–341, 1990.
- Genereux, D. P. and Hemond, H. F.: Naturally occurring Radon 222 as a tracer for streamflow generation: steady state methodology and field example, *Water Resour. Res.*, 26, 3065–3075, 1990.
- Genereux, D. P. and Hemond, H. F.: Determination of gas exchange rate constants for a small stream on Walker Branch Watershed, Tennessee, *Water Resour. Res.*, 28, 2365–2374, 1992.
- Genereux, D. P., Hemond, H. F., and Mulholland, P. J.: Use of radon-222 and calcium as tracers in a three-end-member mixing model for streamflow generation on the West Fork of Walker Branch Watershed, *J. Hydrol.*, 142, 167–211, 1993.
- Gilfedder, B. S., Hofmann, H., and Cartwright, I.: Novel instruments for in situ continuous Rn-222 measurement in groundwater and the application to river bank infiltration, *Environ. Sci. Technol.*, 47, 993–1000, 2012.
- Harte, P. and Kiah, R.: Measured river leakages using conventional streamflow techniques: the case of Souhegan River, New Hampshire, USA, *Hydrogeol. J.*, 17, 409–424, 2009.
- Herczeg, A. L., Torgersen, T., Chivas, A. R., and Habermehl, M. A.: Geochemistry of groundwaters from the Great Artesian Basin, Australia, *J. Hydrol.*, 126, 225–245, 1991.
- Hofmann, H., Gilfedder, B. S., and Cartwright, I.: A novel method using a silicone diffusion membrane for continuous ^{222}Rn measurements for the quantification of groundwater discharge to streams and rivers, *Environ. Sci. Technol.*, 45, 8915–8921, 2011.
- Isotope Hydrology Information System: The ISOHIS Database, available at: <http://www.iaea.org/water/> (last access: 18 November 2012), 2012.
- Jolly, R. L.: Bairnsdale, 1 : 250000 Geological Map Series, Department of Natural Resources and Environment, MDC Fitzroy, Victoria, 3065, 1997.
- Kalbus, E., Reinstorf, F., and Schirmer, M.: Measuring methods for groundwater – surface water interactions: a review, *Hydrol. Earth Syst. Sci.*, 10, 873–887, doi:10.5194/hess-10-873-2006, 2006.
- Kasahara, T. and Wondzell, S. M.: Geomorphic controls on hyporheic exchange flow in mountain streams, *Water Resour. Res.*, 39, 1005, doi:10.1029/2002WR001386, 2003.
- Krause, S., Bronstert, A., and Zehe, E.: Groundwater – surface water interactions in a North German lowland floodplain – implications for the river discharge dynamics and riparian water balance, *J. Hydrol.*, 347, 404–417, 2007.
- Lambs, L.: Interactions between groundwater and surface water at river banks and the confluence of rivers, *J. Hydrol.*, 288, 312–326, 2004.
- Lamontagne, S. and Cook, P. G.: Estimation of hyporheic water residence time in situ using Rn-222 disequilibrium, *Limnol. Oceanogr.-Meth.*, 5, 407–416, 2007.
- Lamontagne, S., Leaney, F. W., and Herczeg, A. L.: Groundwater-surface water interactions in a large semi-arid floodplain: implications for salinity management, *Hydrol. Process.*, 19, 3063–3080, 2005.
- Lamontagne, S., Le Gal La Salle, C., Hancock, G. J., Webster, I. T., Simmons, C. T., Love, A. J., James-Smith, J., Smith, A. J., Ka'mpf, J., and Fallowfield, H. J.: Radium and radon radioisotopes in regional groundwater, intertidal groundwater, and seawater in the Adelaide Coastal Waters Study area: implications for the evaluation of submarine groundwater discharge, *Mar. Chem.*, 109, 318–336, 2008.

- Lerner D, N., Issar A, S., and Simmers, I.: Groundwater recharge, a guide to understanding and estimating natural recharge, International Association of Hydrogeologists, Kenilworth, Rep 8, 1990.
- MacKay, H. M. and Schumann, E. H.: Mixing and circulation in the Sundays river estuary, South Africa, *Estuar. Coast. Shelf S.*, 31, 203–216, 1990.
- Martens, C. S., Kipphut, G. W., and Klump, J. V.: Sediment-water chemical exchange in the coastal zone traced by in situ Radon-222 flux measurements, *Science*, 208, 285–288, 1980.
- McCallum, J. L., Cook, P. G., Brunner, P., and Berhane, D.: Solute dynamics during bank storage flows and implications for chemical base flow separation, *Water Resour. Res.*, 46, W07541, doi:10.1029/2009WR008539, 2010.
- McCallum, J. L., Cook, P. G., Berhane, D., Rumpf, C., and McMahon, G. A.: Quantifying groundwater flows to streams using differential flow gaugings and water chemistry, *J. Hydrol.*, 416, 118–132, 2012.
- McCallum, A. M., Andersen, M. S., and Acworth R. I.: A new method for estimating recharge to unconfined aquifers using differential river gauging, *Ground Water*, in press, 2013.
- Mullinger, N. J., Binley, A. M., Pates, J. M., and Crook, N. P.: Radon in Chalk streams: spatial and temporal variation of groundwater sources in the Pang and Lambourn catchments, UK, *J. Hydrol.*, 339, 172–182, 2007.
- Mullinger, N. J., Pates, J. M., Binley, A. M., and Crook, N. P.: Controls on the spatial and temporal variability of ^{222}Rn in riparian groundwater in a lowland Chalk catchment, *J. Hydrol.*, 376, 58–69, 2009.
- Négrel, P., Petelet-Giraud, E., Barbier, J., and Gautier, E.: Surface water–groundwater interactions in an alluvial plain: chemical and isotopic systematics, *J. Hydrol.*, 277, 248–267, 2003.
- Negulescu, M. and Rojanski, V.: Recent research to determine reaeration coefficients, *Water Res.*, 3, 189–202, 1969.
- Nunes Vaz, R. A., Lennon, G. W., and de Silva Samarasinghe, J. R.: The negative role of turbulence in estuarine mass transport, *Estuar. Coast. Shelf S.*, 28, 361–377, 1989.
- O’Connor, D. J. and Dobbins, W. E.: Mechanisms of reaeration in natural streams, *T. Am. Soc. Civ. Eng.*, 123, 641–684, 1958.
- Peterson, R. N., Santos, I. R., and Burnett, W. C.: Evaluating groundwater discharge to tidal rivers based on a Rn-222 time-series approach, *Estuar. Coast. Shelf S.*, 86, 165–178, 2010.
- Peyrard, D., Delmotte, S., Sauvage, S., Namour, P. H., Gerino, M., Vervier, P., and Sanchez-Perez, J. M.: Longitudinal transformation of nitrogen and carbon in the hyporheic zone of an N-rich stream: a combined modelling and field study, *Phys. Chem. Earth*, 36, 599–611, 2011.
- Rhode, A.: Spring flood: meltwater or groundwater?, *Nord. Hydrol.*, 12, 21–30, 1981.
- Ribolzi, O., Andrieux, P., Valles, V., Bouzigues, R., Bariac, T., and Voltz, M.: Contribution of groundwater and overland flows to storm flow generation in a cultivated Mediterranean catchment, quantification by natural chemical tracing, *J. Hydrol.*, 233, 241–257, 2000.
- Rau, G. C., Andersen, M. S., McCallum, A. M., and Acworth, R. I.: Analytical methods that use natural heat as a tracer to quantify surface water-groundwater exchange, evaluated using field temperature records, *Hydrogeol. J.*, 18, 1093–1110, 2010.
- Ruehl, C., Fisher, A. T., Hatch, C., Los Huertos, M., Stemler, G., and Shennan, C.: Differential gauging and tracer tests resolve seepage fluxes in a strongly-losing stream, *J. Hydrol.*, 330, 235–248, 2006.

- Runkel, R. L.: One-Dimensional Transport with Inflow and Storage (OTIS): A Solute Transport Model for Streams and Rivers, U.S. Geol. Surv. Water Resour. Invest. Rep., 98–4018, 1998.
- Santos, I. R. and Eyre, B. D.: Radon tracing of groundwater discharge into an Australian estuary surrounded by coastal acid sulphate soils, *J. Hydrol.*, 396, 246–257, 2011.
- Santos, I. R., Peterson, R. N., Eyre, B. D., and Burnett, W. C.: Significant lateral inputs of fresh groundwater into a stratified tropical estuary: evidence from radon and radium isotopes, *Mar. Chem.*, 121, 37–48, 2010.
- Silliman, S. E. and Booth, D. F.: Analysis of time-series measurements of sediment temperature for identification of gaining vs. losing portions of Juday Creek, Indiana, *J. Hydrol.*, 146, 131–148, 1993.
- Sophocleous, M.: Interactions between groundwater and surface water: the state of the science, *Hydrogeol. J.*, 10, 52–67, 2002.
- Stacey, M. T., Fram, J. P., and Chow, F. K.: Role of tidally periodic density stratification in the creation of estuarine subtidal circulation. *J. Geophys. Res.*, 113, C08016, doi:10.1029/2007JC004581, 2008.
- Stellato, L., Petrellz, E., Terrasi, F., Bellonie, P., Belli, M., Sansone, U., and Celico, F.: Some limitations in using ^{222}Rn to assess river–groundwater interactions: the case of Castel di Sangro alluvial plain (central Italy), *Hydrogeol. J.*, 16, 701–712, 2008.
- Tsur, Y. and Graham-Tomasi, T.: The buffer value of groundwater with stochastic surface water supplies, *J. Environ. Econ. Manag.*, 21, 201–224, 1991.
- Vandenberg, A. H. M. and Stewart, I. R.: Ordovician terranes of the southeastern Lachlan Fold Belt: stratigraphy, structure and palaeogeographic reconstruction, *Tectonophysics*, 214, 159–176, 1992.
- Victorian Water Resources Data Warehouse: available at: <http://www.vicwaterdata.net/vicwaterdata/home.aspx> (last access: 11 January 2013), 2012.
- Wagner, B. J. and Harvey, J. W.: Experimental design for estimating parameters of rate-limited mass transfer: analysis of stream tracer studies, *Water Resour. Res.*, 33, 1731–1741, 1997.
- Woessner, W. W.: Stream and fluvial plain ground water interactions: rescaling hydrogeologic thought, *Ground Water*, 38, 423–429, 2000.

Chapter 3

Residence times and mixing of water in river banks: implications for recharge and groundwater – surface water exchange

Nicolaas P. Unland^{1,2,*}, Ian Cartwright^{1,2}, Dioni I. Cendón^{3,4}, Robert Chisari³

^[1] School of Geosciences, Monash University, Clayton, Vic, 3800, Australia

^[2] National Centre for Groundwater Research and Training, School of Environment, Flinders University, Adelaide, SA, Australia

^[3] Australian Nuclear Science and Technology Organisation, Kirrawee DC, NSW 2232, Australia

^[4] Connected Waters Initiative, School of BEES, UNSW, Australia

In preparation for publication

Abstract

The residence time of groundwater within 50 m of the Tambo River, South East Australia, has been estimated through the combined use of ³H and ¹⁴C. Groundwater residence times increase towards the Tambo River which implies a gaining river system and not increasing bank storage with proximity to the Tambo River. Major ion concentrations and $\delta^2\text{H}$ and $\delta^{18}\text{O}$ values of bank water also indicate that bank infiltration does not significantly impact groundwater chemistry under baseflow and post-flood conditions, suggesting that the gaining nature of the river may be driving the return of bank storage water back into the Tambo River within days of peak flood conditions. The covariance between ³H and ¹⁴C indicates the leakage and mixing between old (~17,200 years) groundwater from a semi-confined aquifer and younger groundwater (<100 years) near the river where confining layers are less prevalent. The presence of this semi-

confined aquifer has also been used to help explain the absence of bank storage, as rapid pressure propagation into the semi-confined aquifer during flooding will minimise bank infiltration. This study illustrates the complex nature of river groundwater interactions and the potential downfall in assuming simple or idealised conditions when conducting hydrogeological studies.

3.1. Introduction

Documenting water balances in river systems is vitally important to understanding hydrological processes and protecting and managing water resources. While surface runoff and regional groundwater inflows are the two main components of river flow, river banks or floodplain pools may act as sites of transient water storage. Bank storage represents water that infiltrates into alluvial aquifers at high river stage and subsequently returns to the river as the river stage declines (e.g., Chen and Chen, 2003; Singh, 1968; Winter et al., 1998). Bank storage is an important hydrological process that may considerably reduce peak river discharge during floods and maintain river discharge during periods of decreased rainfall. The volume and duration of bank storage for a given river stretch will depend on the flood peak height and flood duration, as well as the hydraulic conductivity of the alluvial aquifer and the hydraulic gradient between the aquifer and river (Chen et al., 2006).

While the concept of bank storage is well understood, quantifying the volume of water that infiltrates the banks and the duration of bank return flows is complicated. Many studies have focused on using analytical and numerical solutions to understand bank storage. Analytical solutions presented by Cooper and Rorabaugh (1963) demonstrate that the duration of bank return flow is related to the duration of the flood period and Pinder and Sauer (1971) showed that hydrographs can be modified by bank storage. Whiting and Pomeranets (1997) indicated a greater storage potential for deep

narrow rivers with wider floodplains and coarse alluvial material. More recently, the potential for significant storage beneath the streambed was identified by Chen and Chen (2003), while Chen et al. (2006) showed that bank storage will return more rapidly in gaining river sections. McCallum et al. (2010) showed that when the concentration of dissolved ions in groundwater is higher than river water, the groundwater returning to a river after bank infiltration can take months or years before returning to the concentration of regional groundwater. Bank slope has also been shown to impact bank storage, with shallower bank slope providing a greater potential for bank storage (Doble et al., 2012).

Most of these studies have concluded that bank storage periods will significantly exceed the duration of flood events. Typically bank storage return to the river will decrease exponentially after flood events, and in the case of sandy river banks with wide floodplains, residence times can be on the order of years (Doble et al., 2012; McCallum, et al., 2010; Whiting and Pomeranets, 1997). While these studies have added to our conceptual understanding of bank storage they often assume ideal or generalised conditions such as aquifer homogeneity, vertical river banks and saturated conditions (Doble et al., 2012), making them difficult to apply to many natural settings. As such, understanding the residence times of bank water may more concisely constrain the time scales and hydrogeological processes controlling bank storage. Field studies focussed on bank storage and the dating of bank water near Australian rivers has been quite limited, however works by Lamontagne et al. (2011) and Cendon et al. (2010) have indicated the presence of relatively young (<50 years) groundwater in river banks, and Cartwright et al., (2010) has shown that preferential recharge is likely to occur near rivers during flooding.

Understanding the geochemistry of water as it enters and exits river banks is important for a range of disciplines. Hydrogeochemical processes occurring within river

banks, such as the bacterial degradation of organic matter and the weathering of minerals can influence the concentrations of DOC, O₂, NO₃, Na, K and other major ions (Bourg and Bertin, 1993). Fukada et al. (2003) identified the continuing denitrification of river water as it infiltrated an alluvial aquifer and demonstrated that the chemistry of infiltrating water is likely to vary according to its residence time within the alluvial aquifer. Understanding the source and load of nutrients in rivers is fundamental in understanding their ecology (Boulton, 1993; Boulton, 2005), while determining the different sources of water in the riparian zone is crucial to effective vegetation management (Cey et al., 1999; Lambs, 2004; Lamontagne et al., 2005; Woessner, 2000). Similarly, the impact of infiltrating river water on water quality in the alluvial aquifer is important when developing groundwater extraction systems for water supply (Hiscock and Grischek, 2002). Accounting for bank storage is also important in conducting groundwater discharge studies, as bank storage will chemically be similar to runoff in comparison to regional groundwater. As such the total groundwater flux to a river will be significantly underestimated if a regional groundwater end member is used during mass balance calculations and bank storage is ignored (McCallum et al., 2010; Unland et al., 2013).

This study investigates bank storage processes in areas immediately adjacent to rivers (within 50 m) by conducting field investigations on the Tambo River, Victoria, Australia. The objectives of the study are to use the hydrogeochemistry of bank water near the Tambo River over changing discharge conditions in order to trace river-bank interactions by (1) characterising the chemistry of water stored in river banks (2) determining the age and likely sources water stored in river banks and (3) identify the factors controlling bank storage and the scale to which bank storage is occurring. While

this study uses data from specific field area, the Tambo River is similar to many others globally and the results may help in understanding bank storage processes in general.

3.1.1 Study Area

Investigations took place on the Tambo River in the Tambo River Basin, South East Australia. The river basin extends southwards from the Eastern Victorian Uplands to the Gippsland Basin (Fig. 1). The Eastern Victorian Uplands are dominated by low-grade metamorphosed Ordovician and Devonian sandstones, shales and turbidites that have been intruded by Devonian granites (Gray and Foster, 2004). The Palaeozoic basement forms a fractured rock aquifer; however, groundwater yields are insignificant in comparison to overlying sedimentary aquifers (Birch, 2003). Coarse gravels and sands eroded from the Eastern Victorian Uplands form an alluvial aquifer in most of the major river valleys in the Gippsland Basin. The Plio-Pleistocene Haunted Hill Gravels is the shallowest aquifer over most of the Gippsland Basin and is primarily composed of quartz with some feldspar, granitic fragments, tourmaline and cassiterite (Kapostasy, 2002). The Haunted Hill Gravels are underlain by the Boisdale Formation which comprises Late Miocene to Early Pliocene sands, gravels and clays with minor Cenozoic basalts, limestones and marls (Birch, 2003). Quaternary alluvium locally covers these formations along the river valleys. Clay layers throughout the Quaternary alluvium, Haunted Hill Gravels and Boisdale formation act as aquitards, separating a number of aquifer horizons that range from unconfined to fully confined (Hocking, 1976). These formations constitute the upper aquifers of the Gippsland Basin and are in total up to ~50 m thick. The deeper aquifers that do not interact with the rivers include the Oligocene-Pliocene Jemmys Point, Tambo River and Lake Wellington Formations (Leonard, 1992; Hofmann and Cartwright, 2013).

The Tambo River is perennial and flows through forest and woodland with cattle grazing on the river floodplains (Department of Agriculture, Fisheries and Forestry, 2006). It discharges into the saline Lake King and the lower ~15 km of the river is estuarine. Average annual precipitation in the catchment increases from 655 mm in the upper reaches to 777 mm in the middle and lower reaches (Bureau of Meteorology, 2013). During the majority of the study period river discharge in the Tambo River ranged from 1.5 to $4.0 \times 10^5 \text{ m}^3/\text{day}$ (Victorian Water Resources Data Warehouse, 2013); however significant rainfall during August 2011 and March 2012 resulted in discharge events that peaked between 2.0×10^7 and $3.0 \times 10^7 \text{ m}^3/\text{day}$, respectively (Fig. 2).

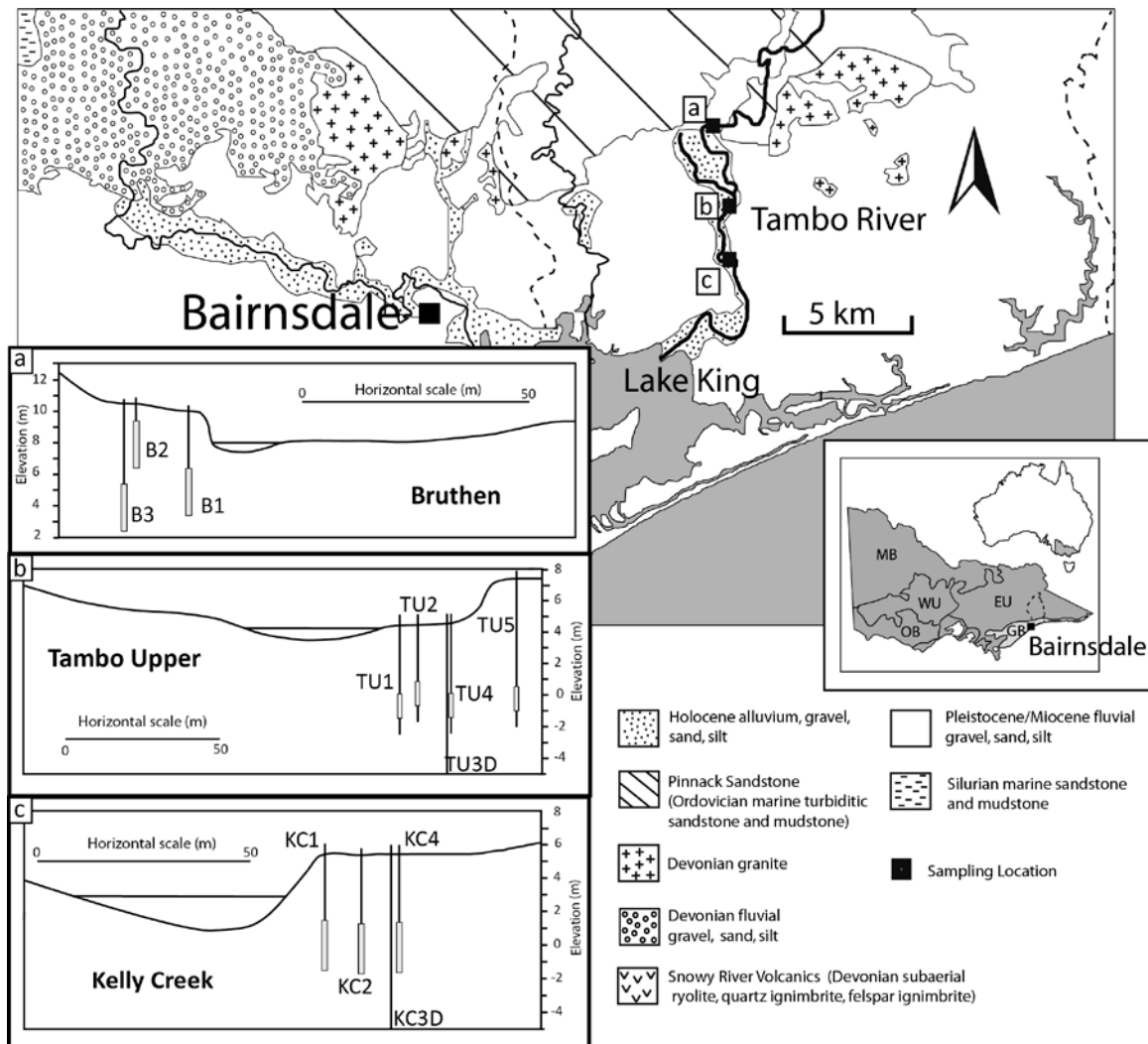


Figure 1. Location of field area and schematic cross sections of bore transects at Bruthen (a), Tambo Upper (b) and Kelly Creek (c). Screened sections indicated by open boxes. Dashed line = Tambo River basin boundary (transects orientated facing upstream).

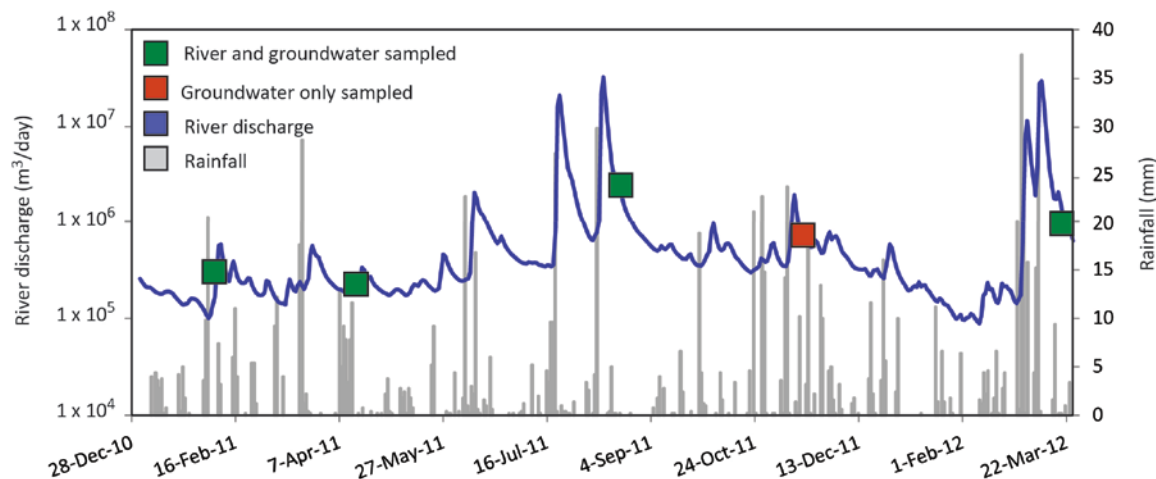


Figure 2. Surface and groundwater sampling frequency superimposed on Tambo River hydrograph (Battens Landing, station 223209) and rainfall (Bairnsdale Airport, station 85279).

Transects of groundwater monitoring bores were set up at three locations on the river banks of the Tambo River with the specific aim of tracing river – bank interactions. Most bores were screened approximately 3 m below the water table in order to capture seasonal variations in the water table while allowing for chemical analysis of groundwater entering the river. A further 2 bores were installed at greater depth (>20 m below ground surface) in order to characterise any deeper groundwater flow systems that may be present near the river. Bores are identified by location and distance from the Tambo River, as indicated by Fig. 1 and Tables 1, 2 and 3. The transect at Bruthen is 28.5 km upstream of Lake King and consists of 3 bores installed at 5.5, 17.6 and 18.3 m distance from the river and 8.0, 5.4 and 7.1 m depth below ground surface, respectively (Fig. 1). The transect at Tambo Upper, 20.2 km upstream of Lake King, consists of 5 bores installed at 8.8, 15.0, 22.3, 23.8 and 37.9 m distance from the Tambo River and 6.7, 6.2, 23.1, 6.7 and 9.8 m depth below ground surface, respectively. The final transect at Kelly Creek, 13.8 km upstream of Lake King, consists of 4 bores installed at 7.0, 17.9, 24.9 and 26.8 m from the Tambo River at depths of 8.1, 7.8, 28 and 7.9 m depth, respectively. Bores at Tambo Upper have 1.5 m screens starting 1 m from the borehole bottom while all other installations have a 3 m screened section set at the bottom of the borehole.

Sediment samples taken during bore installation indicate that the alluvial aquifer at all transects is dominated by coarse sands with clay rich layers variably distributed throughout the profile. All bores have been screened within alluvial sediments, however bores screened at >20 m depth appear to show confined responses, suggesting that clay layers in the profile result in the formation of a semi-confined aquifer at such depths.

3.2. Methods

Bore and river elevation were determined to ± 1 cm relative to the Australian Height Datum (AHD) using a Trimble digital global positioning system (DGPS). Bores were sampled using an impeller pump set at the screened section and at least 3 bore volumes were pumped before sample collection. Five sets of groundwater samples and 4 sets of river samples were collected between February 2011 and March 2012 at each transect. Sampling during February 2011, April 2011 and November 2011 represents conditions close to baseflow while sampling during August 2011 and March 2012 took place ~ 1 week after significant flooding in the catchment (Fig. 2). Rising head slug tests were conducted by pumping bores for ~10 minutes with an impeller pump at a rate of 4 L/minute and then allowing groundwater heads to recover. Changes to groundwater head over the test were recorded using a Rugged TROLL 200 instrument recording pressure changes at 1 second intervals to $\pm 1\%$ accuracy. Hydraulic conductivity was calculated using the Hvorslev method outlined in Fetter (1994).

Electrical conductivity (EC) was measured in field to $\pm 1\%$ using a calibrated TPS pH/EC meter and groundwater levels were measured using an electronic water level tape. Water samples were preserved by refrigeration in air-tight polyethylene bottles. HCO_3^- and dissolved CO_2 were measured within 48 hours of sample collection by titration using a HACH digital titrator with a precision of $\pm 5\%$. Samples were filtered (0.45 μ cellulose nitrate filters) and analysed for anions using a Metrohm ion chromatograph at Monash

University, Clayton, with a precision of $\pm 2\%$ estimated by replicate analysis. Filtered samples were acidified to pH < 2 using twice distilled 16 M nitric acid and analysed for cations by Varian Vista ICP-AES at the Australian National University or at Monash University, Clayton, using a Thermo Finnigan X series II, quadrupole ICP-MS. Drift during ICP-MS analysis was corrected using internal Sc, Y, In, Bi standards, with replicate analysis returning a precision of $\pm 5\%$. Stable isotope ratios were measured at Monash University using ThermoFinnigan MAT 252 and DeltaPlus Advantage mass spectrometers. $\delta^{18}\text{O}$ values of water were measured via equilibration with He- CO_2 at 32°C for 24-48 hours in a ThermoFinnigan Gas Bench. $\delta^2\text{H}$ values of water were measured via reaction with Cr at 850°C using a Finnigan MAT H/Device. $\delta^{18}\text{O}$ and $\delta^2\text{H}$ values were measured relative to internal standards that were calibrated using IAEA SMOW, GISP, and SLAP standards. Data were normalised following (Coplen, 1988) and are expressed relative to V-SMOW where $\delta^{18}\text{O}$ and $\delta^2\text{H}$ values of SLAP are -55.5% and -428% , respectively. The precision (1σ) of the analyses based on replicate analyses is $\delta^{18}\text{O} = \pm 0.2\%$, $\delta^2\text{H} = \pm 1\%$.

Samples for ^{14}C and ^3H were collected during the April 2011 sampling period (Fig. 2). ^3H water samples were distilled and electrolytically enriched prior to analysis by liquid scintillation (Morgenstern and Taylor, 2009). The ^3H concentrations were expressed in tritium units (TU) with uncertainties ranging from $\sim 25\%$ at the quantification limit (0.13 TU) to $< 6\%$ for ^3H concentrations above 1.5 TU. For ^{14}C analysis, the total DIC was converted to CO_2 by acidifying the samples with H_3PO_4 and extracting the liberated CO_2 gas using a custom built extraction line. The CO_2 sample was then heated in a sealed glass tube, containing baked CuO and Ag and Cu wire at 600°C for 2 h – to remove any sulfur compounds that may have been liberated – and followed by graphitisation, graphite targets were analysed by AMS at ANSTO's STAR

accelerator following Fink et al. (2004). The activity of ^{14}C is expressed as per cent of modern carbon (pMC) following Stuiver and Polach (1977). The average error associated with radiocarbon measurements is 0.3%.

3.3. Results

3.3.1 Groundwater elevations and hydraulic conductivities

Groundwater elevation at Bruthen varied between 7.45 m (AHD) in April 2011 and 8.89 m in August 2011. There was less than 6 cm difference across the transect during any given sampling period. Groundwater elevation in B1 and B2 were within 3 cm of each other during all sampling periods, while B3 was 2-6 cm higher than B1 and B2 (Fig. 3). Groundwater elevation at Bruthen was higher than river elevation during all sampling periods. Rising head slug tests at this transect indicate a hydraulic conductivity of $\sim 8.5 \times 10^{-3}$ m/s.

Groundwater elevation in the shallow bores at Tambo Upper ranged from 3.30 m in April 2011 to 4.80 m in August 2011. Elevations in TU5, TU2 and TU1 in individual campaigns were within 3 to 5 cm of each other. Groundwater elevations at TU4 were the lowest in the transect, averaging 3.92 m over the study, approximately 9 cm lower than the average levels in TU1, TU2, and TU5 (Fig. 3). The deeper bore (TU3D) was artesian during all sampling periods; this bore samples a deeper, semi-confined aquifer that has higher heads than the surficial aquifer. During February and April 2011, groundwater elevations in this bore were 4.85 m and 4.69 m, respectively, while in all other sampling periods the elevation exceeded that of the casing (5.04 m). Groundwater elevation at Tambo Upper was greater than river elevation during all periods except April 2011. Slug tests at this transect indicate hydraulic conductivities ranging from 5.1×10^{-4} to 8.6×10^{-5} m/s in the surficial aquifer, and 1.9×10^{-5} m/s in the semi-confined aquifer.

At Kelly Creek, groundwater levels in the shallower bores ranged from 3.07 m in April 2011 to 3.68 m in August 2011 (Fig. 3). Groundwater levels in these bores generally decreased with proximity to the river during all sample periods except April 2011. Groundwater levels in the deeper bore at Kelly Creek (KC3D) were higher than the shallow bores, ranging from 3.82 m in February 2011 to 4.33 m in November 2011. Slug tests at this transect indicate hydraulic conductivities ranging from 2.4 to 3.4×10^{-5} m/s.

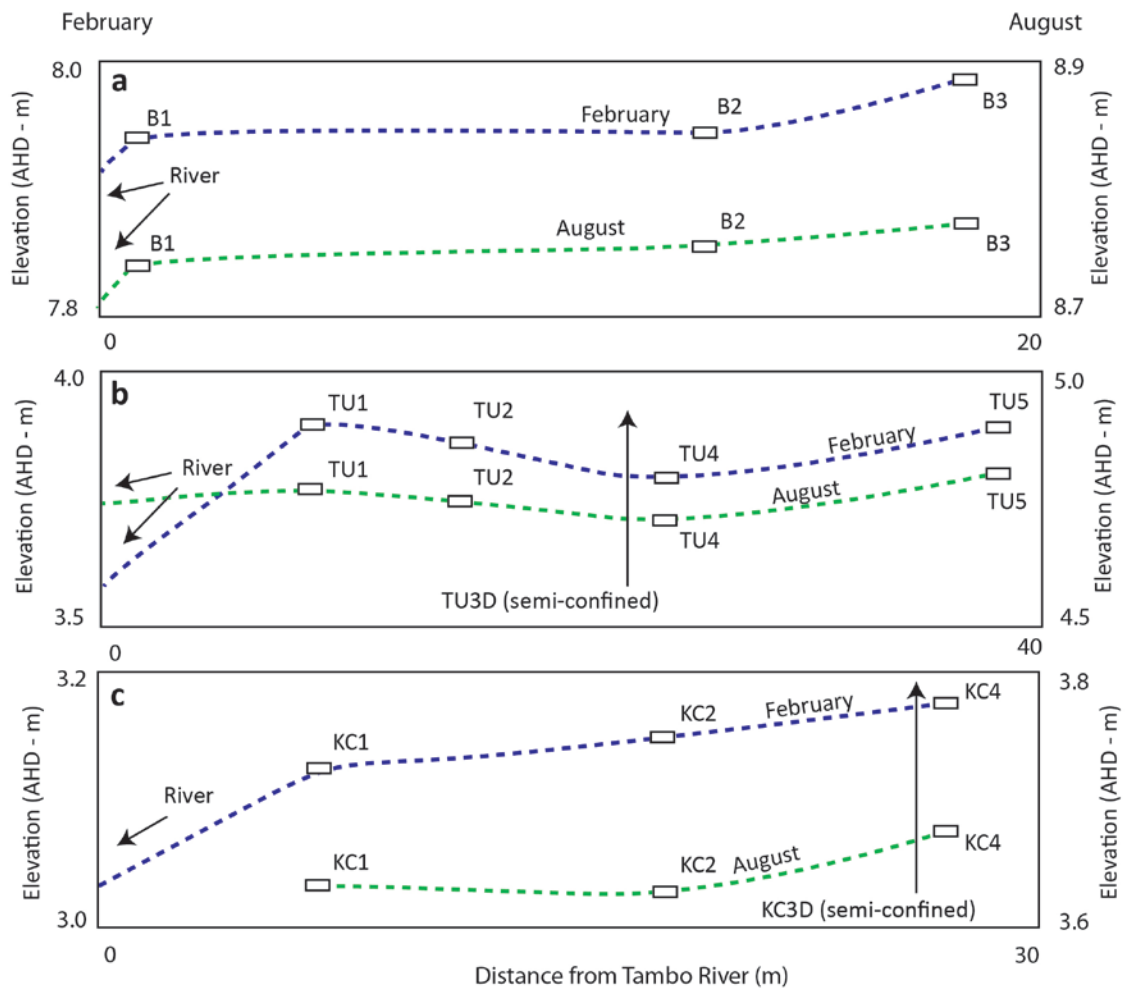


Figure 3. Groundwater elevations during February 2011 and August 2011 at Bruthen (a), Tambo Upper (b) and Kelly Creek (c). White rectangles = measured elevation, dashed lines = interpolated elevations.

3.3.2 Electrical conductivity

Groundwater EC values at Bruthen ranged from 136 to 607 $\mu\text{S}/\text{cm}$. Groundwater at B3 was generally the most saline, ranging from 261 to 607 $\mu\text{S}/\text{cm}$, while that from B1 ranged from 136 to 293 $\mu\text{S}/\text{cm}$. Shallow groundwater at Tambo Upper was more saline

than that from Bruthen, ranging from 717 $\mu\text{S}/\text{cm}$ to 2,682 $\mu\text{S}/\text{cm}$. Shallow groundwater at Tambo Upper was also generally more saline closer to the river than further from the river, averaging 2,110 $\mu\text{S}/\text{cm}$ at TU1 and TU2 over the study period, compared to 980 $\mu\text{S}/\text{cm}$ at TU4 and TU5. Deeper groundwater at Tambo Upper was consistently the most saline in the transect, ranging from 2,490 $\mu\text{S}/\text{cm}$ in April 2011 to 3,250 $\mu\text{S}/\text{cm}$ in August 2011. Groundwater at Kelly Creek was generally more saline than Tambo Upper, with EC's ranging from 2,000 to 2,777 $\mu\text{S}/\text{cm}$ over the study period. Groundwater EC was less variable at Kelly Creek and did not generally increase or decrease with proximity to the Tambo River.

3.3.3 Stable isotopes

$\delta^{18}\text{O}$ and $\delta^2\text{H}$ values generally plot close to the both local and global meteoric water lines (LMWL and GMWL); however river water at Kelly Creek during February 2011 plots to the right of the GMWL (Fig. 4). $\delta^{18}\text{O}$ values at Bruthen ranged from -4.3 to -7.5‰ and were generally higher closer to the river at B1 (average = $-4.8 \pm 0.4\text{‰}$) than those further from the river at B2 and B3 (average = $-5.3 \pm 2.2\text{‰}$). Stable isotope values

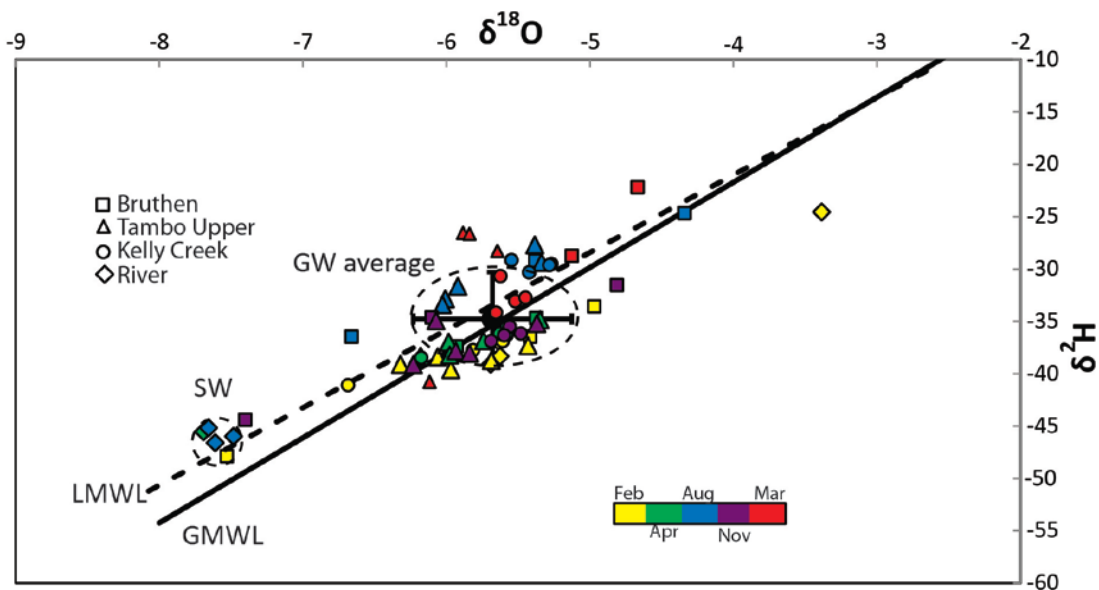


Figure 4. $\delta^{18}\text{O}$ and $\delta^2\text{H}$ values of groundwater (GW) and surface water (SW) from the Tambo River. LMWL defined by Melbourne meteoric water line in Hughes and Crawford, 2012.

were less variable at Tambo Upper with $\delta^{18}\text{O}$ values ranging from -5.3 to -6.3‰.

Groundwater at TU3D, TU1 and TU2 was generally more depleted in ^{18}O (average $\delta^{18}\text{O} = -6.0 \pm 0.2\text{‰}$) than at TU4 and TU5 (average $\delta^{18}\text{O} = -5.6 \pm 0.2\text{‰}$). Shallow groundwater at Kelly Creek showed little variability in $\delta^{18}\text{O}$ values ranging from -5.3 to -5.8‰ over the study. As with EC $\delta^{18}\text{O}$ values showed little variation across the transect, with average $\delta^{18}\text{O}$ values closest to the river at KC1 ($-5.5 \pm 0.2\text{‰}$) and further from the river at KC2 and KC3 ($-5.6 \pm 0.1\text{‰}$) within instrumental error. Deeper groundwater at Kelly Creek had slightly lower $\delta^{18}\text{O}$ values (average $\delta^{18}\text{O} = -5.9 \pm 0.5\text{‰}$) than the shallow groundwater. River water had lower $\delta^{18}\text{O}$ values than groundwater during all sampling periods except February 2011. During this period, $\delta^{18}\text{O}$ values of river water increased from -5.7‰ at Bruthen to -3.4‰ at Kelly Creek. Stable isotopes showed less variation in river water at other times during the study, with $\delta^{18}\text{O}$ values ranging from -7.9 to -7.5‰.

3.3.4 ^3H and ^{14}C

Both ^3H and ^{14}C activities in April 2011 were the highest in groundwater from Bruthen, ranging from 2.7 to 2.8 tritium units and 98.0 to 99.3 pMC, respectively. ^3H activities were higher in groundwater further from the river at Tambo Upper at TU4 and TU5 (^3H activities 1.6 and 1.2 tritium units, respectively) compared to groundwater closer to the river at TU1 and TU2 (^3H activities 0.40 and 0.36 tritium units, respectively). ^3H activities in deep groundwater at TU3D were below detection. ^{14}C activities show a similar variation, with higher activities at TU4 and TU5 (94.5 and 79.2 pMC) compared to groundwater at TU1 and TU2 (35.4 and 38.0 pMC). Deeper groundwater at TU3D had lower ^{14}C activities (10.6 pMC). ^3H activities in groundwater at Kelly Creek decreased from 0.51 tritium units at KC4 to 0.40 and 0.36 tritium units at KC1 and KC2,

respectively. ¹⁴C activities follow a similar trend, decreasing from 84.2 pMC at KC4 to 80.4 pMC at KC1.

3.3.5 Major ions

Despite sampling groundwater from similar aquifers, there are considerable differences in the geochemistry of groundwater from the three transect locations.

Groundwater from Bruthen is a HCO₃-Ca-Na type (Fig. 5). The concentration of most major cations at Bruthen decrease with increasing Cl concentrations, however K has a weak positive correlation with Cl (Fig. 6). Molar Na:Cl ratios at Bruthen generally range from 2 to 4 during periods of lower rainfall in the catchment (February 2011, April 2011 and November 2011), and are generally below 1 during periods of increased rainfall (August 2011 and March 2012). Molar Cl:Br ratios at Bruthen increase from 140 to over 1,000 with increasing Cl concentrations (Fig. 6).

Site	Date	EC μS/cm	Level m	Dist. m	F mg/L	Cl mg/L	Br mg/L	NO ₃ mg/L	SO ₄ mg/L	HCO ₃ mg/L	Na mg/L	K mg/L	Ca mg/L	Mg mg/L	O δ ¹⁸ O	H δ ² H	³ H TU	¹⁴ C Pmc	δ ¹³ C ‰	MGRT years
R	Feb-11	121	7.84	0.00	0.08	9.63	0.03	0.24	1.94	<i>46.44</i>	7.65	1.38	7.77	3.95	-5.69	-39.1				
1	Feb-11	146	7.87	5.56	0.04	9.60	0.05	0.04	6.05	<i>50.93</i>	12.11	1.65	8.33	3.05	-4.97	-33.6				
2	Feb-11	191	7.88	17.56	0.06	5.61	0.02	0.05	23.47	<i>41.31</i>	7.16	3.00	10.36	5.14	-7.53	-47.9				
3	Feb-11	261	7.90	18.34	0.12	13.33	0.07	0.02	11.47	<i>85.05</i>	19.24	2.52	10.27	7.33	-5.42	-36.5				
R	Apr-11	109	7.61	0.00	0.05	3.63	0.01	0.11	0.90											
1	Apr-11	200	7.66	5.56	0.04	6.75	0.10	0.37	5.83	<i>67.06</i>	16.92	2.03	12.16	4.09	-5.37	-34.7	2.65	98.04	-13.9	10.4
2	Apr-11			17.56	0.15	10.31	0.17	0.30	11.42	<i>182.9</i>	27.29	2.68	8.47	7.31	-5.93	-37.4	2.84	99.33	-15.4	8.9
R	Aug-11	145	8.81	0.00	0.04	17.57	0.02	2.17	5.02	<i>38.73</i>	11.71	1.68	6.44	4.85	-7.61	-46.6				
1	Aug-11	179	8.84	5.56	0.06	5.66	0.03	0.20	5.36	<i>52.46</i>	2.52	2.44	11.27	4.91	-4.34	-24.7				
2	Aug-11	173	8.84	17.56	0.12	12.68	0.08	0.03	36.24		BD	2.51	11.47	8.93	-5.38	-29.2				
3	Aug-11	293	8.89	18.34	0.06	18.79	0.04	1.48	30.18		BD	5.28	10.35	6.35	-6.66	-36.5				
1	Nov-11	229	7.91	5.56	0.07	11.09	0.05	0.00	6.07	<i>75.12</i>	15.23	2.10	10.37	5.37	-4.81	-31.6				
2	Nov-11	215	7.88	17.56	0.08	14.62	0.05	2.72	10.10	<i>49.54</i>	13.73	3.91	8.20	4.58	-6.10	-34.6				
3	Nov-11	607	7.94	18.34	0.05	78.22	0.21	0.08	12.10	<i>63.09</i>	33.07	3.32	15.79	14.44	-7.40	-44.4				
R	Mar-12	156	7.47	0.00	0.09	17.48	0.03	0.77	4.12	<i>45.91</i>	11.12	1.53	8.17	5.08	-7.56	-46.2				
1	Mar-12	293	8.36	5.56	0.05	17.80	0.06	0.03	16.53	<i>62.05</i>	9.41	1.72	17.81	6.38	-5.13	-28.7				
2	Mar-12	136	8.36	17.56							6.87	2.43	4.91	2.27						
3	Mar-12	287	8.38	18.34	0.16	23.35	0.07	0.00	22.04	<i>44.73</i>	19.13	1.66	8.43	6.87	-4.67	-22.2				

Table 1. Summary data for Bruthen transect. HCO₃ data in italics = calculated via charge balance. MGRT = mean groundwater residence time as calculated via exponential piston flow modelling (see section 3.4.3).

Groundwater from Tambo Upper is a Cl-Na-Ca type (Fig. 5). At Tambo Upper Na and K concentrations increase and Ca and Mg concentrations decrease with increasing Cl

concentrations (Fig. 8). Groundwater further from the river at Tambo Upper (TU4 and TU5) has Cl concentrations below 10 mmol/L, K concentrations below 0.2 mmol/L and Na concentrations below 7 mmol/L (Table 1). Deeper groundwater from Tambo Upper (TU3D) has Cl concentrations greater than 15 mmol/L, K concentrations greater than 0.8 mmol/L and Na concentrations greater than 16 mmol/L. Groundwater closer to the river at Tambo Upper (TU1 and TU2) contains concentrations of Na, K, Mg and Ca that are an intermediate between that of TU3D and groundwater at TU4 and TU5.

Site	Date	EC μS/cm	Level m	Dist. m	F mg/L	Cl mg/L	Br mg/L	NO ₃ mg/L	SO ₄ mg/L	HCO ₃ mg/L	Na mg/L	K mg/L	Ca mg/L	Mg mg/L	O δ ¹⁸ O	H δ ² H	³ H TU	¹⁴ C Pmc	δ ¹³ C ‰	MGRT years
R	Feb-11	120	3.58	0	0.08	9.78	0.04	0.11	2.04	<i>48.1</i>	7.83	1.74	8.24	3.86	-5.63	-38.3				
1	Feb-11	2395	3.9	8.82	0.14	572	1.88	0.33	25.2	<i>212</i>	279	23	99.6	30.3	-6.06	-38.4				
2	Feb-11	2155	3.86	15	0.12	555	1.77	1.58	14.7	<i>157</i>	280	19.2	62.4	33.9	-5.97	-39.6				
3D	Feb-11	2656	4.85	22.3	0.36	607	1.98	2.54	22.8	<i>316</i>	374	35.4	64.6	29.8	-6.32	-39.1				
4	Feb-11	764	3.78	23.7	0.12	176	0.52	0.07	21.3	<i>60.7</i>	72.8	4.65	33.9	17.7	-5.43	-37.3				
5	Feb-11	1023	3.89	37.9											-5.69	-38.8				
R	Apr-11	112	3.43	0	0.04		0.01	0.08	0.92		16	4.34	10	15.1	-7.88	-61.9				
1	Apr-11	2210	3.38	8.82	0.14	460	1.43	0.22	36.8	291	280	26.9	111	40.7	-5.98	-37	0.4	38	-8.7	52.6
2	Apr-11	2180	3.36	15	0.11	533	1.76	1.24	25.9	272	333	23.1	86.8	52.8	-5.98	-38.2	0.36	35.4	-7.2	52.2
3D	Apr-11	2488	4.69	22.3	0.34	534	1.72	0.33	10.9	439	468	33.8	71.8	41.2	-6.18	-38.3	<0.03	10.6	-5.7	17,200
4	Apr-11	717	3.3	23.7	0.11	140	0.42	0.47	15.9	100	98.1	4.42	37.1	21.2	-5.35	-34.9	1.55	94.5	-10	45.6
5	Apr-11	1043	3.39	37.9	0.11	203	0.61	0.07	50.3	80.5	122	7.1	64.9	20.7	-5.74	-36.9	1.21	79.2	-9.3	60.2
R	Aug-11	148	4.74	0	0.06	18.1	0.02	2.46	4.21	<i>36.5</i>	11.6	1.85	5.87	4.78	-7.66	-45.2				
1	Aug-11	2682	4.77	8.82	0.11	599	1.63	0.53	12.6	<i>406</i>	339	27.3	105	38.2	-6.01	-32.9				
2	Aug-11	2207	4.75	15	0.19	501	1.42	0.27	22.2	<i>279</i>	280	21.3	78	31.7	-5.92	-31.7				
3D	Aug-11	3250	5.04	22.3	0.26	753	2.09	0.11	34.2	<i>799</i>	600	48.4	80.9	45.2	-6.03	-33.4				
4	Aug-11	774	4.7	23.7	0.08	207	0.41	0.12	5.59	<i>89.8</i>	98.3	3.44	32.6	17.6	-5.38	-27.7				
5	Aug-11	1039	4.8	37.9	0.14	227	0.43	0.08	11.6	<i>118</i>	115	3.31	36.5	20.9	-5.34	-29.4				
1	Nov-11	2018	3.74	8.82	0.3	439	1.42	0.56	49.7	<i>383</i>	303	15.5	79.4	26.5	-6.07	-35				
2	Nov-11	2168	3.7	15	0.07	531	1.21	0.12	4.46	<i>294</i>	241	14.2	91.6	54.4	-5.93	-37.9				
3D	Nov-11	2938	>5.04	22.3	0.19	639	2.28	0.21	46.8	<i>760</i>	554	41.2	63.1	38.7	-6.23	-39.1				
4	Nov-11	864	3.61	23.7	0.18	178	0.56	0.21	1.24	<i>170</i>	98.8	4	36	20.1	-5.37	-35.2				
5	Nov-11	1337	3.7	37.9	0.08	276	0.83	0.11	48.3	<i>207</i>	158	6.21	68.4	21.7	-5.84	-38.1				
R	Mar-12	165	3.32	0	0.09	19.6	0.04	0.54	4.21	<i>48.5</i>	12	1.76	8.69	5.47	-7.64	-46.4				
1	Mar-12	1350	4.3	8.82	0.07	385	0.93	0.13	33.5	<i>27.7</i>	141	19.4	68.5	24.2	-5.65	-28.3				
2	Mar-12	1763	4.26	15	0.07	544	1.11	0.07	29.7	<i>BD</i>	190	11.7	70.4	35.7	-5.88	-26.6				
3D	Mar-12	3210	>5.04	22.3	0.24	958	2.46	0.05	41	<i>BD</i>	484	35.2	58.7	33.3	-6.12	-40.8				
4	Mar-12	881	4.22	23.7	0.1	221	0.53	0.09	1.45	<i>73</i>	88.7	4.48	38	19.7	n/a	-34.9				
5	Mar-12	1320	4.32	37.9	0.09	344	0.76	0.3	40.4	<i>57.6</i>	148	6.38	63.3	21.2	-5.84	-26.7				

Table 2. Summary data for Tambo Upper transect HCO₃ data in italics = calculated via charge balance. MGRT = mean groundwater residence time as calculated via exponential piston flow modelling (see section 3.4.3).

Site	Date	EC μS/cm	Level m	Dist. m	F mg/L	Cl mg/L	Br mg/L	NO ₃ mg/L	SO ₄ mg/L	HCO ₃ mg/L	Na mg/L	K mg/L	Ca mg/L	Mg mg/L	O δ ¹⁸ O	H δ ² H	³ H TU	¹⁴ C Pmc	δ ¹³ C ‰	MGRT years
R	Feb-11	18340	3.05	0	0.38	6322	22	0.3	825	<i>899</i>	3558	151	182	521	-3.38	-24.6				
1	Feb-11	2004	3.14	7.02	0.3	518	1.54	0.35	0.43	<i>294</i>	178	3.82	178	33.6	-5.63	-37				
2	Feb-11	2349	3.17	17.9	0.43	597	1.77	0.77	2.01	<i>374</i>	202	3.93	231	32.4	-5.61	-36.9				
3D	Feb-11		3.82	24.9							162	11.4	23.6	9.31	-5.81	-37.8				
4	Feb-11	2364	3.2	26.8	0.38	637	1.92	0.56	1.14	<i>271</i>	197	2.59	229	29.6	-6.68	-41.1				
R	Apr-11	4210		0	0.21	255	0.93	0.13	29.1	<i>8690</i>	2683	153	404	116	-7.69	-45.5				
1	Apr-11	2145	3.15	7.02	0.3	474	1.36	0.27	0.28	446	204	3.29	207	43.6	-5.58	-35.5	0.4	80.4	-2.8	99.1
2	Apr-11	2455	3.07	17.9	0.33	558	1.57	0.43	1	488	252	2.83	289	42.3	-5.63	-36.2	0.37	83.6	-2.9	100.0
3D	Apr-11	2669	3.95	24.9	0.39	413	1.3	0.68	68.9	445	372	17.8	123	48.7	-5.58	-36.3				
4	Apr-11	2099	3.15	26.8	0.57	630	1.83	1.87	0.78	591	313	3.12	340	47.8	-6.17	-38.5	0.51	84.2	-3.7	96.0
R	Aug-11	170		0	0.05	21.6	0.03	2.24	4.82	<i>39</i>	13.8	2.38	6.33	5.03	-7.48	-46				
1	Aug-11	2568	3.63	7.02	0.24	590	1.4	0.84	0.38	<i>256</i>	146	4.27	219	42.8	-5.27	-29.5				
2	Aug-11	2777	3.63	17.9	0.26	655	1.44	0.18	1.56	<i>355</i>	135	3.73	286	49.8	-5.28	-29.6				
3D	Aug-11	2438	4.3	24.9	0.23	608	1.3	2.12	61.4	292	218	12.1	186	51	-5.55	-29.2				
4	Aug-11	2717	3.68	26.8	0.26	513	1.26	0.01	0.52	<i>291</i>	73.4	2.28	263	35.5	-5.42	-30.3				
1	Nov-11	2742		7.02	0.45	533	1.7	2.7	0.68	<i>848</i>	286	6.14	249	48.7	-5.56	-35.5				
2	Nov-11	2542	3.36	17.9	0.32	563	1.62	0.13	51.4	<i>711</i>	269	3.26	268	42.9	-5.69	-36.9				
3D	Nov-11	2738	4.33	24.9	0.41	436	1.44	0.04	0.57	998	338	11	192	50.7	-5.6	-36.3				
4	Nov-11	2218	3.41	26.8	0.35	532	1.71	2.48	0.54	<i>552</i>	226	2.49	230	34.4	-5.48	-36.2				
R	Mar-12	195		0	0.08	33.4	0.09	0.21	7.25	<i>465</i>	82.1	11.9	47.4	30.1	-7.58	-45.5				
1	Mar-12	2770		7.02	0.3	598	1.48	0.04	2.44	<i>397</i>	218	4.39	215	37.9	-5.52	-33.1				
2	Mar-12	2495		17.9	0.41	605	1.53	0.1	1.11	<i>430</i>	219	3.72	238	32.8	-5.45	-32.8				
3D	Mar-12	2345		24.9	0.37	560	1.45	0.16	0.46	<i>637</i>	292	8.75	199	41.6	-5.65	-34.2				
4	Mar-12	2715		26.8	0.32	713	1.64	0.13	43.4	<i>24.3</i>	189	3.42	218	27.6	-5.62	-30.7				

Table 3. Summary data for Kelly Creek transect. HCO₃ data in italics = calculated via charge balance. MGRT = mean groundwater residence time as calculated via exponential piston flow modelling (see section 3.4.3).

Shallow groundwater at Kelly Creek is Cl- Ca-Na type. At Kelly Creek, shallow groundwater has Cl concentrations that range from 11.6 to 20.1 mmol/L and Ca concentrations that range from 3.1 to 8.5 mmol/L (Fig. 7). Ca, Na, K, and Mg concentrations generally increase with Cl concentrations. Deeper groundwater from Kelly Creek shows similar trends in major ion concentrations but contains a higher proportion of Na and Mg and a lower proportion of Ca in comparison to shallower groundwater. Molar Cl:Br ratios in groundwater at Kelly Creek increase from ~650 to ~1,000 while Na:Cl ratios decrease from 1.4 to 0.4 as Cl concentrations increase.

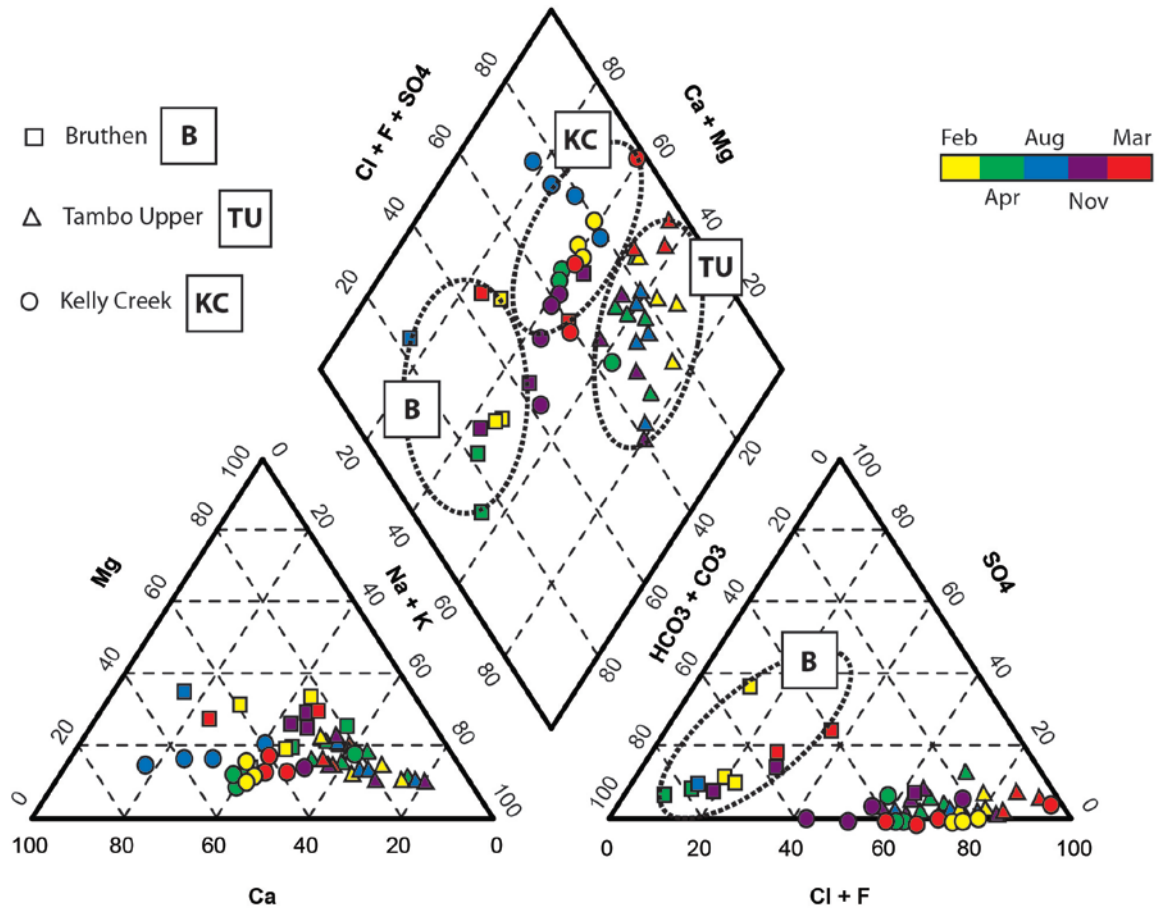


Figure 5. Piper plot of bank water from the Tambo River.

3.4. Discussion

The following section focusses on identifying the source of water stored in the banks of the Tambo River. Through groundwater dating, the prevalence of bank storage is evaluated and patterns in groundwater recharge and flow are identified. These evaluations are further coupled with major ion and stable isotope analysis under changing hydrological conditions, in order to identify processes controlling the chemistry of bank water and the potential impacts to river and groundwater quality.

3.4.1 Hydrogeochemical processes

Na:Cl ratios at Bruthen and Kelly Creek were higher during periods of lower rainfall compared to periods of higher rainfall. This suggests that periods of lower rainfall

may drive longer groundwater residence times in the aquifer, which may facilitate greater water-rock interaction and the dissolution of Na bearing minerals such as plagioclase (Edmunds, 2009; Herczeg et al., 2001). The increase in Cl:Br ratios at Bruthen and Kelly Creek with increasing Cl concentrations (Figs 6, 7) indicates an input of Cl rather than evapotranspiration (which would not impact Cl:Br ratios). An absence of evaporation is also supported by $\delta^2\text{H}$ and $\delta^{18}\text{O}$ values at Bruthen which plot close to the local meteoric water line rather than along evaporation trends (Fig. 4) (Cartwright et al., 2010; Herczeg et al., 2001). Fig. 4 does suggest an evapotranspiration trend in February; however this is skewed by a surface water sampled at Kelly Creek when low flow conditions allowed saline water from Lake King (with an evaporated signature) to migrate upstream (to Kelly Creek). This trend is not apparent at other times or in the groundwater system. Increased Cl:Br ratios may result from halite (NaCl) dissolution which could also shift Na:Cl ratios towards 1 as Cl concentrations increase.

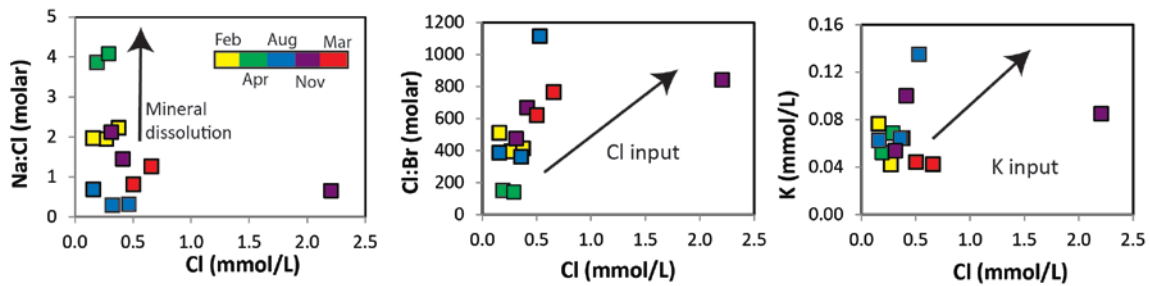


Figure 6. Trends in major ion chemistry at Bruthen indicating mineral dissolution, the input of Cl into groundwater and the input of K into groundwater.

However, there are no obvious stores of halite in the catchment and Na:Cl ratios of <1 at Kelly Creek are difficult to explain by halite dissolution. An alternative source of Cl is KCl fertilizers that are used locally (Department of Environment and Primary Industries, 2013). K:Cl ratios decrease with increasing Cl concentrations at Bruthen (Fig. 6), however, K is non-conservative and may be removed from the soil profile by vegetation (e.g., Schachtman and Schroder, 1994). It is also possible that these samples

have interacted with weathered and potentially parent shale, where K could be sorbed by illite (Griffioen, 2001). In any case, increased Cl concentrations during periods increased rainfall suggests that infiltration facilitates the transport of Cl from the land surface and/or the soil profile into shallow groundwater (Panno et al., 2006).

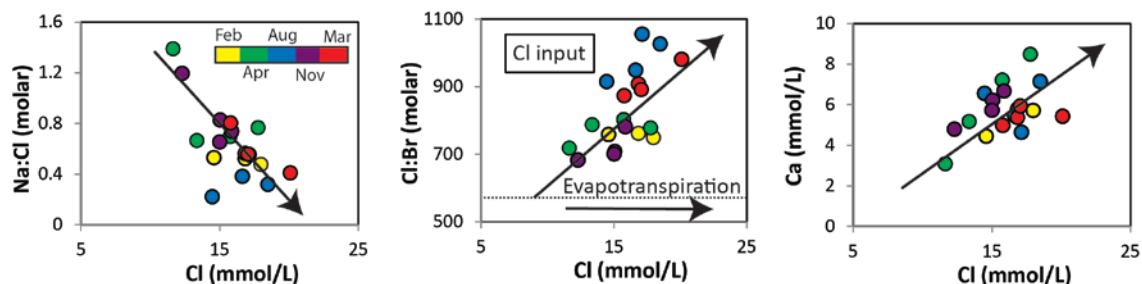


Figure 7. Trends in major ion chemistry at Kelly Creek indicating Cl inputs during increased rainfall.

At Tambo Upper, the groundwater from TU1, TU2 and TU5 has Cl concentrations consistent with the mixing between deep groundwater from TU3D (Cl concentrations of 17.11 to 27.03 mmol/L) and shallow groundwater from TU4 (Cl concentrations of 3.94 to 6.24 mmol/L) (Fig. 8). Molar Na:Cl ratios and K:Cl ratios in the deeper groundwater are generally higher than in shallow groundwater, while Ca:Cl and Mg:Cl ratios are generally lower than in shallow groundwater. This suggests that higher groundwater residence times in the deeper aquifer have facilitated the dissolution of Na and K minerals such as plagioclase and orthoclase feldspar, while Ca and Mg bearing minerals such as gypsum and calcite are likely to be less prevalent. The geochemistry of shallow groundwater throughout the Tambo Upper transect may be explained by mixing trend between shallow groundwater and deep groundwater (Fig.8). This especially occurs during the wetter periods of August 2011 and March 2012, suggesting that hydraulic loading of the deeper, semi-confined aquifer is driving increased leakage of deep groundwater into the overlying alluvial aquifer.

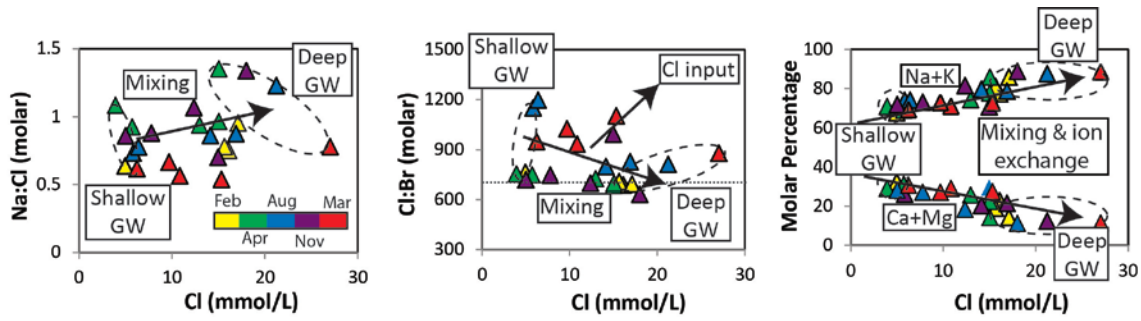


Figure 8. Trends in major ion chemistry at Tambo Upper indicating mixing between groundwater in the shallow, unconfined aquifer and groundwater from the deeper, semi-confined aquifer.

3.4.2 Aquifer interactions

The ^{14}C and ^3H activities in groundwater may be predicted from their atmospheric concentrations and groundwater residence times. The activities of these isotopes in the atmosphere were elevated due to the atmospheric nuclear tests that occurred mainly in the 1960s (the so-called “bomb pulse”). For this study, calculations are based on a rainfall weighted ^3H activity of 3.2 tritium units for the period July 2005 to June 2011 in the Melbourne area (Tadros et al., 2014, unpublished), and we assume that pre-bomb pulse tritium activities are similar to these as indicated by Allison and Hughes (1977). Unlike ^3H , ^{14}C activities of atmospheric CO_2 were similar in the northern and southern hemispheres (Fontes, 1983). The data of Hau et al. (2013) were used to approximate the activity of ^{14}C in precipitation from 1950 to 2010. Pre 1950, ^{14}C activities are assumed to have decreased from 100 pMC in 1905 to 97.5 pMC in 1950 due to fossil fuel burning (Suess, 1971).

Le Gal La Salle et al. (2001) presented a renewal rate model where the shallow aquifer is treated as a reservoir in which each year a certain proportion of water leaks to deeper groundwater and is replaced by recharge. The ^3H or ^{14}C activity in groundwater at time t (C_t) is given by:

$$C_t = (1 - R_n) C_{t-1} e^{-\lambda} + R_n C_i \quad (1)$$

where λ is the decay constant ($5.63 \times 10^{-3} \text{ yr}^{-1}$ for ^3H , $1.21 \times 10^{-4} \text{ yr}^{-1}$ for ^{14}C), C_i is the activity of ^3H or ^{14}C in precipitation in year i and R_n is the aquifer renewal rate.

The assumption that the aquifer acts as a single well-mixed homogeneous zone is unlikely to apply to anything but the top few meters. Lumped-parameter models may also be used to describe groundwater flow in shallow unconfined aquifers and semi-confined aquifers (Małozzewski and Zuber, 1991; Małozzewski and Zuber, 1982; Morgenstern, 2010; Zuber et al., 2005). Piston flow models assume that no mixing takes place between recharge and water in the aquifer, and is suitable for settings where dispersion is low. Conversely, the exponential flow model assumes a vertical stratification of groundwater ages in an aquifer and is suitable for the sampling of fully penetrating wells or surface water bodies fed by aquifers receiving homogeneous recharge. This study uses the exponential piston flow model (EPFM) which combines a portion of piston flow followed by a portion of exponential flow and is appropriate for unconfined to semi-confined aquifers screened below the water table, such that precludes sampling of groundwater with very short residence times (Morgenstern, 2010; Cartwright and Morgenstern, 2012).

For the EPFM C_t is given by:

$$C_t = \int_0^{\infty} C_i(t - \tau)g(\tau)e^{(-\lambda\tau)}d\tau \quad (2)$$

where τ is the transit time and $g(\tau)$ is the system response function. The system response function is given by:

$$g(\tau) = 0 \quad \text{for } \tau < T(1-f) \quad \text{and} \quad (3a)$$

$$g(\tau) = (fT)^{-1} e^{(-\tau/ft)+1/f-1} \quad \text{for } \tau > T(1-f) \quad (3b)$$

where T is the mean residence time and f is the ratio of exponential flow to piston flow for the total flow volume (Cartwright and Morgenstern, 2012; Zuber et al., 2005). f has been estimated at 0.8 for shallow bores neighbouring the Tambo River on the basis of bore depth, screen length and aquifer lithology.

While the specific model adopted results in different estimates of groundwater residence times, the predicted variation in ^{14}C and ^3H activities are similar in all flow models that involve attenuation of the bomb-pulse peak of ^3H and ^{14}C during flow. The covariance of ^{14}C and ^3H activities constrains mixing within the groundwater system (Le Gal La Salle et al., 2001; Cartwright et al., 2007, 2013). Mixing between recently-recharged groundwater and older groundwater with low ^{14}C and negligible ^3H activities will displace water compositions to the left of the predicted ^{14}C vs. ^3H trends. Closed-system calcite dissolution lowers ^{14}C but which does not impact ^3H concentrations produces a similar displacement. The co-variance between ^3H and ^{14}C for groundwater samples is shown in Fig. 9, with the expected trends for eqn 1.

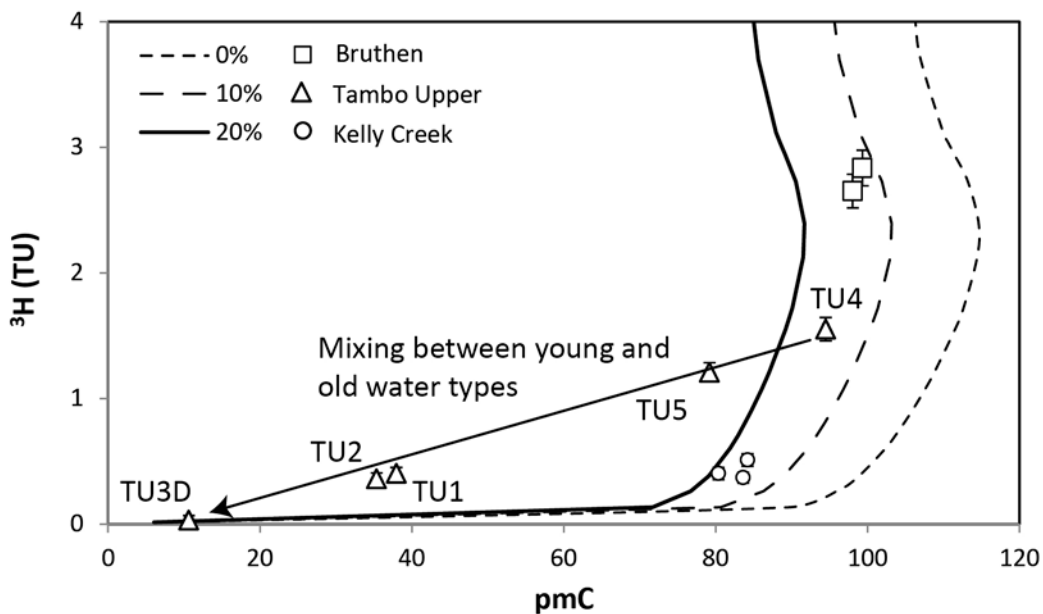


Figure 9. Co-variance of ^3H and ^{14}C in groundwater and that predicted by eqn 1 for 0%, 10% and 20% DIC input from closed systems calcite dissolution.

This indicates that groundwater from Bruthen has a relatively high renewal rate compared to groundwater from Kelly Creek and <20% closed system calcite dissolution, as is consistent with aquifers dominated by siliclastic sediments (Vogel, 1970; Clark and Fritz, 1997). By contrast, groundwater from TU1, TU2 and TU5 at Tambo Upper follow a trend consistent with the mixing between groundwater in the shallow aquifer that has higher renewal rates (TU4), and groundwater in the deeper semi-confined aquifer that has lower renewal rates (TU3D) (Fig. 9). The trend indicates increased leakage from the deeper aquifer into the surface aquifer closer to the river at TU1 and TU2. This is consistent with higher groundwater levels and electrical conductivities at TU1 and TU2 (Fig. 3) that would result from increased connectivity with artesian groundwater in the deeper, semi-confined aquifer. This connection may have resulted from erosion of the clay layers closer to the Tambo River during periodic flooding.

3.4.3 Groundwater residence times and mixing

Groundwater residence times were calculated using the ^3H activities and the EPFM with $f = 0.8$. Groundwater from Bruthen has relatively short residence times of 2 to 4 years. Groundwater from Kelly Creek has longer residence times (96 to 100 years), which is consistent with the higher degrees of mineral dissolution at Kelly Creek discussed previously. Groundwater from TU4 at Tambo Upper has an intermediate residence time of 27 years. The ^3H and ^{14}C activities of these samples are similar to what is expected where there has been minimal mixing between older and younger groundwater (c.f. Le Gal La Salle et al., 2001). To assess the sensitivity of these results, f values in this study were varied between 0.6 and 1.0. This results in variations of < 0.1 years at Bruthen and < 15 years at Kelly Creek. Uncertainties in groundwater age based on the uncertainty of ^3H activities were <1 year at Bruthen (based on an uncertainty of 0.14 tritium units) and < 1.5 years at Kelly Creek (based on an uncertainty of 0.04 tritium

units). As deeper groundwater from Tambo Upper site is ^3H free, residence times were calculated from ^{14}C activities. Making the assumption of 15% calcite dissolution, age estimates based on Clarke and Fritz (1997, their Eq. 2 pg. 206) are ~17,200 years.

The relatively young groundwater residence times from the shallow aquifers implies that groundwater recharge in the area is dominantly local, probably within a few hundreds of metres of the Tambo River. Mean groundwater residence times from the Bruthen bores are similar and within analytical uncertainty, preventing calculation of horizontal flow velocities. Mean groundwater residence times at Kelly Creek increase from 96 years at KC4 to 100 years at KC2. The age of groundwater at KC1 is 99 years and within the analytical uncertainty of groundwater at KC2. Based on these data, groundwater at Kelly Creek has a horizontal flow velocity of between 1.3 and 6.5 m/year towards the river.

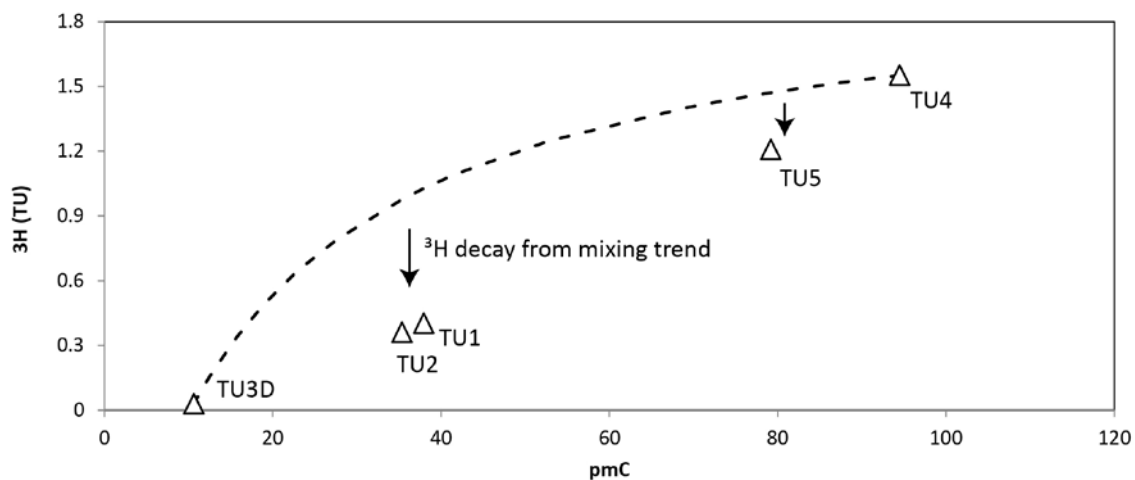


Figure 10. ^3H and ^{14}C activities of groundwater at Tambo Upper and predicted trend for mixing between deep groundwater (TU3D) and shallow groundwater (TU4). Curve based on DIC, ^3H and ^{14}C activities from Table 2.

The ^3H and ^{14}C activities predicted by the mixing between groundwater from TU4 and deeper groundwater are shown in Fig. 10. While it is possible that groundwater from TU4 has already undergone some mixing with deeper groundwater (and C inputs from the aquifer are less than 10% opposed to the 10-20% indicated), this remains difficult to

define. As such, mixing estimates at Tambo Upper will be conservative with respect to the input of deep groundwater. Groundwater from TU1, TU2 and TU5 plot below the mixing trend in Fig. 10. While there are uncertainties in these calculations it is possible that ^3H activities are lower than expected due to the decay of ^3H in shallow groundwater. Exponential piston flow modelling of water at TU1 and TU2 indicates that a residence time of ~20 years would be required to cause the observed deviation in ^3H activities from the mixing trend shown in Fig. 10. This suggests a horizontal flow rate of 1.8 ± 0.6 m/year towards the Tambo River at the Tambo Upper transect. This is consistent with shallow groundwater recharge on the floodplains of the Tambo River and groundwater flow towards the river, as is consistent with a gaining river section as indicated by Unland et al. (2013).

3.4.4 Implications for groundwater – surface water interaction

The distribution of groundwater residence times does not support increased bank storage in the area immediately (within 10's of meters) neighbouring the Tambo River. If this was so, groundwater closer to the Tambo River would contain a higher proportion of younger water than groundwater further from the river and groundwater ages would decline towards the river. Instead, increasing groundwater age with proximity of the Tambo River was found at Kelly Creek and Tambo Upper, while groundwater at Bruthen was approximately the same age at 18 m and 6 m distance from the Tambo River.

As the ^3H and ^{14}C activities were analysed for groundwater sampled in April 2011, these data can only be used to evaluate bank storage for the hydrological conditions leading up to sampling. This included a discharge event that increased river height by 0.5 m approximately 2 weeks prior to sampling. As such, these data indicate that an increase in river height of 0.5 m is not large enough to produce bank storage 5 to 10 m distance from the river for a period greater than 2 weeks. Major ions and stable isotopes were

analysed at several times, including after flood events which increased river height by ~5 m. Again there is little evidence of river water infiltrating into the river banks following these events. The curves expected for the mixing between shallow groundwater furthest from the river, deep groundwater, and river water at each transect with respect to Cl:Br, Na:Cl, and K:Cl ratios are shown in Fig. 11.

Data are shown for February 2011 and August 2011 to represent baseflow conditions when bank infiltration is likely to have the least impact on groundwater chemistry and post flood conditions, when bank infiltration is most likely to impact groundwater chemistry. The composition of groundwater from the two bores closest to the Tambo River at each transect are not consistent with the trends expected for mixing between river water and deep or shallow groundwater further from the river.

These observations indicate that either river water penetrates <5 m into the banks during flooding, or that the hydrogeological processes outlined above including aquifer mixing, water rock interaction or the mobilisation and infiltration of Cl from the soil profile have a greater impact on the chemistry of water in the river banks than bank infiltration (Fig. 12). Similarly, $\delta^2\text{H}$ and $\delta^{18}\text{O}$ values of groundwater closer to the Tambo River do not decline after significant flooding, as would be expected for the infiltration of river water with the lower $\delta^2\text{H}$ and $\delta^{18}\text{O}$ values observed during flooding. Again, this suggests limited bank infiltration. The absence of significant bank infiltration may result from similar processes to those identified in Vekerdy and Meijerink (1998) and Wett et al. (2002), who found bank infiltration to be minimal in confined and semi-confined aquifers where pressure loading from the flood wave propagated rapidly into the neighbouring aquifers, limiting bank infiltration. While most bores near the Tambo River are screened in the alluvial aquifer which is unconfined, leakage of the underlying semi-confined aquifer into the alluvial aquifer does occur (Fig. 9).

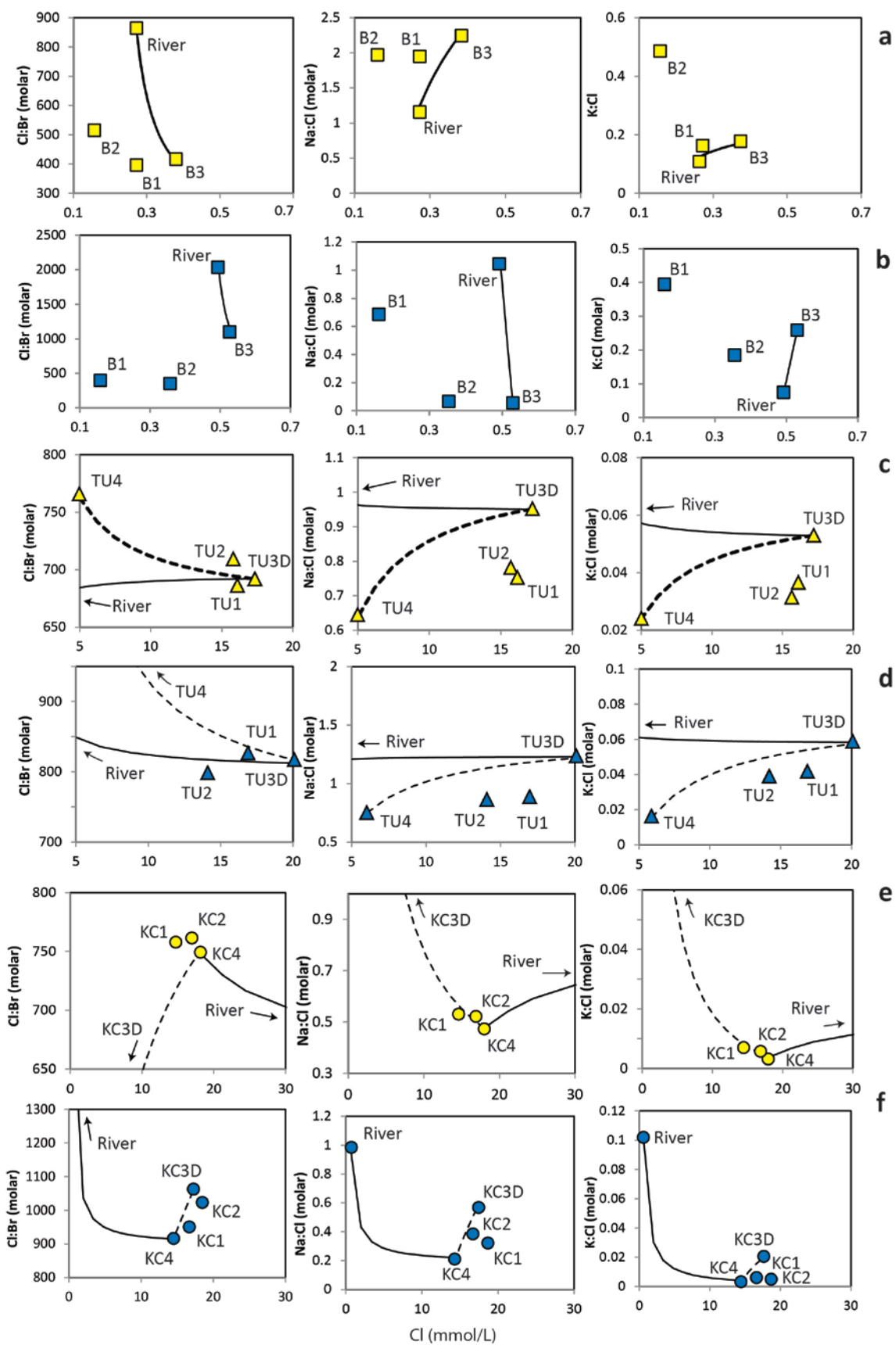


Figure 11. Predicted mixing curves between river water and groundwater at Bruthen (a,b), Tambo Upper (c,d) and Kelly Creek (e,f). Yellow data points = February 2011, blue data points = August 2011.

As such, it may be that pressure has propagated rapidly into the semi-confined aquifers of the area, and subsequently into the alluvial aquifer where confining layers are less prevalent – as is expected in river banks where erosive processes will actively diminish the formation of confining layers (Rinaldi and Darby, 2007).

It is however possible that bank storage is occurring, but that the gaining nature of the Tambo River near these transects is driving the return of bank water back into the river before sampling has taken place (Fig. 12). If this is the case, the storage period is significantly shorter than predicted by modelling eg: (Cooper, 1963; Doble et al., 2012; McCallum et al., 2010; Whiting and Pomeranets, 1997), with no discernible chemical change in bank water within ~1 week of a flood peak. In terms of groundwater age, it is possible that a higher proportion of recently infiltrated river water does remain in the river bank closer to the river, but horizontal groundwater flow velocities are slower than estimated. For example, if groundwater at Kelly Creek had a horizontal flow velocity half that of the 3.9 m/year estimated (1.95 m/year), groundwater closer to the river would have a mean residence time of 177 years instead of the 99 years modelled.

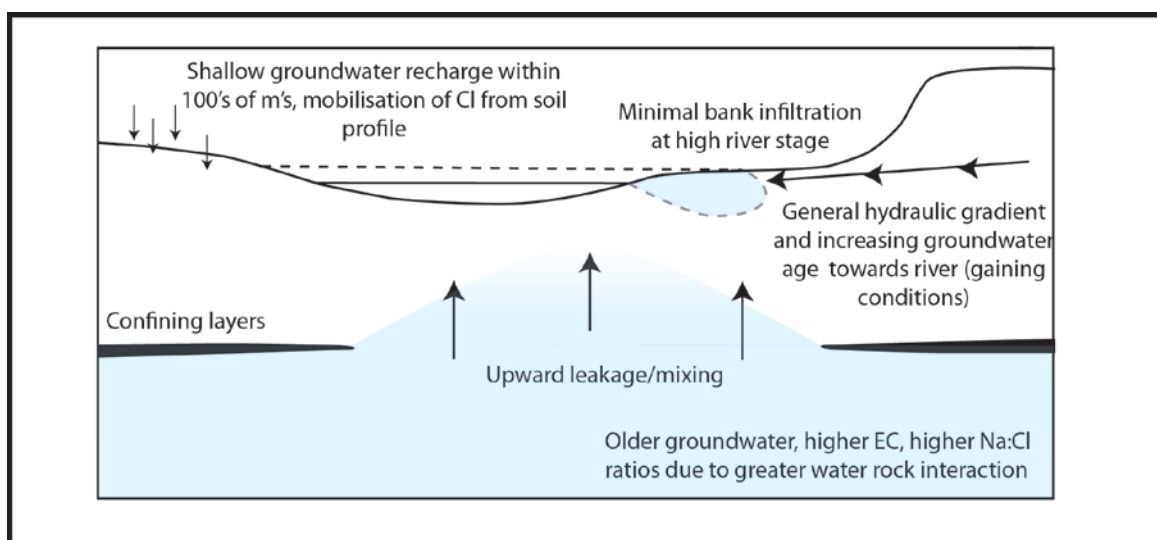


Figure 12. Schematic representation of the Tambo River and major hydrogeochemical processes in the presence of discontinuous semi-confining layer at baseflow (solid line) and high flow (dashed line) conditions.

It could be that this is this case, and that increased mixing between river water and groundwater closer to the river has resulted in the groundwater residence times that have been calculated. Under this scenario, it would require only a 10% input of river water to increase the ^3H activity to the observed 0.40 TU (assuming river water has an atmospheric ^3H activity). While this would also cause an increase in the ^{14}C activities, a 10% input of river water containing modern ^{14}C activities could be offset by an extra 2% DIC input from carbonate dissolution, which is possible. In any case, these results suggest that if a higher proportion of infiltrated river water is present closer to the river, it does not chemically reflect a significant proportion groundwater compared to locally recharged groundwater. This shows that if bank storage processes are occurring, the impact of such processes on groundwater chemistry may be insignificant with respect to groundwater discharge studies, riparian ecology and river chemistry.

3.5 Conclusions

The mean groundwater residence times and horizontal flow velocities of groundwater in the alluvial aquifer system peripheral to the Tambo River determined using ^3H and ^{14}C activities indicates that recharge is dominantly local (within 100's of meters of the Tambo River). The covariance between ^3H and ^{14}C activities show that mixing between relatively old groundwater from a deeper semi-confined aquifer, and younger groundwater from the unconfined alluvial aquifer is occurring in parts of the Tambo River bank. It is further shown that by coupling ^3H and ^{14}C to define a mixing trend, deviations in the activity of ^3H from the trend can be used to estimate the likely age of groundwater along its flow path. Na:Cl ratios >1 in groundwater sampled during baseflow conditions and in older groundwater from the area indicate the dissolution of Na bearing minerals and is consistent with the weathering of silicic sands in the aquifer. Increasing Cl:Br ratios and increasing Cl concentrations during periods of increased

rainfall indicate an input of Cl, as is consistent with the mobilisation of Cl accumulated in the soil profile through the use of fertilizers. Increasing groundwater age with proximity to the Tambo River is consistent with the gaining nature of the Tambo River, but does not suggest that exchange between groundwater and surface water increases with increasing proximity to the river. Major ions, $\delta^2\text{H}$ and $\delta^{18}\text{O}$ values support this and do not show trends consistent with an increased input of river water to the groundwater closer to the river. These results suggest that either the strongly gaining nature of the Tambo River at the study locations is preventing significant lateral infiltration of river water into the bank, or that the rapid propagation of pressure into the underlying semi-confined aquifer, followed by leakage into the above unconfined aquifer is preventing significant bank infiltration. These results are indicative of the highly complex nature of groundwater and surface water processes that may be occurring within river banks and illustrates that while models can significantly help in conceptualising our understanding of groundwater-surface water interactions, field studies can offer complementary information that may otherwise be overlooked.

Acknowledgements

We would like to thank Massimo Raveggi and Rachelle Pierson for their help with major ion analyses. ^3H and ^{14}C analysis at ANSTO was conducted with the help of AINSE funding. Further funding for this research was provided by the National Centre for Groundwater Research and Training, an Australian Government initiative, supported by the Australian Research Council and the National Water Commission.

References

Allison, G.B., Hughes, M.W., 1977. The history of tritium fallout in southern Aust and inferred from rainfall and wine samples. *Earth and Planetary Sci. Lett.* 36, 334-340.

-
- Birch, W.D., 2003. *The Geology of Victoria*. Geological Society of Australia (Victorian Division), Sydney.
- Boulton, A.J., 1993. Stream ecology and surface-hyporheic hydrologic exchange: Implications, techniques and limitations. *Marine and Freshwater Research*, 44(4): 553-564.
- Boulton, A.J., 2005. Chances and challenges in the conservation of groundwaters and their dependent ecosystems. *Aquatic Conservation: Marine and Freshwater Ecosystems*, 15(4): 319-323.
- Bourg, A.C.M., Bertin, C., 1993. Biogeochemical processes during the infiltration of river water into an alluvial aquifer. *Environmental Science & Technology*, 27(4): 661-666.
- Bureau of Meteorology: Commonwealth of Australia, available at: <http://www.bom.gov.au> (last access: 28 August 2013), 2013.
- Cartwright, I., Morgenstern, U., 2012. Constraining groundwater recharge and the rate of geochemical processes using tritium and major ion geochemistry: Ovens catchment, southeast Australia. *Journal of Hydrology*, 475(0): 137-149.
- Cartwright, I., Weaver, T. R., Simmons, C. T., Fifield, L. K., Lawrence, C. R., and Chisari, R., 2010. Physical hydrogeology and environmental isotopes to constrain the age, origins, and stability of a low-salinity groundwater lens formed by periodic river recharge: Murray Basin, Australia. *Journal of Hydrology*, 380(1-2): 203-221.
- Cartwright, I., Weaver, T.R., Stone, D., Reid, M., 2007. Constraining modern and historical recharge from bore hydrographs, ^3H , ^{14}C , and chloride concentrations: Applications to dual-porosity aquifers in dryland salinity areas, Murray Basin, Australia. *Journal of Hydrology*, 332(1-2): 69-92.
- Cendón D.I., Larsen J.R., Jones B.G., Nanson G.C., Rickleman D., Hankin S.I., Pueyo J.J. Maroulis J., 2010. Freshwater recharge into a shallow saline groundwater system, Cooper Creek floodplain, Queensland, Australia. *Journal of Hydrology* 392, 150-163.
- Cey, E.E., Rudolph, D.L., Aravena, R., Parkin, G., 1999. Role of the riparian zone in controlling the distribution and fate of agricultural nitrogen near a small stream in southern Ontario. *Journal of Contaminant Hydrology*, 37(1-2): 45-67.
- Chen, X., Chen, D.Y., Chen, X.-h., 2006. Simulation of baseflow accounting for the effect of bank storage and its implication in baseflow separation. *Journal of Hydrology*, 327(3-4): 539-549.
- Chen, X., Chen, X., 2003. Stream water infiltration, bank storage, and storage zone changes due to stream-stage fluctuations. *Journal of Hydrology*, 280(1-4): 246-264.
- Coplen, T.B., 1988. Normalisation of oxygen and hydrogen isotope data. *Chemical Geology: Isotope Geoscience section*, 72(4): 293-297.
- Cooper, H.H., Rorabaugh, M.I., 1963. Ground-water movements and bank storage due to flood stages in surface streams, United States Department of the Interior, Geological Survey Water-Supply Paper, Washington.
- Clark, I.D., Fritz, P., 1997. *Environmental Isotopes in Hydrogeology*. Lewis, New York, USA, 206 pp.
- Doble, R., Brunner, P., McCallum, J., Cook, P.G., 2012. An Analysis of River Bank Slope and Unsaturated Flow Effects on Bank Storage. *Ground Water*, 50(1): 77-86.
- Department of Environment and Primary Industries: available at: <http://vro.dpi.vic.gov.au/dpi/vro/vrosite.nsf/pages/water-gw-quality-quantity> (last access: 5 July 2013), 2013.
-

- Department of Agriculture, Fisheries and Forrestry: available at:
<http://adl.brs.gov.au/water2010/pdf/catchment2230summary.pdf> (last access: 19 November 2012), 2006.
- Edmunds, W.M., 2009. Geochemistry's vital contribution to solving water resource problems. *Applied Geochemistry*, (24): 1058-14073.
- Fetter, C. W. 1994. *Applied Hydrogeology*. Merrill, New Jersey.
- Fink, D., Hotchkis, M., Hua, Q., Jacobsen, G., Smith, A.M., Zoppi, U., Child, D., Mifsud, C., Vender Gaast, H., Williams, A., Williams, M., 2004. The Antares AMS facility at ANSTO. *Nuclear Instruments and Methods in Physics Research*, 109-115.
- Fontes, J.-Ch., 1983. Dating of Groundwater. *Guidebook on Nuclear Techniques in Hydrology*. Technical Reports Series No. 91, IAEA, Vienna. pp. 285–317.
- Fukada, T., Hiscock, K.M., Dennis, P.F., Grischek, T., 2003. A dual isotope approach to identify denitrification in groundwater at a river-bank infiltration site. *Water Research*, 37(13): 3070-3078.
- Gray, D.R., Foster, D.A., 2004. Tectonic evolution of the Lachlan Orogen, southeast Australia: historical review, data synthesis and modern perspectives. *Australian Journal of Earth Sciences*, 51(6): 773-817.
- Griffioen J., 2001, Potassium adsorption ratios as an indicator for the fate of agricultural potassium in groundwater: *Journal of Hydrology*, 254(1–4), 244–254.
- Herczeg, A.L., Dogramaci, S.S., Leany, F.W., 2001. Origin of dissolved salts in a large, semi-arid groundwater system: Murray Basin, Australia. *Marine Freshwater Research*, (51): 41-52.
- Hiscock, K.M., Grischek, T., 2002. Attenuation of groundwater pollution by bank filtration. *Journal of Hydrology*, 266(3–4): 139-144.
- Hocking, J.B., 1976. Definition and revision of Tertiary stratigraphic units, onshore Gippsland Basin, Geological Survey of Victoria.
- Hofmann, H., Cartwright, I., 2013. Using hydrogeochemistry to understand inter-aquifer mixing in the on-shore part of the Gippsland Basin, southeast Australia. *Applied Geochemistry*, 33(0): 84-103.
- Hughes, C. E., and Crawford, J., 2012. A new precipitation weighted method for determining the meteoric water line for hydrological applications demonstrated using Australian and global GNIP data: *Journal of Hydrology*, 464–465(0): 344-351.
- Hua, Q., Barbetti, M., Rakowski, A.Z., 2013. Atmospheric Radiocarbon for the period 1950–2010. *Radiocarbon*, 55(4): 2059-2072.
- Kapostasy, S., 2002. Haunted Hill Gravel: Deposition and Neotectonic History along the Southern Australian Coast. In: Palmer, B.A. (Ed.), *Keck Geology Consortium*, Wisconsin, USA.
- Lambs, L., 2004. Interactions between groundwater and surface water at river banks and the confluence of rivers. *Journal of Hydrology*, 288(3–4): 312-326.
- Lamontagne, S., Leaney, F.W., Herczeg, A.L., 2005. Groundwater-surface water interactions in a large semi-arid floodplain: implications for salinity management. *Hydrological Processes*, 19(16): 3063-3080.
- Lamontagne, S., Taylor, A.R., Cook, P.G., Barrett, C., 2011. Interconnection of Groundwater Systems – River Losses from Losing/Disconnected Streams. Gwydir River Site Report. Gwydir River site report. CSIRO: Water for a Healthy Country National Research Flagship, Adelaide. 31 pp
- Le Gal La Salle, C., C., Marlin, C., Leduc, C., Taupin J.D., Massault, M. and Favreau, G. 2001. Renewal rate estimation of groundwater based on radioactive tracers (^3H , ^{14}C)

- in an unconfined aquifer in a semi-arid area, Iullemeden Basin, Niger. *Journal of Hydrology*, 254(1–4): 145-156.
- Leonard, J.G., 1992. An overview of Victoria's groundwater resources. Background report S3, short term planning guidelines. Drought management plan for Victoria's water resources, Department of Water Resources, Melbourne, Victoria.
- Maloszewski, P., Zuber, A., 1991. Influence of Matrix Diffusion and Exchange Reactions on Radiocarbon Ages in Fissured Carbonate Aquifers. *Water Resources Research*, 27(8): 1937-1945.
- Małoszewski, P., Zuber, A., 1982. Determining the turnover time of groundwater systems with the aid of environmental tracers: 1. Models and their applicability. *Journal of Hydrology*, 57(3–4): 207-231.
- McCallum, J.L., Cook, P.G., Brunner, P., Berhane, D., 2010. Solute dynamics during bank storage flows and implications for chemical base flow separation. *Water Resour. Res.*, 46(7): W07541.
- Morgenstern, U., Stewart, M.K., Stenger, R., 2010. Dating of streamwater using tritium in a post-bomb world: continuous variation of mean transit time with streamflow. *Hydrol. Earth Syst. Sci.* (14): 2289-2301.
- Morgenstern, U., Taylor, C.B., 2009. Ultra low-level tritium measurement using electrolytic enrichment and LSC. *Isot. Environ. Health.*, (45) 96–117.
- Panno, S.V. et al., 2006. Source identification of sodium and chloride in natural waters: Preliminary results. *Ground Water*, 44(2): 176-187.
- Pinder, G.F., Sauer, S.P., 1971. Numerical simulation of flood wave modification due to bank storage effects. *Water Resources Research*, 7(1): 63-70.
- Rinaldi, M., Darby, S.E., 2007. 9 Modelling river-bank-erosion processes and mass failure mechanisms: progress towards fully coupled simulations. In: Helmut Habersack, H.P., Massimo, R. (Eds.), *Developments in Earth Surface Processes*. Elsevier, pp. 213-239.
- Schachtman, D.P., Schroeder, J.I., 1994. Structure and transport mechanism of a high-affinity potassium uptake transporter from higher plants. *Nature*, 370(6491): 655-658.
- Singh, K.P., 1968. Some Factors Affecting Baseflow. *Water Resources Research*, 4(5): 985-999.
- Stuiver, M. and Polach, H.A., 1977. Reporting of ^{14}C data. *Radiocarbon*, 19, 355-363.
- Suess, H., 1971. Climatic changes and atmospheric radiocarbon. *Palaeogeography Palaeoclimatology Palaeoecology* 10, 199–202.
- Tadros, C.V., Hughes, C.E., Crawford, J.C., Hollins, S.E. and Chisari, R., 2014. Tritium in Australian precipitation: a 50 year record. *Under review, Journal of Hydrology*.
- Unland, N.P. et al., 2013. Investigating the spatio-temporal variability in groundwater and surface water interactions: a multi-technical approach. *Hydrol. Earth Syst. Sci. Discuss.*, 10(3): 3795-3842.
- Vekerdy, Z., Meijerink, A.M.J., 1998. Statistical and analytical study of the propagation of flood-induced groundwater rise in an alluvial aquifer. *Journal of Hydrology*, 205(1–2): 112-125.
- Victorian Water Resources Data Warehouse: available at:
<http://www.vicwaterdata.net/vicwaterdata/home.aspx> (last access: 28 August 2013), 2013.
- Vogel, J.C., 1970. Groningen radiocarbon dates IX. *Radiocarbon* 12, 444–471.
- Wett, B., Jarosch, H., Ingerle, K., 2002. Flood induced infiltration affecting a bank filtrate well at the River Enns, Austria. *Journal of Hydrology*, 266(3–4): 222-234.

- Whiting, P.J., Pomeranets, M., 1997. A numerical study of bank storage and its contribution to streamflow. *Journal of Hydrology*, 202(1–4): 121-136.
- Winter, T.C., Harvey, J.W., Franke, O.L., Alley, W.M., 1998. Ground water and surface water a single resource, U.S. Geological Survey Circular.
- Woessner, W.W., 2000. Stream and fluvial plain ground water interactions: Rescaling hydrogeologic thought. *Ground Water*, 38(3): 423-429.
- Zuber, A. et al., 2005. Groundwater dating with ^3H and SF_6 in relation to mixing patterns, transport modelling and hydrochemistry. *Hydrological Processes*, 19(11): 2247-2275.

Chapter 4

The dynamics and modelling of river – groundwater exchange in river banks

N .P. Unland^{1,2}, I. Cartwright^{1,2}, E. Daly^{2,3}, B. S. Gilfedder^{1,2,4}, A.P. Atkinson^{1,2}

^[1] *School of Geosciences, Monash University, Clayton, Vic. 3800, Australia*

^[2] *National Centre for Groundwater Research and Training, GPO box 2100, Flinders University, Adelaide, SA 5001, Australia*

^[3] *Department of Civil Engineering, Monash University, Clayton, Vic. 3800, Australia*

^[4] *Department of Hydrology, University Bayreuth, Bayreuth, Germany*

In preparation for publication

Abstract

Understanding groundwater-surface water exchange in river banks is crucial for a range of different scientific disciplines and effective water management. While much research has focussed on understanding these processes analytically and numerically, many studies assume idealised, simple and homogeneous aquifer systems. This paper presents a field study of the Tambo River (South East Australia) that interacts with an unconfined aquifer containing relatively young and low salinity young groundwater (<500 $\mu\text{S}/\text{cm}$ and <100 years old), which is receiving upward leakage from an underlying artesian, semi-confined aquifer that contains relatively old and saline groundwater ($\text{EC} > 2,500 \mu\text{S}/\text{cm}$ and > 10,000 years old). Continuous groundwater elevation and EC monitoring along the river bank within the different aquifers and the river suggests that the degree of mixing between the two aquifers and the river varies significantly in response to changing hydrological conditions. Numerical modelling using MODFLOW indicates that saline

water moves into the river bank during flooding as hydraulic gradients reverse. This water then returns during flood recession as baseflow hydraulic gradients are re-established. Modelling also indicates that this process will increase groundwater concentrations for up to ~34 days between 20 and 40 meters of the river for flood events as large as 9.7 m in height. For the same flood event, groundwater concentrations within 10 m of the river will increase for only ~15 days as the infiltrating low salinity river water drives groundwater dilution. Average groundwater fluxes to the river stretch estimated using Darcy's Law were $7 \text{ m}^3/\text{m}/\text{day}$ compared to 26 and $3 \text{ m}^3/\text{m}/\text{day}$ for the same periods via ^{222}Rn and Cl mass balance, respectively. This study shows that by coupling numerical modelling with continuous groundwater-surface water monitoring, the transient nature of groundwater-surface water exchange can be better evaluated, leading to a better understanding of the hydrological system and better interpretation of hydrochemical data.

4.1. Introduction

Hydraulic gradients orientated towards a river drive the discharge of groundwater from alluvial aquifers into gaining river sections under baseflow conditions. However, during increased river stage, the hydraulic gradient may be reversed resulting in the infiltration of river water into the alluvial aquifer. As flood events subside and river height falls, streamward hydraulic gradients re-establish and the recently infiltrated water will return to the river. Although this process, termed bank storage, is conceptually well understood (eg: Hantush et al., 2002; Nowinski et al., 2012; Sophocleous, 2002; Winter, 1995), such complex interactions between rivers and alluvial aquifers are commonly overlooked in hydrological studies (Burt et al., 2002). Understanding these interactions is important for calculating water balances in river basins (Pinder and Sauer, 1971), investigating chemical cycling in river banks (Bourg and Bertin, 1993; Fukada et al., 2003), maintaining healthy river and riparian ecology (Boulton, 1993; Boulton, 2005;

Brunke and Gonser, 1997; Cey et al., 1999; Lambs, 2004; Lamontagne et al., 2005; Woessner, 2000), developing water extraction systems (Hiscock, 2005) and calculating groundwater discharge to rivers (McCallum et al., 2010; Unland et al., 2013).

Bank storage may be simulated using both analytical solutions (Cooper and Rorabaugh, 1963; Moench and Barlow, 2000; Moench et al., 1974; Zlotnik and Huang, 1999) and numerical models (Chen et al., 2006; Pinder and Sauer, 1971; Squillace, 1996; Whiting and Pomeroy, 1997). While such studies have significantly added to the understanding of bank exchange processes, most assume simplified or ideal conditions, making results hard to apply to settings where conditions are more complex (Doble et al., 2012). For example, the majority of numerical bank storage studies involve single homogeneous, unconfined and/or infinite aquifers which may not be a good approximation of specific field examples.

In Chapter 3, the age, geochemical evolution and flow regime of water stored in the banks of the Tambo River, in South East Australia, was investigated by discrete geochemical sampling under hydrological conditions ranging from baseflow to post flood. Groundwater dating via ^3H and ^{14}C analysis indicated that relatively young groundwater (<100 years) is stored in the river banks of the Tambo River, and that these waters increase in age with proximity to the river, as is consistent with gaining conditions and not increased bank storage near the river. Further to this, trends given by major ions, oxygen isotopes and hydrogen isotopes were not consistent with mixing between river water and local or regional groundwater. The study also identified a deeper, semi-confined aquifer in the area that contains significantly older (>10,000 years) and more saline water than the overlying unconfined aquifer. The study suggests that in contrast to many of the above papers which assert significant bank storage for months to years after flooding, bank storage in the Tambo River is minimal, resulting in very little change in

the mean groundwater residence time or the geochemistry of the bank water for days to weeks after flooding.

It was hypothesized that either the strongly gaining nature of the Tambo River or the presence of the semi-confined aquifer in the area reduces the potential for bank storage. This paper tests these hypotheses by combining continuous groundwater-river monitoring and numerical modelling using MODFLOW to investigate processes that may impact groundwater - surface water exchange in the banks of the Tambo River. Through the use of high frequency data collection (30 minutes) over an extended time period (~2 years), the exchange between groundwater and surface water under changing hydrological conditions may be investigated, allowing better groundwater flux estimates and an improved understanding of hydrochemical processes occurring in river banks. Ultimately this study aims to provide insight into the complexities of groundwater-surface water processes in river banks under changing hydrological conditions, and to analyse the impact that the presence of semi-confined aquifers have on bank storage.

4.2 Methods

4.2.1 Study Area

Investigations took place on the Tambo River in the Tambo River Basin, South East Australia. The Tambo River Basin extends southwards from the Eastern Victorian Uplands to the Gippsland Basin (Fig. 1). The Eastern Victorian Uplands are dominated by low-grade metamorphosed Ordovician and Devonian sandstones, shales and turbidites that have been intruded by Devonian granites (Gray and Foster, 2004). The Gippsland Basin hosts a complicated aquifer system that is underlain by Palaeozoic basement. While the basement acts as a fractured rock aquifer, groundwater yields are insignificant in comparison with overlying sedimentary aquifers (Birch, 2003).

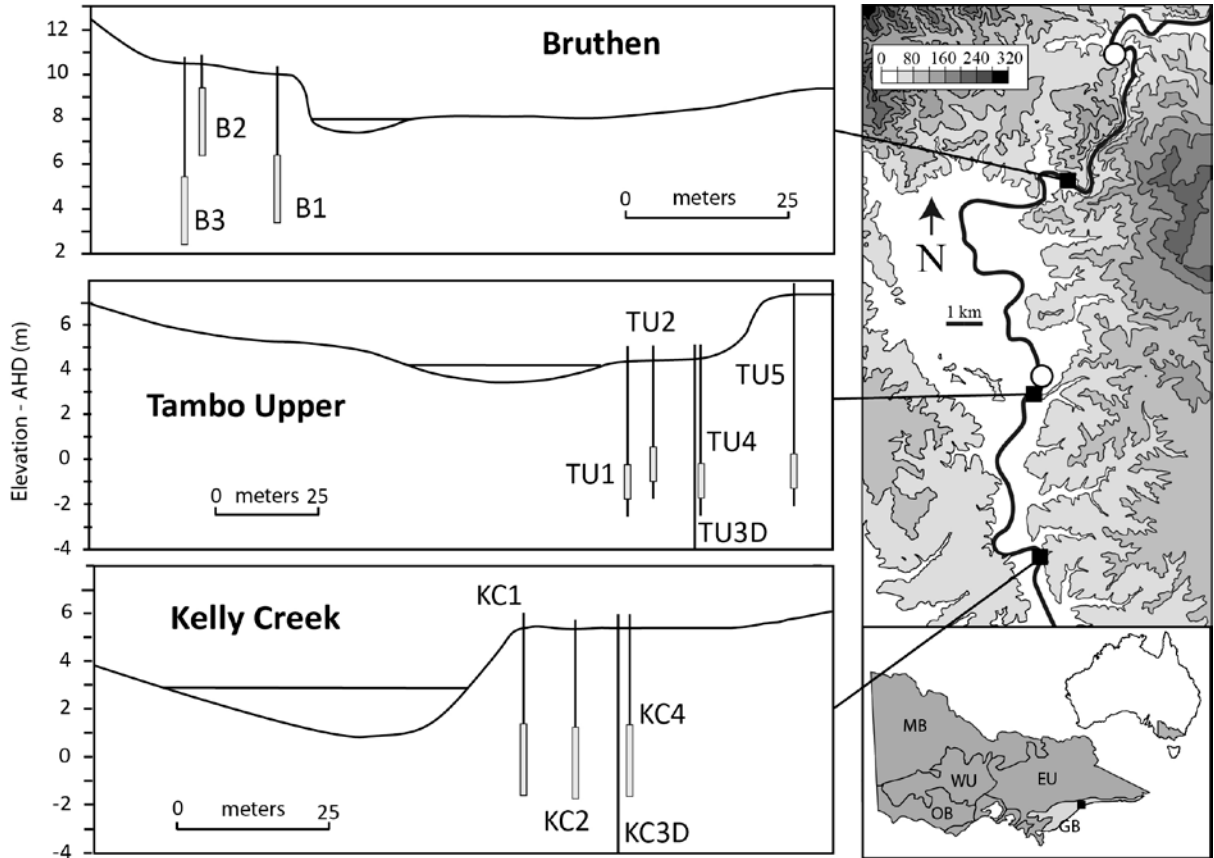


Figure 1. Schematic representation of monitoring bores along the Tambo River bank at Bruthen, Tambo Upper and Kelly Creek. Local elevation (m) and location of field area with respect to regional geology from Jolly (1997) on right, GB=Gippsland Basin, EU=Eastern Victorian Uplands, WU=Western Victorian Uplands, OB=Otway Basin, MB=Murray Basin. Black squares = field sites, white circles = river gauging stations.

The Plio-Pleistocene Haunted Hill Gravels is the shallowest aquifer over most of the Gippsland Basin. It is primarily composed of quartz with some feldspar, granitic fragments, tourmaline and cassiterite (Kapostasy, 2002). The Haunted Hill Gravels are underlain by the Late Miocene to Early Pliocene Boisdale Formation which is composed of sands, gravels and clays interlayed with minor Tertiary basalts, limestones and marls (Birch, 2003). These formations are locally covered by Quaternary alluvium derived from the Eastern Victorian Uplands along the major river valleys. Clay layers throughout the Quaternary alluvium, Haunted Hill Gravels and Boisdale Formations behave as aquitards, separating a number of aquifer horizons. This results in a complex aquifer system throughout the region with highly variable connectivities (Hocking, 1976). While a

number of deeper aquifers occur in the Gippsland Basin (including the Oligocene-Pliocene Jemmys Point, Tambo River and Lake Wellington Formations), they are >50 m deep and do not interact with rivers in the area (Hofmann and Cartwright, 2013; Leonard, 1992).

Annual rainfall in the Tambo River Basin is ~700 mm (Bureau of Meteorology, 2013). The Tambo River is perennial and flows south from the Victorian Uplands through the Gippsland Basin before reaching the saline and tidal Lake King. Under baseflow conditions the lower ~15 km of the river becomes estuarine through mixing with Lake King, however the length of this section is significantly reduced under high flow conditions. Throughout the period of this study (2011-2012), Tambo River discharge varied from $8.9 \times 10^4 \text{ m}^3/\text{day}$ under baseflow conditions to $6.4 \times 10^7 \text{ m}^3/\text{day}$ under high flow conditions.

Continuous monitoring of groundwater elevations and electrical conductivities (EC) took place at three transects (as outlined Fig. 1 of Chapter 3). These include 3 monitoring bores at Bruthen (25.8 km upstream of Lake King) which are 5.5, 17.6 and 18.3 m from the Tambo River and 8.0, 5.4 and 7.1 m below ground surface, respectively (Fig. 1). Five monitoring bores at Tambo Upper (20.2 km upstream of Lake King) which are 8.8, 15.0, 22.3, 23.8 and 37.9 m from the Tambo River and 6.7, 6.2, 23.1, 6.7 and 9.8 m below ground surface, respectively. Four monitoring bores at Kelly Creek (13.8 km upstream of Lake King) which are 7.0, 17.9, 24.9 and 26.8 m from the Tambo River and 8.1, 7.8, 28 and 7.9 m below ground surface, respectively. At Kelly Creek and Bruthen, screened sections are set at the bottom of the bore and are 3 m long while bores at Tambo Upper are screened 1 m from the bottom of the bore and are 1.5 m in length. The deeper bores at both Tambo Upper and Kelly Creek are screened within a semi-confined artesian aquifer, while all other bores are screened in the alluvial aquifer.

4.2.2 Analytical procedure

River and groundwater EC were measured in the field in February 2011, April 2011, August 2011 and March 2012 using a TPS pH/EC meter. The pressure, electrical conductivity (EC) and temperature of groundwater in the monitoring bores were recorded at 30 minute intervals between February 2011 and October 2012 using a combination of Win-Situ Rugged TROLL 100 and Win-Situ Aqua TROLL 200 loggers. Barometric pressure corrections were made using a Rugged Baro TROLL that was deployed at the Tambo Upper site. Measurement precision is $\pm 0.1\%$ for pressure, $\pm 0.1^\circ\text{C}$ for temperature and $\pm 0.5\%$ for EC. Bore heights and river levels were referenced to the Australian Height Datum (AHD) using a Trimble digital global positioning system (DGPS) to $\pm 1\text{cm}$ accuracy. Groundwater elevations were calculated from the pressures using manual measurements made via an electronic water level tape. River levels were measured at the Ramrod Creek and Battens Landing flow gauging stations (Victorian Water Resource Warehouse, 2013) located $\sim 40\text{ km}$ and $\sim 20\text{ km}$ upstream of Lake King (Fig. 1). The river height at Bruthen was calculated by interpolating river height data from Battens Landing and Ramrod Creek station with DGPS data as outlined in Unland et al. (2013).

4.3. Results

4.3.1 Groundwater and surface water elevations

Groundwater elevation at Bruthen was monitored in B1 and B2 during the study (Fig. 2). Groundwater elevations in these bores were generally similar, ranging from 7.38 to 13.91 m at B1 and 7.34 to 13.91 m at B2, while river elevation ranged from 7.27 to 15.15 m. An increase in river and groundwater elevation to $\sim 8.5\text{ m}$ occurred during June 2011, November 2011 and August 2012 in response to increased rainfall in the catchment (Fig. 2). These events were superseded by significant rainfall in the catchment during July 2011, August 2011, March 2012 and June 2012 that resulted in river and groundwater

elevations of 10 to 15 m and flooding in the Tambo Catchment. Groundwater elevations were generally higher than river elevation at Bruthen, however this did reverse during flooding. Groundwater elevations in B1 and B2 over the study were similar (average difference = 0.02 m), however responses in B1 during flooding were quicker than in B2 (giving a maximum difference of 0.55m).

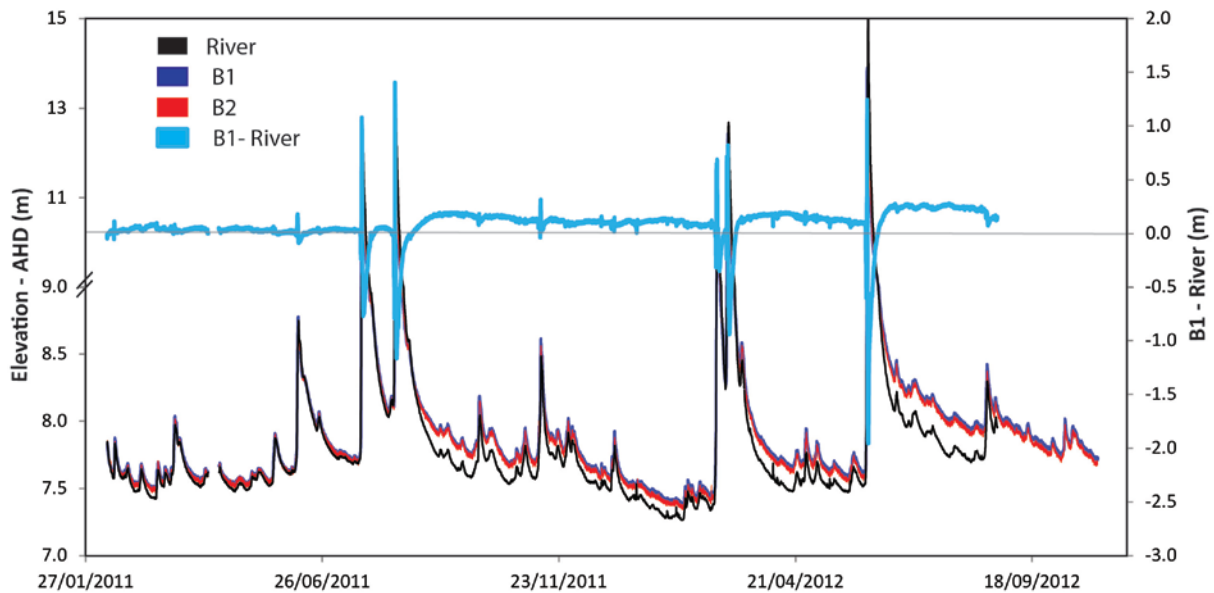


Figure 2. River and groundwater elevation at Bruthen. Difference between groundwater and surface water elevation (B1-River) based on groundwater elevation at B1 and interpolated river elevation at Bruthen. Positive B1-River values = groundwater discharge, negative B1-River values = groundwater recharge. Note break in primary y axis.

Under baseflow conditions, surface water and shallow groundwater elevations at Tambo Upper were ~3.5 m and varied by less than 0.5 m (Fig. 3). The groundwater elevation in the deeper bore at Tambo Upper (TU3D) was generally much higher than in the river or shallow groundwater with minimum elevations of 4.65 m during January and February 2012. Elevations in TU3D exceeded the casing height (5.1 m) for periods of ~1 month during increased rainfall and river flow in June, July, August and November 2011 and March 2012. After the largest flow event in June 2012 the groundwater elevation in TU3D exceeded the casing height for a period of ~100 days. Groundwater elevations in TU1 (8.8 m from river) were generally the highest of the shallow bores, averaging 3.81 m

over the study (Fig. 3). Elevations in TU2 (15.0 m from river) were the next highest (av. = 3.78 m) followed by TU 5 (37.9 m from river) which averaged 3.77 m. Groundwater elevation was generally the lowest in TU4 (23.8 m from river) with an average elevation of 3.69 m. Surface water and shallow groundwater elevations exceeded 4.0 m during June 2011, November 2011 and August 2012. Again, significant rainfall during July 2011, August 2011, March 2012 and June 2012 resulted in flooding throughout the Tambo Catchment, giving rise to increased surface and groundwater elevation at Tambo Upper (>8.0 m, Fig. 3). Surface water elevation was generally lower than groundwater elevation at Tambo Upper, averaging 3.7 m over the study with an average difference of 0.11 m between TU1 and the river (Fig. 3). However as the rivers response to rainfall was more rapid than groundwater, gradients were reversed when river height exceeded 4.0 m.

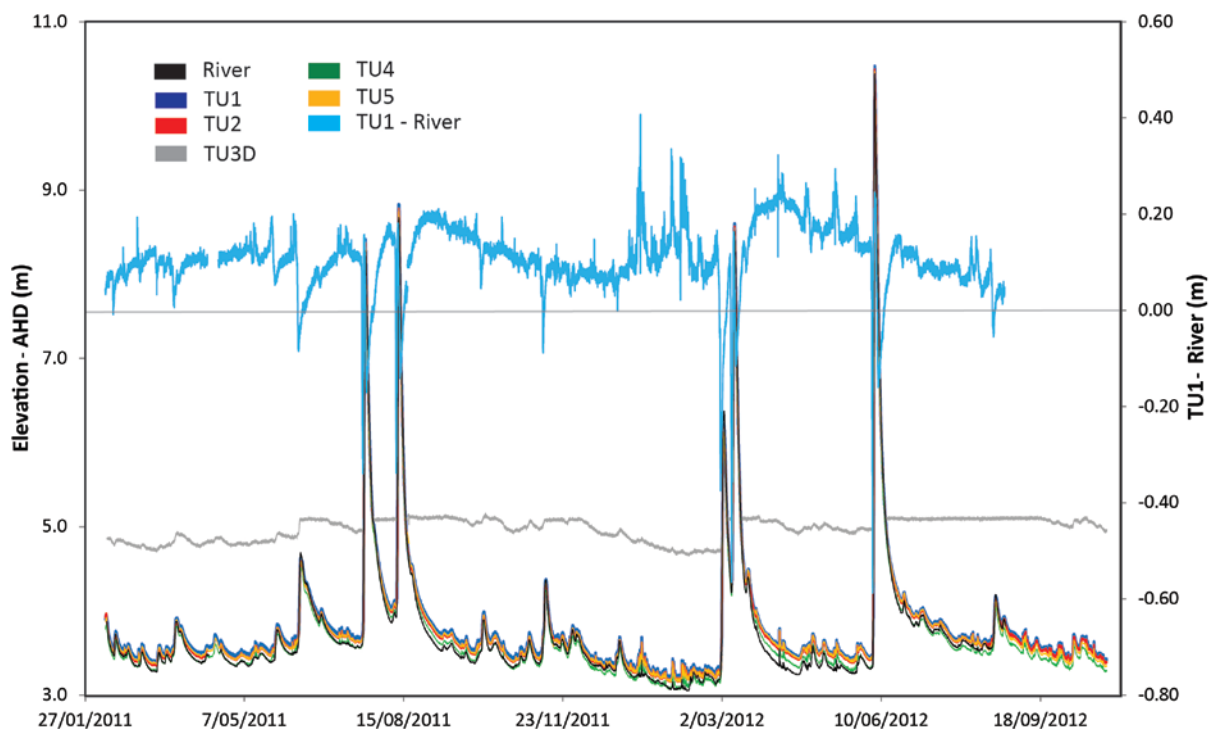


Figure 3. River and groundwater elevation at Tambo Upper. Difference between groundwater and surface water elevation (TU1-River) based on groundwater elevation at TU1 and interpolated river elevation at Tambo Upper. Positive TU1-River values = groundwater discharge, negative TU1-River values = groundwater recharge.

Average groundwater elevations in the shallow bores at Kelly Creek (KC1, KC2 and KC4) were 3.35, 3.33 and 3.38 m, respectively, and were less variable than at Bruthen or Tambo Upper (Fig. 4). Unlike the Bruthen and Tambo Upper sites only the flood events of July 2011, August 2011, March 2012 and June 2012 resulted in groundwater elevations of >5.0 m, and smaller increases in river height were not reflected by increases in groundwater elevation. Similar to Tambo Upper, groundwater elevation in the deeper bore (KC3D, 24.9 m from the Tambo River) was higher than in the shallow bores, ranging from approximately 4 to 5 m under baseflow conditions throughout the study. Under baseflow conditions, groundwater elevation at Kelly Creek showed a periodic increase and decrease of ~0.20 m over ~2 week cycles. This is particularly prevalent prior to flooding in July 2011 and between flooding in March and June 2012 (Fig. 4). Groundwater elevation closest to the Tambo River at Kelly Creek (KC1) was generally higher than the groundwater elevation further from the Tambo River at KC2, with an average difference of 0.02 m. However groundwater elevations in both KC1 and KC2 were lower than the elevations furthest from the Tambo River at KC4, with average differences of 0.05 m and 0.07 m, respectively.

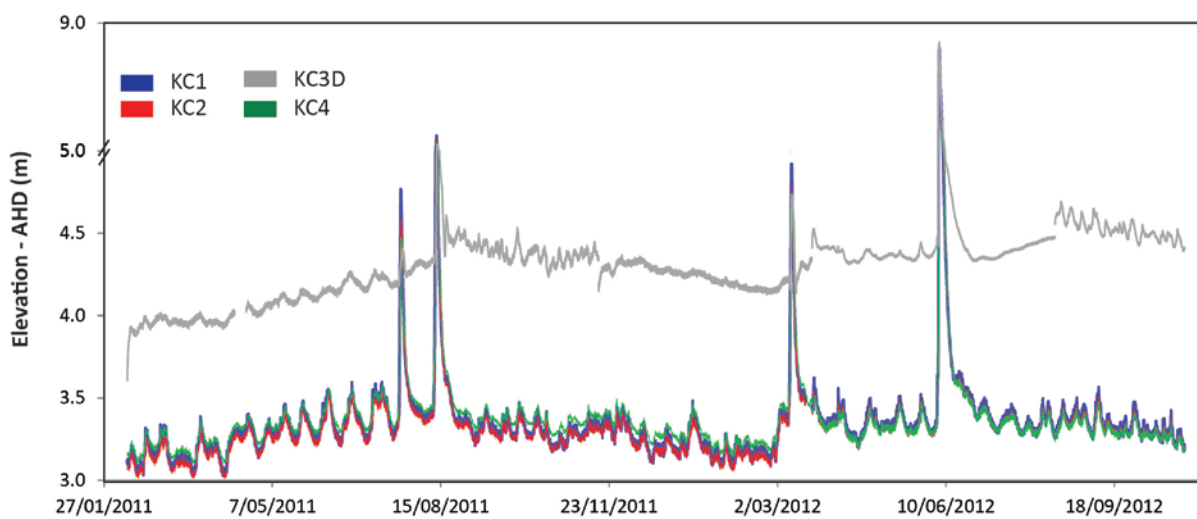


Figure 4. Groundwater elevation at Kelly Creek. River elevation at Kelly Creek not interpolated. Note break in y axis.

4.3.2 Electrical conductivity

River EC values at Bruthen and Tambo Upper were very similar, ranging from 121 to 156 $\mu\text{S}/\text{cm}$ and from 120 to 165 $\mu\text{S}/\text{cm}$, respectively. During baseflow conditions in February 2011 and April 2011, river EC at Kelly Creek was significantly higher (18,300 and 4,200 $\mu\text{S}/\text{cm}$, respectively), indicating the transition into an estuarine environment. During August 2011 and March 2012, river EC at Kelly Creek was more similar to Bruthen and Tambo Upper, with EC values of 170 and 195 $\mu\text{S}/\text{cm}$, respectively.

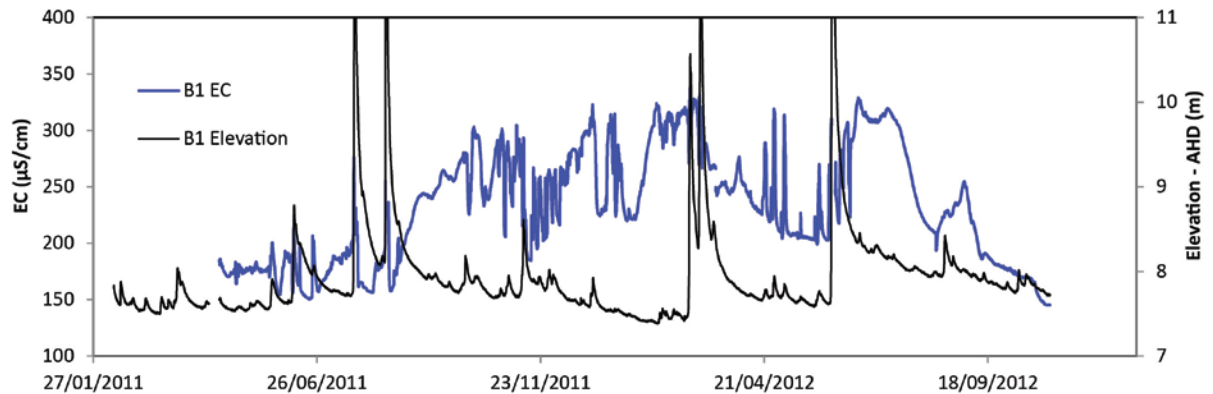


Figure 5. Electrical conductivity of groundwater at Bruthen (B1) and groundwater elevation at Bruthen (B1).

Groundwater EC was generally higher than river EC. At Bruthen, groundwater EC at B1 ranged from 145 to 338 $\mu\text{S}/\text{cm}$ over the study (Fig. 5). While highly variable, groundwater EC tended to increase as groundwater elevation increased, before declining in the days following peaks in groundwater elevation (Fig. 5). Groundwater EC at Tambo Upper showed a similar trend, increasing as groundwater elevation increased and declining in the following days (Fig. 6). Groundwater EC was the highest and most variable closer to the river in TU1, ranging from 1,130 to 3,330 $\mu\text{S}/\text{cm}$ with an average EC of 1,840 $\mu\text{S}/\text{cm}$ over the study. Groundwater EC in TU2 was similar to TU1, ranging from 1,050 to 3,080 $\mu\text{S}/\text{cm}$ with an average of 1,710 $\mu\text{S}/\text{cm}$. Groundwater further from

the river at TU5 had a lower EC than TU 1 or TU2, ranging from 695 to 2,630 $\mu\text{S}/\text{cm}$ with an average of 943 $\mu\text{S}/\text{cm}$ over the study (Fig. 6). The EC of deep groundwater in TU3D was higher and less variable than shallow groundwater at Tambo Upper with an average EC of $2,910 \pm 340$ $\mu\text{S}/\text{cm}$.

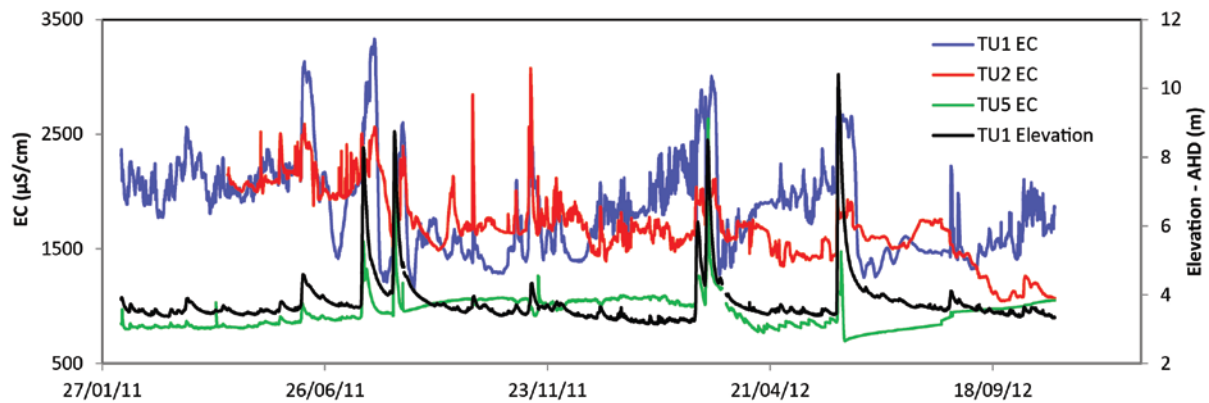


Figure 6. Electrical conductivity of groundwater at Tambo Upper (TU1, TU2 and TU5) superimposed on groundwater elevation (TU1).

Groundwater EC was generally higher at Kelly Creek than at Tambo Upper or Bruthen (Fig. 7). EC ranged from 1,580 to 3,880 $\mu\text{S}/\text{cm}$ at KC1 with an average of 2,700 $\mu\text{S}/\text{cm}$, while EC ranged from 1,990 to 2,760 $\mu\text{S}/\text{cm}$ at KC2 with an average of 2,580 $\mu\text{S}/\text{cm}$. Groundwater in the deeper semi-confined aquifer in KC3D was similar to that in the rest of the transect and showed little variation with an average EC of 2550 ± 190 $\mu\text{S}/\text{cm}$. Groundwater EC at Kelly Creek did not increase with increasing groundwater elevation as at Bruthen and Tambo Upper; however, EC did decline in KC2 after flooding in July 2011, March 2012 and June 2012 (Fig. 7). Abrupt changes in groundwater EC were recorded during April 2011, August 2011 and March 2012 after groundwater sampling occurred. This suggests that water drawn into the monitoring bore during pumping had a different EC to that within the bore prior to pumping. Between March 2012 and June 2012, groundwater EC in KC1 showed a negative correlation with groundwater elevation, while EC in KC2 showed a small positive correlation with

groundwater elevation. These variations are cyclic and occur over periods of approximately 2 weeks.

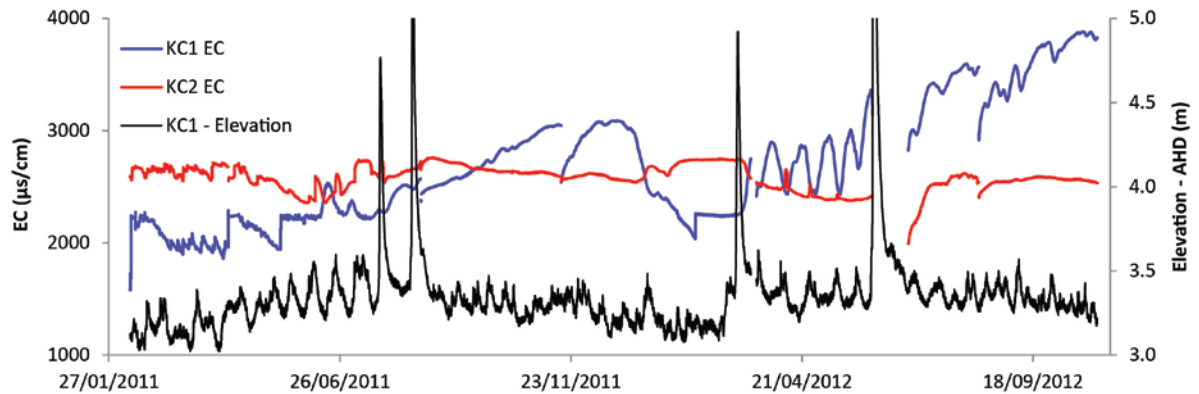


Figure 7. EC of groundwater at Kelly Creek (KC1 and KC2) superimposed over groundwater elevation (KC1).

4.4. Discussion

In this section, the dynamics of groundwater – surface water exchange in river banks are investigated using the high frequency monitoring data from the three sites at different flow conditions, and further evaluated using MODFLOW. Continuous volumetric groundwater fluxes at the groundwater-surface water interface are estimated using Darcy's Law, and are assessed in reference to the conceptual framework provided by numerical modelling and results given by chemical tracing methods (Unland et al., 2013).

4.4.1 The dynamics of groundwater surface water exchange

As river EC at both Bruthen and Tambo Upper transects is lower than groundwater EC, and high EC waters through the area are dominated by Cl which is largely conservative (Chapter 3), the movement of river water into and out of the river bank at these locations can be traced using EC. Bank infiltration will occur when surface water elevation increases above groundwater elevation (Hantush et al., 2002; Sophocleous, 2002). The volume of river water stored in the river bank will continue to

increase during a flood event until surface water elevation returns below groundwater elevation. Thus, bank storage will typically increase from the initial stages of flooding and peak shortly after a flood peak has passed (eg: Chen et al., 2006). Accordingly, the infiltration of low EC river water into the river bank should reduce the EC of near-river groundwater during the early stages of flooding until sometime after the flood peak has passed. However, at both Bruthen and Tambo Upper there is an increase in groundwater EC as river stage rises (Figs 5 and 6). Such responses are shown in Fig. 8 for moderate (a,d), major (b,e) and minor (e,f) flood events that resulted in an increase in groundwater elevation of ~1 m, greater than 3 m and ~0.3 m, respectively. The increase in both groundwater elevation and EC in Fig. 8 suggests that the simple infiltration of river water into the bank is not the major process controlling groundwater salinity at these sites.

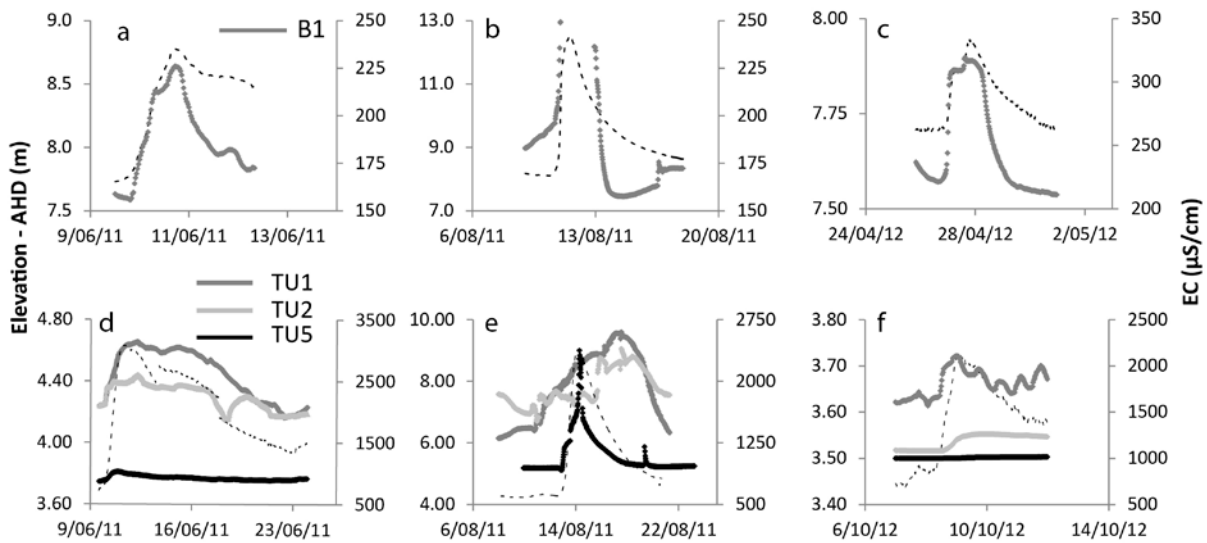


Figure 8. Changes in groundwater elevation (dashed line) and EC at Bruthen (a,b,c) and Tambo Upper (d,e,f). Groundwater elevations from B1 at Bruthen and TU1 at Tambo Upper.

^3H and ^{14}C activities (Chapter 3) indicate that water from the deeper, semi-confined aquifer is significantly older (mean groundwater residence time >10,000 years at Tambo Upper) than groundwater from the shallow unconfined aquifer (mean groundwater residence time <100 years at all locations). Furthermore, groundwater in the

deeper, semi-confined aquifer is far more saline (EC ~3,000 $\mu\text{S}/\text{cm}$, Cl >500 mg/L) than groundwater in the shallow aquifer (EC <1,000 $\mu\text{S}/\text{cm}$, Cl ~15 mg/L). At Tambo Upper, trends in ^3H activities, ^{14}C activities and EC values at TU1 and TU2 indicate increased upward leakage of the deeper groundwater into the surface aquifer close to the river (Fig. 8).

The increase in groundwater EC close to the Tambo River during the early stages of flooding suggests that the leakage from the semi-confined aquifer increases during flooding, possibly as a response to the propagation of pressure into the deeper aquifer via floodplain recharge or increased river stage further upstream. This can happen during flooding as pressure responses in confined and semi-confined aquifers is significantly faster than in unconfined aquifers (Wett et al., 2002). For example, pressure head propagation in sandy aquifers similar to this study may be on the order of several kilometres per day in for confined systems (Sophocleous, 1991), but only tens to hundreds of metres per day in unconfined systems (Vekerdy and Meijerink, 1998). While deeper screened bores were not installed at the Bruthen transect to confirm deep aquifer leakage, similar EC responses during flooding suggest that the hydrogeology at Bruthen is similar to that at Tambo Upper. As such, it is presumed that leakage from that deeper aquifer has occurred at Bruthen in response to flooding.

Increases in groundwater EC at Bruthen and Tambo Upper occurred during both minor (~0.3 m) and major (> 5 m) changes in groundwater elevation, suggesting that even small increases in groundwater elevation may be driving increased upward leakage from the deeper aquifer (Fig. 8). Changes in groundwater EC at Tambo Upper are also relative to changes in groundwater elevation, with increases in groundwater elevation of 0.25, 0.93 and 4.51 m at TU1 corresponding with increases in groundwater EC of 399, 917 and 1,084 $\mu\text{S}/\text{cm}$ (Fig. 8 d,e,f). This suggests that even during large flood events when

increases in river stage are close to 5 m, pressure loading on the deeper aquifer will be similarly increased and bank infiltration diminished. Leakage also appears to increase with proximity to the Tambo River, with generally greater EC responses at TU2 compared to TU5, and generally greater EC responses at TU1 compared to TU2. This effect of proximity is illustrated in Fig. 8f which suggests that an increase in groundwater elevation of 0.25 m is not significant enough to drive upward leakage at TU5, minor leakage at TU2 and significant leakage at TU1. This data suggests that the confining layer separating the shallow and deep aquifer at Tambo Upper is breached closer to the Tambo River.

In contrast to Bruthen and Tambo Upper, groundwater at Kelly Creek does not show a correlation between increases in groundwater elevation and EC. This may be because groundwater in the shallow aquifer at Kelly Creek has a relatively high EC compared to other transects (average EC = 2550 ± 310 $\mu\text{S}/\text{cm}$). As such leakage from the deeper, confined aquifer at Kelly Creek (average EC = 2350 ± 230 $\mu\text{S}/\text{cm}$) may be difficult to constrain using EC (EC values based on periodic sampling, Chapter 3, Table 3). It is however possible to resolve bank infiltration, as river EC during flood events was less than 200 $\mu\text{S}/\text{cm}$ at Kelly Creek and should cause a reduction in groundwater EC. EC variations in KC1 and KC2 suggests that bank infiltration has not occurred during 2011, as even during significant (~2 m) flood events, groundwater EC changed very little at Kelly Creek (Fig. 7). As aquifer leakage at this site cannot be excluded, pressure propagation and aquifer leakage remains a plausible mechanism for limited bank infiltration during 2011.

After flooding during March 2012, groundwater EC in the bore closest to the river at Kelly Creek decreased periodically in response to increases in groundwater elevation (Fig. 9). This suggests that during flooding in March 2012, relatively fresh water from the

Tambo River has infiltrated into the bank at Kelly Creek, and subsequent tidal variations in river elevation have driven the movement of this low EC water within the river bank as hydraulic gradients change. While the March 2012 flood event did not cause the greatest increase in river or groundwater elevation in the Tambo Catchment, the succession of two large events within 1 week at this time produced a particularly long period of increased river elevation (river elevation ~1 m above baseflow elevation for >3 weeks at Tambo Upper). As such, it is possible that bank infiltration has only occurred at Kelly Creek during March 2012 as a result of this prolonged period of increased river stage.

While this river section is ungauged and river elevations/groundwater – surface water gradients could not be determined, the gradient between KC1 and KC2 is away from the river at this time (KC1 head > KC2 head), and this gradient increases when the EC in KC1 decreases (Fig. 9). This supports the movement of fresh water into the bank as river elevation increases and groundwater flows away from the river are increased. While the gradient between KC1 and KC2 does not generally become negative (which would indicate the return of higher EC groundwater towards the river), variations in river elevation are likely to be greater than groundwater elevation. As such it is likely that as the gradient between KC1 and KC2 approaches 0, river elevation will fall below groundwater elevation at KC1 and groundwater flow towards the river will occur.

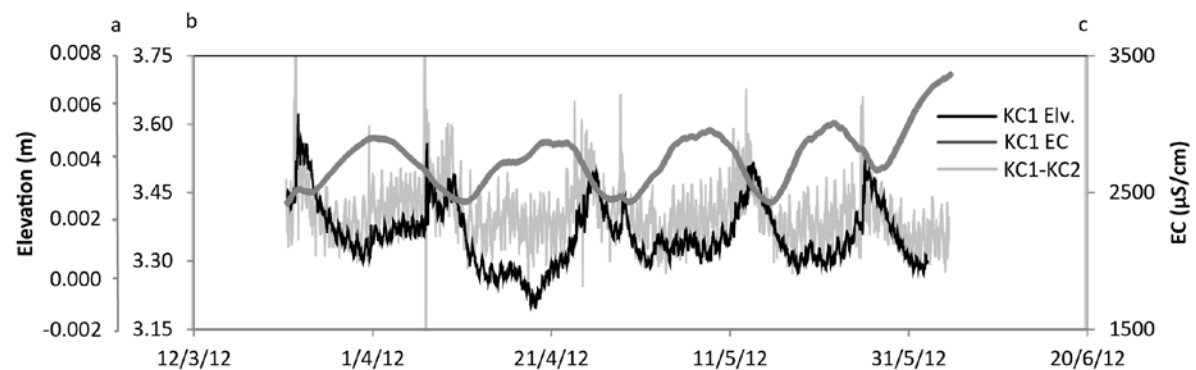


Figure 9. Tidally cyclic EC and groundwater elevation variations at Kelly Creek. Axis (a) = gradient between KC1 and KC2, axis (b) = groundwater elevation at KC1, axis (c) = EC at KC1.

4.4.2 Numerical modelling

The following section considers the infiltration of low salinity river water into an alluvial aquifer connected to a confined aquifer using MODFLOW. The model considers an aquifer cross section 100 m long (x direction), 40 m thick (z direction) and 1 m deep (y direction). The model has 100 columns in the x direction and 43 layers in the z direction. Grid spacing is 1×1 m throughout the model except for 4 layers between 14 and 15 m which are 0.25 m thick (z direction). The model is set up with an unconfined aquifer of 25 m that overlies a confined aquifer of 14 m. The confining layer is absent within 15 m of the right model boundary, 0.25 m thick between 15 and 25 m from the right boundary, 0.5 m thick between 25 and 30 m of the right boundary and 1 m thick throughout the rest of the model (Fig. 10a). This represents a confining layer that becomes less prevalent closer to the Tambo River, which is consistent with field observations. Where the thickness of the confining layer is reduced to 0.5, 0.25 and 0 m, the thickness of the unconfined aquifer is increased to 25.5, 25.75 and 26 m, respectively. The hydraulic conductivity (K) of the unconfined aquifer and the confined aquifer are 3.0×10^{-4} m/s and 2.0×10^{-5} m/s, respectively (from the rising head tests described in Chapter 3). The hydraulic conductivity of the confining layer has been set at 1.0×10^{-9} m/s which is appropriate for clays (Freeze and Cherry, 1979).

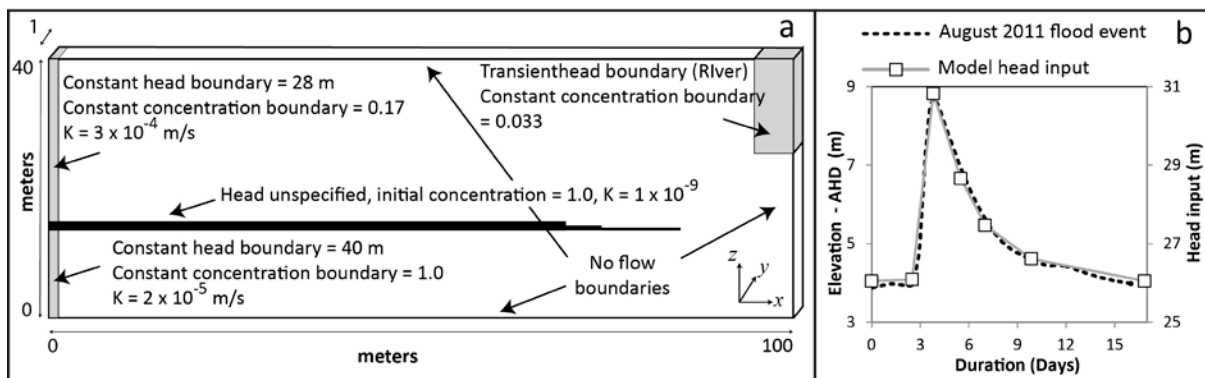


Figure 10. Schematic of model setup (a) and head condition at river boundary (b).

For simplicity, the river was modelled as being non-penetrating by varying the head at the top right boundary of the model, (c.f. McCallum et. al 2010), rather than using the river or stream packages. The initial elevation of the river was 26 m. The unconfined aquifer has a constant head boundary of 28 m at the left margin which produces an initial hydraulic gradient of 0.02 towards the river, which is consistent with the observed hydraulic gradient at Tambo Upper (Fig. 3). The left margin of the confined aquifer is a constant head boundary of 40 m; this results in the head in the confined aquifer at 20 m from the river being ~1.5 m higher than that in the unconfined aquifer, which is consistent with the observed head difference between TU4 and TU3D (Fig. 3). Constant dimensionless concentration boundaries of a conservative tracer have been set at 1 at the left boundary of the confined aquifer, 0.17 at the left boundary of the unconfined aquifer and 0.033 at the right boundary. Initial solute concentrations were also set at 1 in the confined aquifer and clay layer, 0.17 in the unconfined aquifer and 0.33 in the river. The relative differences in solute concentrations are similar to the observed differences in EC of ~3,000 (deep aquifer) ~500 (shallow aquifer) and ~100 $\mu\text{S}/\text{cm}$ (river), respectively.

While MODFLOW initialises with hydraulic heads in steady state, the model was run for a period representing 100 days prior to flood simulations to allow solute concentrations to achieve steady state. Flood waves modelled by varying the head at the river boundary according to a flood event in the Tambo River during August 2011. This involved an increase in head of 4.7 m over 1.3 days, followed reductions in head of 2.1 m over 1.7 days, 1.2 m over 1.5 days, 0.8 m over 2.9 days and finally 0.6 m over 7 days (Fig. 10b). The predicted change in groundwater concentrations in response to flooding was recorded using concentration observation bores at 10, 20 and 40 m distance from the right model boundary with screens at 16.5 m elevation. The model results show that under baseflow conditions, mixing will occur between groundwater from the semi-confined

aquifer and groundwater from the unconfined aquifer closer to the river, where the confining layer is absent.

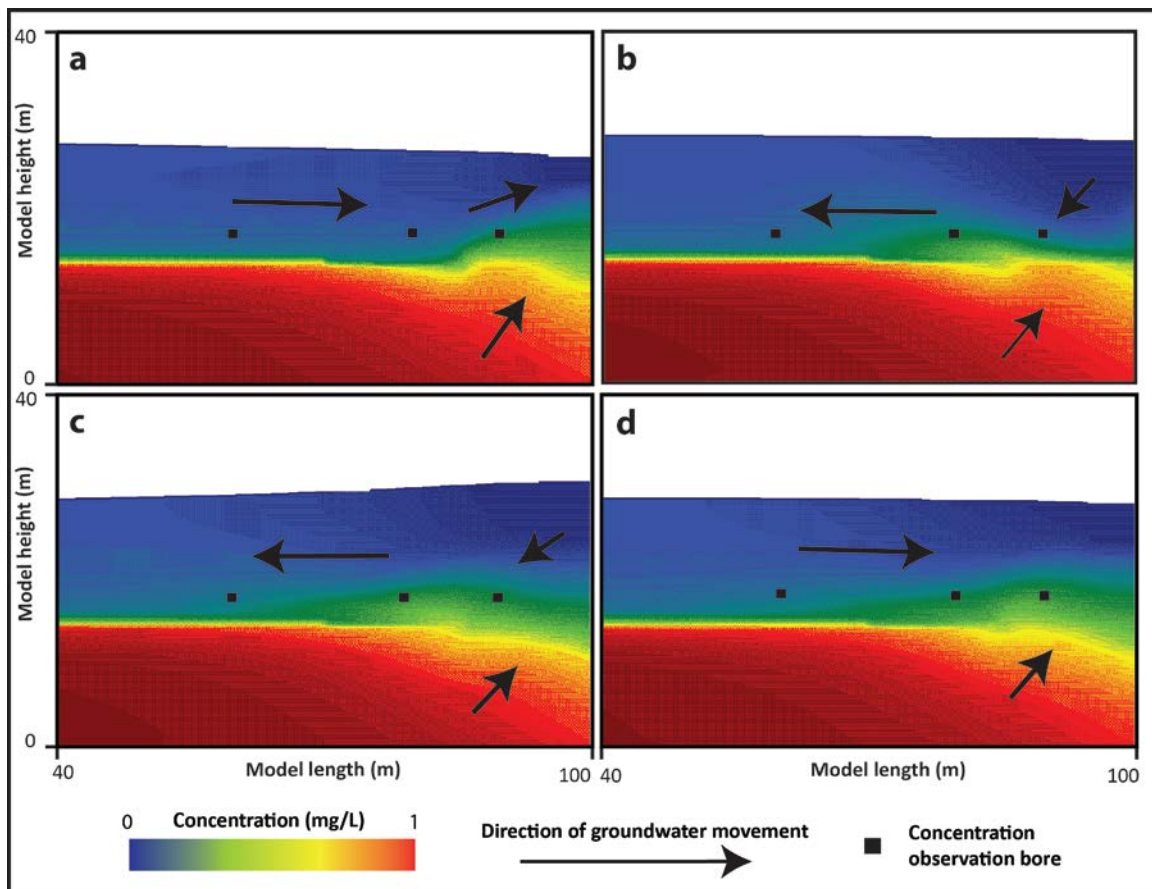


Figure 11. Model results showing water table (shaded area below white fill), changes in groundwater solute concentration (colour gradient) and flow direction (black arrows) prior to flooding (a), during initial stages of flooding (b), during flood (c) and during flood recession (d).

The degree of mixing in the unconfined aquifer increases with increasing proximity to the river, with solute concentrations at the 10 m model bore exceeding those at the 20 m or 40 m model bores (Figs 11a, 12b). During the initial stages of flooding, the hydraulic gradient near the river reverses, resulting in the infiltration of river water into the unconfined aquifer. As solute concentrations in groundwater close to the river are comparatively high, hydraulic gradient reversal results in the movement of this high concentration water away from the river into the unconfined aquifer (Fig 11b). As flooding continues however, the sustained infiltration of river water causes groundwater dilution in the unconfined aquifer close to the river. Finally, as the flood event subsides,

toward river hydraulic gradients are re-established, causing the high concentration groundwater to move back toward the river (Fig. 11d). The predicted changes in solute concentrations during flooding in model bores are shown in Fig. 12. Groundwater from 10 m shows an initial increase in concentration during the preliminary stages of flooding followed by a decrease due to the infiltration of low concentration river water. Secondary increases in concentration are then observed as the high concentration water flows back towards the river during flood recession.

The impact of K on the changes to solute concentration in the banks was evaluated by varying K in the unconfined aquifer between 8.5×10^{-5} and 5.0×10^{-4} m/s (the highest and lowest values recorded in the unconfined aquifer, Chapter 3). For both higher and lower K values, the infiltration of river water and the movement of high concentration groundwater further into the river bank occurred. When K is reduced, however, lateral groundwater movement is reduced. As such, during baseflow conditions, the flow of high concentration groundwater towards the river is reduced, resulting in higher pre-flood groundwater concentrations at 10 m (Fig. 12c). Additionally, groundwater concentrations at 40 m do not increase as much for lower K values as the movement of high concentration groundwater into the bank during flooding is reduced (Fig. 12c). Conversely, when K is increased, lateral groundwater movement is increased, allowing for greater flow of high concentration groundwater towards the river under baseflow conditions, giving lower initial groundwater concentrations at 10 m (Fig. 12a). Higher K values also allow greater movement of the high concentration groundwater into the bank during flooding, causing greater concentration increases at 40 m (Fig. 12a). The infiltration of river water is also increased at higher K values, causing greater dilution of groundwater at 10 m during flooding.

A series of flood waves with a similar shape to the August 2011 event were modelled ranging in magnitude from a 2 day, 0.5 m flood to 40 day, 9.7 m flood. The duration for which groundwater concentrations changed in response to these flood waves is shown in Fig. 13. In order to remove small concentration variations within the model that were not associated with the simulated flood waves, dilution was only considered to occur when solute concentrations were less than 90% of pre-flood concentrations ($C < 0.9C_0$), while increases were considered to occur when concentrations exceeded 110% of pre-flood concentrations ($C > 1.1C_0$). Increases in solute concentrations first occurred after 8 days of flooding at the 10 and 20 m model bores and after 16 days of flooding at the 40 m model bore. The model indicates that the residence time of the groundwater with higher solute concentrations will increase linearly with flood duration (Fig. 13a). The model also indicates that during larger flood events (≥ 16 days) the residence time of groundwater with higher solute concentrations will be greater further from the river (at 20 and 40 m), as solute concentrations closer to the river (at 10 m) will be lowered by infiltrating river water.

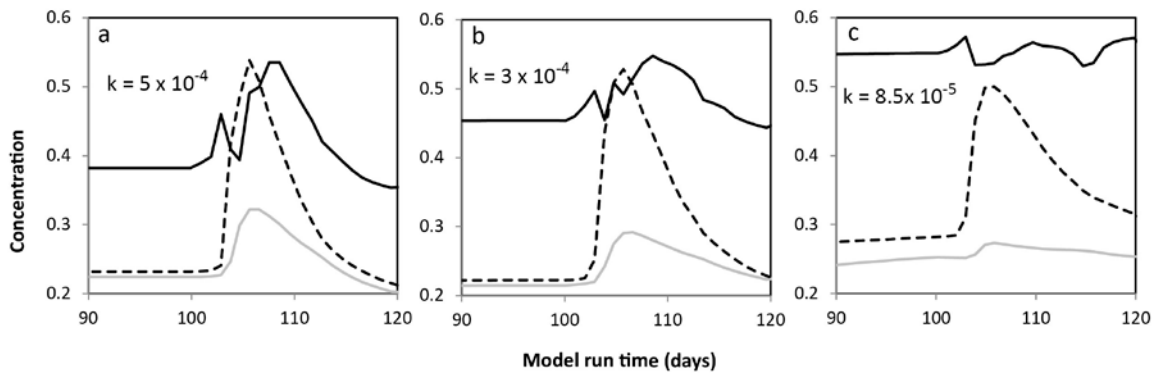


Figure 12. Modelled groundwater concentrations at 10 (solid black line), 20 (dashed black line) and 40 m (grey line) model bores at 10 m depth for $K = 8.5 \times 10^{-5}$ (a), $K = 3 \times 10^{-4}$ (b) and $K = 5 \times 10^{-4}$ (c).

For the flood waves modelled, groundwater dilution ($C < 0.9C_0$) was only recorded in the 10 m model bore (Fig. 13b). The duration of dilution at 10 m also increased linearly with flood duration. The dilution of solute concentrations was not

recorded at the 20 or 40 m model bores, indicating that exceptionally large flood events (>40 days in length or >9.7 m in height) would be required to dilute groundwater solute concentrations ≥ 20 m distance from the river via bank infiltration. The model further indicates that for this system, flood events > 4 m in height and > 15 days in duration would be required to cause the dilution of groundwater via bank infiltration within 10 m of the river. Additionally, such flooding may actually increase solute concentrations in the groundwater via the migration of saline groundwater away from the river.

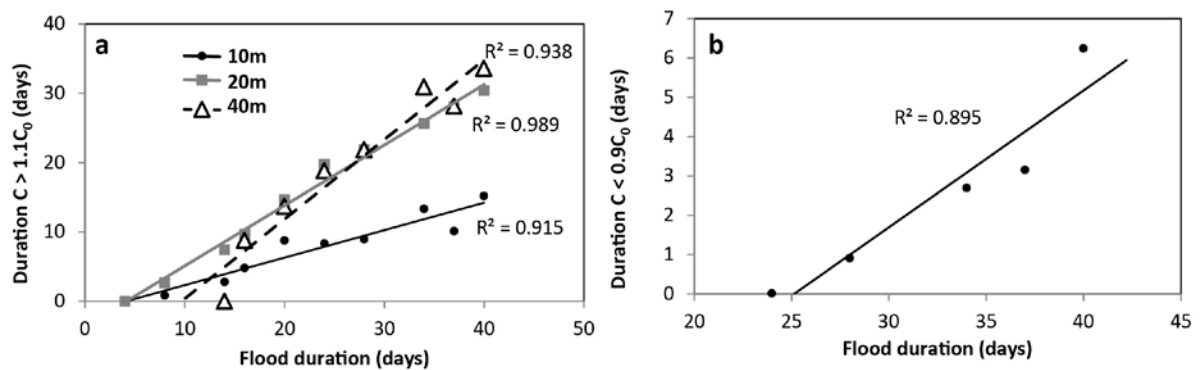


Fig. 13. Duration of increased groundwater concentrations (a) and groundwater dilution (b) for different flood lengths at 10, 20 and 40 m model bores.

The modelled solute concentration responses in the river bank show a number of similarities to those observed on the Tambo River (Fig. 8). Firstly, both model results and field observations indicate an increase in groundwater concentrations within 40 m of the river in response to flood events ranging from 0.3 to >4.0 m height. Secondly, both the model and field observations suggest that areas further from the river will only show an increase in solute concentrations during larger flood events. This is shown in EC responses at Tambo Upper (Fig. 8 d,e,f) where groundwater EC at TU5 (37.9 m) did not increase during smaller flood events (<1.0 m), but did increase after larger (>4 m) flood events. Both the model and field observations also indicate that such increases in EC will happen more readily closer to the river (10 m model bore and TU1) in response to smaller flood events (<2 m and <1 m, respectively). These results suggest that the EC

responses shown in in Fig. 8 may not be a result of increased upward leakage from the semi-confined aquifer through the rapid propagation of pressure that occurs in confined aquifers, but may be the result of saline groundwater movement away from the river as hydraulic gradients reverse during flooding.

4.4.3 Groundwater flux estimates

As indicated in section 4.4.2, complex aquifer interactions and mixing in river banks will change the geochemistry of groundwater in river banks during flooding, making water flux estimates via chemical methods difficult to constrain (c.f. McCallum et al., 2010). The flux of groundwater into and out of the Tambo River bank (q in $\text{m}^3/\text{m}^2/\text{day}$) was estimated via Darcy's Law: $q = -K (dh/dl)$ (Darcy, 1856), where K is hydraulic conductivity (m/day) and dh/dl is the hydraulic gradient. These have been adjusted for river width at each monitoring site to give water fluxes per unit length (m) of river ($\text{m}^3/\text{m}/\text{day}$). Hydraulic gradients were calculated between the monitoring bore closest to the river and the river while hydraulic conductivities are based on the average conductivity ($25.7 \text{ m}/\text{day}$) in the unconfined aquifer (Chapter 3). Fluxes were estimated at the Bruthen and Tambo Upper transects but not the Kelly Creek transect where river height is affected by tidal forcing.

Continuous groundwater fluxes via the Darcy equation are illustrated in Fig. 14. Groundwater fluxes at both Bruthen and Tambo Upper generally indicate groundwater discharge (positive groundwater fluxes) – as is consistent with the dominantly gaining nature of the Tambo River (Unland et al., 2013). However both data sets indicate groundwater recharge (negative groundwater fluxes) during periods of increased river height. This is consistent with the infiltration of river water into the alluvial aquifer as indicated by numerical modelling. Groundwater fluxes at Bruthen are more variable than Tambo Upper, ranging from -137 to $98.5 \text{ m}^3/\text{m}/\text{day}$ compared to -42.9 to $29.7 \text{ m}^3/\text{m}/\text{day}$,

respectively. This may be a result of flood peak attenuation with increasing distance downstream and changes to channel geometry. This will cause flood peaks to be higher and last for shorter periods at Bruthen compared to Tambo Upper, producing a greater variations between groundwater and surface water elevations. K values in the unconfined aquifer near the Tambo River are variable, ranging from 7.4 to 44 m/day and as q scales linearly with K, this represents the greatest source of uncertainty in groundwater flux calculations. Based on this range of K values, the average uncertainty with respect to q estimates in Fig. 14 are ~71%.

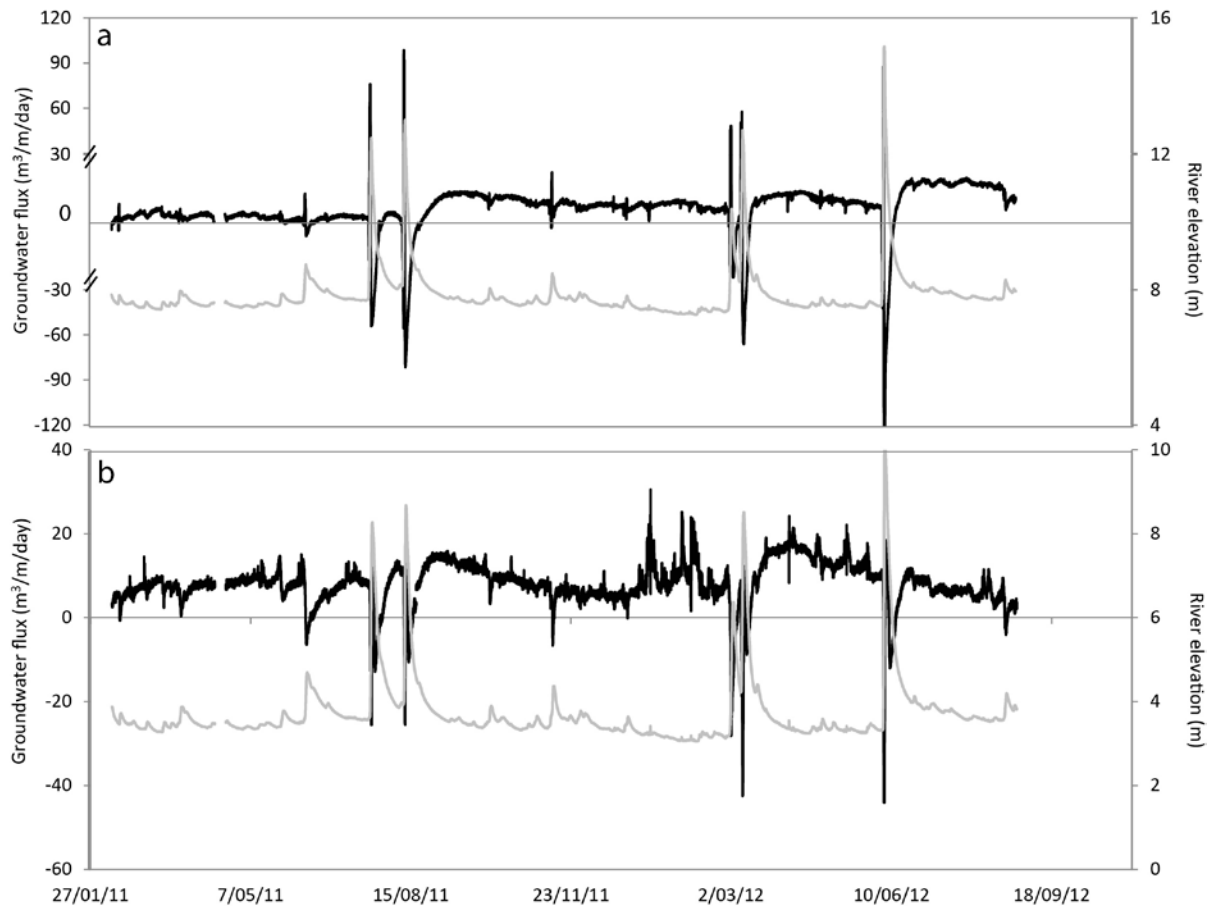


Figure 14. Groundwater flux estimates superimposed on river height data at Bruthen (a) and Tambo Upper (b). Positive fluxes represent groundwater discharge and negative fluxes indicate groundwater recharge

Both locations show similar responses to changing hydrological conditions with groundwater fluxes generally below $10 \text{ m}^3/\text{m}/\text{day}$ under baseflow conditions and negative

fluxes when river height increases. At Bruthen, increases in river height of as little as 0.5 m caused bank infiltration, while bank infiltration at Tambo Upper occurred with increases in river height of as little as 0.3 m. Groundwater fluxes to the Tambo River were generally the highest in the days to weeks following flood peak, when a combination of recent groundwater recharge and declining river elevation are likely to produce higher toward river hydraulic gradients. These results are consistent with results from modelling that indicate the infiltration of river water into the Tambo River bank during flooding.

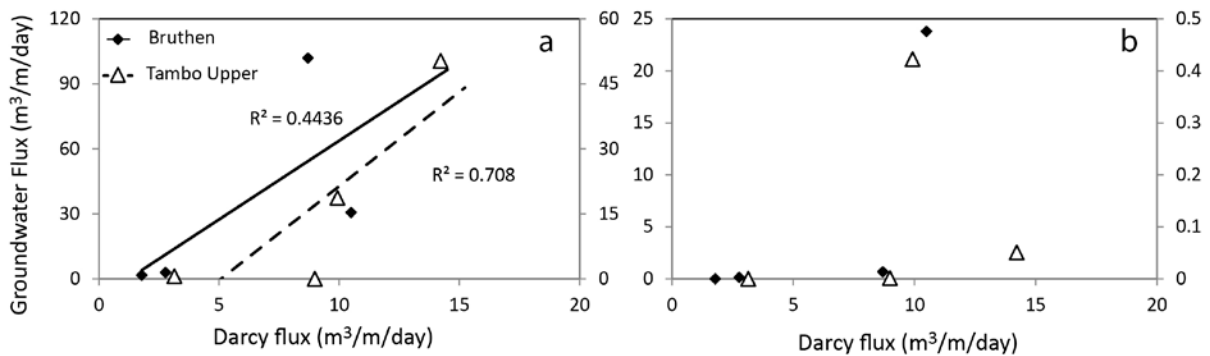


Figure 15. Covariance between Darcy flux estimates (x axis) and estimates from ^{222}Rn (a) and Cl mass balance (b) from Unland et al., 2013 at Tambo Upper (primary y axis) and Bruthen (secondary y axis).

Darcy flux estimates have been plotted in Fig. 15 against flux estimates given by chemical mass balance for similar time periods at the Bruthen and Tambo Upper sites (Unland et al., 2013). While flux estimates via ^{222}Rn mass balance and the Darcy equation show a weak positive correlation, Darcy flux estimates are considerably less variable, ranging from 1.79 to 14.22 $\text{m}^3/\text{m}/\text{day}$ compared to ^{222}Rn mass balance which ranges from 0 to 100.5 $\text{m}^3/\text{m}/\text{day}$. Correlations between Darcy flux estimates and estimates from Cl mass balance are very poor (Fig. 15b) as flux estimates by Cl mass balance are extremely low ($<1 \text{ m}^3/\text{m}/\text{day}$) for all but two time periods.

Discrepancies in flux estimates may be driven by many factors. Firstly, the above numerical modelling and field results suggest complex river-aquifer interactions that will significantly affect near groundwater chemistry, making accurate characterisation of groundwater end members for mass balance difficult. Secondly, the variability in K has only been calculated at two locations along the Tambo River, leaving a level of uncertainty with respect to groundwater fluxes calculated by the Darcy's Law. Finally, there are likely to be differences in the calculated groundwater fluxes due to the inherent differences in the methods used. More specifically, Darcy fluxes are based on measurements at one point spatially where chemical mass balance integrates any processes that have affected surface and groundwater chemistry along their relative flow paths (Cook, 2012).

While physical and numerical methods often contrast with chemical methods (Cartwright et al., 2013), their combined use still offers complementary information. Though the use of multiple chemical tracers offers a more elegant and robust approach for calculating groundwater fluxes, and provides information on the spatial distribution of gaining and losing reaches, geochemical flux estimates only represent the conditions under which sampling occurs (Cook, 2012; McCallum et al., 2010). Conversely, numerical modelling and continuous Darcy flux estimates, as used in this study, yield information on the dynamics of groundwater – surface water interaction under changing hydrologic conditions. In this context, the Darcy fluxes and numerical modelling above are able to characterise the rapid change between gaining and losing conditions, and the likely changes in groundwater chemistry that will result from such exchange. This allows for improved interpretation of hydrochemical data and more robust evaluation of groundwater flux estimates via chemical mass balance.

Ultimately, these results show that in the presence of complex aquifer-river interactions where the application of chemical tracer methods may be impeded, a combination of physical hydrological methods and numerical modelling may help to better interpret hydrochemical data, leading a better understanding of groundwater – surface water exchange.

4.5 Conclusions

This study demonstrates the potential complexities that may exist during river-aquifer exchange. The presence of a confined aquifer close to a river can significantly complicate river-groundwater interaction during flooding. In this example, upward leakage of deeper groundwater into an unconfined aquifer limits the dilution of groundwater via bank infiltration during the initial stages of flooding, inhibiting bank storage as it is classically envisaged (eg: Hantush et al., 2002; Nowinski et al., 2012; Sophocleous, 2002; Winter, 1995). Such complexities also have significant implications for the chemistry of groundwater being discharged to rivers. For example, diminished bank storage may reduce the processing of nutrients that may otherwise take place in these settings (Bourg and Bertin, 1993; Cey et al., 1999; Fukada et al., 2003).

Additionally, the groundwater from the semi-confined aquifer at Tambo Upper is anoxic (Chapter 3) and the upwards leakage of this water has the potential to change the redox conditions in the river bank, even though both the river water and shallow groundwater are oxic. This shows that the highly variable nature of river-groundwater interactions (on both spatial and temporal scales) needs to be considered when interpreting the results of periodic geochemical surveys designed to characterise river behaviour with respect to linkages to groundwater.

In complex aquifer systems, the exchange between rivers and aquifers can be significantly improved by continuous monitoring of river and groundwater EC at a

number of locations and aquifers. Through the use of basic numerical modelling, these complex interactions can be further resolved to provide a better conceptual understanding of how such systems operate. Given this, basic hydrological principles such as Darcy flux estimates can be applied in order to calculate water exchanges at the groundwater-surface water interface. By understanding these interactions qualitatively and quantitatively over space and time, the applicability of other techniques used in quantifying groundwater-river exchange such as chemical mass balance can be better evaluated.

Acknowledgements

Funding for this research was provided by the National Centre for Groundwater Research and Training, an Australian Government initiative, supported by the Australian Research Council and the National Water Commission.

References

- Bureau of Meteorology: Commonwealth of Australia, available at: <http://www.bom.gov.au> (last access: 11 January 2013), 2012.
- Birch, W.D., 2003. The Geology of Victoria. Geological Society of Australia (Victorian Division), Sydney.
- Boulton, A.J., 1993. Stream ecology and surface-hyporheic hydrologic exchange: Implications, techniques and limitations. *Marine and Freshwater Research*, 44(4): 553-564.
- Boulton, A.J., 2005. Chances and challenges in the conservation of groundwaters and their dependent ecosystems. *Aquatic Conservation: Marine and Freshwater Ecosystems*, 15(4): 319-323.
- Bourg, A.C.M., Bertin, C., 1993. Biogeochemical processes during the infiltration of river water into an alluvial aquifer. *Environmental Science & Technology*, 27(4): 661-666.
- Brunke, M., Gonser, T.O.M., 1997. The ecological significance of exchange processes between rivers and groundwater. *Freshwater Biology*, 37(1): 1-33.
- Burt, T.P. et al., 2002. Water table fluctuations within the floodplain of the River Severn, England. *Journal of Hydrology*, 262(1-4): 1-20.
- Cartwright, I., Gilfedder, B., Hofmann, H., 2013. Contrasts between chemical and physical estimates of baseflow help discern multiple sources of water contributing to rivers. *Hydrology and Earth Systems Science Discussion*, 10(5): 5943-5974.
- Cey, E.E., Rudolph, D.L., Aravena, R., Parkin, G., 1999. Role of the riparian zone in controlling the distribution and fate of agricultural nitrogen near a small stream in southern Ontario. *Journal of Contaminant Hydrology*, 37(1-2): 45-67.

- Chen, X., Chen, D.Y., Chen, X.-h., 2006. Simulation of baseflow accounting for the effect of bank storage and its implication in baseflow separation. *Journal of Hydrology*, 327(3–4): 539-549.
- Cook, P. G., 2012. Estimating groundwater discharge to rivers from river chemistry surveys, *Hydrological Processes*, doi:10.1002/hyp.9493, 2012.
- Cooper, H.H., Rorabaugh, M.I., 1963. Ground-water movements and bank storage due to flood stages in surface streams, United States Department of the Interior, Geological Survey Water-Supply Paper, Washington.
- Darcy, H., 1856. *Les fontaines publiques de la ville de Dijon.*, Victor Dalmont, Paris.
- Doble, R., Brunner, P., McCallum, J., Cook, P.G., 2012. An Analysis of River Bank Slope and Unsaturated Flow Effects on Bank Storage. *Ground Water*, 50(1): 77-86.
- Freeze, R.A. & Cherry, J.A., 1979. *Groundwater*. Prentice-Hall, Englewood Cliffs, New Jersey.
- Fukada, T., Hiscock, K.M., Dennis, P.F., Grischek, T., 2003. A dual isotope approach to identify denitrification in groundwater at a river-bank infiltration site. *Water Research*, 37(13): 3070-3078.
- Gray, D.R., Foster, D.A., 2004. Tectonic evolution of the Lachlan Orogen, southeast Australia: historical review, data synthesis and modern perspectives. *Australian Journal of Earth Sciences*, 51(6): 773-817.
- Hantush, M., Harada, M., Mariño, M., 2002. Hydraulics of Stream Flow Routing with Bank Storage. *Journal of Hydrologic Engineering*, 7(1): 76-89.
- Hiscock, K.M., 2005. *Hydrogeology Principles and Practice*. Blackwell Science, Victoria.
- Hocking, J.B., 1976. Definition and revision of Tertiary stratigraphic units, onshore Gippsland Basin, Geological Survey of Victoria.
- Hofmann, H., Cartwright, I., 2013. Using hydrogeochemistry to understand inter-aquifer mixing in the on-shore part of the Gippsland Basin, southeast Australia. *Applied Geochemistry*, 33(0): 84-103.
- Jolly, R. L., 1997. Bairnsdale, 1 : 250 000 Geological Map Series, Department of Natural Resources and Environment, MDC Fitzroy, Victoria.
- Kapostasy, S., 2002. Haunted Hill Gravel: Deposition and Neotectonic History along the Southern Australian Coast. In: Palmer, B.A. (Ed.), *Keck Geology Consortium*, Wisconsin, USA.
- Lambs, L., 2004. Interactions between groundwater and surface water at river banks and the confluence of rivers. *Journal of Hydrology*, 288(3–4): 312-326.
- Lamontagne, S., Leaney, F.W., Herczeg, A.L., 2005. Groundwater-surface water interactions in a large semi-arid floodplain: implications for salinity management. *Hydrological Processes*, 19(16): 3063-3080.
- Leonard, J.G., 1992. An overview of Victoria's groundwater resources. Background report S3, short term planning guidelines. Drought management plan for Victoria's water resources, Department of Water Resources, Melbourne, Victoria.
- McCallum, J.L., Cook, P.G., Brunner, P., Berhane, D., 2010. Solute dynamics during bank storage flows and implications for chemical base flow separation. *Water Resour. Res.*, 46(7): W07541.
- Moench, A.F., Barlow, P.M., 2000. Aquifer response to stream-stage and recharge variations. I. Analytical step-response functions. *Journal of Hydrology*, 230(3–4): 192-210.
- Moench, A.F., Sauer, V.B., Jennings, M.E., 1974. Modification of routed streamflow by channel loss and base flow. *Water Resources Research*, 10(5): 963-968.

- Nowinski, J.D., Cardenas, M.B., Lightbody, A.F., Swanson, T.E., Sawyer, A.H., 2012. Hydraulic and thermal response of groundwater–surface water exchange to flooding in an experimental aquifer. *Journal of Hydrology*, 472–473(0): 184-192.
- Pinder, G.F., Sauer, S.P., 1971. Numerical Simulation of Flood Wave Modification Due to Bank Storage Effects. *Water Resources Research*, 7(1): 63-70.
- Sophocleous, M., 2002. Interactions between groundwater and surface water: the state of the science. *Hydrogeology Journal*, 10(1): 52-67.
- Sophocleous, M., 1991. Combining the soilwater balance and water-level fluctuation methods to estimate natural groundwater recharge: Practical aspects. *Journal of Hydrology*, 124(3-4): 229-241.
- Squillace, P.J., 1996. Observed and simulated movement of bank-storage water. *Ground Water*, 34(1): 121.
- Unland, N.P., Cartwright, I., Andersen, M. S., Rau, G. C., Reed, J., Gilfedder, B. S., Atkinson, A. P., Hofmann, H., 2013. Investigating the spatio-temporal variability in groundwater and surface water interactions: a multi-technical approach. *Hydrology Earth Syst. Sci.* 17: 3437-3453.
- Vekerdy, Z., Meijerink, A.M.J., 1998. Statistical and analytical study of the propagation of flood-induced groundwater rise in an alluvial aquifer. *Journal of Hydrology*, 205(1–2): 112-125.
- Victorian Water Resources Data Warehouse, 2013: available at: <http://www.vicwaterdata.net/vicwaterdata/home.aspx> (last access: 11 November, 2013).
- Wett, B., Jarosch, H., Ingerle, K., 2002. Flood induced infiltration affecting a bank filtrate well at the River Enns, Austria. *Journal of Hydrology*, 266(3–4): 222-234.
- Whiting, P.J., Pomeranets, M., 1997. A numerical study of bank storage and its contribution to streamflow. *Journal of Hydrology*, 202(1–4): 121-136.
- Winter, T.C., 1995. Recent advances in understanding the interaction of groundwater and surface water. *Reviews of Geophysics*, 33(S2): 985-994.
- Woessner, W.W., 2000. Stream and fluvial plain ground water interactions: Rescaling hydrogeologic thought. *Ground Water*, 38(3): 423-429.
- Zlotnik, V.A., Huang, H., 1999. Effect of shallow penetration and streambed sediments on aquifer response to stream stage fluctuations (analytical model). *Ground Water*, 37(4): 599-605.

Chapter 5

Transient groundwater - surface water interactions in a tidal estuary: a case study from the Tambo River, Eastern Victoria

N .P. Unland ^{1,2}, B. S. Gilfedder^{1,2,3}, I. Cartwright ^{1,2}, A.P. Atkinson^{1,2}

^[1] *School of Geosciences, Monash University, Clayton, Vic. 3800, Australia*

^[2] *National Centre for Groundwater Research and Training, GPO box 2100, Flinders University, Adelaide, SA 5001, Australia*

^[3] *Department of Hydrology, University Bayreuth, Bayreuth, Germany*

In preparation for publication

Abstract

Quantifying groundwater discharge and its chemical impact in the upper and middle reaches of rivers has been widely studied, however comparatively few studies consider groundwater-surface water interactions in coastal estuaries. Groundwater discharge in estuaries can have significant impacts on nutrient loads and biogeochemical cycling as nutrient concentrations in groundwater are often significantly higher than in surface water and runoff. Understanding biogeochemical pathways within estuaries is important as estuaries represent the dynamic interface between terrestrial and marine environments, and are often the site of significant biological diversity. Continuous high temporal resolution monitoring of ²²²Rn activities in the stratified tidal estuary of the Tambo River in South East Australia indicates significant variation in groundwater-surface water interactions over a ~5 day period. In contrast to the limited number of studies in similar

areas, ^{222}Rn mass balance indicates that the groundwater fraction varies tidally in the subsurface section of the Tambo River estuary but not in the surface section (the upper 50 cm of the water column). The maximum groundwater fraction estimated in the subsurface typically ranged from ~4% to ~8% of total river discharge over individual tidal cycles. While this is partially attributed to varying degrees of mixing between subsurface water and surface water over tidal cycles, the input of groundwater during flow reversal is also likely to affect the groundwater fraction. It is proposed that in a tidal estuary, river water may receive groundwater inputs during both downstream movement at tidal minimum and upstream movement at tidal maximum, resulting in higher groundwater fractions during tidal maximums. A reduction in the maximum groundwater fraction in the surface section (from ~11 to ~2%) coincides with increased rainfall in the catchment and a reduction in $\delta^2\text{H}$ values (from -42 to -62‰), suggesting the dilution of groundwater via inputs from rainfall and runoff. This study shows the dynamic nature and variability in groundwater – surface water interactions in estuaries that can occur over a time period of hours to days.

5.1. Introduction

Coastal estuaries represent a dynamic interface between marine and freshwater environments and are often the site of biogeochemically diverse reactions (Charette and Sholkovitz, 2006; Cifuentes et al., 1989; Harris, 1999; Morris et al., 1978). While groundwater discharge represents only a small percentage of the total freshwater flux to coastal areas (Burnett et al., 2006), it may still provide a significant proportion of nutrient loads as nutrient concentrations in groundwater are typically much higher than in rivers (Santos et al., 2008). Thus, quantification of groundwater discharge to estuaries is not only important for calculating global nutrient fluxes to the ocean, but also for the effective management of coastal waterways, as nutrient inputs to coastal waterways has

been shown to result in algal blooms, reductions in biodiversity and eutrophication (eg: Anderson et al., 2002; Cloern, 2001; Howarth and Marino, 2006).

Environmental tracers including radiogenic isotopes, stable isotopes and major ions offer an effective approach to calculating groundwater fluxes to surface water bodies (Appendix A, Cartwright et al., 2011; Cook, 2012; Cook et al., 2006; Genereux and Hemond, 1992, 1990; Lamontagne et al., 2008; Swarzenski, 2007). The effectiveness of this approach relies on the accurate characterisation of a tracer, the concentration of that tracer being sufficiently different in groundwater compared to surface water, and the ability to accurately quantify a tracers sources and sinks. ^{222}Rn has proven particularly useful as a tracer of groundwater inflows to surface water bodies as activities of ^{222}Rn are commonly 2 to 3 orders of magnitude higher in groundwater compared to surface water, it is chemically inert, and degassing to the atmosphere (and decay) reduces its activity in surface water so that high ^{222}Rn activities only occur in regions of groundwater inflows. Further to this, the effects of degassing and ingrowth in river and coastal environments have been well researched, making ^{222}Rn ideal for groundwater-surface water studies (Cartwright et al., 2011; Cook et al., 2006; Genereux and Hemond, 1992; Kawabata et al., 2003; Mullinger et al., 2007).

Traditionally, dissolved ^{222}Rn has been measured on discrete water samples using scintillation (eg: Cook et al., 2006; Freyer et al., 1997; Hoehn and Von Gunten, 1989; Mullinger et al., 2007; Mullinger et al., 2009; Murakami and Horiuchi, 1979). This approach can be both expensive and logistically difficult, as samples need to be shipped to a laboratory within a few days of sampling. Over the last decade, however, the development of continuous ^{222}Rn in field measurements (Burnett et al., 2001) has allowed a number of studies to investigate the variability of ^{222}Rn activities in surface water bodies at high spatial and temporal frequencies (Crusius et al., 2005; Dulaiova et al.,

2005; Gilfedder et al., 2012; Hofmann et al., 2011; Knee and Jordan, 2013; Peterson et al., 2010; Santos et al., 2008; Santos et al., 2011; Santos and Eyre, 2011).

As continuous measurement of ^{222}Rn has only developed over the last decade, there is still much to be gained from investigations focussed on assessing high temporal variations in groundwater-surface water interactions over tidal cycles. This study investigates the variability of groundwater discharge to the stratified tidal estuary of the Tambo River, a dominantly gaining river system in southeast Australia (Unland et al., 2013). The highly dynamic nature of estuaries makes groundwater tracing in these systems particularly difficult. As such, studies of this nature require parameters such as salinity, temperature, hydraulic gradients and chemical tracers such as ^{222}Rn to be monitored on a continuous, high frequency time series in order to assess the changing nature of groundwater discharge over tidal cycles. Most previous studies of groundwater discharge to estuaries using continuous ^{222}Rn data have considered either non-stratified water columns or focussed on the surface (fresh) water in the estuary (Burnett et al., 2010; Knee and Jordan, 2013; Santos and Eyre, 2011; Santos et al., 2010). The limited studies that have monitored ^{222}Rn activities and groundwater discharge to both surface and subsurface waters have focussed on relatively fresh groundwater systems (Peterson et al., 2010).

This research focuses on a section of the Tambo River where the groundwater is relatively saline. The inflow of groundwater to the estuary is assessed over a number of tidal cycles by combining continuous monitoring of ^{222}Rn , EC, hydraulic head and temperature with periodic sampling for O and H isotopes. Studies focussed on evaluating groundwater fluxes in tidal estuaries via continuous monitoring are still relatively novel and therefore have the potential to add to our understanding of groundwater-surface water processes in these settings.

5.1.1 Study Area

The Tambo River is a perennial river that flows southwards from the Eastern Victorian Uplands through the Gippsland Basin before discharging at Lake King (Fig. 1). Lake King is a saline lake that is connected to Tasman Sea through an outlet at Lakes Entrance which allows tidal water movement through the lower section of the Tambo River. The transition from fresher upstream water ($\sim 150 \mu\text{S}/\text{cm}$) and saline water from Lake King ($\sim 30,000 \mu\text{S}/\text{cm}$) varies with changing hydrologic conditions. The boundary is sharper and further upstream ($\sim 15 \text{ km}$ upstream of Lake King) under lower flow conditions and more gradual and further downstream ($\sim 3 \text{ km}$ upstream of Lake King) under high flow conditions (Unland et al., 2013).

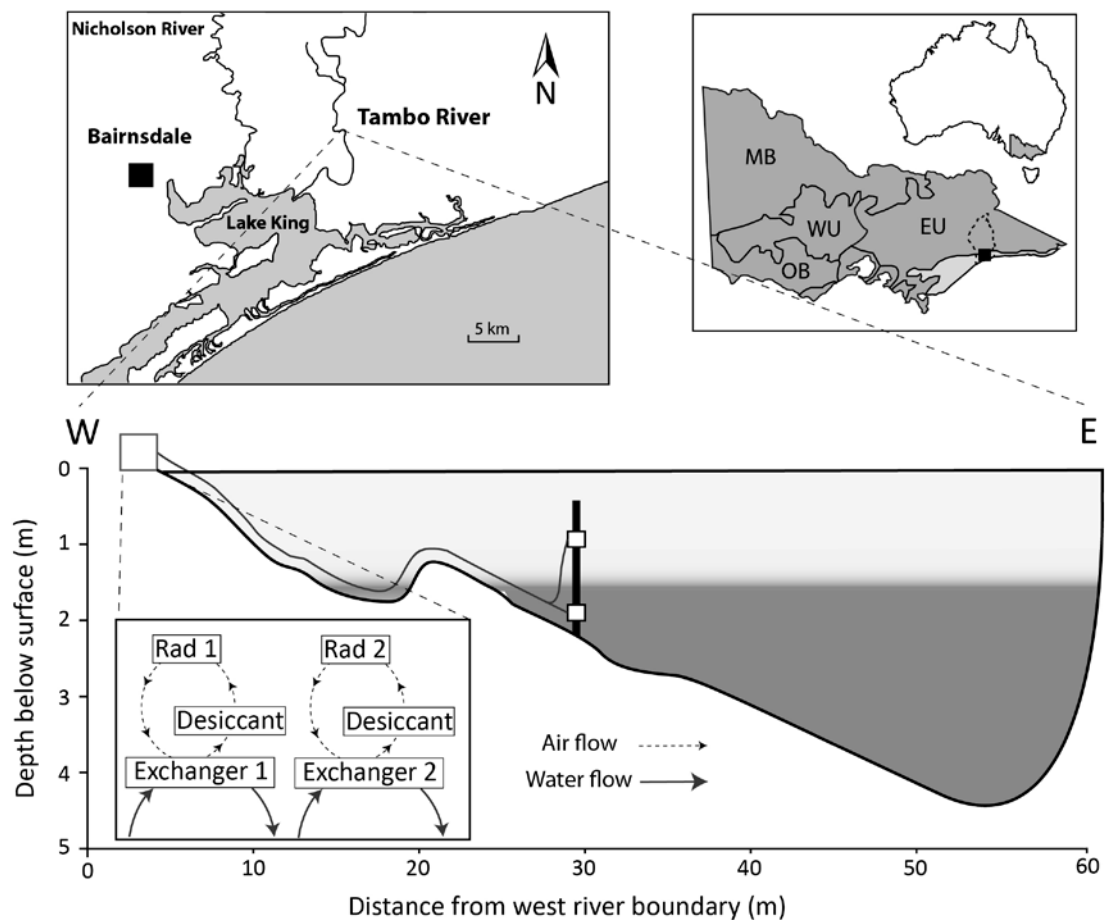


Figure 1. Field area and experimental setup facing upstream. Dark grey areas in estuary cross section indicate more saline river water. White box on the west bank indicates RAD7 setups, white boxes in estuary indicates location of EC/temperature/ head loggers as well as water intakes for RAD7's and water sampling.

Average annual rainfall in the catchment ranges from 655 mm in the upper reaches of the catchment to 777 mm in the middle and lower reaches. Average daily river discharge upstream of the tidal section generally varies between $\sim 1 \times 10^4$ m³/day at low flow to $\sim 5 \times 10^7$ m³/day at high flow conditions, with an average daily river discharge of $\sim 1 \times 10^6$ m³/day.

The Gippsland Basin contains a heterogeneous aquifer system; however the near-surface aquifers with which the Tambo River interacts are dominated by Quaternary and Tertiary coarse siliceous sands and gravels that are interbedded with clays. These clay layers produce a number of aquifer horizons that range from confined to unconfined. The Tambo River catchment is covered by forest and woodland in its upper reaches, with cattle grazing on river floodplains in its lower reaches (Department of Agriculture, Fisheries and Forestry, 2006). The Gippsland Lakes system to which the Tambo River discharges is a complex saline lakes system that is commonly affected by algal blooms arising from nutrient influxes (Cook et al., 2010; Grayson et al., 1997; Hallegraeff, 1992). The Tambo River is a predominantly gaining river system with groundwater discharge in the ~ 20 km section upstream of the estuary contributing between 7 and 21% of total river discharge (Unland et al., 2013).

5.2. Methods

Investigations took place between April 13 and April 18, 2011 under relatively low flow conditions when groundwater is expected to comprise a relatively high fraction of river water. Studies took place ~ 13.8 km upstream from Lake King on a stratified section of the Tambo River that is affected by tidal forcing.

5.2.1 Continuous monitoring

The activity of ²²²Rn in river water was continuously measured using an exchanger similar to that described by Burnett et al., (2001). Water was continuously

pumped from the river via polyethylene tubing and into an acrylic chamber via a spray nozzle which increases the rate of degassing of ^{222}Rn from the water. The temperature and EC within the chamber was monitored continuously to $\pm 0.1^\circ\text{C}$ and $\pm 1\%$, respectively, using a Win-Situ Aqua TROLL 200 logger, and the water:air ^{222}Rn ratio ($K_{\text{w/air}}$) was corrected using:

$$\ln \beta = a_1 + a_2\left(\frac{100}{T}\right) + a_3\ln\left(\frac{T}{100}\right) + S\left[b_1 + b_2\left(\frac{T}{100}\right) + b_3\left(\frac{T}{100}\right)^2\right] \quad (1a)$$

$$\text{and } K_{\text{w/air}} = \beta \cdot \frac{T}{273.15} \quad (1b)$$

(Schubert et al., 2012), where a_1 to b_3 are empirically derived coefficients for the partitioning of ^{222}Rn between the atmosphere and water under changing temperature (T) and salinity (S) conditions. The air within the chamber was cycled through a RAD-7 radon-in-air detector via a desiccant using the built in air pump of the RAD-7. The RAD-7 detectors integrated the activity of ^{222}Rn over 20 minute periods. Two exchangers were used to monitor the activity of ^{222}Rn in the river both above the pycnocline (~ 50 cm below the river surface) and below the pycnocline (~ 200 cm below river surface). Water was pumped from these depths via polyethylene tubing secured to a steel star picket ~ 25 m distance from the river bank (Fig. 1). As salt wedge movement and inter layer mixing throughout the study make sampling of water within and across the pycnocline likely, the terms “surface” and “sub-surface” sections have been adopted for the upper ~ 50 cm of the water column and the remainder of the water column, respectively.

Win-Situ Aqua TROLL 200 loggers were secured to the star picket at the same depth as the tubing to monitor water pressure (to $\pm 0.1\%$) and electrical conductivity (EC) (to $\pm 0.1\%$) at 5 minute intervals. The EC and elevation of groundwater in a 8.1 m deep monitoring bore ~ 7 m from the river and ~ 30 m upstream of the monitoring site was

logged at 30 minute intervals during the study using a Win-Situ Aqua TROLL 200 logger. Water pressure was corrected for barometric pressure changes using a Rugged Baro TROLL set above the groundwater level and converted to head levels using a Trimble digital global positioning system and electrical measuring tape. River flow was calculated via the tidal prism method used in Peterson et al. (2010), which approximates river flow by dividing changes in the volume of a river section by the cross sectional area of the river at its bottom boundary. The volume of water in the study stretch was calculated using river widths measured along the study stretch, continuously measured depth at the lower boundary, and river depth data from the Victorian Water Resources Data Warehouse (2013) at the upstream boundary.

5.2.2 Sampling and analysis

Groundwater ^{222}Rn activities are based on activities determined by equilibration of streambed sediments with ^{222}Rn free water over >8 weeks as outlined in Unland et al. (2013). Briefly, four ~1.45 kg sediment samples were allowed to equilibrate with ~500 ml of water in air tight polyethylene containers before 150 ml of water was extracted and analysed. The activity of ^{222}Rn in water was measured using a RAD-7 radon-in-air detector by the method outlined in Burnett and Dulaiova (2006) and are reported in Bq/m^3 . ^{222}Rn was degassed from 150 ml of water for 5 minutes into an air-tight loop of known volume and total counting times were 40 minutes, yielding an average uncertainty of 15% based on replicate analysis. The ingrowth of ^{222}Rn via the decay of ^{226}Ra in river water was calculated by collecting two 1L samples (one saline and one fresh) of river water in air tight polyethylene bottles and allowing the ^{222}Rn and ^{226}Ra in the sample to achieve secular equilibrium over a period of >3 months. 500 ml of this sample was then degassed via the method outlined above for twelve 2 hr counting periods, yielding an uncertainty based on replicate analysis of ~20%.

River water was sampled throughout the study from the exchanger outlets in resealable polyethylene bottles. Stable isotopes were measured at Monash University using ThermoFinnigan MAT 252 and DeltaPlus Advantage mass spectrometers. $\delta^{18}\text{O}$ values of water were measured via equilibration with He- CO_2 at 32°C for 24-48 hours in a ThermoFinnigan Gas Bench. $\delta^2\text{H}$ values of water were measured via reaction with Cr at 850°C using a Finnigan MAT H/Device. $\delta^{18}\text{O}$ and $\delta^2\text{H}$ values were measured relative to internal standards that were calibrated using IAEA SMOW, GISP, and SLAP standards. Data were normalised following Coplen (1988) and are expressed relative to V-SMOW where $\delta^{18}\text{O}$ and $\delta^2\text{H}$ values of SLAP are -55.5‰ and -428‰ , respectively. The precision (1σ) of the analyses based on replicate analyses is $\delta^{18}\text{O} = \pm 0.2\text{‰}$, $\delta^2\text{H} = \pm 1\text{‰}$.

5.3. Results

5.3.1 Surface section (~50 cm depth)

As the absolute elevation of the river is not known, river heights have been referenced to the head logger at ~50 cm depth. During the study, the river height varied by ~20 cm, however the variation in any given tidal cycle was less than 10 cm (Fig. 2). River levels generally declined over the study, with a tidal maximum height of 0.64 m above the logger on April 14 and a tidal maximum height of 0.54 m above the logger on April 18. The greatest change in river height over a single tidal cycle occurred during the 15th of April, with a variation in height of ~10 cm. The smallest change in river height over a single tidal cycle occurred during the 18th of April with a variation in height of ~5 cm.

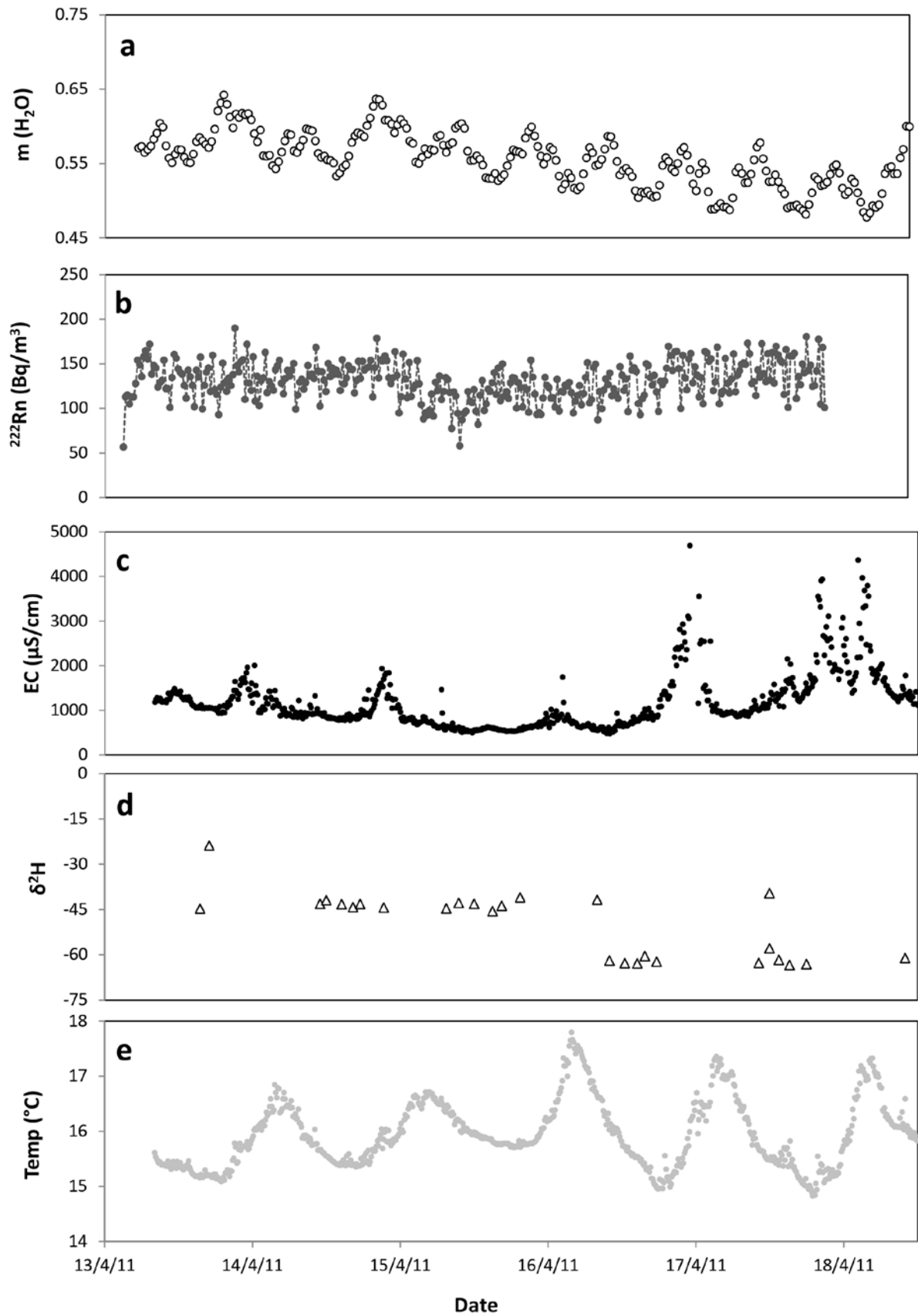


Figure 2. Variation over the study period of (a) Height of river above logger, (b) ^{222}Rn activity, (c) electrical conductivity, (d) δ^2H values and (e) temperature at ~50 cm depth in the Tambo River.

^{222}Rn activities in the surface section ranged from 60 to 190 Bq/m³ but did not show any periodic increases or decreases with tidal cycles. The average ^{222}Rn activity throughout the study was relatively constant at 130 ± 20 Bq/m³, however a decline in ^{222}Rn activity from 180 to 60 Bq/m³ occurred during April 15 (Fig. 2). Between April 13 and April 17 the EC of the surface section generally increased from ~1,000 to ~2,000 $\mu\text{S/cm}$ during tidal maximums while a sharp increase in EC from ~1,000 to ~10,000 $\mu\text{S/cm}$ occurred during April 17. EC was more variable after April 17, ranging from ~1,000 to ~5,000 $\mu\text{S/cm}$. The temperature of the surface section varied between 14 and 18 °C throughout the study. Diurnal variations were ~2°C with minimum daily temperatures occurring at ~3:00 am and daily maximum temperatures occurring at ~4:00 pm.

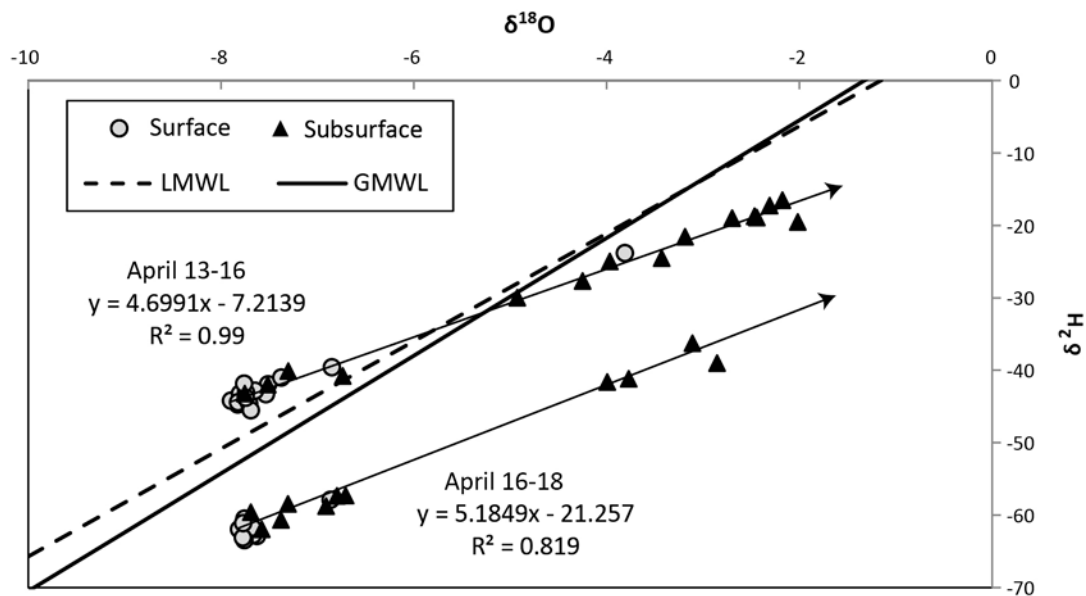


Figure 3. $\delta^2\text{H}$ and $\delta^{18}\text{O}$ values of surface and subsurface river water in the Tambo River against the Global meteoric water line (GMWL) and local (Melbourne) meteoric water line (LMWL) after Hughes et al. (2012). Arrowed lines = trend lines for water sampled April 13-16 and April 16-18.

$\delta^{18}\text{O}$ and $\delta^2\text{H}$ values in the surface section generally ranged from -7.9 to -6.9‰ and from -64 to -40‰, respectively, and plot close to the local and global meteoric water lines. This range however excludes a single anomalous sample with $\delta^2\text{H}$ and $\delta^{18}\text{O}$ values of -3.8‰ and -24‰, respectively, that was given for a sample taken on April 17 at

11:00am during a tidal maximum (Fig. 3). The majority of water from the surface section defines two distinct populations. The first population represents water sampled between April 13 and 8:00 am on April 16, with average $\delta^{18}\text{O}$ and $\delta^2\text{H}$ values of 7.5‰ and 42‰, respectively. The second population represents water sampled between 10:00 am on April 16 and April 18, with average $\delta^{18}\text{O}$ and $\delta^2\text{H}$ values of -7.6‰ and -60‰, respectively.

5.3.2 Subsurface section (~200cm depth)

The EC of water in the subsurface section of the Tambo River estuary was generally higher and more variable than in the surface section, with EC varying between ~32,000 and ~23,000 $\mu\text{S}/\text{cm}$ during April 14 (the smallest change over a tidal cycle), and between ~2,400 and ~32,000 $\mu\text{S}/\text{cm}$ during April 16 (the largest change over a tidal cycle). Subsurface temperature was generally higher than in the surface section, ranging from ~17 to ~20 °C over the study. Temperature in the subsurface shows a strong correlation with EC, with the greatest change in temperature (from 16.6 and 19.7 °C) correlating with the greatest change in EC during April 16 (Fig. 9c). ^{222}Rn activities in the subsurface section showed significantly higher variations than those in the surface section. ^{222}Rn activities varied between 50 and 220 Bq/m^3 and generally show a positive correlation with EC, temperature and river height (Fig. 4). The greatest increase in ^{222}Rn activities during a single tidal cycle occurred during the greatest increase in river height over a tidal cycle (~10 cm) on April 15, with ^{222}Rn activity increasing from ~100 to ~220 Bq/m^3 . EC increased from 10,000 to 30,200 $\mu\text{S}/\text{cm}$ during this tidal cycle. The lowest change in ^{222}Rn activity during a tidal cycle occurred on April 14 varying between ~100 and ~150 Bq/m^3 .

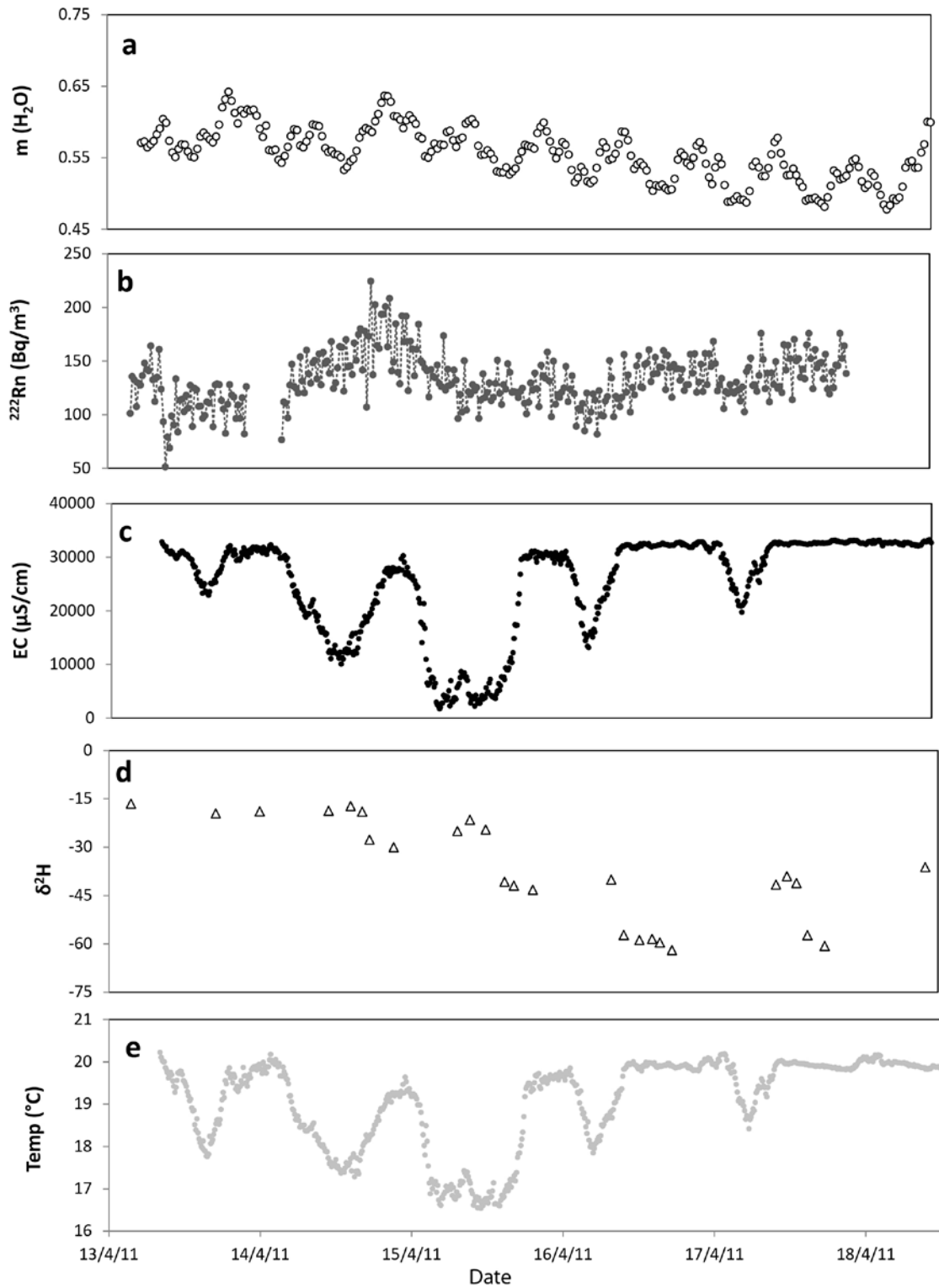


Figure 4. Variation over the study period of (a) height of river above logger, (b) ^{222}Rn activity, (c) electrical conductivity, (d) $\delta^2\text{H}$ values and (e) temperature at ~ 200 cm depth in the Tambo River.

$\delta^2\text{H}$ and $\delta^{18}\text{O}$ values of the subsurface water were also more variable than those from the surface section, with $\delta^2\text{H}$ and $\delta^{18}\text{O}$ values ranging from -7.8 to -2.0% and from $-$

62 to -17‰, respectively. Elevated $\delta^2\text{H}$ and $\delta^{18}\text{O}$ values in the deeper water tend to occur during tidal maximums when river EC is higher. The $\delta^2\text{H}$ and $\delta^{18}\text{O}$ values of subsurface waters again define two distinct groups (Fig. 3). Samples taken between April 13 and 8:00 am on April 16 define a linear trend (slope ~ 4.7) with $\delta^2\text{H}$ ranging from -43 to -17‰ and $\delta^{18}\text{O}$ values ranging from -7.8 to -2.0‰. Samples taken between 10:00 am on April 16 and April 18 define a linear trend (slope ~ 5.2) with $\delta^2\text{H}$ ranging from -62 to -36‰ and $\delta^{18}\text{O}$ values ranging from -7.7 to -2.9‰.

5.3.3 Groundwater

While groundwater elevations adjacent to the Tambo River estuary showed fluctuations consistent with tidal cycles, the range was considerably smaller than in the estuary, with only 0.07 m variation over the study (Fig. 5). Changes in groundwater elevation during individual cycles correlate with changes in river height, with the greatest increase occurring during April 15 (0.05 m). As with river water, groundwater levels declined over the study with a maximum elevation of 3.32 m above sea level (AHD) on April 15 and a maximum of 3.29 m on April 18. There was little variation in groundwater salinity over the study with an average EC of $2,234 \pm 4$ $\mu\text{S}/\text{cm}$. Lower groundwater EC's during the initial stages of monitoring may reflect the recovery of the monitoring bore following pumping prior to deploying the logger. Groundwater temperature remained constant over the study at 16.9 ± 0.1 °C. The activity of ^{222}Rn in water from sediment ingrowth experiments ranged from 3,740 to 1,900 Bq/m^3 with an average activity of $2,650 \pm 600$ Bq/m^3 ; these activities are similar to the ^{222}Rn activities of much of the groundwater in the Tambo catchment (Unland et al., 2013).

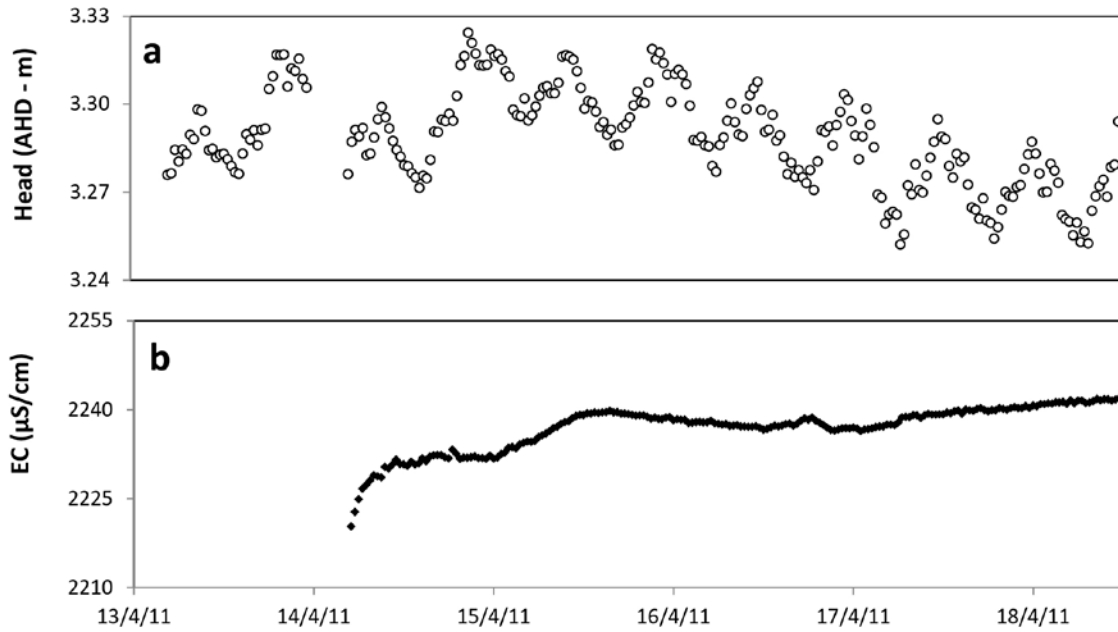


Figure 5. Head and electrical conductivity of groundwater ~7 m from the Tambo River at the study site.

5.4. Discussion

The following section considers the impact of tidal cyclicity in the Tambo River estuary with respect to fluctuations in salinity (EC), temperature, stable isotopes and ^{222}Rn in both surface and subsurface waters. The balance of ^{222}Rn and groundwater in the estuary is determined and the results compared to those of previous studies in similar hydrological settings.

5.4.1 Modelling groundwater fluxes

Groundwater fluxes into the surface section of the Tambo River estuary were modelled using continuous time series ^{222}Rn data and the minimum/maximum model (Burnett et al., 2010; Peterson et al., 2010; Santos et al., 2011) described by Eqs (2) and (3):

$$Q_{\text{gw-min}} = Q \times \left[\frac{(^{222}\text{Rn}_{\text{sw}} - ^{222}\text{Rn}_{\text{bkgd}})}{^{222}\text{Rn}_{\text{gw}}} \right] \quad (2)$$

$$Q_{\text{gw-max}} = Q \times \left[\left[\frac{(^{222}\text{Rn}_{\text{sw}}) + \left(\frac{J_{\text{atm}} \times R}{D} \right) - ^{222}\text{Rn}_{\text{bkgd}}}{e^{\lambda R}} \right] / ^{222}\text{Rn}_{\text{gw}} \right] \quad (3)$$

where $Q_{\text{gw-min}}$ is the minimum possible volume of groundwater discharged to the river stretch (m^3/day), assuming all groundwater is discharged at the sample point, and $Q_{\text{gw-max}}$ is the maximum possible volume of groundwater discharged to the river stretch, assuming all groundwater was discharged upstream (at the river gauging station). It is important to note that Q_{gw} represents the volume of groundwater discharge that is fluxing through the vertical plane at the point of time series measurement and is not an instantaneous representation of actual groundwater discharge. As such, negative Q_{gw} values indicate groundwater movement upstream and not losing conditions in the river.

As there are no ^{222}Rn sinks in Eq (2), groundwater discharge is simply calculated by subtracting $^{222}\text{Rn}_{\text{bgd}}$ (the input of ^{222}Rn via the decay of ^{226}Ra in river water) from the measured river ^{222}Rn activity ($^{222}\text{Rn}_{\text{sw}}$). This value is then divided by the activity of ^{222}Rn in groundwater ($^{222}\text{Rn}_{\text{gw}}$) to get the groundwater fraction in the river and multiplied by river discharge (Q , m^3/day) to get the volume of groundwater discharge to the stretch. Eq (3) takes into account the loss of ^{222}Rn to the atmosphere (J_{atm} , $\text{Bq}/\text{m}^2/\text{day}$) and decay ($\lambda = 0.18 \text{ day}^{-1}$) during the residence time (R , days) from the upstream boundary of the model. The atmospheric evasion of ^{222}Rn in the surface box was calculated using Eq's (4) and (5):

$$J_{\text{atm}} = k (^{222}\text{Rn}_{\text{sw}} - \alpha ^{222}\text{Rn}_{\text{air}}) \quad (4)$$

$$k = 1.719w^{0.5}D^{-0.5} \quad (5)$$

(Borges et al., 2004; Santos and Eyre, 2011) where $^{222}\text{Rn}_{\text{sw}}$ and $^{222}\text{Rn}_{\text{air}}$ are the activities of ^{222}Rn in river water and air (Bq/m^3), respectively, k is the gas transfer velocity (given in cm/h and converted to m/day), α is the Ostwald solubility coefficient for the ^{222}Rn fluid-gas ratio, w is river velocity (cm/sec) and D is river depth (m). While

there are a number of models that can be used to calculate k , the above model is suitable for this section of the Tambo River as river turbulence is likely to be dominated by river current and not wind speed, as steep river banks and cliffs ~50 m in height (Unland et al., 2013) protect the study area from high wind velocities. Additionally, similar models previously used in this river section (the Negulescu and Rojanski (1969) model as modified by Genereux and Hemond (1992) and Mullinger et al. (2007)) give similar k values for the study period. After converting the k values given by the Negulescu and Rojanski model to m/day by accounting for river depth, an average k value of 0.55 ± 0.1 m/day was given for the study period. This value is very similar to the average k given by Eqn (5) over the study (0.47 ± 0.2 m/day, Table 1), indicating that k model variability in this river section is unlikely to have significant impacts on groundwater discharge estimates.

As the RAD-7 instruments were measuring ^{222}Rn activities in river water throughout the study it was not possible to concurrently measure atmospheric ^{222}Rn activities, however previous studies have shown typical atmospheric activities to be <10 Bq/m³ (eg: Kenawy and Morsy, 1991). Atmospheric activities of 0 Bq/m³ have been assumed here to give the maximum J_{atm} value and thus the maximum groundwater discharge estimate. The exact value of $^{222}\text{Rn}_{\text{air}}$ has very little impact on groundwater flux estimates, with the average maximum $Q_{\text{gw-max}}$ value in the surface section reduced by only 15% when assuming an atmospheric activity of 20 Bq/m³.

Eqs (2) and (3) have also been used to describe the discharge of groundwater in the subsurface section of the estuary. As the subsurface section of the estuary is not in contact with the atmosphere it is not subject to degassing and the J_{atm} term in Eq (3) is redundant. Both surface and subsurface sections of the estuary will receive diffusive ^{222}Rn inputs via direct emanation from streambed and river bank sediments, and

from diffusive inputs of ^{222}Rn from in pore water. As this section of the Tambo River is gaining, groundwater discharge is likely to purge porewater prior to significant ingrowth, limiting diffusive inputs. As such, these inputs are likely to be negligible and are not considered in Eqs (2) and (3).

Box	R Days	Q m ³ /day	Rn _{bckgd} Bq/m ³	Rn _{gw}	k m/day	J _{atm} Bq/m ² /day	Q _{min} m ³ /day	Q _{max} m ³ /day	Groundwater Fraction (%)
Surface	0.76±.04	688	59±13	2640	0.47±0.16	61±24	19	49	3 to 7
Subsurface		1,808	52±8	±600			63	142	4 to 8

Table 1. Average model parameters and groundwater discharge values from Eqs (2) and (3).

Model parameters in Eqs (2) and (3) have been summarised in Table 1. River velocity based on the tidal prism method ranged from 1,540 m/day upstream to 2,370 m/day downstream. The residence time of water varied little over the study, ranging from 0.62 to 0.80 days with an average of 0.76±0.04 days. The average k value was 0.47±0.16 m/day while atmospheric evasion averaged 61±24 Bq/m²/day. River discharge values in the surface section ranged from 45,380 m³/day upstream to 70,040 m³/day downstream, with an average of 687 m³/day downstream. Maximum groundwater discharge in the surface section ranged from 5,540 upstream to 9,800 m³/day downstream and minimum groundwater discharge ranged from 1,745 m³/day upstream to 2,510 m³/day downstream (Fig. 6). The maximum groundwater fraction in the surface section ranged from 1.3 to 14% of total discharge and the minimum from 0.1 to 4.9% of total discharge (Fig. 6). River discharge in the subsurface section ranged from 170,100 m³/day upstream to 270,150 m³/day downstream with an average of 1,810 m³/day downstream. The maximum groundwater fraction in the subsurface section ranged from 3.7 to 14.2% of total discharge while the minimum ranged from 0.2 to 7.2% of total discharge (Fig. 6). These fractions correlate with groundwater discharge volumes of 20,100 m³/day upstream

to 32,000 m³/day downstream and 9,430 m³/day upstream to 10,300 m³/day downstream, respectively.

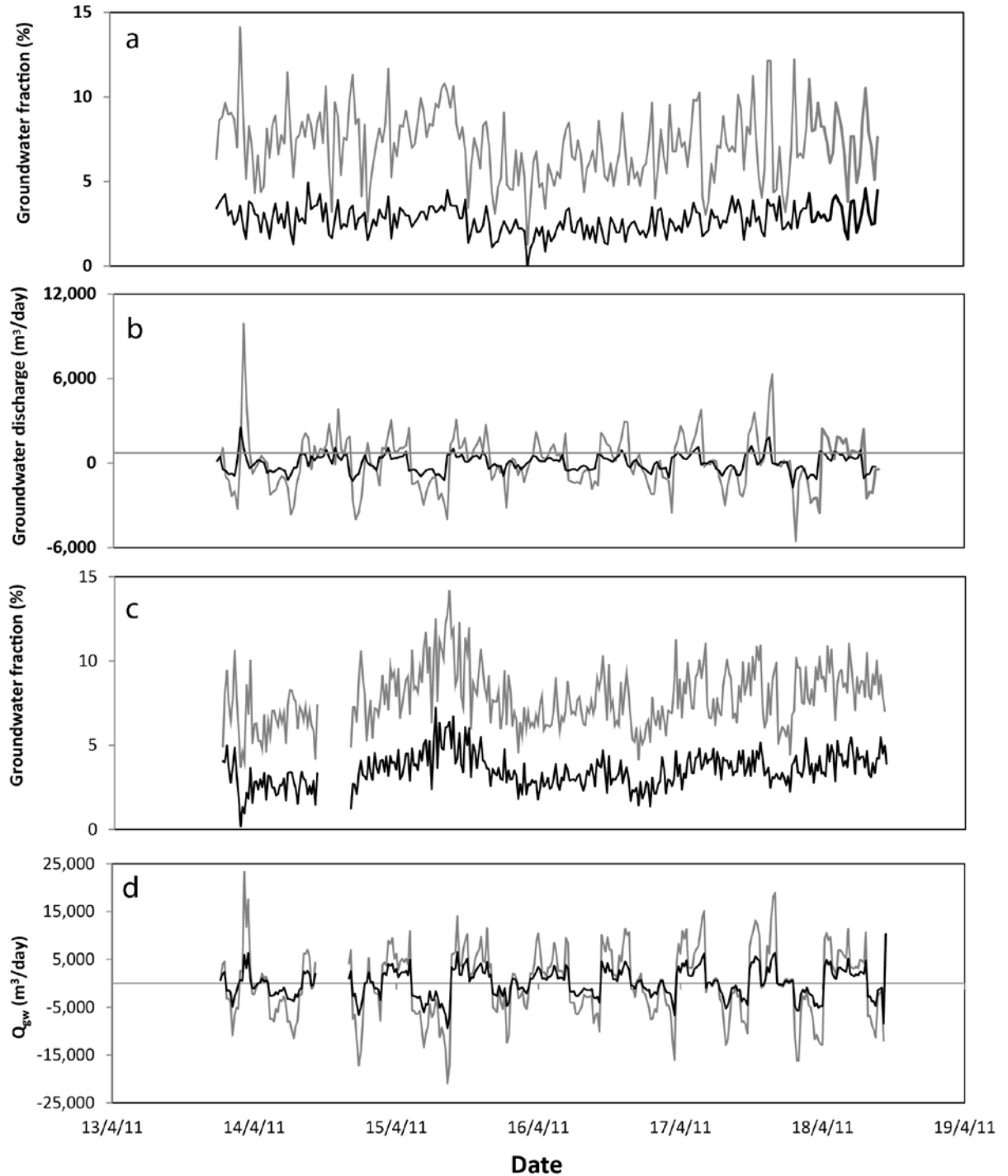


Figure 6. Modelled groundwater fractions in surface water (a), groundwater discharge volume in surface section (b), groundwater fraction in subsurface section (c), groundwater discharge volume in subsurface section (d). Minimum estimates = black lines, maximum estimates = grey lines.

5.4.2 Uncertainty and sensitivity analysis

While it has been shown that there are uncertainties associated with the derivation of Q via the tidal prism method (Luketina, 1998), it may provide a more realistic estimate of river flow in stratified estuaries, as the tidal prism method integrates changes in the height of the entire water column as opposed to single point current measurements (Peterson et al., 2010). As Q is estimated using changes in the volume of the study section, the uncertainty of Q will be a function of the measured river height, width and depth. Uncertainties with respect to changes in river height are likely to be small as these changes are measured using a logger with an instrumental error of $\pm 0.1\%$. The river depth and width were measured in field by tape measure to ± 1 cm, while the length of the study stretch was measured using satellite imagery. The uncertainty associated with length was assessed by taking several measurements ($n=6$), yielding an uncertainty of 54 m (0.9%).

The largest uncertainty with respect to Q is the variability in depth and width between measurement points. Ripples ~ 30 cm in height dominate the streambed morphology in this section of the Tambo River, giving an approximate uncertainty of 16.2% based on the average depth of the river stretch. While the average depth of the study stretch was interpolated from river height data at measurement sites, change in depth between sites was not measured during the study and as such remains unconstrained. The average width of the study stretch was also interpolated using the width measured at the upstream and downstream measurement sites. The uncertainty associated with this assumption was estimated by measuring the actual river width every 100 m using satellite imagery (Fig. 7), giving an average uncertainty 10.9% with respect to average river width. The overall uncertainty of Q based on the above estimates is 19.5%.

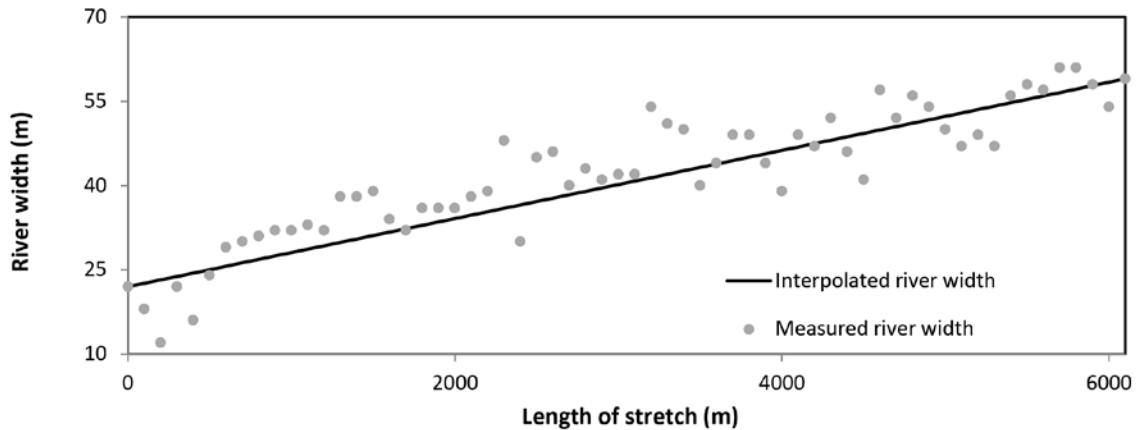


Figure 7. Interpolated river width vs river width every 100m measured using satellite imagery.

For ^{222}Rn activities less than $1,000 \text{ Bq/m}^3$ (surface water), analytical uncertainties are typically less than 15%, while activities greater than $1,000 \text{ Bq/m}^3$ (groundwater) typically yield an analytical uncertainty of less than 5% (e.g. Cartwright et al., 2011; Unland et al., 2013). The uncertainty of $^{222}\text{Rn}_{\text{gw}}$ based on the variability of ^{222}Rn in water equilibrated with different sediment samples was slightly higher than analytical precision, with a standard deviation 22% from the mean. Background ^{222}Rn activities were relatively low, yielding slightly higher analytical uncertainties based on replicate analysis (22% and 18% in for the surface and subsurface sections, respectively). Based on the above, the overall uncertainty with respect to GW_{min} estimates is 39%.

The uncertainty of GW_{max} requires the uncertainty of k to be evaluated but not residence time (as the uncertainty of R relies upon depth, width and length measurements which are already accounted for in Q uncertainty analysis). The uncertainty of k used to calculate J_{atm} in Eq (3) was estimated by comparison between the Negulescu and Rojanski (1969) and the Borges et al. (2004) gas transfer models. These models yield an uncertainty of 9.7% with respect to average k estimates. k values estimated by the Negulescu and Rojanski model are generally higher than the Borges model, resulting in slightly higher average groundwater estimates. The average uncertainty in GW_{max}

estimates resulting from discrepancies in k values is 16.8% and is considered negligible in the context of this study.

River discharge imposes the greatest control on variations in the calculated groundwater discharge in (Fig. 6). This is because in both Eq (2) and (3), the calculated groundwater fraction is multiplied by Q . The groundwater fraction varies by less than 15% in both the surface and subsurface sections while Q varies by >5 orders of magnitude in both the surface and subsurface sections. As a result, groundwater discharge has a linear correlation with Q (Fig. 8), with downstream groundwater flow increasing during tidal minimums and upstream groundwater flow increasing during tidal maximums.

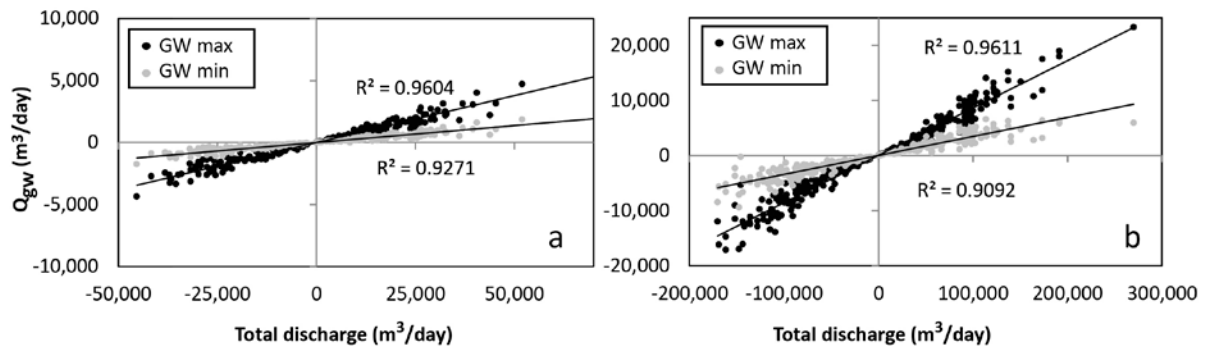


Figure 8. Total discharge vs groundwater discharge in surface (a) and subsurface (b) water in the Tambo River estuary.

In contrast, variations in the groundwater fraction over the study relied most heavily on $^{222}\text{Rn}_{\text{sw}}$, as $^{222}\text{Rn}_{\text{sw}}$ is the most variable parameter in Eq (2) and (3) other than the total river discharge. While accounting J_{atm} does increase the estimated maximum groundwater fraction in surface waters during the study, variations in k and R over the study are minor, so variations in J_{atm} are mostly a result of variations in $^{222}\text{Rn}_{\text{sw}}$. Furthermore, the $^{222}\text{Rn}_{\text{gw}}$ and $^{222}\text{Rn}_{\text{bckgd}}$ parameters in Eq (3) are fixed. As such, they will alter the baseline groundwater fraction (with higher $^{222}\text{Rn}_{\text{gw}}$ and $^{222}\text{Rn}_{\text{bckgd}}$ values giving lower groundwater fractions), but will have no impact on variations in the groundwater

fraction calculated throughout the study. In this context $^{222}\text{Rn}_{\text{gw}}$ will have a greater impact on the groundwater fraction than $^{222}\text{Rn}_{\text{bckgd}}$, as the all terms in Eq (3) are divided by $^{222}\text{Rn}_{\text{gw}}$ (giving a 1:1 change in the groundwater fraction in response to $^{222}\text{Rn}_{\text{gw}}$), while $^{222}\text{Rn}_{\text{bckgd}}$ is only subtracted from the atmospheric evasion corrected $^{222}\text{Rn}_{\text{sw}}$ term in Eq (3) (giving ~1:4 changes in the groundwater fraction in response to $^{222}\text{Rn}_{\text{bckgd}}$).

5.4.3 Tidal dynamics and groundwater-surface water interactions

Fluctuations in water temperature of 2 to 3 °C in the surface section are consistent with diurnal atmospheric temperature fluctuations (Fig. 9a). Fluctuations are approximated by a sine curve (mean difference = 0.33 °C) with an amplitude of 0.94 °C from the median temperature of 15.9 °C over a 24 hr period. As such, temperature fluctuations in the surface section are not indicative of mixing with warmer lake water or the discharge of groundwater over the study which would cause significant deviations from the sine curve in Fig. 9a. The EC spike in the surface section on April 17 (Fig. 2) represents a period of mixing with more saline water in the subsurface section that was driven by boat activity in the estuary and is not indicative of natural conditions. EC increases in the surface section from ~1,000 to ~2,000 $\mu\text{S}/\text{cm}$ on April 14, 15, 16 and from ~1,000 to ~4,000 on April 18 occur during tidal maximums and are indicative of varying degrees of mixing with the more saline water in the subsurface. This indicates that the estuary is partially mixed and that the degree of mixing throughout the water column varies as a function of changing river flow over tidal cycles.

While groundwater fractions and ^{222}Rn activities do not show tidal cyclicity in the surface section (Fig. 2), a reduction in the maximum groundwater fraction (from 11 to 2%) and ^{222}Rn activities (from 153 to 58 Bq/m^3) did occur during April 15. This was also followed by a reduction in both the $\delta^2\text{H}$ and $\delta^{18}\text{O}$ values of water in the estuary. These observations coincide with increased rainfall in the area, with 7.8 mm of rainfall on April

15 and 11.6 mm of rainfall on April 16 (Bureau of Meteorology, 2013). As such, the reduction in ^{222}Rn activity and groundwater fraction may be the result of dilution through the addition of ^{222}Rn free rainwater (c.f., Santos et al., 2010). Simultaneously the input of rainfall and runoff with a different $\delta^2\text{H}$ and $\delta^{18}\text{O}$ signature to river water will alter the $\delta^2\text{H}$ and $\delta^{18}\text{O}$ value of river water (Kennedy et al., 1986). This may explain the two distinct populations of $\delta^2\text{H}$ and $\delta^{18}\text{O}$ values in Fig. 3, with higher $\delta^2\text{H}$ values representing pre event upstream water and lower $\delta^2\text{H}$ values representing a mixture of pre event upstream water and event water.

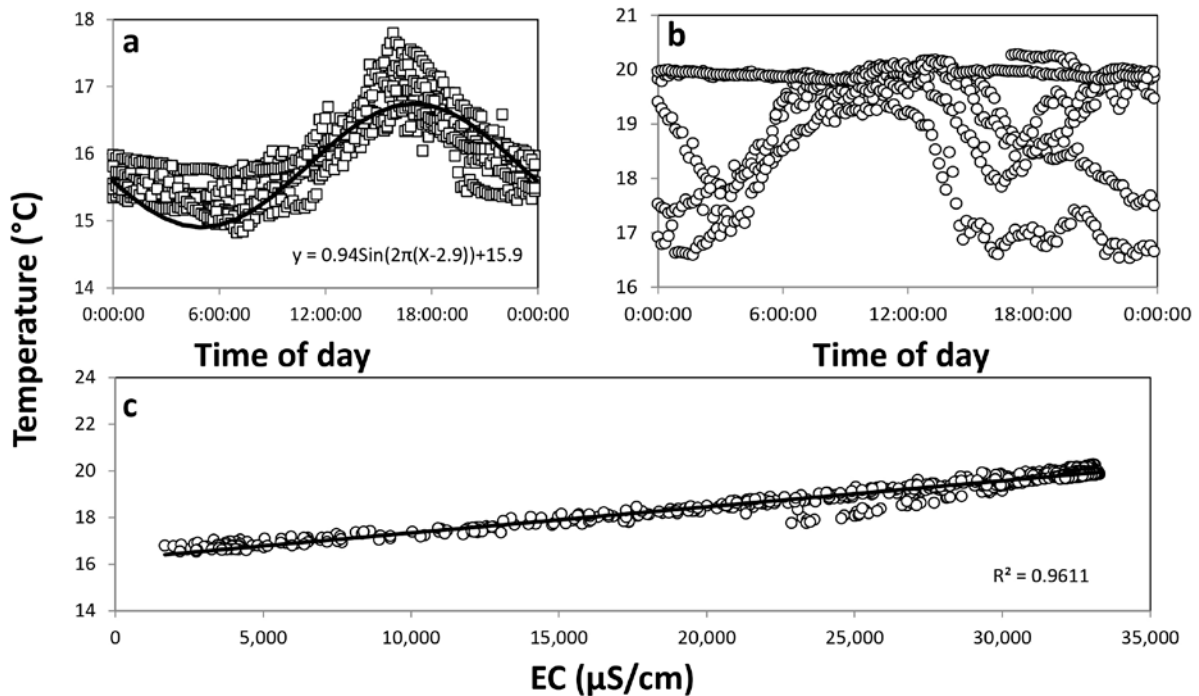


Figure 9. Daily temperature fluctuations at ~50 cm depth (a) and ~200 cm depth (b) and covariance between EC and temperature at ~200 cm depth.

As upstream water has an EC of $\sim 150 \mu\text{S}/\text{cm}$ and downstream water has an EC of $\sim 33,000 \mu\text{S}/\text{cm}$, relatively small inputs of saline water ($<3\%$) would be required to produce the background EC of $1,000 \mu\text{S}/\text{cm}$ observed in the surface section throughout most of the study. Additionally, tidal variations in EC ($1,000$ to $4,000 \mu\text{S}/\text{cm}$ at ~ 50 cm) would be driven by relatively minor increases in the saline water fraction (from $\sim 3\%$ to

~12%). ^{222}Rn activities in the surface section support this assertion as significant inputs of subsurface water with higher ^{222}Rn activities would be expected to result in an increase in the activity of ^{222}Rn in the surface section, which does not occur. $\delta^2\text{H}$ and $\delta^{18}\text{O}$ values in the surface section are also consistent with minor inputs of subsurface water and do not generally increase during tidal maximums as would be expected for increased inputs of subsurface water.

In contrast, groundwater fractions, EC, temperature, ^{222}Rn activities, $\delta^2\text{H}$ and $\delta^{18}\text{O}$ values all increase during tidal maximums in the subsurface of the Tambo River estuary, indicating higher variations in the mixing between fresh upstream and saline lake water in subsurface section compared to the surface section of the estuary. Mixing estimates based on end members of 150 and 33,000 $\mu\text{S}/\text{cm}$ indicate a variation in the saline water fraction of between 5% and 100%. This mixing trend is further supported by a linear correlation between with EC and temperature (Fig. 9c) and the absence of diurnal variations similar to atmospheric temperature fluctuations.

While groundwater discharge in the subsurface section of the estuary increase during tidal minimums, this is a function of the models reliance on Q and does not reflect increasing groundwater inputs, as the groundwater fraction in the estuary actually decreases during tidal minimums. This observation is different to other studies in similar settings which have indicated increasing groundwater discharge during tidal minimums, driven by elevated groundwater–surface water gradients as surface water levels decline (Knee and Jordan, 2013; Peterson et al., 2010; Santos and Eyre, 2011; Santos et al., 2010). While river height was not corrected to the Australian Height Datum and exact groundwater – surface water gradients could not be established, the relative height of groundwater and surface water have been shown in Fig 10. This shows that on a number of occasions (eg: ~16:00 on April 15,16,17) the groundwater fraction declined (to 4.5, 4.1

and 4.5%, respectively) when the relative height of groundwater to surface water increased (to 0.89, 0.91 and 0.93, respectively). Conversely, the highest maximum groundwater fractions in the subsurface (14.2%) occurred early in the morning of April 15, when the relative height of groundwater to surface water was the lowest (0.82 m). This suggests that groundwater fraction increases in the subsurface have a greater reliance on mixing than groundwater-surface water gradients.

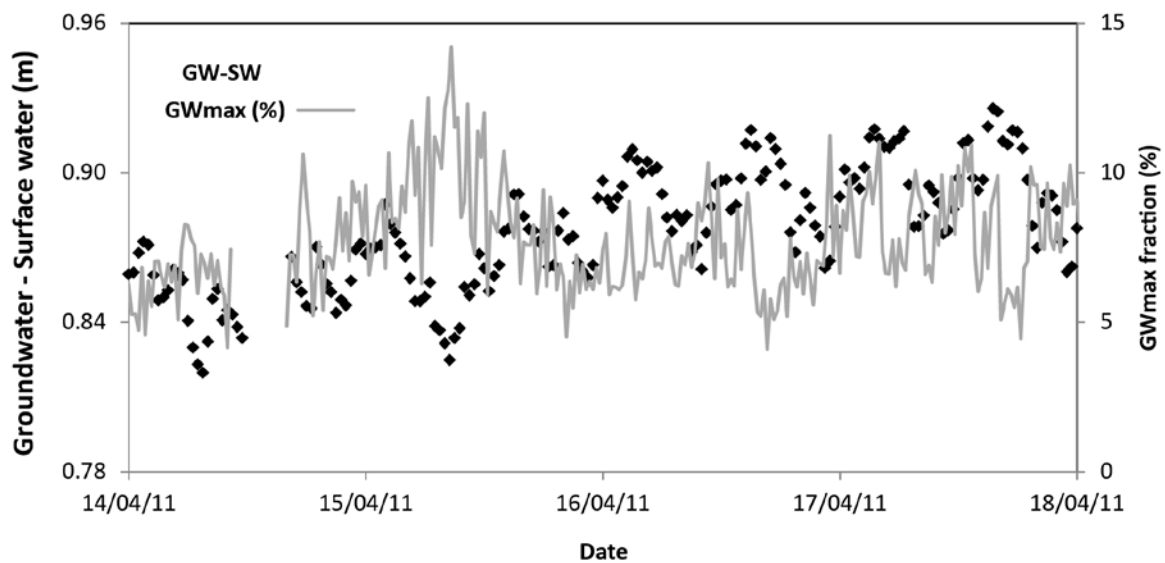


Figure 10. Groundwater elevation (AHD-m) minus average river depth (m) over the study vs maximum groundwater fraction estimates in the subsurface section of the Tambo River estuary.

While previous studies have considered either fully stratified (Santos et al., 2010; Peterson et al., 2010) or well mixed (Burnett et al., 2010; Crusius et al., 2005; Santos and Eyre, 2011) estuaries, results from this study indicate a varying degrees of mixing in the Tambo River estuary. As such, reductions in ^{222}Rn activities in the subsurface of the estuary during tidal minimums may be attributed to mixing between surface water that has lower ^{222}Rn activities and subsurface water with higher ^{222}Rn activities. However, mixing can not be solely responsible for the observed ^{222}Rn activities in the subsurface as trends in EC do not mirror those in ^{222}Rn activities. It is also apparent that the greatest increase in ^{222}Rn activities in the subsurface occurs not only during one of many increases

in EC ($\sim 32,000 \mu\text{S}/\text{cm}$) but also during the greatest tidal maximum (Fig. 4), when tidal increases will cause the greatest upstream flow in an estuary. As such, it may be that subsurface water receives groundwater inputs as it migrates downstream, and that the same body of water receives further groundwater inputs as it moves back upstream during flow reversal at high tide (Fig. 11). It is also important to note that similar processes may be occurring in the surface section of the estuary, but processes such as degassing of ^{222}Rn and dilution of groundwater from rainfall and runoff make it difficult to capture. Furthermore, flow reversal is likely to be greater in subsurface than the surface section of the estuary, resulting in greater upstream movement and a greater potential for secondary groundwater inputs.

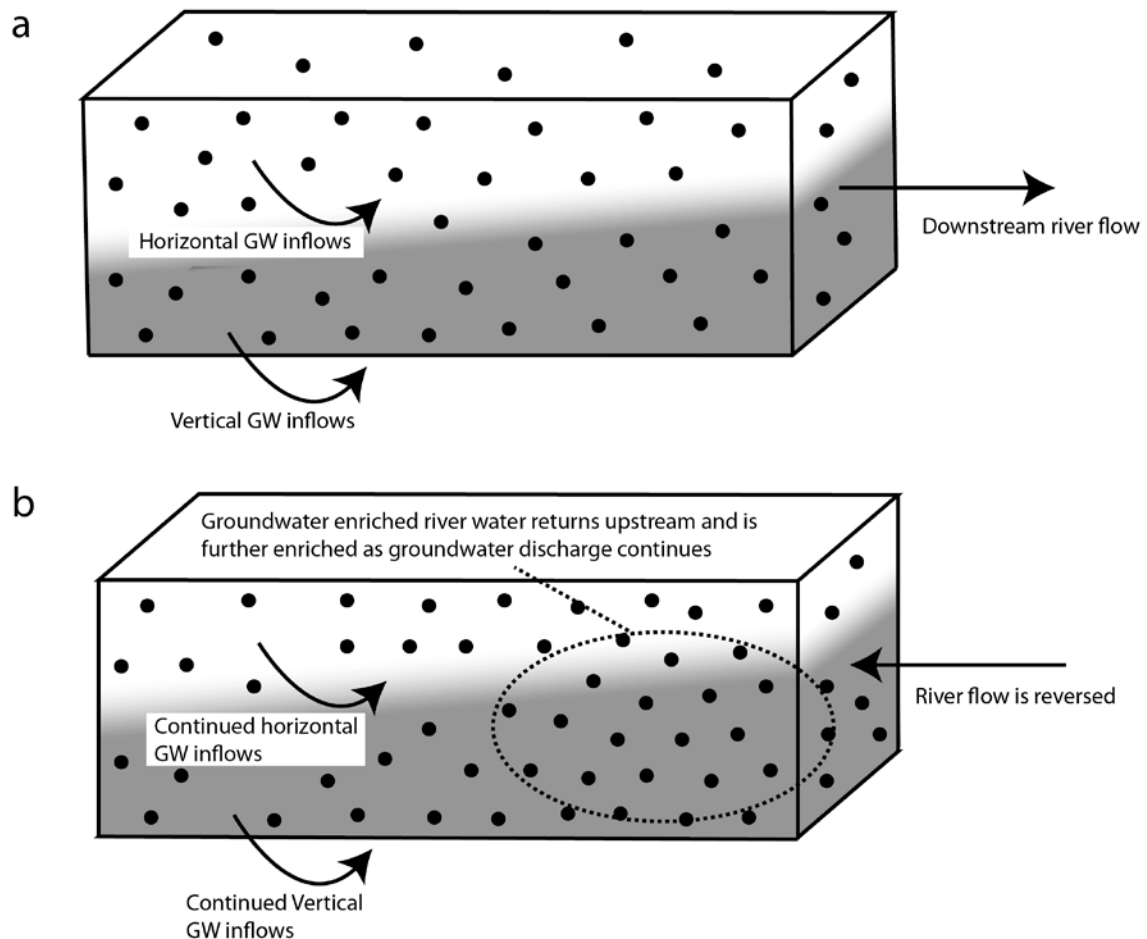


Figure 11. Schematic representation of groundwater (black dots) inputs to the Tambo River estuary during tidal minimums (a) and tidal maximums (b). Grey shading indicates saline subsurface waters.

In any case, this is a mechanism that has not previously been explored in similar studies and may contribute to changes in the groundwater fraction in other tidal estuaries. Even in estuaries where downstream flow is reduced during tidal maximums, but not completely reversed, similar processes may be occurring. Under these conditions, if groundwater discharge remains constant while downstream river discharge is reduced, the fraction of groundwater in the estuary will begin to increase as river discharge decreases. This will of course have no impact on the total nutrient load carried by rivers via groundwater pathways (as groundwater discharge is not considered to vary here), however failure to account for such processes has the potential to lead to poor groundwater discharge and nutrient load estimates. If for example, the load of a nutrient via groundwater discharge is based on average daily river discharge, and a groundwater fraction has been calculated during a tidal minimum, the groundwater fraction and nutrient load via groundwater discharge may be underestimated. These processes are indicative of the highly transient nature of groundwater-surface water interactions in tidal estuaries, and demonstrates the value in analysing such interactions at a high frequency when conducting groundwater-surface water studies.

5.5 Conclusions

This study applies established ^{222}Rn mass balance models to a tidal estuary in southeast Australia to explore groundwater inflows over tidal cycles. The main conclusions of the study are (1) ^{222}Rn activities in the surface water fraction were generally lower than in the subsurface due to the degassing of ^{222}Rn in surface waters (2) decreases in ^{222}Rn activities of the surface water fraction during the study are consistent with the input of low ^{222}Rn rainfall and runoff (3) increasing ^{222}Rn activities in the subsurface of the estuary during tidal maximums can be mostly attributed to mixing between low ^{222}Rn surface water and higher ^{222}Rn subsurface waters (4) fluctuations in

the ^{222}Rn activity of subsurface water is greater than simple mixing indicates, suggesting secondary inputs of groundwater into the subsurface during flow reversal at larger tidal maximums. While the continuous ^{222}Rn method has been previously applied in tidal estuaries and coastal areas to assess groundwater inputs (Burnett et al., 2010; Burnett et al., 2008; Crusius et al., 2005; Knee and Jordan 2013; Peterson et al., 2008; Peterson et al., 2010; Santos and Eyre 2011; Santos et al., 2013), this study is the first (to the authors knowledge) to combine this method with analysis of oxygen and hydrogen isotopes, allowing for the determination of groundwater dilution via increased rainfall and runoff. Further to this, most of these and other studies have found ^{222}Rn activities to increase at low tide due to changes in groundwater- surface water gradients and tidal pumping (Burnett et al., 2008; Crusius et al., 2005; Santos et al., 2008; Santos and Eyre 2011; Santos et al., 2013). In contrast, this study found ^{222}Rn activities to increase during tidal maximums in the subsurface section of the estuary. While such trends have previously resulted from degassing (Peterson et al., 2010), this study has identified sampling and mixing across the pycnocline as the major driver of tidal ^{222}Rn variations. Further variations have been attributed to constant groundwater discharge during changes in river discharge over tidal cycles, a mechanism not previously explored in other studies.

This study shows how continuous ^{222}Rn monitoring in both surface and subsurface estuary waters can be combined with oxygen and hydrogen isotope analysis to understand tidal groundwater-surface water dynamics. The findings highlight a number of processes that can affect the groundwater fraction in estuaries on the time scales of hours to days, and that failure to account for such processes may lead to poor groundwater discharge and nutrient load estimates. These outcomes have the potential to better understand water balances, nutrient loads and the biogeochemical processes in estuaries.

Acknowledgements

Funding for this research was provided by the National Centre for Groundwater Research and Training, and Australian Government initiative, supported by the Australian Research Council and the National Water Commission.

References

- Anderson, D., Glibert, P., Burkholder, J., 2002. Harmful algal blooms and eutrophication: Nutrient sources, composition, and consequences. *Estuaries*, 25(4): 704-726.
- Bureau of Meteorology, 2013: Commonwealth of Australia, available at: <http://www.bom.gov.au> (last access: 28 August 2013).
- Borges, A.V., Gazeau, F., Abril, G., Frankignoulle, M., 2004. Gas transfer velocities of CO₂ in three European estuaries (Randers Fjord, Scheldt, and Thames). *Limnology and Oceanography*, 49(5): 1630-1641.
- Burnett, W.C., Aggarwal, P. K., Aureli, A., Bokuniewicz, H., Cable, J. E., Charette, M. A., Kontar, E., Krupa, S., Kulkarni, K. M., Loveless, A., Moore, W. S., Oberdorfer, J. A., Oliveira, J., Ozyurt, N., Povinec, P., Privitera, A. M. G., Rajar, R., Ramessur, R. T., Scholten, J., Stieglitz, T., Taniguchi, M., Turner, J. V., 2006. Quantifying submarine groundwater discharge in the coastal zone via multiple methods. *Science of The Total Environment*, 367(2–3): 498-543.
- Burnett, W.C., Dulaiova, H., 2006. Radon as a tracer of submarine groundwater discharge into a boat basin in Donnalucata, Sicily. *Continental Shelf Research*, 26(7): 862-873.
- Burnett, W.C., Kim, G., Lane-Smith, D., 2001. A continuous monitor for assessment of ²²²Rn in the coastal ocean. *Journal of Radioanalytical and Nuclear Chemistry*, 249(1): 167-172.
- Burnett, W.C., Peterson, R., Moore, W.S., de Oliveira, J., 2008. Radon and radium isotopes as tracers of submarine groundwater discharge – Results from the Ubatuba, Brazil SGD assessment intercomparison. *Estuarine, Coastal and Shelf Science*, 76(3): 501-511.
- Burnett, W.C., Peterson, R.N., Santos, I.R., Hicks, R.W., 2010. Use of automated radon measurements for rapid assessment of groundwater flow into Florida streams. *Journal of Hydrology*, 380(3–4): 298-304.
- Cartwright, I., Hofmann, H., Sirianos, M.A., Weaver, T.R., Simmons, C.T., 2011. Geochemical and ²²²Rn constraints on baseflow to the Murray River, Australia, and timescales for the decay of low-salinity groundwater lenses. *Journal of Hydrology*, 405(3–4): 333-343.
- Charette, M.A., Sholkovitz, E.R., 2006. Trace element cycling in a subterranean estuary: Part 2. Geochemistry of the pore water. *Geochimica Et Cosmochimica Acta*, 70(4): 811-826.
- Cifuentes, L.A., Fogel, M.L., Pennock, J.R., Sharp, J.H., 1989. Biogeochemical factors that influence the stable nitrogen isotope ratio of dissolved ammonium in the Delaware Estuary. *Geochimica Et Cosmochimica Acta*, 53(10): 2713-2721.
- Cloern, J.E., 2001. Our evolving conceptual model of the coastal eutrophication problem. *Marine Ecology Progress Series*, 210: 223-253.

- Coplen, T.B., 1988. Normalisation of oxygen and hydrogen isotope data. *Chemical Geology: Isotope Geoscience section*, 72(4): 293-297..
- Cook, P.G., 2012. Estimating groundwater discharge to rivers from river chemistry surveys. *Hydrological Processes*, 27(25): 3694-3707.
- Cook, P.G., Lamontagne, S., Berhane, D., Clark, J.F., 2006. Quantifying groundwater discharge to Cockburn River, southeastern Australia, using dissolved gas tracers ^{222}Rn and SF_6 . *Water Resources Research*, 42(10): W10411.
- Cook, P.L.M., Holland, D.P., Longmore, A.R., 2010. Effect of a flood event on the dynamics of phytoplankton and biogeochemistry in a large temperate Australian lagoon. *Limnology and Oceanography*, 55(3): 1123-1133.
- Crusius, J., Koopmans, D., Bratton, J.F., Charette, M.A., Kroeger, K., Henderson, P., Ryckman, L., Halloran, K., Colman, J.A., 2005. Submarine groundwater discharge to a small estuary estimated from radon and salinity measurements and a box model.
- Department of Agriculture, Fisheries and Forestry, 2006: available at: <http://adl.brs.gov.au/water2010/pdf/catchment2230summary.pdf> (last access: 19 November 2012).
- Dulaiova, H., Peterson, R., Burnett, W.C., Lane-Smith, D., 2005. A multi-detector continuous monitor for assessment of ^{222}Rn in the coastal ocean. *Journal of Radioanalytical and Nuclear Chemistry*, 263(2): 361-363.
- Freyer, K., Treutler, H.C., Dehnert, J., Nestler, W., 1997. Sampling and measurement of radon-222 in water. *Journal of Environmental Radioactivity*, 37(3): 327-337.
- Genereux, D.P., Hemond, H.F., 1992. Determination of gas exchange rate constants for a small stream on Walker Branch Watershed, Tennessee. *Water Resources Research*, 28(9): 2365-2374.
- Genereux, D.P., Hemond, H.F., 1990. Naturally Occurring Radon 222 as a Tracer for Streamflow Generation: Steady State Methodology and Field Example. *Water Resour. Res.*, 26: 3065-3075.
- Gilfedder, B.S., Hofmann, H., Cartwright, I., 2012. Novel instruments for in situ continuous Rn-222 measurement in groundwater and the application to river bank infiltration. *Environmental Science & Technology*, 47(2): 993-1000.
- Grayson, R.B., Gippel, C.J., Finlayson, B.L., Hart, B.T., 1997. Catchment-wide impacts on water quality: the use of 'snapshot' sampling during stable flow. *Journal of Hydrology*, 199(1-2): 121-134.
- Hallegraef, G.M., 1992. Harmful algal blooms in the Australian region. *Marine Pollution Bulletin*, 25(5-8): 186-190.
- Harris, G.P., 1999. Comparison of the biogeochemistry of lakes and estuaries: ecosystem processes, functional groups, hysteresis effects and interactions between macro- and microbiology. *Marine and Freshwater Research*, 50(8): 791-811.
- Hoehn, E., Von Gunten, H.R., 1989. Radon in groundwater: A tool to assess infiltration from surface waters to aquifers. *Water Resources Research*, 25(8): 1795-1803.
- Hofmann, H., Gilfedder, B.S., Cartwright, I., 2011. A Novel Method Using a Silicone Diffusion Membrane for Continuous ^{222}Rn Measurements for the Quantification of Groundwater Discharge to Streams and Rivers. *Environmental Science & Technology*, 45(20): 8915-8921.
- Howarth, R.W., Marino, R., 2006. Nitrogen as the limiting nutrient for eutrophication in coastal marine ecosystems: evolving views over three decades. *Limnol. Oceanogr.*, 51(1): 364-376.
- Hughes, C. E., and Crawford, J., 2012. A new precipitation weighted method for determining the meteoric water line for hydrological applications demonstrated

- using Australian and global GNIP data: *Journal of Hydrology*, 464–465(0): 344–351.
- Kawabata, H., Narita, H., Harada, K., Tsunogai, S., Kusakabe, M., 2003. Air-Seas gas transfer velocity in stormy winter estimated from radon deficiency. *Journal of Oceanography*, 59: 651–661.
- Kennedy, V.C., Kendall, C., Zellweger, G.W., Wyerman, T.A., Avanzino, R.J., 1986. Determination of the components of stormflow using water chemistry and environmental isotopes, Mattole River basin, California. *Journal of Hydrology*, 84(1–2): 107–140.
- Kenawy, M.A., Ahmed Morsy, A., 1991. Measurements of environmental radon-222 concentration in indoor and outdoors in Egypt. *International Journal of Radiation Applications and Instrumentation. Part D. Nuclear Tracks and Radiation Measurements*, 19(1–4): 343–346.
- Knee, K., Jordan, T., 2013. Spatial Distribution of Dissolved Radon in the Choptank River and Its Tributaries: Implications for Groundwater Discharge and Nitrate Inputs. *Estuaries and Coasts*: 1–16.
- Lamontagne, S., Le Gal La Salle, C., Hancock, G.J., Webster, I.T., Simmons, C.T., Love, A.J., James-Smith, J., Smith, A.J., Kämpf, J., Fallowfield, H.J., 2008. Radium and radon radioisotopes in regional groundwater, intertidal groundwater, and seawater in the Adelaide Coastal Waters Study area: Implications for the evaluation of submarine groundwater discharge. *Marine Chemistry*, 109(3–4): 318–336.
- Luketina, D., 1998. Simple tidal prism models revisited. *Estuarine, Coastal and Shelf Science*, 46(1): 77–84.
- Morris, A.W., Mantoura, R.F.C., Bale, A.J., Howland, R.J.M., 1978. Very low salinity regions of estuaries: important sites for chemical and biological reactions. *Nature*, 274(5672): 678–680.
- Mullinger, N.J., Binley, A.M., Pates, J.M., Crook, N.P., 2007. Radon in Chalk streams: Spatial and temporal variation of groundwater sources in the Pang and Lambourn catchments, UK. *Journal of Hydrology*, 339(3–4): 172–182.
- Mullinger, N.J., Pates, J.M., Binley, A.M., Crook, N.P., 2009. Controls on the spatial and temporal variability of ²²²Rn in riparian groundwater in a lowland Chalk catchment. *Journal of Hydrology*, 376(1–2): 58–69.
- Murakami, Y., Horiuchi, K., 1979. Simultaneous determination method of radon-222 and radon-220 by a toluene extraction-liquid scintillation counter. *J. Radioanal. Chem.*, 52(2): 275–283.
- Negulescu, M., Rojanski, V., 1969. Recent research to determine reaeration coefficients. *Water Res.*, 3: 189–202.
- Peterson, R.N., Santos, I.R., Burnett, W.C., 2010. Evaluating groundwater discharge to tidal rivers based on a Rn-222 time-series approach. *Estuarine, Coastal and Shelf Science*, 86(2): 165–178.
- Santos, I.R., Burnett, W.C., Chanton, J., Mwashote, B., Suryaputra, I. G. N. A., Dittmar, T., 2008. Nutrient biogeochemistry in a Gulf of Mexico subterranean estuary and groundwater-derived fluxes to the coastal ocean. *Limnol. Oceanogr.*, 52(2): 805–718.
- Santos, I.R., de Weys, J., Eyre, B.D., 2011. Groundwater or Floodwater? Assessing the Pathways of Metal Exports from a Coastal Acid Sulfate Soil Catchment. *Environmental Science & Technology*, 45(22): 9641–9648.
- Santos, I.R., Eyre, B.D., 2011. Radon tracing of groundwater discharge into an Australian estuary surrounded by coastal acid sulphate soils. *Journal of Hydrology*, 396(3–4): 246–257.

- Santos, I.R., Peterson, R.N., Eyre, B.D., Burnett, W.C., 2010. Significant lateral inputs of fresh groundwater into a stratified tropical estuary: Evidence from radon and radium isotopes. *Marine Chemistry*, 121(1–4): 37-48.
- Schubert, M., Paschke, A., Lieberman, E., Burnett, W.C., 2012. Air–Water Partitioning of ^{222}Rn and its Dependence on Water Temperature and Salinity. *Environmental Science & Technology*, 46(7): 3905-3911.
- Swarzenski, P.W., 2007. U/Th Series Radionuclides as Coastal Groundwater Tracers. *Chemical Reviews*, 107(2): 663-674.
- Unland, N.P., Cartwright, I., Andersen, M. S., Rau, G. C., Reed, J., Gilfedder, B. S., Atkinson, A. P., Hofmann, H., 2013. Investigating the spatio-temporal variability in groundwater and surface water interactions: a multi-technical approach. *Hydrol. Earth Syst. Sci. Discuss.*, 10(3): 3795-3842.
- Victorian Water Resources Data Warehouse: available at:
<http://www.vicwaterdata.net/vicwaterdata/home.aspx>(last access: 11 January 2013), 2013.

Chapter 6

Assessing the hydrogeochemical impact and distribution of acid sulphate soils, Heart Morass, West Gippsland, Victoria

N .P. Unland^{1,3}, H.L. Taylor¹, B.R. Bolton^{1,2}, I. Cartwright^{1,2}

^[1] *School of Geosciences, Monash University, Clayton, Vic. 3800, Australia*

^[2] *Water Studies Centre, Monash University, Clayton, Vic. 3800, Australia*

^[3] *National Centre for Groundwater Research and Training, GPO box 2100, Flinders University, Adelaide, SA 5001, Australia*

Published in Applied Geochemistry (27, 2001-2009)

Abstract

The hydrogeochemical processes associated with the precipitation and oxidation of pyrite during the development of acid sulphate soils was investigated in the coastal floodplain environment of the Heart Morass, Victoria, Australia. During drought conditions in 2009, low-lying areas of the floodplain (0–2 m elevation) were the most affected by acid sulphate soils, with a median soil pH (pH_e) of 3.56 to approximately 50 cm depth. Soils below ~100 cm depth in these areas contain pyrite and have reduced inorganic S concentrations of up to 0.85 wt%. Higher areas of the floodplain (2–6 m) do not contain acid sulphate soils, with a median pH of 4.74 to approximately 50 cm depth, an average neutralising capacity of 3.87 kg H₂SO₄/t, and no appreciable unoxidised pyrite. In low-lying areas concentrations of Co, Ni, Zn, Mn and Fe in soil increased from <2.0, 4.0, 10, 20 and 2000 mg/kg, respectively, at 56 cm depth to 10, 20, 45, 152 and 15,000 mg/kg at 221 cm depth. In areas of higher elevation, concentrations of Co, Ni, Zn

and Fe increased from 6, 11, 21 and 12,500 mg/kg at 44 cm depth to 10, 19, 47 and 19,400 mg/kg at 239 cm depth. These data indicate acidic leaching of metals from the upper soil profile in both low-lying and more elevated areas. The lowest concentrations of Al, Co, Fe, Mn and Ni in surface water or pit water from low-lying areas were 2.43, 0.06, 2.90, 2.89 and 0.09 mg/L, respectively. These concentrations are 1–2 orders of magnitude higher than in any potential water sources around the morass and are higher than can be accounted for by evapotranspiration, indicating the leaching of metals into surface water and groundwater. Excess SO_4^{2-} from pyrite oxidation in the central low-lying area of the morass was characterised by molar Cl: SO_4 ratios <5 and $\delta^{34}\text{S}$ values <10‰. The Cl: SO_4 ratios combined with $\delta^{34}\text{S}$ values define zones of SO_4^{2-} depletion during reduction (Cl: SO_4^{2-} , $\delta^{34}\text{S}$ = 22.7‰) and contemporary SO_4^{2-} reduction of water enriched with oxidised pyritic SO_4^{2-} (Cl: SO_4^{2-} = 9.9, $\delta^{34}\text{S}$ = 26.2‰). Average concentrations of Fe in the upper soil profile decreased from 129 g/kg during drought conditions to 15.2 g/kg after flooding in 2011, suggesting the dissolution of Fe mineral salts accumulated in the upper soil profile. Average concentrations of Al, Ni, Cr and Cu increased in the upper soil profile from 9,522, 18.4, 17.0 and 14.4 mg/kg during drought to 12,800, 22.4, 22.6 and 22.4 mg/kg after flooding, suggesting that metal precipitation and dissolution is the result of changing pH and redox chemistry during flooding. This highlights the need for continuous measurement and sampling during flood events in order to better constrain these processes.

6.1. Introduction

Coastal floodplains, wetlands and swamps that contain sulphide bearing or hypersulfidic sediments cover over 17 million ha worldwide (Nordmyr et al., 2008a; Sullivan et al., 2010). In Australia, coastal floodplains are commonly drained for agriculture, reducing the level of local water tables (White et al., 1997). Excess drainage

and lower rainfall during drought conditions may expose these sediments to the atmosphere, leading to oxidation and the production of sulphuric acid. These sediments are termed acid sulphate soils (ASS's), and the acidification and environmental degradation resulting from the development of these has been well documented (e.g. Ritsema et al., 1992; Dent and Pons, 1995; Åström and Björklund, 1995; Cook et al., 2004; Johnston et al., 2009, 2010). Much work has been conducted on the export of acidity from such ASS affected areas (Cook et al., 2000; Österholm and Åström, 2008; Toivonen and Österholm, 2011) and the associated impacts on water quality and ecology (Sammut et al., 1995; Gosavi et al., 2004). These studies commonly use pH, Cl:SO₄ ratios and soil characteristics such as S concentrations and mineral properties to trace the extent and impacts of ASS.

Recent studies conducted across Australia and Northern Europe have focused on tracing the mobilisation and export of metals in ASS landscapes (Österholm and Åström, 2002; Nordmyr et al., 2008b). Most of this work has focused on the impacts of seasonal variability (Österholm and Åström, 2004, 2008) and individual rain events on the export of metals and acidity from ASS (Green et al., 2006; Santos et al., 2011). Metal mobilisation in ASS environments during floods has also been simulated in laboratory experiments by rewetting dried samples (e.g. Burton et al., 2008a; Fitzpatrick et al., 2009). However as extreme climatic events such as extensive drought and severe flooding occur infrequently, there are fewer opportunities to conduct field studies that assess the impacts of flooding in ASS environments. Given that the behaviour of metals in ASS environments is not always simple and relationships with parameters such as pH and SO₄²⁻ are often complicated, such field studies are valuable in understanding processes involved in metal mobilisation.

Sulphur isotopes may also be used to understand processes occurring in ASS environments (Simpson et al., 2008; Kilminster and Cartwright, 2011). Reduced S species such as biogenic pyrite have low $\delta^{34}\text{S}$ values (-52‰ to -14‰: Clark and Fritz, 1997) while SO_4^{2-} derived from seawater has higher $\delta^{34}\text{S}$ values that are close to that of the oceans (20.7‰: Mörrh and Torssander, 1995). In many regions, surface water bodies and rainfall contain dissolved SO_4^{2-} with low $\delta^{34}\text{S}$ values due to anthropogenic S inputs. In contrast, rainfall derived SO_4^{2-} throughout most of Australia has $\delta^{34}\text{S}$ values close to those of seawater, as sources of anthropogenic S are generally minor (Bridgman, 1992). Rainfall in SE Australia has $\delta^{34}\text{S}$ values -20‰ (Dogramaci et al., 2001), while rivers in SE Australia have $\delta^{34}\text{S}$ values generally between 12‰ and 20‰ (Cartwright, unpublished data). Additionally, surficial gypsum in SE Australia has $\delta^{34}\text{S}$ values of 21‰ near the coast, decreasing to -14‰ further inland (Chivas et al., 1991). Thus SO_4^{2-} derived from gypsum dissolution or rainfall will have higher $\delta^{34}\text{S}$ values than those from pyrite oxidation.

This study combines major ion geochemistry and S isotopes to better understand the nature of ASS in a coastal wetland in Victoria, SE Australia. The magnitude of acidification and the behaviour of metals are also examined during flooding following extensive drought. By understanding the chemical processes that occur during the transition from drought to flood conditions in ASS wetlands, predictions on the future impact of changing climatic conditions can be made. This is important for the understanding of local ecological processes and for the effective management of ASS wetlands.

6.2. Methods

6.2.1 Field area

The Heart Morass is a coastal wetland system located in SE Australia. It occupies ~18,000 ha and lies on the northern floodplain of the Latrobe River near the town of Sale (Fig. 1). This section of the Latrobe River is variably saline as it becomes estuarine towards its discharge point in Lake Wellington, ~1500 m to the east of the morass. In the early 1800's the morass was drained for beef and dairy production. Since then it has been identified as a wetland of significant importance under the Ramsar convention, with recent efforts aimed at the rehabilitation of the wetland system. The morass exhibits typical floodplain morphology with a gentle decline in elevation from the levee bank of the Latrobe River (~6 m above sea level) towards the centre of the floodplain (~0 m above sea level), before an increase in elevation to ~10 m at its northern boundary. For the purpose of this study, environmental characterisation of GHD (2005) was used to separate the morass into three areas: the low-lying sedgeland and aquatic swamp scrub; the floodplain riparian woodland and scrub; and the uplands (Fig. 1).

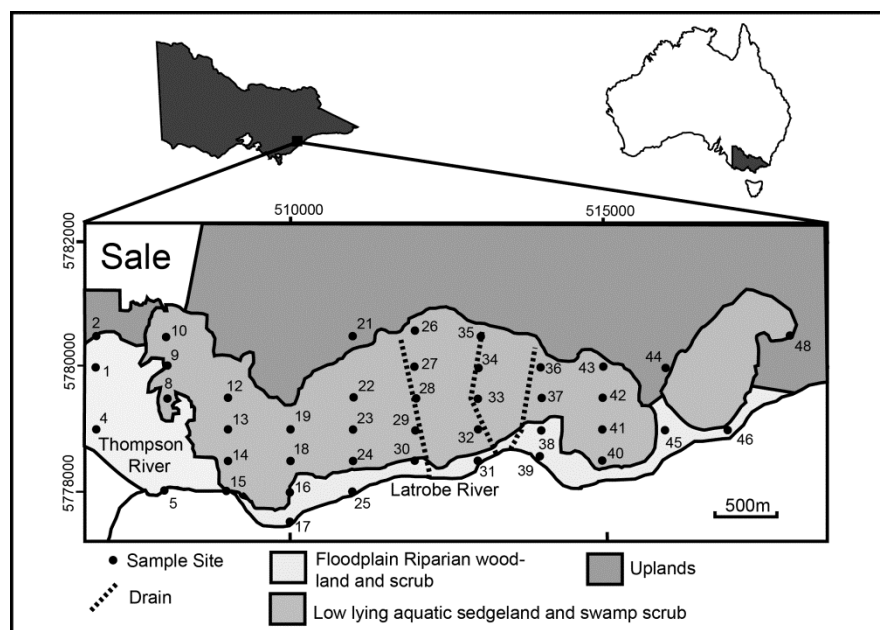


Fig. 1. Location of the Heart Morass, sample sites and vegetation/landform zones.

The area receives an average annual rainfall of 598 mm, with a mean daily maximum temperature of 19.6°C (Bureau of Meteorology, 2010). Historically the Heart Morass has experienced seasonal flooding from the Latrobe River, however drainage of the morass and extensive drought (1996–2010; Fig. 2), has resulted in an extended period of drying in the morass. Wetland degradation and soil pH < 2 in the area reported by Boon et al. (2007) suggests the oxidation of ASS during this time. High rainfall in the area during 2011 resulted in significant flooding in the Morass through runoff, inflow from uncontrolled drains and overbank flooding from the Latrobe River.

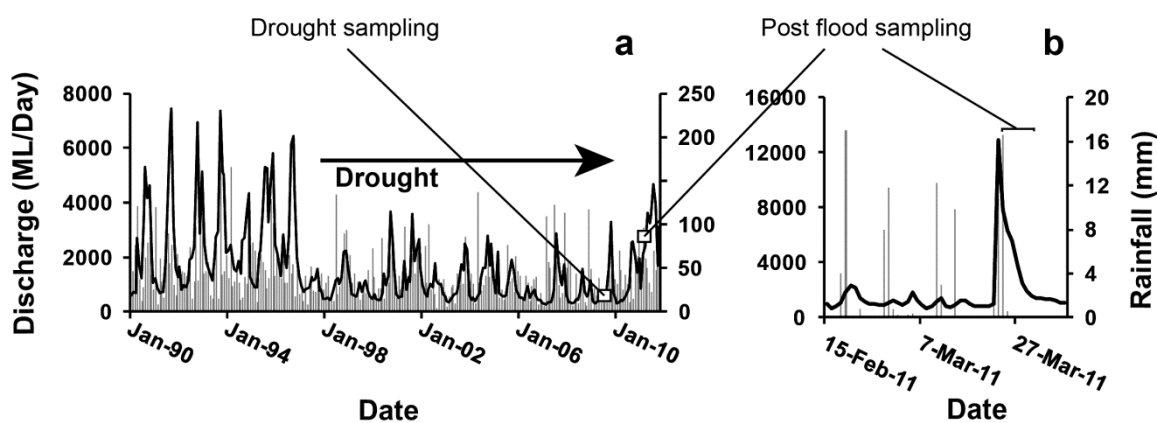


Fig. 2. Sampling periods under changing meteorological conditions. Discharge of the Latrobe River (station 226005) indicated by black line on left y axis, and precipitation (Sale Airport – station 085072) indicated by grey bars on right y axis. a = monthly average discharge and rainfall, b = daily average discharge and rainfall.

6.2.2 Field survey

Initial field studies of 42 sites took place during April 2009 in order to characterise drought conditions in the morass. These sites are on a 500 m by 1000 m grid (Fig. 1), with sites surveyed using a Garmin Etrex GPS to 5 m accuracy. Landforms and vegetation were recorded at each site and soil horizon descriptions were made in ~50 cm soil pits using the classification of McDonald et al. (1990). Soil pH (pH_F) measurements were made on 1:1 mixed soil water samples from each horizon using a calibrated Hanna HI 98130 pH/EC meter (Ahern et al., 2004). Soil was reacted with 1 M HCl and examined for effervescence as an indicator of CaCO_3 . Readily extractable acidity tests

were conducted on surface soil samples by mixing 50 g of soil with 100 mL of deionised water and waiting 5 min for suspended matter to settle. A 10 mL filtrate of the sample was taken using 1.2 μ m cellulose acetate filter, diluted to 100 mL with deionised water and titrated against a standard 0.3636 N NaOH solution in the presence of phenolphthaleine indicator using a HACH 16900 digital titrator. Measurement of pH and EC was made in situ on 4 surface water and 18 pit water samples using a calibrated Hanna HI 98130 pH/EC meter. Additional acidity and pH testing was conducted during December 2010, with further limited sampling conducted during 2011 after increased rainfall and flooding in the morass during March (Fig. 2).

6.2.3 Sampling

Soil samples were taken from each soil horizon to ~50 cm depth or where the water table was encountered. Further soil samples were taken at ~20 cm intervals to ~250 cm depth at sites 25 and 30 by hand auger. In order to prevent pyrite oxidation, soil samples were collected in re-sealable polyethylene bags, placed on ice in the field and frozen in a domestic freezer upon return from the field. Samples were oven dried at 80°C upon return to the laboratory (Ahern et al., 2004). Surface water samples were taken from 4 sites in the Heart Morass and five representative pit water sites. Water was sampled from Lake Wellington, an upland groundwater bore and at three locations along the Latrobe River. Surface and pit water samples were taken and filtered in the field using 0.2 μ m cellulose acetate filters for anion and isotope analysis. Subsamples were subsequently acidified in the field to a pH < 2 using 16 M HNO₃ for cation analysis. Samples were placed on ice in the field and refrigerated at ~4°C upon return.

6.2.4 Laboratory analysis

Soil samples were tested for acid neutralising capacity (ANC) through titration of 1.0 g of soil with NaOH following acidification by 25 mL addition(s) of 0.1 M HCl to pH

< 3 (Ahern et al., 2004). Results are reported with a precision of $\pm 1.0\%$ based on replicate analysis. Reduced inorganic S (RIS) concentrations were obtained by reducing oven dried soil samples with an acidic Cr(II) solution in a sealed reaction chamber and diffusing the produced H_2S into an alkaline Zn solution (Burton et al., 2008b). This was used as a proxy for pyrite concentrations (Johnston et al., 2010). Scanning electron microscope images were taken on sediment/resin thin sections using a JOEL JSM-7001F field emission scanning electron microscope at Monash University, Clayton. The concentration of metals in soil was determined by inductively coupled plasma atomic emission spectrometry (ICP-AES) at ALS-Melbourne. Digestion of soil for ICP-AES followed method 200.2 of the USEPA (1994), with treatment by 2 mL of 35% HNO_3 and 10 mL of 6.4% HCl at 95°C for 30 min, addition of 2 mL 30% H_2O_2 for 30 min after cooling and dilution to 50 mL. Particulate metal concentrations are reported with a precision of ± 50 mg/kg for Fe and Al, ± 5 mg/kg for Mn and Zn, and ± 2 mg/kg for Co and Ni. The concentration of major anions in water samples was determined using a Metrohm ion chromatograph at Monash University, with a precision of $\pm 2\%$ based on replicate analysis. The concentration of metals in water samples was determined by octopole reaction cell inductively coupled plasma mass spectrometry at ALS-Sydney. Dissolved metal concentrations are reported with a precision of ± 5 $\mu\text{g/L}$ for Al, ± 2 $\mu\text{g/L}$ for Fe, ± 1 $\mu\text{g/L}$ for Ni, ± 0.5 $\mu\text{g/L}$ for Mn and ± 0.1 $\mu\text{g/L}$ for Co and Ni. Particle size analysis was conducted on gently disaggregated sediment samples in deionised water using an LS100 Beckman–Coulter Counter at Monash University, Clayton. Particle size distributions had a precision of $< 8\%$ based on replicate analysis. The mineralogy of sediments was determined on raw sediment, sediment heated to 550°C and sediment heated to 550°C and treated with glycol using a Siemens D5000 X-Ray Diffractometer at Latrobe University, Bundoora. Isotopic analysis of S was conducted on BaSO_4 precipitates using

the method outlined in Kilminster and Cartwright (2011). $\delta^{34}\text{S}$ values are expressed in ‰ relative to the Canon Diablo Troilite (CDT) standard with a precision of $\pm 0.85\text{‰}$ based on replicate analysis.

6.3. Results

6.3.1 Soils

The uppermost soil horizons in the Heart Morass contain penetrating roots and decaying organic matter, producing a layer containing ~10% organic matter by weight. The morass is dominated by Holocene floodplain sediments that range from coarse sands to clays, with surface sediments dominated by fine sands and coarse silts. Surface sediments range from poorly to very poorly sorted and are generally coarser in the riparian woodland scrub than in the low-lying sedgeland.

6.3.1.1 Low-lying sedgeland

The central low-lying sedgeland was most affected by ASS with pH_F values as low as 1.98 (Fig. 3).

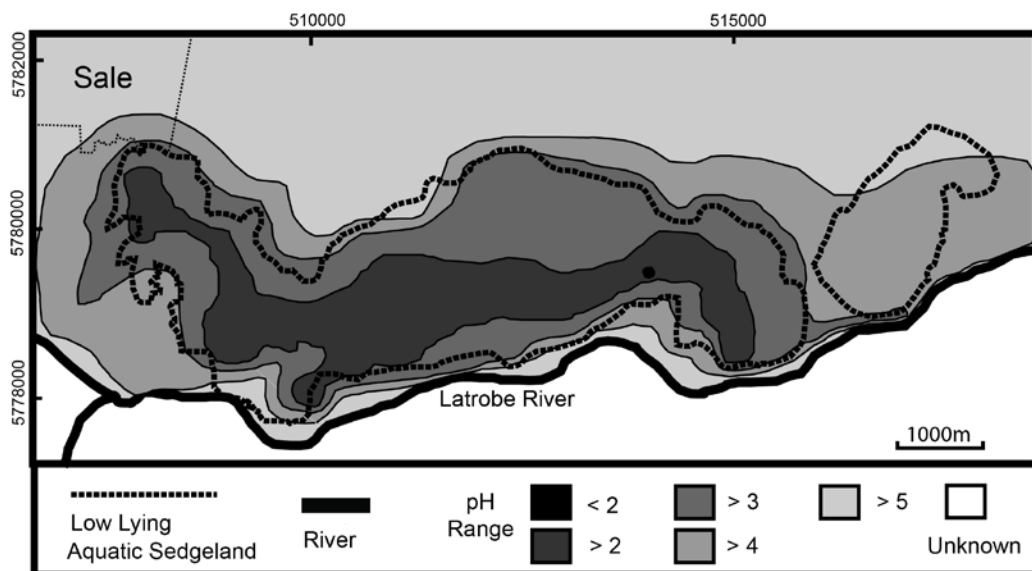


Fig. 3. Contour map of surface soil pH_F during drought conditions in 2009.

Soil horizons in these areas to about 50 cm depth had a median pH_F of 2.95 at the surface and 3.80 below the surface. The uppermost soil horizon exhibited orange staining while lower horizons showed orange–red mottling that was more prevalent near deeper penetrating roots.

XRD analysis indicated the presence of ferroxalohydrate ($\text{FeSO}_4 \cdot 6\text{H}_2\text{O}$) and sideronatrite ($\text{Na}_2\text{Fe}(\text{SO}_4)_2(\text{OH}) \cdot 3\text{H}_2\text{O}$) throughout the soil profile of the sedgeland. Acid neutralising capacities (ANC) were below detection for 25 of the 27 surface samples taken from the sedgeland, and there was no apparent reaction of samples treated with 1 M HCl. Representative samples from site 30 show a gradual increase in ANC from 0.00 kg $\text{H}_2\text{SO}_4/\text{t}$ at ~100 cm depth to 11.9 kg $\text{H}_2\text{SO}_4/\text{t}$ at 248 cm depth (Fig. 4). pH_F and RIS concentrations show similar trends, with pH_F increasing from 3.43 at ~100 cm to 5.98 at 173 cm, and RIS increasing from <0.01% at ~100 cm to 0.85% at 248 cm. SEM images from sediment thin sections at 248 cm depth indicates the presence of spherical framboidal pyrite (Fig. 5). Metal concentrations also increase with depth in the low-lying sedgeland (Fig. 6). At site 30, concentrations of Co, Ni, Zn, Mn and Fe increase from <2.0, 4.0, 10, 20 and 2,000 mg/kg, respectively, at 56 cm depth, to 10, 20, 45, 152 and 15,000 mg/kg, respectively, at 221 cm depth.

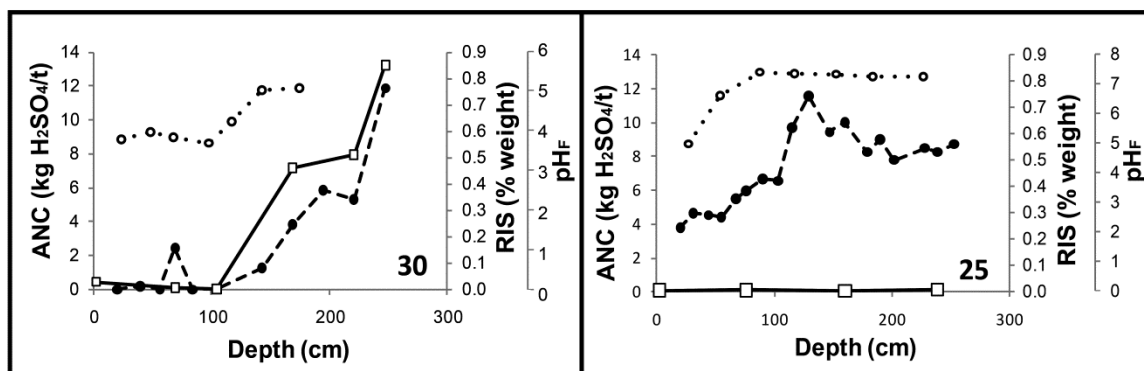


Fig. 4. Neutralising capacity (dashed line with black circles), reduced inorganic S concentrations (solid line with white squares) and soil pH_F (white circles with dotted line) with depth at site 30 (low lying sedgeland) and site 25 (riparian woodland scrub).

6.3.1.2 Floodplain riparian woodland scrub and uplands

There is a gradual rise in surface soil pH_F away from the central low-lying sedgeland towards the riparian woodland scrub and uplands (Fig. 3). These areas have a median pH of 4.92 at the surface with little variation to ~50 cm depth. Only isolated soils in the riparian woodland scrub have a pH_F value <4 . Soil horizons in these areas are coherent, moist and dusky brown to dark brown and do not show orange or red staining/mottles. The mineralogy of these sediments is dominated by quartz and muscovite and does not show any secondary minerals associated with pyrite oxidation. Average RIS concentrations were 0.01% for all surface soil samples analysed, and SEM imaging of representative samples did not indicate the presence of pyrite.

The average acid neutralising capacity of surface samples from riparian woodland scrub and uplands was 3.71 kg $\text{H}_2\text{SO}_4/\text{t}$. Representative samples from site 25 show an increase in ANC with depth (Fig. 4) from 6.56 kg $\text{H}_2\text{SO}_4/\text{t}$ at 104 cm to 11.56 kg $\text{H}_2\text{SO}_4/\text{t}$ at 129 cm. pH_F values also increase with depth from 4.63 at 19.5 cm to 7.49 at 111 cm. Metal concentrations show a similar trend with Co, Ni, Zn and Fe concentrations increasing from 6, 11, 21 and 12,500 mg/kg, respectively, at 44 cm to 10, 19, 47 and 19,400 mg/kg, respectively, at 239 cm.

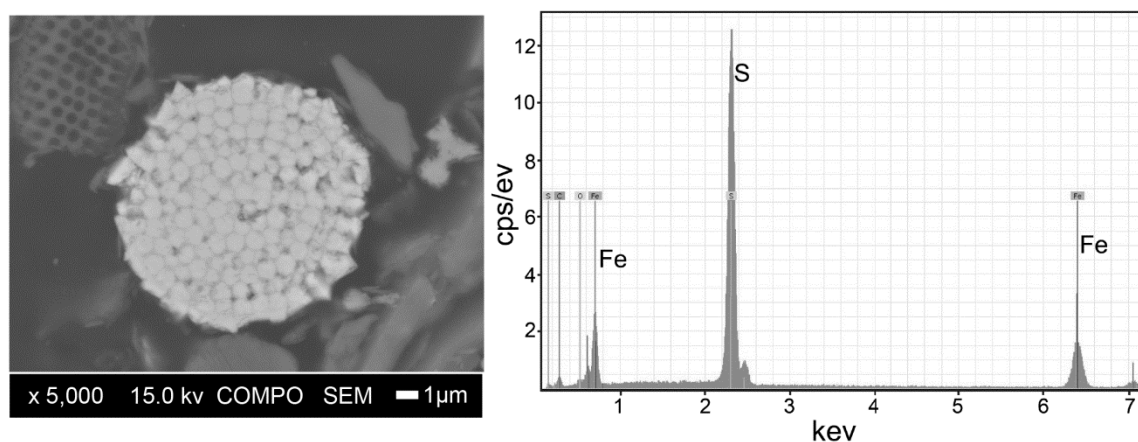


Fig. 5. Electron backscatter image and energy-dispersive X-ray spectrum of framboidal pyrite in sediment thin section from 248 cm depth at site 30.

6.3.2 Hydrochemistry

The median pH of pit water was 3.89 in the low-lying sedgeland and ranged from 5.51 to 6.23 in the riparian woodland scrub and uplands, while surface water pH ranged from 2.54 to 2.96 in the low-lying sedgeland and from 4.42 to 5.45 in the riparian woodland scrub and uplands (water from site 35 was included as “upland” as it sources upland runoff). The average EC of water in the Heart Morass was 13.6 mS/cm in pit water and 4.72 mS/cm in surface water. Pit water from the low-lying sedgeland had an average EC of 15.3 mS/cm while the surface water had an average EC of 12.0 mS/cm. Groundwater, pit water and surface water samples contain higher concentrations of Cl⁻ than surrounding potential water sources (such as the uplands and the Latrobe River). Molar Cl:Br ratios ranged from 341 to 811 and did not increase with increasing salinity.

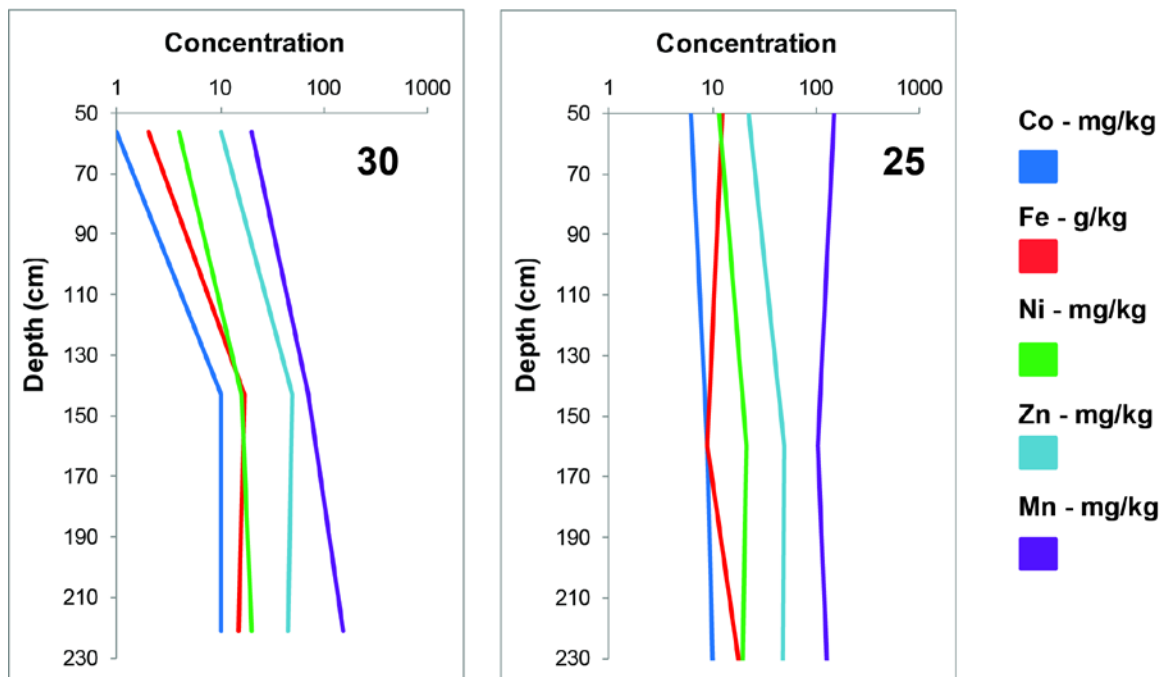


Fig. 6. Changes in concentration of Co, Fe, Ni, Zn and Mn in soil samples with depth at site 30 (low lying sedgeland) and 25 (riparian woodland scrub).

Low molar Cl:SO₄ ratios (<4) occur in 7 of the 9 surface and pit water samples from the morass and correlate spatially with low water pH (Fig. 9a). These Cl:SO₄ ratios are significantly lower than sea water (~20: Johnston et al., 2011) or the nearby saline

Lake Wellington (18.9). Pit water from site 31 and the Latrobe River have intermediate Cl:SO₄ ratios (7.18–12.2), while groundwater from the uplands and surface water from site 48 have high Cl:SO₄ ratios (31.9 and 23.9, respectively). The lowest concentrations of

Al, Co, Fe, Mn, Ni and Zn measured in the low-lying sedgeland were 2.64, 0.06, 2.90, 2.89, 0.09 and 0.18 mg/L, respectively, in surface water, and 2.43, 0.10, 208, 8.26, 0.13 and 0.41 mg/L, respectively, in pit water.

The δ³⁴S values of surface water throughout the central region of the low-lying sedgeland ranged from 4.8‰ to 8.1‰ (Fig. 9b), and are below that expected in sea water or river water in SE Victoria (12–20‰) (Bridgman, 1992; Mörrh and Torssander, 1995; Dogramaci et al., 2001). Water with high δ³⁴S values occurs at sites 31 (26.2‰) and 48 (22.7‰), exceeding those expected in sea water or river water in SE Australia, while surface water from site 35 has an intermediate δ³⁴S value of 11.7‰.

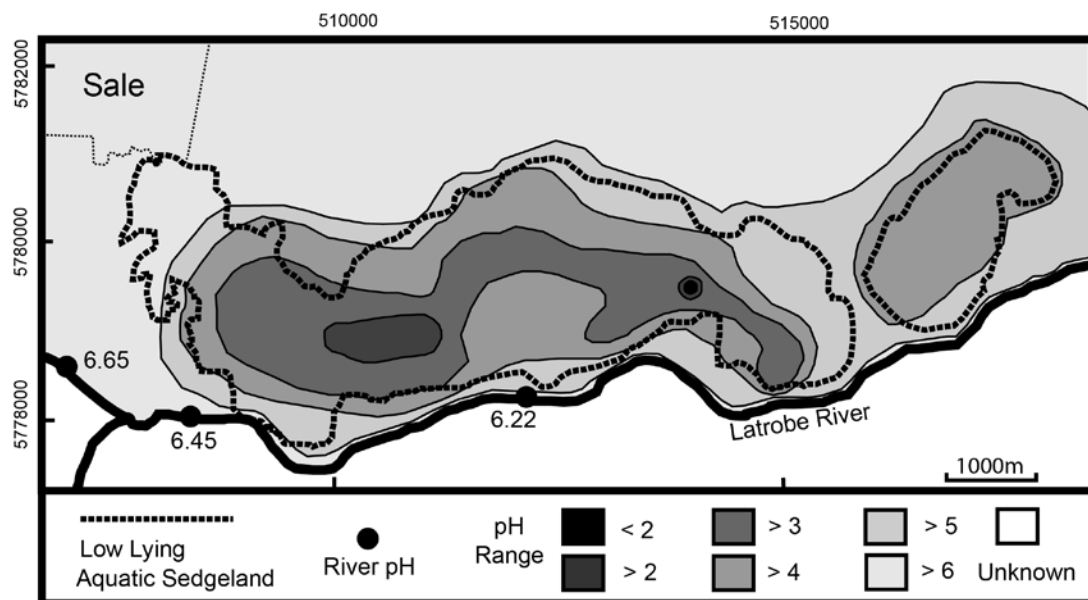


Fig. 7. Contour map of water pH in the Heart Morass during 2009.

6.3.3 Post-flood conditions

Following flooding, the median soil pH was 3.8 in the low-lying sedgeland and 4.45 in the floodplain riparian woodland scrub. Surface water pH in the low-lying

sedgeland ranged from 3.41 to 3.98 and the average EC was 8.34 mS/cm. The Cl:SO₄ ratio of surface waters in the low-lying sedgeland ranged from 4.17 to 5.79 with an average of 4.44 ± 0.79 . These values are still below the ratios in the Latrobe River, upland groundwater and Lake Wellington which range from 31.9 to 7.18.

Average surface soil concentrations of Fe and Mn decreased from 129 g/kg and 266 mg/kg, respectively, during drought conditions to 15.2 g/kg and 62.3 mg/kg, respectively, after flooding. The concentrations of Zn, As, Co and Cd also decreased after flooding, with average concentrations of 46.8, 12.6, 5.5 and 2.5 mg/kg, respectively, during drought conditions and average concentrations of 42.0, 9.3, 5.3, and <1.0 mg/kg, respectively, after flooding. Conversely, average concentrations of Al, Ni, Cr and Cu increased from 9,522, 18.4, 17.0 and 14.4 mg/kg during drought conditions to 12,800, 22.4, 22.6 and 22.4 mg/kg after flooding. Dissolved metal concentrations also generally increased in groundwater and surface water, with average Al, Co, Mn, Ni and Zn concentrations of 45.3, 0.36, 11.3, 0.47, 1.38 mg/L after flooding compared to 8.8, 0.18, 8.54, 0.24 and 0.63 mg/L, respectively, during drought.

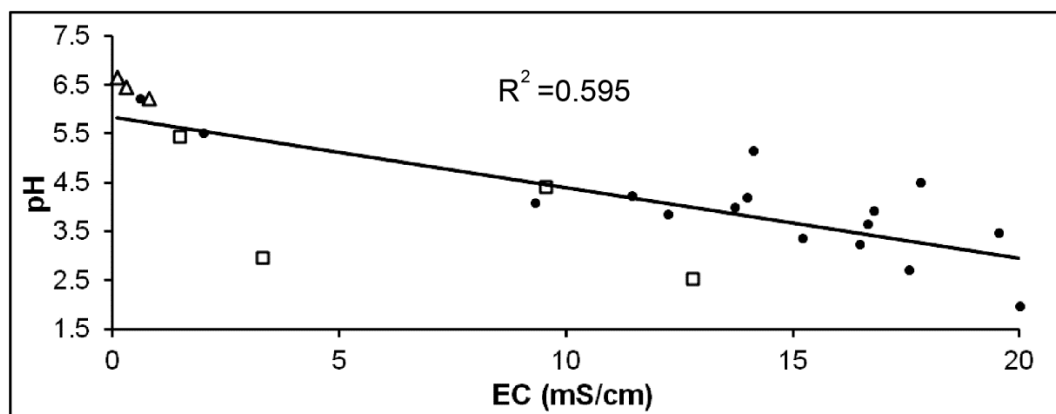


Fig. 8. Inverse correlation of pH with EC in water from the Latrobe River (white triangles), pit water (black circles) and surface water (white squares) from the Heart Morass during 2009.

6.4. Discussion

The geochemistry of the soils, groundwater and surface water allow processes involved in the generation of ASS in the Heart Morass under drought conditions and after flooding to be understood.

6.4.1 Pre-flood conditions in the low lying sedgeland

The central areas of the low-lying sedgeland exhibit characteristics consistent with oxidation of pyrite in ASS (Sullivan et al., 2010). This includes soil pH_F values as low as 1.98 and the orange/red staining and mottling that is typical of pyrite oxidation (Simpson et al., 2008). Mottling at depth was commonly associated with penetrating roots, suggesting that oxidation deeper in the profile has been facilitated by the transport of O_2 through air filled intercellular spaces of root material (cf., Flessa, 1994). This is further supported by the presence of secondary minerals associated with pyrite oxidation, such as ferroxahydroxide and sideronatrite (Fitzpatrick et al., 2009). The absence of carbonate minerals, as shown by XRD analysis, lack of effervescence under 1M HCl additions, and acid neutralising capacities below detection for 93% of surface soil samples, indicates that the neutralising capacity of these soils has largely been exceeded.

Water pH follows a similar spatial distribution to soil pH_F (Fig. 7), indicating that leaching of acid from the soil profile into groundwater and surface water has occurred. There is an inverse correlation between EC and pH (Fig. 8) that is likely to have resulted from evapotranspiration in the upper profile. Evapotranspiration results in both the concentration of solutes and the oxidation of pyrite, forming low pH water with high EC values (Fitzpatrick et al., 2009). Molar Cl:Br ratios of 341–811 also indicate that evapotranspiration exerts the largest control over salinity in the morass, as Cl:Br ratios of 15,000–20,000 would be expected if halite dissolution was responsible (Cartwright et al., 2006). This is because halite contains very little Br relative to Cl and as it is dissolved,

Cl:Br ratios will become elevated over that of local rainfall (typically 400–650). In addition, pyrite oxidation is likely to result in elevated concentrations of SO_4^{2-} in the groundwater and surface water, further increasing the EC (Österholm and Åström, 2008).

Molar Cl: SO_4 ratios in pit water and surface water (Fig. 9a) are well below those of sea water, Lake Wellington or the Latrobe River, indicating the presence of excess SO_4^{2-} in the system. The Cl: SO_4 ratios correlate spatially with low water pH, indicating the input of H_2SO_4 during pyrite oxidation. This is further supported by low $\delta^{34}\text{S}$ values (4.8‰ to 8.1‰) of water from the central regions of the low-lying sedgeland (Fig. 9b). As reduced S species have low $\delta^{34}\text{S}$ values (-52‰ to -14‰: Clark and Fritz, 1997) and SO_4^{2-} derived from sea water, rainfall and river water in SE Australia has higher $\delta^{34}\text{S}$ values (12–20‰: Mörth and Torssander, 1995; Dogramaci et al., 2001; Cartwright, unpublished data), data from the sedgeland indicates the mixing between SO_4^{2-} from reduced S species with SO_4^{2-} from other nearby sources including rainfall, runoff and the Latrobe River. These results are consistent with pyrite-derived SO_4^{2-} in ASS landscapes (Boman et al., 2008), and $\delta^{34}\text{S}$ values that range from 0‰ to 6‰ in ASS drainage waters in Finland (Åström and Spiro, 2000).

While site 35 resides in the low-lying sedgeland, it is partly fed by a drain sourcing water from the uplands. As such the intermediate $\delta^{34}\text{S}$ value of 11.7‰ suggests a greater influence of rainwater/runoff than the water in the central region of the morass. The Cl: SO_4 ratio of water at this site however is the lowest in the morass (2.03), suggesting the most excess SO_4^{2-} . This is likely to reflect low Cl^- concentrations at this site (112 mg/L), consistent with a higher proportion of rainfall/runoff. As a result, even the input of relatively low amounts of SO_4^{2-} at this location will greatly affect Cl: SO_4 ratios in the mixed water. The high Cl: SO_4 ratio (31.9) and high $\delta^{34}\text{S}$ value (22.7‰) of surface water in the eastern part of the low-lying sedgeland is consistent with the

depletion of SO_4^{2-} and enrichment of $\delta^{34}\text{S}$ that occurs during bacterial SO_4 reduction (e.g. Thode et al., 1951; Rees, 1973; Massmann et al., 2003; Johnston et al., 2011). The mixing between water affected by pyrite oxidation and water that has undergone SO_4 reduction is demonstrated by the co-variance of SO_4^{2-} concentrations and $\delta^{34}\text{S}$ values (Fig. 10). This demonstrates the effectiveness in combining S isotopes, SO_4^{2-} concentrations and Cl: SO_4 ratios in determining the processes surrounding the development and impact of ASS.

An increase in pH_F , ANC and RIS below ~100 cm depth in the soil profile of the sedgeland indicates that a redox boundary exists, preventing extensive oxidation of pyrite (Fig. 4). This conclusion is supported by SEM images of spherical framboidal pyrite at 248 cm depth (Fig. 5), which is consistent with contemporary pyrite formation in dysoxic sedimentary environments (Wilkin et al., 1996). Similar trends in metal concentrations with depth (Fig. 6) are consistent with the mobilisation and exportation of metals associated with the movement of acidified water through the upper part of the soil profile (Golez and Kyuma, 1997; Österholm and Åström, 2002; Nordmyr et al., 2008a). These data indicate that in the upper ~100 cm of the soil profile of the low-lying sedgeland, extensive pyrite oxidation has resulted in acid production that has exceeded the natural buffering capacity of the soil, resulting in the mobilisation and export of metals. This can further elevate the EC of these waters through the additional input of solutes (e.g. Österholm and Åström, 2004; Burton et al., 2008a).

The lowest concentrations of Al, Co, Fe, Mn and Ni measured in surface water or pit water from the low-lying sedgeland are 1–2 orders of magnitude higher than any of the potential water sources around the Heart Morass (including the Latrobe River, uplands groundwater and Lake Wellington, Table 1).

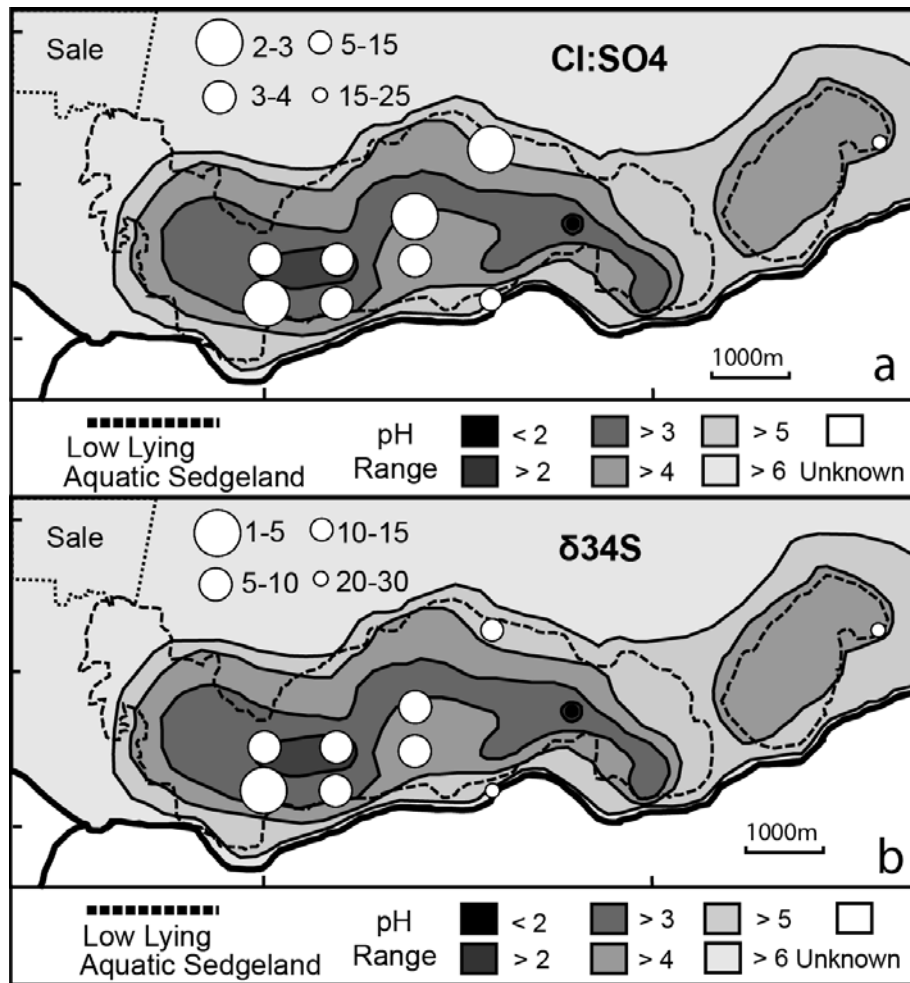


Fig. 9. Spatial distribution of Cl:SO₄ ratios (a) and δ³⁴S values of dissolved SO₄²⁻ (b) in relation to water pH.

Estimates of the potential concentration of these metals by evapotranspiration were made assuming that Cl⁻ behaves conservatively. Of the average metal concentrations in surface water from the low-lying sedgeland, evapotranspiration could only account for 43% of Al, 14% of Mn and 2.1% of Fe. In pit water from the low-lying sedgeland, evapotranspiration could again only account for 14% of Al, 8% of Mn and 1.1% of Fe. This indicates the presence of excess metals in water from the low-lying sedgeland and is consistent with the leaching of metals from the soil profile by acidic water. These estimates assumed the Latrobe River as the source of water in the low-lying sedgeland, as it had the highest metal:Cl⁻ ratio of the potential water sources. Thus, estimates of excess metal calculations are conservative.

6.4.2 Pre-flood conditions in the floodplain riparian woodland and uplands

The riparian woodland scrub and uplands were largely unaffected by ASS, with a median surface pH_F of 4.92 and little variation to ~50 cm depth. While incubation experiments (e.g., as described by Sullivan, 2009) were not performed on these samples, high pH_F values, average RIS concentrations of 0.01% and the absence of visible pyrite in SEM images indicates that these areas are hyposulfidic (Sullivan et al., 2010). These areas also had a higher average ANC (3.71 kg $\text{H}_2\text{SO}_4/\text{t}$) than the low-lying sedgeland, indicating that the buffering capacity in these areas has not been exceeded.

While both ANC and pH_F increase with depth in the riparian woodland scrub (Fig. 4), the absence of RIS at depth does not provide evidence for a continuing redox boundary within the profile. It is possible that under changing hydrological conditions, acidified water from the central areas of the morass has infiltrated through the upper layers of the profile in the riparian woodland scrub, reducing the ANC and pH_F in these areas.

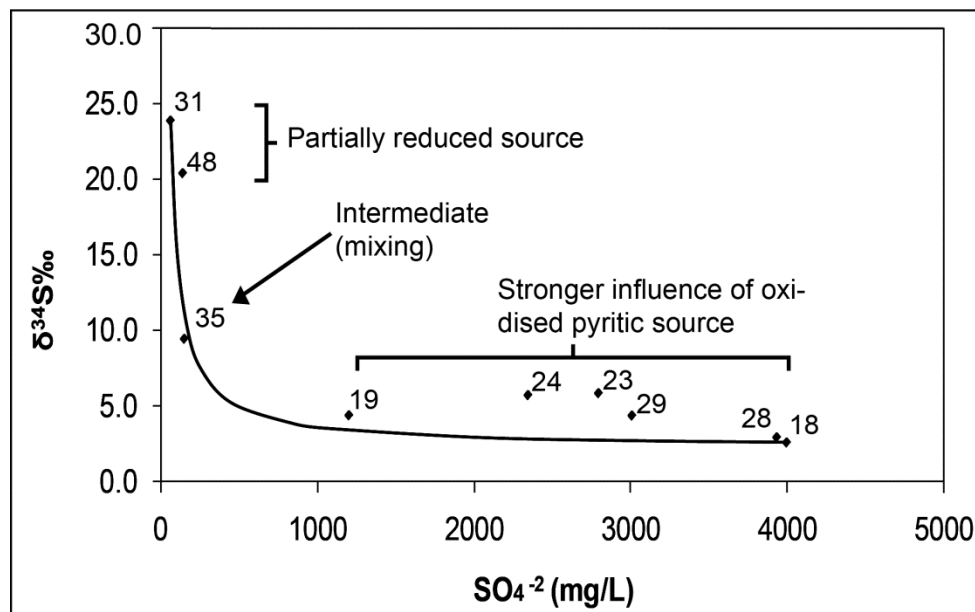


Fig. 10. $\delta^{34}\text{S}$ values and SO_4^{2-} concentrations of surface and groundwater in the Heart Morass along a mixing curve.

Similar to the low lying sedgeland, comparatively low concentrations of Co, Ni, Zn and Fe (Fig. 4) in the upper soil profile of these areas supports the mobilisation and export of metals during the movement of acidic water. While this provides evidence for the occurrence of acidic leaching, concentrations of Co, Ni, Zn, and Fe are only 36–55% lower in the upper profile of this area, compared to 78–87% lower in the upper profile of the low-lying sedgeland. This indicates that if acidic mobilisation has occurred in the riparian woodlands, it is less severe than in the low-lying sedgeland.

Intermediate molar Cl:SO₄ ratios (7.18–12.2) of pit water in the riparian woodlands (site 31) and water from the Latrobe River are likely to reflect the mixing between water with lower Cl:SO₄ ratios such as that from the low-lying sedgeland (<4), and water with higher Cl:SO₄ ratios such as those in estuaries or sea water (~20: Johnston et al., 2011). Water at site 31 however has a $\delta^{34}\text{S}$ value of 26.6‰, which is consistent with the enrichment of ³⁴S during bacterial SO₄²⁻ reduction. This suggests that water at this location has previously been influenced by SO₄²⁻ inputs during pyrite oxidation, and the subsequent reduction of this water has resulted in a high $\delta^{34}\text{S}$ value. This would result in water with a high $\delta^{34}\text{S}$ value and a low Cl:SO₄ ratio (Fig. 11).

6.4.3 Post-flood conditions

An increase of 0.85 in the median pH surface soil in the low-lying sedgeland indicates that flooding has resulted in the export of acid from the upper soil profile in these areas. In contrast, the riparian woodland scrub did not show any appreciable change in pH_F during flooding. While the median pH of surface water increased from 2.75 to 3.53 in the low-lying sedgeland, the average EC decreased from 12.03 to 8.43 mS/cm, indicating that increases in pH may be attributed to dilution and not the export of acid. Average Cl:SO₄ ratios of 4.44 ± 0.79 in surface water from the sedgeland were still well below those from the Latrobe River and other nearby sources (31.9–9.67), suggesting that

during flooding, minor overbank input from the Latrobe River has occurred and more significant inputs have come from relatively fresh upland runoff and precipitation. These fresher sources will increase water pH and decrease the EC of water in the morass, while having little impact the ratio of Cl:SO₄.

Site Name/Number	Al (mg/L)	Co (mg/L)	Fe (mg/L)	Mn (mg/L)	Ni (mg/L)	Zn (mg/L)	Cl (mg/L)	Br (mg/L)
Lake Wellington	0.02	bd	0.01	0.03	bd	0.01	10,709	34.78
Latrobe River 1	0.04	bd	0.17	0.03	bd	0.11	61.32	0.17
Latrobe River 2	0.13	bd	0.22	0.06	bd	0.25	194.6	0.66
Uplands (GW)	bd	bd	bd	0.02	bd	bd	1,065	11.61
LLS 2009 18	32.1	0.38	298	13.0	0.52	1.34	4,026	19.67
LLS 2009 19	4.68	0.06	2.90	2.89	0.09	0.18	1,357	5.46
LLS 2009 23	2.64	0.15	356	8.69	0.22	0.54	3,398	10.61
LLS 2009 24	7.89	0.28	208	8.26	0.28	0.76	3,365	9.82
LLS 2009 28	2.94	0.12	398	9.38	0.17	0.53	3,638	11.41
LLS 2009 29	2.43	0.10	368	9.00	0.13	0.41	4,335	14.33
LLS 2011 2	22.10	0.19	4.92	7.32	0.26	0.62	2,932	8.37
LLS 2011 3	113.00	0.71	44.80	20.70	0.99	3.13	n/a	n/a
LLS 2011 4	16.30	0.15	2.21	6.19	0.20	0.49	n/a	n/a
LLS 2011 6	12.30	0.11	2.78	4.85	0.15	0.37	2,089	6.36
LLS 2011 7	62.60	0.64	138.00	17.50	0.76	2.26	5,433	15.75

Table 1. Concentration of dissolved Al, Co, Fe, Mn, Ni, Zn and Cl during drought (2009) and flood (2011) conditions. bd = below detection, n/a = not available.

The mobilisation of metals from soils throughout the Heart Morass during flooding was demonstrated by a decrease in the average concentration of Fe and Mn from 129 g/kg and 266 mg/kg, respectively, to 15.2 g/kg and 62 mg/kg, respectively. Minor levels of mobilisation are suggested by small decreases in average Zn, As, Co and Cd concentrations, while concentrations of Al, Ni, Cr and Cu increased during flooding. These results are somewhat consistent with flood simulation experiments (Simpson et al., 2008) that concluded that precipitation and sorption of Al, Cr and Cu occurred during the inundation of ASS with river water. The mobilisation of Mn, Zn, Co and Cd observed in the morass is consistent with observations in similar ASS environments (Sohlenius and Öborn, 2004; Nordmyr et al., 2008b), however, the apparent mobilisation of Fe conflicts with the limited Fe mobilisation reported in these studies. Iron mobilisation may instead result from the dissolution of immobile secondary Fe(III) minerals such as sideronatrite

($\text{Na}_2\text{Fe}(\text{SO}_4)_2(\text{OH}) \cdot 3\text{H}_2\text{O}$) under reducing conditions. This process has been documented in other areas during the early stages of flooding (Burton et al., 2008a) and tidal inundation (Johnston et al., 2011). The average concentrations of Fe in water samples decreased from 271 mg/L during drought to 38.5 mg/L after flooding (Table 1). This is conflicts somewhat with the Fe dissolution proposed above, as Fe dissolution should increase the concentration of dissolved Fe in soil water. However, as the majority of sampling occurred in the week following the flood peak, it is possible that the dissolution and exportation of Fe had already occurred.

Increased concentrations of Al, Co, Mn, Ni and Zn in surface water after flooding may indicate the mobilisation of species complexed with Fe(III) during mineral salt dissolution. However this is unlikely as Fe concentrations declined during flooding, suggesting metal export. Metal mobilisation may instead be the result of changes pH and redox chemistry during flooding, causing the precipitation and dissolution of different metal species at different times throughout a flood event (Santos et al., 2011). Limited access to sites during flooding, heterogeneity in water samples and non-continuous measurement of pH and redox conditions make these processes difficult to constrain and more work in this area needs to be conducted to better resolve this issue.

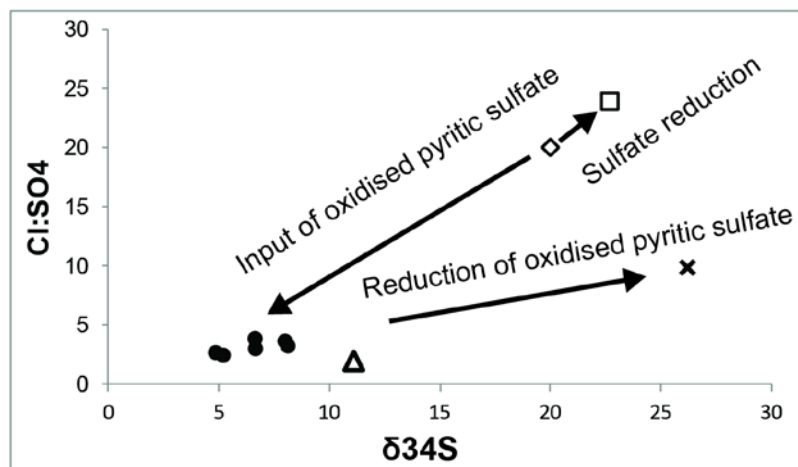


Fig. 11. Processes controlling the deviation of Cl:SO₄ ratios and δ³⁴S value of water in the low lying sedgeland (black circles), site 48 (white square), site 35 (white triangle), site 31 (cross), from oceanic water (white diamond).

6.5 Conclusions

During drought conditions, the upper soil horizons in the low lying sedgeland of the Heart Morass contain material resulting from pyrite oxidation. These layers are low in soil pH, have little to no acid neutralising capacity and have significantly lower metal concentrations than horizons lower in the profile, indicating acidic leaching subsequent to pyrite oxidation. Other areas of the morass such as the riparian woodland scrub and uplands are less impacted by ASS with significantly higher pH_F values, however lower ANC and metal concentrations in the upper soil profile of these areas suggests previous acidification. Low water pH and high metal concentrations during drought correlate with low soil pH, indicating the leaching of acid and metals from the upper soil profile into the hydrological system. By combining the use of Cl:SO₄ ratios with $\delta^{34}\text{S}$ values, the reduction of SO₄²⁻ in water previously affected by oxidised pyritic SO₄²⁻ was identified. This is something that could not be identified by using either method alone, and emphasises the value of using a combined approach in analysing ASS wetlands. Post-flood conditions are characterised by the dilution of water in the morass with a high proportion of precipitation and upland runoff, and a comparatively low proportion of overbank flooding. Lower Fe concentrations in surface soil samples and water samples is consistent with the dissolution and export of Fe mineral salts during the initial flooding stages of ASS affected areas. The behaviour of many other metals is not as clear as this process and may reflect dissolution and precipitation of different metals under changing pH and redox conditions during the stages of inundation. This highlights the need for continuous monitoring and sampling during flood events to better constrain metal behaviour in ASS wetlands.

This study has successfully characterised the extent, distribution and processes involved in the development of ASS in a wetland in SE Australia. It has demonstrated

that by combining S isotopes with other well developed ASS techniques such as Cl:SO₄ ratios, a better understanding of pyrite formation and oxidation can be gained.

Furthermore, by sampling during drought and after severe flooding, the potential impact of extreme climatic conditions on ASS wetlands is demonstrated. This study also highlights the need for continuous sampling and measurement during the flooding of ASS, in order to better constrain the behaviour of metals during changes in redox and pH conditions.

Acknowledgements

Funding for this project was provided by the West Gippsland Catchment Authority and the National Centre for Groundwater Research and Training, an Australian Government initiative, supported by the Australian Research Council and the National Water Commission. We would like to thank Gary Howard and Matt Bowler for their assistance during the field campaigns and Massimo Raveggi for his help in the laboratory. We also thank the reviewers for their helpful comments during the review process.

References

- Ahern, C.R., McElnea, A.E., Sullivan, L.A., 2004. Acid Sulfate Soils Laboratory Methods Guidelines. Queensland Department of Natural Resources, Mines and Energy, Indooroopilly, Queensland, Australia.
- Åström, M., Björklund, A., 1995. Impact of acid sulfate soils on stream water geochemistry in western Finland. *J. Geochem. Explor.* 55, 163–170.
- Åström, M., Spiro, B., 2000. Impact of isostatic uplift and ditching of sulfidic sediments on the hydrochemistry of major and trace elements and sulfur isotope ratios in streams, Western Finland. *Environ. Sci. Technol.* 34, 1182–1188.
- Boman, A., Åström, M., Fröjdö, S., 2008. Sulfur dynamics in boreal acid sulfate soils rich in metastable iron sulphide – the role of artificial drainage. *Chem. Geol.* 255, 68–77.
- Boon, P.I., Raulings, E., Morris, K., Roache, M., Robinson, R., Hatton, M., Salter, J., 2007. Ecology and Management of the Lake Wellington Wetlands, Gippsland Lakes: A Report on the RD Project, 2003–2006. Institute for Sustainability and Innovation, Victoria, Australia.
- Bridgman, H.A., 1992. Evaluating rainwater contamination and sources in southeast Australia using factor analysis. *Atmos. Environ.* 26, 2401–2412.

- Bureau of Meteorology, 2010. Commonwealth of Australia Bureau of Meteorology. <www.bom.gov.au>.
- Burton, E.D., Bush, R.T., Sullivan, L.A., Johnston, S.G., Hocking, R.K., 2008a. Mobility of arsenic and selected metals during re-flooding of iron- and organic-rich acid sulfate soil. *Chem. Geol.* 253, 64–73.
- Burton, E.D., Sullivan, L.A., Bush, R.T., Johnston, S.G., Keene, A.F., 2008b. A simple and inexpensive chromium-reducible sulfur method for acid-sulfate soils. *Appl. Geochem.* 23, 2759–2766.
- Cartwright, I., Weaver, T.R., Fifield, L.K., 2006. Cl/Br ratios and environmental isotopes as indicators of recharge variability and groundwater flow: an example from southeast Murray Basin, Australia. *Chem. Geol.* 231, 38–56.
- Chivas, A.R., Andrew, A.S., Lyons, W.B., Bird, M.I., Donnelly, T.H., 1991. Isotopic constraints on the origin of salts in Australian playas. 1.. Sulphur Palaeogeol. Palaeoclimatol. Palaeoecol. 84, 309–332.
- Clark, I.D., Fritz, P., 1997. *Environmental Isotopes in Hydrogeology*. Lewis, New York, USA.
- Cook, F.J., Hicks, W., Gardner, E.A., Carlin, G.D., Froggatt, D.W., 2000. Export of acidity in drainage water from acid sulphate soils. *Mar. Pollut. Bull.* 41, 319–326.
- Cook, F.J., Dobos, S.K., Carlin, G.D., Millar, G.E., 2004. Oxidation rate of pyrite in acid sulfate soils: in situ measurements and modelling. *Aust. J. Soil Res.* 42, 499–507.
- Dent, D.L., Pons, L.J., 1995. A world perspective on acid sulphate soils. *Geoderma* 67, 263–276.
- Dogramaci, S.S., Herczeg, A.L., Schiff, S.L., Bone, Y., 2001. Controls on d34S and d18O of dissolved sulfate in aquifers of the Murray Basin, Australia and their use as indicators of flow processes. *Appl. Geochem.* 16, 475–488.
- Fitzpatrick, R.W., Grealish, G., Shand, P., Simpson, S.L., Merry, R.H., Raven, M.D., 2009. Acid Sulfate Assessment in Finnis River, Currency Creek, Black Swamp and Goolwa Channel, South Australia. CSIRO Land and Water Technical Report 26/09, Australia.
- Flessa, H., 1994. Plant-induced changes in the redox potential of the rhizospheres of the submerged vascular macrophytes *Myriophyllum verticillatum* L. and *Ranunculus circinatus* L. *Aquat. Bot.* 47, 119–129.
- GHD, 2005. Heart Morass Feasibility Study Final Report. West Gippsland Catchment Management Authority.
- Golez, N.V., Kyuma, K., 1997. Influence of pyrite oxidation and soil acidification on some essential nutrient elements. *Aquacult. Eng.* 16, 107–124.
- Gosavi, K., Sammut, J., Gifford, S., Jankowski, J., 2004. Macroalgal biomonitors of trace metal contamination in acid sulfate soil aquaculture ponds. *Sci. Total. Environ.* 324, 25–39.
- Green, R., Macdonald, B.C.T., Melville, M.D., Waite, T.D., 2006. Hydrochemistry of episodic drainage waters discharged from an acid sulfate soil affected catchment. *J. Hydrol.* 325, 356–375.
- Johnston, S.G., Bush, R.T., Sullivan, L.A., Burton, E.D., Smith, D., Martens, M.A., McElnea, A.E., Ahern, C.R., Powell, B., Stephens, L.P., Wilbraham, S.T., VanHeel, S., 2009. Changes in water quality following tidal inundation of coastal lowland acid sulfate soil landscapes. *Estuar. Coast Shelf Sci.* 81, 257–266.
- Johnston, S.G., Burton, E.D., Bush, R.T., Keene, A.F., Sullivan, L.A., Smith, D., McElnea, A.E., Ahern, C.R., Powell, B., 2010. Abundance and fractionation of Al, Fe and trace metals following tidal inundation of a tropical acid sulfate soil. *Appl. Geochem.* 25, 323–335.

- Johnston, S.G., Keene, A.F., Bush, R.T., Burton, E.D., Sullivan, L.A., Isaacson, L., McElnea, A.E., Ahern, C.R., Smith, C.D., Powell, B., 2011. Iron geochemical zonation in a tidally inundated acid sulfate soil wetland. *Chem. Geol.* 280, 257–270.
- Kilminster, K., Cartwright, I., 2011. A sulfur-stable-isotope-based screening tool for assessing impact of acid sulfate soils on waterways. *Mar. Freshw. Res.* 62, 152–161.
- Massmann, G., Tichomirowa, M., Merz, C., Pekdeger, A., 2003. Sulfide oxidation and sulfate reduction in a shallow groundwater system, Oderbruch Aquifer, Germany. *J. Hydrol.* 278, 231–243.
- McDonald, R.C., Isbell, R.F., Speight, J.G., Walker, J., Hopkins, M.S., 1990. *Australian Soil and Land Survey Field Handbook*, second ed. Inkata Press, Melbourne, Australia.
- Mörth, C.M., Torssander, P., 1995. Sulfur and oxygen isotope ratios in sulphate during an acidification reversal study at Lake Gårdjsön, Western Sweden. *Water Air Soil Pollut.* 79, 261–278.
- Nordmyr, L., Åström, M., Peltola, P., 2008a. Metal pollution of estuarine sediments caused by leaching of acid sulphate soils. *Estuar. Coast Shelf Sci.* 76, 141–152.
- Nordmyr, L., Österholm, P., Åström, M., 2008b. Estuarine behaviour of metal loads leached from coastal lowland acid sulphate soils. *Mar. Environ. Res.* 66, 378–393.
- Österholm, P., Åström, M., 2002. Spatial trends and losses of major and trace elements in agricultural acid sulphate soils distributed in the artificially drained Rintala area, W. Finland. *Appl. Geochem.* 17, 1209–1218.
- Österholm, P., Åström, M., 2004. Quantification of current and future leaching of sulfur and metals from Boreal acid sulfate soils, western Finland. *Aust. J. Soil Res.* 42, 547–551.
- Österholm, P., Åström, M., 2008. Meteorological impacts on the water quality in the Pajuluoma acid sulphate area, W. Finland. *Appl. Geochem.* 23, 1594–1606.
- Rees, C.E., 1973. A steady-state model for sulphur isotope fractionation in bacterial reduction processes. *Geochim. Cosmochim. Acta* 37, 1141–1162.
- Ritsema, C.J., Groenenberg, J.E., Bisdom, E.B.A., 1992. The transformation of potential into actual acid sulphate soils studied in column experiments. *Geoderma* 55, 259–271.
- Sammut, J., Melville, M.D., Callinan, R.B., Fraser, G.C., 1995. Estuarine acidification: impacts on aquatic biota of draining acid sulphate soils. *Aust. Geogr. Stud.* 33, 89–100.
- Santos, I.R., Weys, J.D., Eyre, B.D., 2011. Groundwater or floodwater? Assessing the pathways of metal exports from a coastal acid sulfate soil catchment. *Environ. Sci. Technol.* 45, 9641–9648.
- Simpson, S., Fitzpatrick, R., Shand, P., Angle, B., Spadaro, D., Merry, R., Thomas, M., 2008. *Acid, Metal and Nutrient Mobilisation Following Rewetting of Acid Sulfate Soils in the Lower Murray*. CSIRO Land and Water Technical Report CLW27/08, Australia.
- Sohlenius, G., Öborn, I., 2004. Geochemistry and partitioning of trace metals in acid sulphate soils in Sweden and Finland before and after sulphide oxidation. *Geoderma* 122, 167–175.
- Sullivan, L.A., 2009. Improved identification of sulfidic soil materials by a modified incubation method. *Geoderma* 149, 33–38.

- Sullivan, L.A., Fitzpatrick, R.W., Bush, R.T., Burton, E.D., Shand, P., Ward, N.J., 2010. The Classification of Acid Sulfate Soil Materials: Further Modifications. Southern Cross Geoscience Technical Report 310.
- Thode, H.G., Kleerekoper, H., Mcencheran, D.E., 1951. Isotopic fractionation in the bacterial reduction of sulphate. *Research* 4, 581–582.
- Toivonen, T., Österholm, P., 2011. Characterization of acid sulfate soils and assessing their impact on a humic boreal lake. *J. Geochem. Explor.* 110, 107–117.
- USEPA, 1994. Sample Preparation procedure for Spectrochemical Determination of Total Recoverable Elements, Method 200.2, Revision 2.8.
- White, I., Melville, M.D., Wilson, B.P., Sammut, J., 1997. Reducing acidic discharges from coastal wetlands in eastern Australia. *Wetland Ecol. Manag.* 5, 55–72.
- Wilkin, R.T., Barnes, H.L., Brantley, S.L., 1996. The size distribution of framboidal pyrite in modern sediments: an indicator of redox conditions. *Geochim. Cosmochim. Acta* 60, 3897–3912.

Chapter 7

Major findings and concluding remarks

This thesis presents detailed findings that help define the connectivity of groundwater and surface water in the Gippsland Basin, Eastern Victoria, Australia. These findings define not only changes in the volumetric exchange of water between groundwater and surface water reservoirs over space and time, but how such variability may impact geochemical processes and water quality. These outcomes have the potential to aid water management practices in the Gippsland Lakes region which relies heavily on local groundwater and surface water for agriculture, drinking, fishing, boating, recreation and tourism.

7.1 Detailed findings as discussed by chapter

7.1.1 Investigating the spatio-temporal variability in groundwater and surface water interactions: a multi-technique approach

- Groundwater discharge to the Tambo River is spatially controlled by topography, with areas of increased topographic variation providing greater potential for the establishment of higher groundwater-surface water gradients and increased groundwater discharge.
- The highest volumes of groundwater discharge to the Tambo and Nicholson Rivers occurs in the days to weeks following significant rainfall in the catchment, when river levels have receded but recent groundwater recharge has elevated groundwater levels.

- The volume of groundwater discharge to the Tambo River estimated by Cl mass balance differs significantly to that estimated by ^{222}Rn mass balance and differential flow gauging. This is due to spatial heterogeneity in the Cl end member that is driven by aquifer interactions and river-groundwater exchange.

7.1.2 Residence times and mixing of water in river banks: implications for recharge and groundwater – surface water exchange

- Groundwater in the unconfined aquifer neighbouring the Tambo River has a mean groundwater residence time of <100 years in age while deeper groundwater in the unconfined aquifer has a mean residence time of ~17,200 years.
- Groundwater in the unconfined aquifer increases in age with proximity to the Tambo River yielding a horizontal flow velocity between 1 and 10 m/year towards to river. This is consistent with the gaining nature of the Tambo River and relatively local groundwater recharge within 100's of meters of the river boundary.
- ^3H and ^{14}C activities indicate that some areas closer to the Tambo River are receiving upward leakage from the deeper, semi-confined aquifer, presumably because the confining layer is not present closer to the river where erosion due to periodic flooding prevents its preservation.
- Major ions, $\delta^2\text{H}/\delta^{18}\text{O}$ values and $^3\text{H}/^{14}\text{C}$ activities of groundwater in the banks of the Tambo River do not support the increased prevalence of river water storage closer to the river margin. These results suggest that either the strongly gaining nature of the Tambo River at the study locations is preventing significant lateral infiltration of river water into the bank, or that the rapid propagation of pressure into the underlying semi-confined aquifer, followed by leakage into the above unconfined aquifer is preventing significant river infiltration.

7.1.3 The dynamics of river – groundwater exchange in river banks

- The upward leakage of saline water from the deeper, semi-confined aquifer neighbouring the Tambo River limits the dilution of groundwater in the unconfined aquifer via bank infiltration as classically envisaged.
- During flooding, saline water that has leaked into the unconfined aquifer moves away from the river due to the reversal of the hydraulic gradient. This causes groundwater in the area 10 to 50 m from the Tambo River to increase in salinity during the initial stages of flooding.
- Continued flooding will cause groundwater dilution in the unconfined aquifer immediately neighbouring the Tambo River, however as flooding subsides, high salinity groundwater that has moved away from the river will return, elevating the salinity of groundwater closer to the river.
- By combining high frequency groundwater-surface water monitoring with numerical modelling, complex river-groundwater interactions can be identified, leading to a better understanding of groundwater-surface water systems and better evaluation of geochemical data.

7.1.4 Transient groundwater - surface water interactions in a tidal estuary: a case study from the Tambo River, Eastern Victoria

- The surface section of the Tambo River estuary is characterised by relatively low ^{222}Rn activities due to degassing and do not vary tidally.
- Rainfall in the Tambo Catchment will reduce the activity of ^{222}Rn in the surface section of the Tambo River estuary via the input of low ^{222}Rn water. These inputs may be traced simultaneously via $\delta^2\text{H}$ and $\delta^{18}\text{O}$ analysis.

- Increasing ^{222}Rn activities in the subsurface section of the estuary during tidal maximums can be mostly attributed to mixing between low ^{222}Rn surface water and higher ^{222}Rn subsurface waters.
- Fluctuations in the ^{222}Rn activity of subsurface water is greater than simple mixing indicates, suggesting secondary inputs of groundwater into the subsurface during flow reversal at larger tidal maximums.

7.1.5 Assessing the hydrogeochemical impact and distribution of acid sulphate soils, Heart Morass, West Gippsland, Victoria.

- During drought conditions when the local water table is likely to be lower, pyritic soils in the central area of the Heart Morass have become oxidised.
- Low metal concentrations, pH and neutralising capacities in these soils is indicative of acidic and metalliferous drainage into the local groundwater, and is supported by high concentrations of dissolved metals in the associated waters.
- While other areas in the Heart Morass do not currently exhibit low pH conditions consistent with pyrite oxidation, low neutralizing capacities and low metal concentrations in the upper soil horizons of these areas is consistent with previous acidification and metalliferous drainage.
- Sulphate $\delta^{34}\text{S}$ values and $\text{Cl}:\text{SO}_4$ ratios of water from the morass were able to characterise the changing nature of pyrite oxidation and sulphate reduction in different areas of the morass in response to changing redox conditions.
- Increased rainfall, water table elevation and soil moisture was found to remediate the impact of pyrite oxidation, yielding higher soil and water pH and the export of various metals.

7.2 Implications of research

The research presented in this thesis provides a number of findings with respect to groundwater and surface water interaction at both a local and catchment scale in the Gippsland region. At a regional scale, it appears that groundwater recharge is occurring at the margin between the Eastern Victorian Uplands and the Gippsland Basin and draining roughly east towards the coastline. Confining layers throughout the basin appear to result in the separation of this regional groundwater component from local recharge. Where confining layers are less prevalent, such as incised rivers, mixing between this older groundwater and locally recharged groundwater is occurring. More specific outcomes of the thesis are listed as follows:

- The contribution of groundwater to the lower 40 km sections of the Tambo and Nicholson Rivers has been estimated to vary from ~5% of total river discharge during periods of increased rainfall to ~20% of river discharge under baseflow conditions.
- Shallow groundwater in the unconfined aquifer of the Tambo River basin is of relatively high quality ($<500 \mu\text{S/cm}$), is relatively modern (<100 years old) and is recharged relatively locally. Deeper water in the underlying semi-confined aquifer is more saline ($\sim 3,000 \mu\text{S/cm}$), much older ($\sim 17,200$ years old) and poses a contamination risk to the above lying unconfined aquifer.
- Water stored in the banks of the Tambo River may be of lower water quality than further from the river, as confining layers appear to be less prevalent and increased leakage from the semi-confined aquifer has been shown to occur in these areas.
- During flooding, saline water from the semi-confined aquifer may penetrate further into the unconfined aquifer due to hydraulic gradient reversal. As such, groundwater quality in the unconfined aquifer may be reduced during flooding.

- During floodplain drainage and reduced rainfall, pyrite oxidation, acid generation and metal mobilisation reduce the quality of surface and groundwater surrounding the Heart Morass. Water quality may however improve after significant rainfall through the dilution and export of metals and acid. By discontinuing anthropogenic drainage of the morass, water managers may be able to remediate the acidic and metalliferous groundwater and surface conditions in the morass.

7.3 Further research

Much of the work presented in this thesis characterises the chemical nature of groundwater and surface water systems under different hydrological conditions. Such characterisations took place during particularly dry periods and after significant rainfall and flooding. The transition from wet to dry conditions however remains relatively unconstrained with respect to groundwater and surface water chemistry. This is an area that is still relatively under-researched as such studies are logistically difficult to conduct, requiring sampling and analysis during periods of increased rainfall. Thus, researchers and analytical equipment must be mobilised on short notice based on meteorological forecasts.

Despite this, such research has the potential to help understand the transient nature of groundwater-surface water systems. For example, Chapters 3 and 4 identify increasing groundwater EC in response to flooding – however the relative impacts of aquifer leakage versus mineral salt dissolution and mobilisation from the soil zone into the shallow groundwater remains unconstrained. Similarly, the behaviour of dissolved metals in acid sulphate soil environments (Chapter 6) is hard to constrain without monitoring redox potential and metal speciation during rainfall events. In this context, combining continuous monitoring of parameters such as temperature, pH, redox potential and ^{222}Rn activity with periodic sampling of surface water and groundwater for major ions and

dissolved metals has the potential to better characterise the geochemical processes occurring in groundwater-surface water systems in response to rainfall. This is of particular interest in the Gippsland Lakes system as nutrient and solute loads carried by flood waters to the lower lakes has been shown to cause algal blooms (Cook et al., 2010). As such, understanding the exact chemical pathways that nutrients and solutes takes may help facilitate effective water management.

Research presented in this thesis also highlights a number of assumptions and approximations within ^{222}Rn mass balance models that leads to uncertainties in groundwater discharge estimates. These include the gas transfer velocity (k) and characterization of ^{222}Rn in groundwater. While a variety of models exist that can be used to approximate k , it has been shown that selecting the appropriate model for a particular river system can be difficult (Genereux and Hemond, 1992). It would be useful for future work to focus on characterising river systems based on factors such as morphology in order to allow the appropriate application of k models. It has also been widely recognised that accurate characterisation of ^{222}Rn in groundwater remains one of the largest uncertainties when calculating groundwater fluxes (Cook, 2012). This is a response to not only the spatial variability of ^{222}Rn in groundwater that results from aquifer lithology, but also temporal changes due to variable groundwater residence times and flow rates through aquifers. For example, Chapters 2, 3 and 4 highlight river-bank interactions and groundwater leakage as drivers of ^{222}Rn variability, both of which vary spatially and temporally near the Tambo River. Recent developments in ^{222}Rn monitoring (Gilfedder et al., 2012; Hofmann et al., 2011) facilitates continuous ^{222}Rn monitoring in groundwater, allowing the impact of such processes on groundwater ^{222}Rn activities to be evaluated, and thus better characterisation of the groundwater ^{222}Rn end member.

References

- Cook, P.G., 2012. Estimating groundwater discharge to rivers from river chemistry surveys. *Hydrological Processes*, 27(25): 3694-3707.
- Cook, P.L.M., Holland, D.P., Longmore, A.R., 2010. Effect of a flood event on the dynamics of phytoplankton and biogeochemistry in a large temperate Australian lagoon. *Limnol. Oceanogr.*, 55(3): 1123-1133.
- Genereux, D.P., Hemond, H.F., 1992. Determination of gas exchange rate constants for a small stream on Walker Branch Watershed, Tennessee. *Water Resources Research*, 28(9): 2365-2374.
- Gilfedder, B.S., Hofmann, H., Cartwright, I., 2012. Novel instruments for in situ continuous Rn-222 measurement in groundwater and the application to river bank infiltration. *Environmental Science & Technology*, 47(2): 993-1000.
- Hofmann, H., Gilfedder, B.S., Cartwright, I., 2011. A novel method using a silicone diffusion membrane for continuous ²²²Rn measurements for the quantification of groundwater discharge to streams and rivers. *Environmental Science & Technology*, 45(20): 8915-8921.

Appendix A

A multi-tracer approach to quantifying groundwater inflows to an upland river; assessing the influence of variable groundwater chemistry

A. P. Atkinson,^{1,2*} I. Cartwright,^{1,2} B. S. Gilfedder,^{1,2} H. Hofmann,¹ N. P. Unland,^{1,2}
D. I. Cendón^{3,4} and R. Chisari³

¹ School of Geosciences, Monash University, Clayton, Vic, 3800, Australia

² National Centre for Groundwater Research and Training, GPO Box 2100, Flinders University, Adelaide, SA 5001, Australia

³ Australian Nuclear Science and Technology Organisation, Menai, NSW 2232, Australia

⁴ School of Biological Earth and Environmental Sciences, The University of New South Wales, Sydney, NSW 2052, Australia

Abstract:

Understanding the behaviour and variability of environmental tracers is important for their use in estimating groundwater discharge to rivers. This study utilizes a multi-tracer approach to quantify groundwater discharge into a 27 km upland reach of the Gellibrand River in southwest Victoria, Australia. Ten sampling campaigns were conducted between March 2011 and June 2012, and the distribution of ²²²Rn activities, Cl and ³H concentrations imply the river receives substantial groundwater inflows. Mass balances based on ²²²Rn, Cl and ³H yield estimates of groundwater inflows that agree to within $\pm 12\%$, with cumulative inflows in individual campaigns ranging from 24 346 to 88 467 m³/day along the studied river section. Groundwater discharge accounts for between 10 and 50% of river flow dependent on the time of year, with a high proportion (>40 %) of groundwater sustaining summer flows. Groundwater inflow is largely governed by regional groundwater flowpaths; between 50 and 90% of total groundwater inflows occur along a narrow 5–10 km section where the river intersects the Eastern View Formation, a major regional aquifer. Groundwater ²²²Rn activities over the 16 month period were spatially heterogeneous across the catchment, ranging between 2000 Bq/m³ and 16 175 Bq/m³. Although groundwater ²²²Rn activities display temporal variation, spatial variation in groundwater ²²²Rn is a key control on ²²²Rn mass balances in river catchments where groundwater and river ²²²Rn activities are within an order of magnitude of each other. Calculated groundwater discharges vary from 8.4 to 15 m³/m/day when groundwater ²²²Rn activities are varied by $\pm 1 \sigma$. Copyright © 2013 John Wiley & Sons, Ltd.

KEY WORDS groundwater; geochemistry; ²²²Rn; ³H; baseflow; Gellibrand

Received 6 May 2013; Accepted 21 November 2013

INTRODUCTION

Groundwater (GW) and surface water (SW) in the form of rivers, lakes and wetlands are intrinsically linked. Instead of being two isolated components of the water cycle, they are coupled reservoirs, with changes in one potentially affecting the other (Winter *et al.*, 1998; Sophocleous, 2002). This inter-connection is of vital importance not only in the hydrological cycle for water balances, but also from an ecological perspective, with consequences for water quality and groundwater-dependent ecosystems (Hancock *et al.*, 2005). In the case of rivers, an understanding of groundwater inflows enables sustainable rates of groundwater extraction to be estimated, protec-

tion of river flows, and can provide important information on the pathways of nutrients and pollutants.

Recent advances in our understanding of GW-SW connectivity have shown that exchange between the two water reservoirs occurs along a variety of flowpaths, each with a unique transmission time (McDonnell *et al.*, 2010). Regional flowpaths refer to groundwater that discharges into rivers 100's to 1000's of years after initially entering the aquifer (Larkin and Sharp, 1992). On the regional scale, rivers may be gaining (where they receive groundwater), or losing (where the net flux is from the river to the adjacent aquifer) (Cendón *et al.*, 2010; Banks *et al.*, 2011). Rivers are likely to have both gaining and losing reaches distributed along their course and this distribution may change at different flows, with a transition from gaining behaviour at low flows to losing at high flows.

Imposed on these regional flows are smaller scale hyporheic (Boulton *et al.*, 1998; Mutz and Rohde, 2003)

*Correspondence to: A. P. Atkinson, School of Geosciences, Monash University, Clayton, Vic, 3800, Australia.

E: [REDACTED]

and parafluvial flows (Deforet *et al.*, 2009). Here, water travels several metres or less within the streambed sediments, re-emerging within a matter of hours to days. Though knowledge of both processes is important in order to accurately estimate groundwater inflows, at the catchment scale, regional groundwater provides the largest quantities of water, with many river systems dependent on groundwater contributions during periods of drought.

A range of techniques may be used to assess the direction and magnitude of the flux between groundwater and rivers. These include analysis of stream hydrographs (Nathan *et al.*, 1990; Aksoy *et al.*, 2009), numerical modelling (Arnold *et al.*, 1993), Darcy flux calculations (Kroeger *et al.*, 2007) and detailed temperature profiles in the river bed (Hatch *et al.*, 2006). Groundwater fluxes can also be determined using environmental tracers (Cook, 2012), including electrical conductivity (EC) (Oxtobee and Novakowski, 2003), chloride (Cartwright *et al.*, 2011), dissolved gases in the form of ^{222}Rn and chlorofluorocarbons (CFCs) (Cook *et al.*, 2003, 2006; Mullinger *et al.*, 2007; Burnett *et al.*, 2010) and the stable isotopes of water (Tetzlaff and Soulsby, 2008; Liu *et al.*, 2008). The use of geochemical tracers to estimate groundwater fluxes into rivers relies on the groundwater having significantly different concentrations of the tracers to river water and the concentrations of these tracers in groundwater being uniform, or any variations being well known. Tracers may be conservative such as Cl and the stable isotopes, or have well-defined non-conservative behaviour (such as degassing rates or radioactive decay in the case of ^{222}Rn or CFCs).

With the evolution of both discrete (Freyer *et al.*, 1997) and continuous (Burnett *et al.*, 2010; Hofmann *et al.*, 2011) field measurement techniques, ^{222}Rn has increasingly been used to estimate groundwater influxes into rivers. ^{222}Rn is produced by the decay of ^{226}Ra in the ^{238}U - ^{206}Pb decay chain. With a half life of 3.8 days, the activity of ^{222}Rn reaches secular equilibrium with ^{226}Ra in the aquifer matrix over a few weeks (Cecil and Green, 2000). Concentrations of ^{226}Ra in minerals in the aquifer matrix are several orders of magnitude higher than the dissolved ^{226}Ra concentrations in surface water (Ellins *et al.*, 1990; Cecil and Green, 2000; Stellato *et al.*, 2008; Mullinger *et al.*, 2009) or the suspended ^{226}Ra in river sediments (Santos and Eyre, 2011); hence, groundwater ^{222}Rn activities are commonly two or three orders of magnitude higher than those of surface water. Consequently, high ^{222}Rn activities in rivers indicate groundwater inflows. Due to its relatively short half-life and degassing to the atmosphere, ^{222}Rn activities decline downstream from these zones of groundwater inflow (Ellins *et al.*, 1990; Genereux and Hemond, 1990; Cook *et al.*, 2003; Mullinger *et al.*, 2007).

Tritium (^3H) is another powerful tracer for determining the movement and residence time of water in the hydrosphere. ^3H has a half life of 12.43 years and is generally used as a technique for dating recently (<100 years) recharged groundwater (Han *et al.*, 2012; Manning *et al.*, 2012). Although not commonly used in this way, the inflow of old groundwater with low ^3H into surface water that has high ^3H concentrations can also be used to detect groundwater inflows.

This study uses ^{222}Rn , ^3H , EC, chloride and stable isotopes ($\delta^{18}\text{O}$ & $\delta^2\text{H}$) over a 16 month period to estimate groundwater fluxes into the upland catchment of the Gellibrand River, Victoria, Australia. In particular, the spatial and temporal variability in groundwater ^{222}Rn activities are assessed to understand the impact that variations in groundwater chemistry have on groundwater fluxes calculated using ^{222}Rn .

Hydrogeological setting

The Gellibrand River is located in southwest Victoria and has a catchment area of ~950 km². It rises in the Otway Ranges and flows west and southwest for 75 km, before entering the ocean via Bass Strait. This study focuses on a 27 km section of river within the upland plain of the catchment (Figure 1a), which covers an area of ~250 km². This part of the catchment consists of a mixture of cool temperate rainforest and wet sclerophyll on the valley sides and in the headwaters, whilst the river plains have been cleared for dairy farming. With an average annual rainfall of between 800 and 1200 mm per year, the area is one of the wettest in Victoria with the majority of rainfall falling in the Australian winter between June and September (Figure 2).

Situated in the Otway Basin which was formed by late Jurassic to early Cretaceous rifting, Cretaceous volcanolithic sandstone, siltstone and mudstone of the Otway Group form the basement of the catchment. This unit crops out in the southern and eastern margins of the upper catchment (Tickell, 1990). The primary aquifer in the upland area is the Eastern View Formation; this is composed of non-marine sands with lenses of silt and clay, and has an average thickness across the catchment of 150 m (Leonard *et al.*, 1981). Together, the Eastern View Formation and near-stream Quaternary alluvial deposits constitute the likely sources of groundwater discharging into the Gellibrand River. To the northeast of the river, the Eastern View Formation is overlain by a regional clay aquitard — the Gellibrand Marl; this and a number of intrusions of the basaltic Quaternary Newer Volcanics confine the aquifer in this area.

The Gellibrand River has a shallow gradient (0.9 m/km) with relatively low turbulence along the study reach and no significant rapids or pool and riffle sequences. Its width is between 5 and 10 m along most of its length, and depth

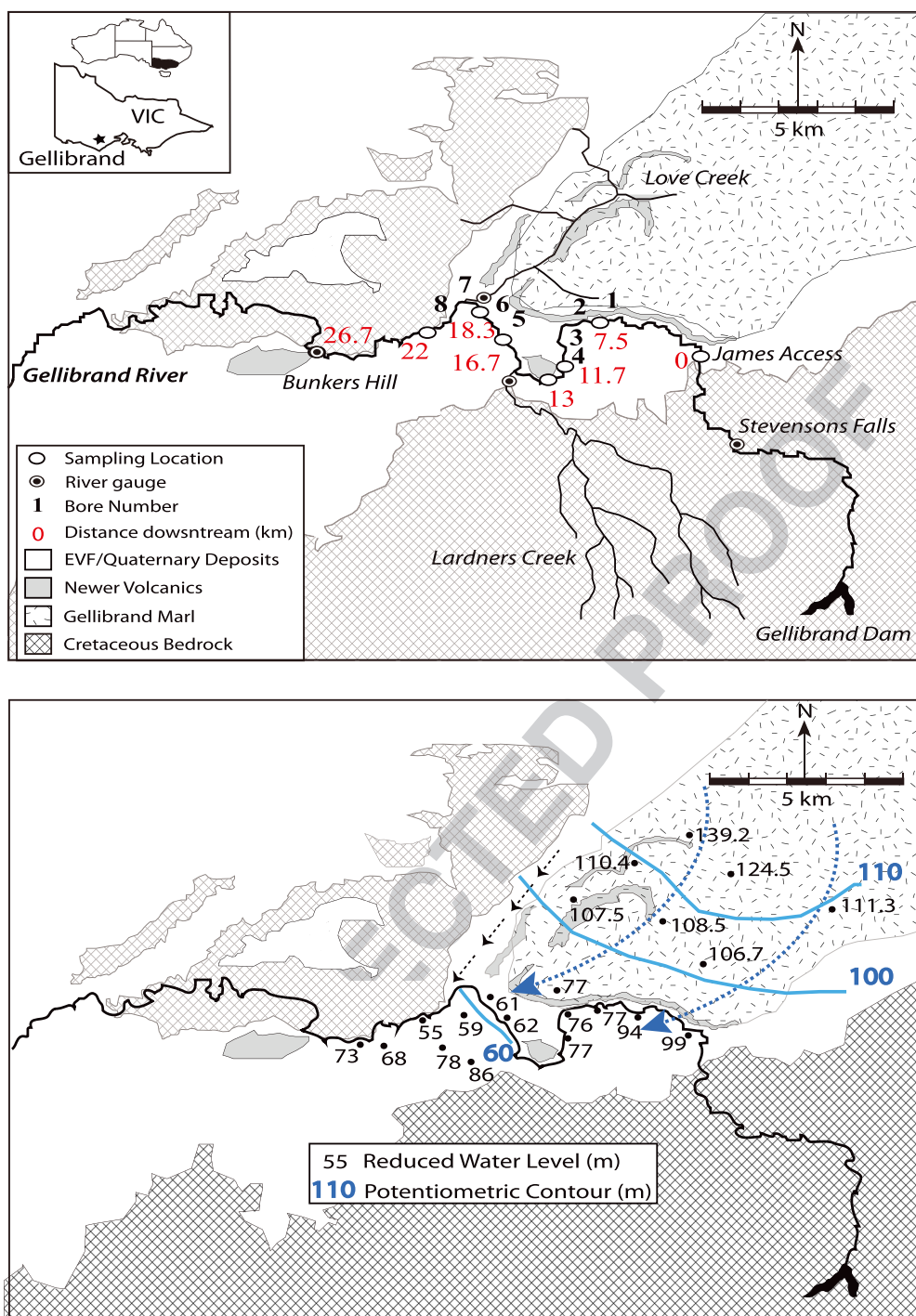


Figure 1. (a) Location map of the Gellibrand catchment, showing the generalized geology and sampling locations. (b) Potentiometric flow map constructed from local bore network; regional groundwater flow is predominantly in a SW direction toward the river

varies dependent on flow conditions between 1 and 6 m. Outflow from the Gellibrand Dam is gauged, with a further two gauges located in the upper catchment (Stevensons Falls) and at the end of the study reach (Bunkers Hill) (Figure 1a). Annual flow at Stevensons Falls ranges between 10 and 100 ML/day and Bunkers Hill between 50

and 500 ML/day (Victorian Water Resources Data Warehouse, 2012), with high flows occurring during the wet season (June – September) and low flows during the summer months (Figure 2). A number of small gauged tributaries enter the Gellibrand River in the study region; the largest of these joining from the south, Lardners Creek,

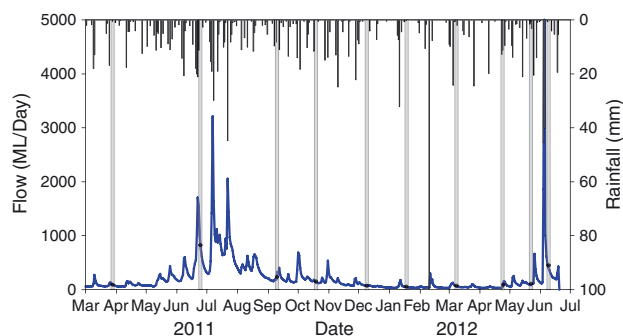


Figure 2. Bunkers Hill discharge record. Sampling times are indicated by vertical grey lines

has flows of 20–100 ML/day, and Love Creek joining from the North, has flows of 1–50 ML/day (Victorian Water Resources Data Warehouse, 2012).

Groundwater flow in the Eastern View Formation is towards the river (Victorian Water Resources Data Warehouse, 2012), indicating a potentially gaining system (Figure 1b). Over the 16 month study period, the stream was sampled 10 times between March 2011 and June 2012 in order to encompass a range of different flow conditions and to assess temporal variations in groundwater discharge. The majority of these sampling campaigns were conducted during baseflow conditions; however, June 2011 and June 2012 sampling was conducted on the recession curves of major flood peaks (Figure 2).

METHODOLOGY AND ANALYTICAL TECHNIQUES

River water was sampled longitudinally downstream over a 27 km stretch at eight sites; these are designated as distance downstream from James Access (0 km), where the river first encounters the region of the catchment underlain by the Eastern View Formation aquifer (Figure 1a). Samples were taken ~1 m below the river surface to ensure a representative sample of well mixed river water. Groundwater from the Eastern View Formation was sampled from eight bores that are part of the Victorian State Observation Bore Network. The bores have screen depths of 11–16 m, are <25 m from the river and are located in a 14 km² area of the catchment. Bores were pumped using an impeller pump set in the screen, purging two to three bore volumes before sampling. EC and pH of groundwater were measured in the field using a calibrated TPS WP-81 conductivity/pH meter and probes. Rainfall samples were also collected in the catchment throughout the study period.

Cations were analysed on a Thermo Finnigan X Series II Quadrupole ICP-MS on samples that had been filtered through 0.45 µm cellulose nitrate filters and acidified to

pH < 2. Anions were measured on filtered unacidified samples using a Metrohm ion chromatograph. The precision of major ion concentrations based on replicate analyses is ± 2%. Charge balances are within ± 5%. Stable isotope ratios were measured using Finnigan MAT 252 and ThermoFinnigan DeltaPlus Advantage mass spectrometers. δ¹⁸O values were measured via equilibration with He-CO₂ at 32 °C for 24–48 h in a Finnigan MAT Gas Bench whilst δ²H values were measured by the reaction of water samples with Cr at 850 °C using a Finnigan MAT H/Device. Both δ¹⁸O and δ²H were measured against an internal standard that has been calibrated using the IAEA, SMOW, GISP and SLAP standards. Data was normalized following methods outlined by Coplen (1988) and are expressed relative to V-SMOW where δ¹⁸O and δ²H values of SLAP are –55.5‰ and –428‰, respectively. Precision is ± 1‰ for δ²H and ± 0.2‰ for δ¹⁸O.

²²²Rn activities in groundwater and surface water were determined using a portable radon-in-air, RAD-7 monitor (Durrige) following methods described by Burnett and Dulaiova (2006) and are expressed in Becquerels per m³ of water (Bq/m³). Water sample, 500 cm³, was collected by bottom filling a glass flask and ²²²Rn was degassed into a closed air loop of known volume. Counting times are 2 h for river water and 15 min for groundwater and typical relative precisions are <3% at 10 000 Bq/m³ increasing to ~10% at 100 Bq/m³.

³H concentrations were measured in a number of near-river shallow groundwater bores in April 2012 and at four river sites in March 2012 and April 2012. Tritium (³H) concentrations were measured at the Australian Nuclear Science and Technology Organisation's (ANSTO) Low Level Laboratory. Samples for ³H were distilled and electrolytically enriched prior to being analysed by liquid scintillation counting (Neklapilova, 2008a, b). ³H concentrations are expressed in Tritium Units (TU) with a relative uncertainty of ± 5% and a quantification limit of 0.13 – 0.14 TU.

RESULTS

SW & GW geochemistry, major ion concentrations and stable isotopes

Both GW and SW are sodium chloride-bicarbonate type waters. River water has an average pH of 6–8 and an EC that varies between 80 and 250 µS/cm³ dependent on flow conditions. Cl concentrations in the Gellibrand River increase downstream in all sampling campaigns from 22 to 28 mg/l at James Access, to 35–49 mg/l at Bunkers Hill (Figure 3a). A similar increase occurs for major ions such as Na (Figure 3b) which increases downstream from 15–22 mg/l (James Access) to 18–32 mg/l (Bunkers

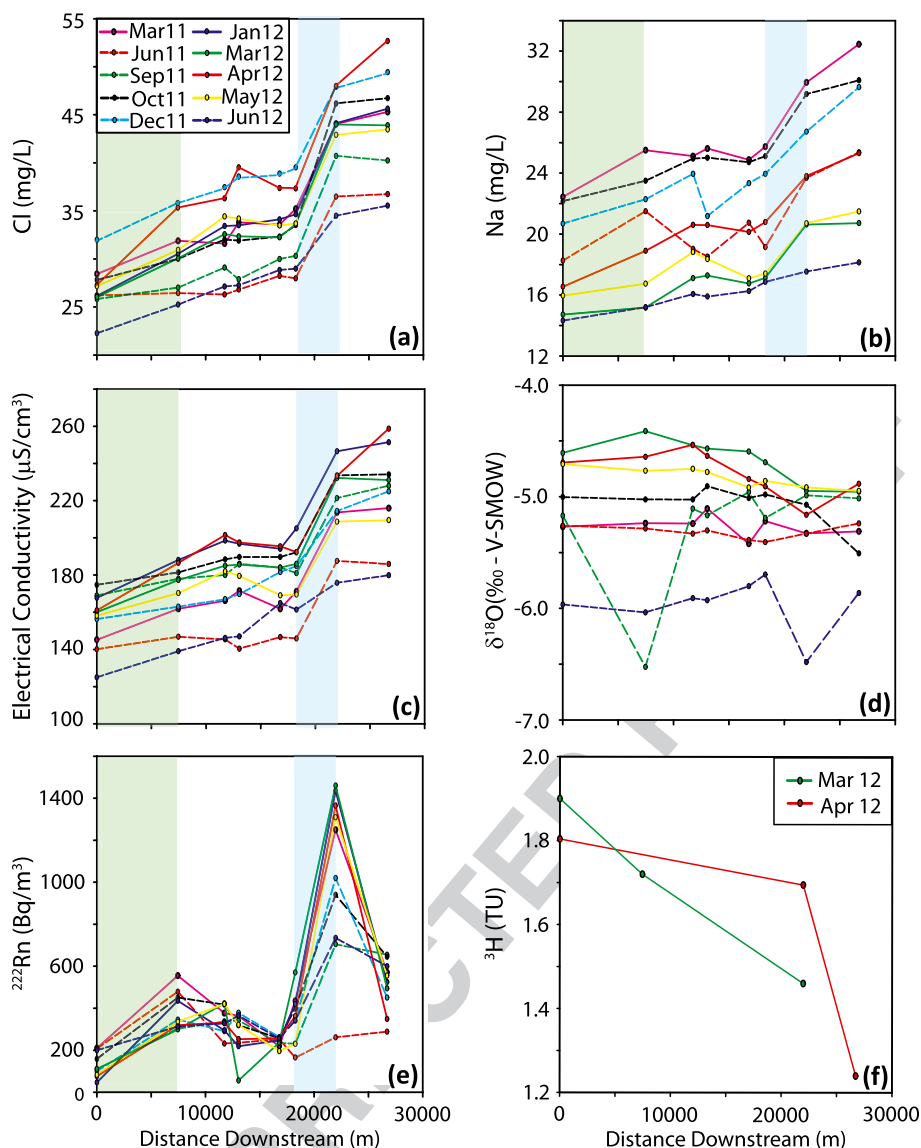


Figure 3. Chloride (3a), sodium (3b), EC (3c), ^{18}O (3d), ^{222}Rn activities (3e) and ^3H (3f) concentrations over ten sampling campaigns. Major increases in Cl, Na, EC and ^{222}Rn are seen between two reaches at 0–7.5 (green) and 16.8–22 km (blue)

Hill), Mg from 4.7 to 6.3 mg/l and Li from 0.7 $\mu\text{g}/\text{l}$ to 1.7 $\mu\text{g}/\text{l}$. The increase in solute concentrations corresponds to an increase in EC values downstream from 125–175 to 179–251 $\mu\text{S}/\text{cm}^3$ over the sampling campaigns (Figure 3c).

Major increases in EC values and Cl and Na concentrations occur between sampling points at 0–7.5 km and 16.8–22 km downstream. This spatial pattern is observed in all sampling campaigns (Figure 3 a,b,c). A notable decrease in EC and Cl occurs between 13 and 16.8 km; this is due to low EC water from the upper catchment entering the Gellibrand River via Lardners Creek.

The EC of regional groundwater is substantially higher than river water, ranging between 200 and 500 $\mu\text{S}/\text{cm}^3$. Major ion concentrations are also higher: Na (32–94 mg/l),

Mg (2.5–13.4 mg/l), K (2–8.5 mg/l) and Li (1–10 $\mu\text{g}/\text{l}$). $\delta^{18}\text{O}$ and $\delta^2\text{H}$ values of groundwater and river water from all campaigns lie close to the local meteoric water line which is defined by rainfall samples in the catchment and the meteoric water line for Melbourne some 150 km to the East (Figure 4). There are no substantial changes in $\delta^{18}\text{O}$ and $\delta^2\text{H}$ values downstream in any of the sampling rounds (Figure 3d).

^{222}Rn activities in the Gellibrand river

^{222}Rn activities in the Gellibrand River range between 100 and 1500 Bq/m^3 across all sampling campaigns. Highest activities were recorded during summer months (March 2011) and lowest during the winter (June 2011).

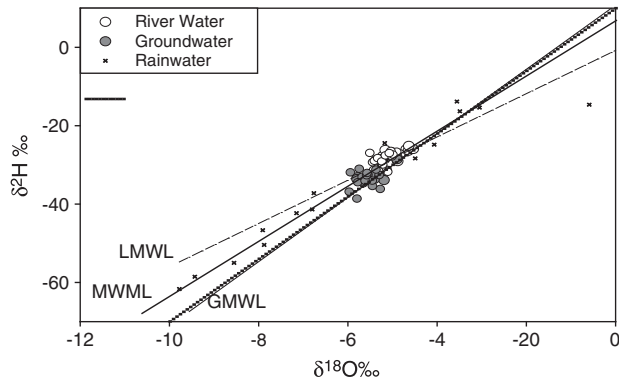


Figure 4. $\delta^{18}\text{O}$ v $\delta^2\text{H}$ values for SW, GW and rainfall in the Gellibrand Catchment. The Global Meteoric Water Line (GMWL) Melbourne Meteoric Water Line (MMWL) and Local Meteoric Water Line (LMWL) are shown

^{222}Rn activities vary systematically downstream for all sampling rounds (Figure 3e). ^{222}Rn activities are lowest ($46\text{--}210\text{ Bq/m}^3$) at 0 km (James Access) and increase downstream between 0 and 7.5 km ($302\text{--}555\text{ Bq/m}^3$). This is followed by a more substantial increase in ^{222}Rn activities between 16.8 and 22 km ($705\text{--}1460\text{ Bq/m}^3$). The reaches characterized by increases in ^{222}Rn activities are separated by a large reach between 7.5 and 16.8 km that has lower ^{222}Rn activities ($200\text{--}400\text{ Bq/m}^3$). These spatial trends in ^{222}Rn well correlate with changes in major ions, with high ^{222}Rn activities associated with increases in EC values and chloride concentrations.

^{222}Rn activities and chloride concentrations in groundwater samples

Groundwater ^{222}Rn activities for the eight near-river bores range from 1700 to 16 000 Bq/m^3 , with an average ^{222}Rn for all groundwater samples of 5636 Bq/m^3 and standard deviation ($\pm 1\sigma$) of 2781 Bq/m^3 . There is no systematic spatial variability of groundwater ^{222}Rn activity within the catchment, and little relationship between groundwater ^{222}Rn activity and screen depth. As well as spatial variations in groundwater ^{222}Rn activities, temporal variations in groundwater ^{222}Rn activities are observed between sampling campaigns, as shown by the lower and upper quartiles for each sampled F5 bore (Figure 5). The degree of temporal variation differs between bores. Large variations in the interquartile range are observed in a few bores (Bore 7: $8704\text{--}12963\text{ Bq/m}^3$, Bore 3: $3608\text{--}5405\text{ Bq/m}^3$); however, the majority remain relatively stable (Bore 1: $3166\text{--}3542\text{ Bq/m}^3$, Bore 2: $2181\text{--}2521\text{ Bq/m}^3$, Bore 6: $7138\text{--}7269\text{ Bq/m}^3$). No systematic pattern to this temporal variation in terms of screen depths or position in the catchment was observed.

Average groundwater chloride concentrations exhibit a large range ($38.6\text{--}125.5\text{ mg/l}$), with a $\sim 325\%$ difference between highest and lowest values, albeit

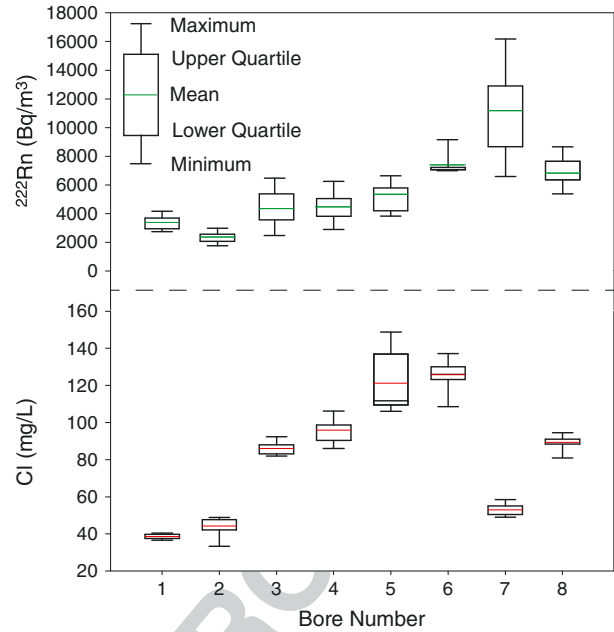


Figure 5. Variation in groundwater ^{222}Rn activities and Cl concentrations; the mean and interquartile range values for each bore are calculated over all sampling campaigns

lower than the magnitude of variation observed in average groundwater ^{222}Rn activities ($\sim 470\%$ difference between highest and lowest values). Temporal variations of chloride are significantly lower, with interquartile ranges generally no higher than 6 mg/l with the exception of Bore 5 ($109.8\text{--}131.6\text{ mg/l}$).

^3H concentrations in surface-water and groundwater samples

The ^3H concentration in near-river groundwater from bores 1–8 was below the quantification limit (0.14 TU). ^3H concentrations of river water in both March and April 2012 (Figure 3f) decline downstream, from 1.9 to 1.46 TU in March 2012 and 1.8 to 1.24 TU in April 2012. Though the largest decreases in ^3H occur in different reaches, between 7.5 and 22 km in March 2012, and 22 and 27 km in April 2012, the lowest ^3H concentrations in both campaigns occur after 20 km.

DISCUSSION

With the combination of major ions, ^{222}Rn activities and ^3H concentrations, patterns of groundwater–surface water interaction in the Gellibrand can be distinguished. Over the 27 km of river studied, there are downstream increases in the concentrations of all major ions and a decrease in ^3H concentrations, and ^{222}Rn activities show a pronounced increase between 0 and 7.5 km and 18.3 and 22 km. In the following sections, the changes in geochemistry are used

to quantify groundwater influxes and compare calculated groundwater fluxes from different tracers.

Constraining groundwater inputs using ²²²Rn

Groundwater inflows (I in m³/m/day) may be estimated via:

$$I = \frac{(Q \frac{dC_r}{dx} - wEC_r + kdWC_r + \lambda dWC_r)}{(C_i - C_r)} \quad (1)$$

(Mullinger *et al.*, 2007; Cartwright *et al.*, 2011; Cook *et al.*, 2012) where C_i is the ²²²Rn activity in groundwater and C_r is the ²²²Rn activity in the river (Bq/m³). Q is river discharge (m³/day), w is river width (m) and d is river depth (m). E is the evaporation rate (m/day), λ is the radioactive decay rate (0.181 day⁻¹) and k is the reaeration coefficient (day⁻¹). Evaporation rates (E) are taken from the nearest meteorological station at Mt Gellibrand, Colac, and range between 10⁻² and 10⁻³ m/day through the year (Bureau of Meteorology, 2012). In agreement with these low evaporation rates, the δ¹⁸O and δ²H values of river water lie on the meteoric water line rather than defining evaporation trends (Figure 4) and do not increase downstream (Figure 3d). Evaporation is, therefore, unlikely to significantly increase the concentration of solutes in the river. Groundwater ²²²Rn activities are taken as the mean value from bores sampled during each campaign.

The reaeration coefficient (k) is related to river turbulence and defines the rate of exchange or degassing of ²²²Rn across the air–water interface. River velocity and depth are the two most important factors in driving degassing. k is estimated using Equations (2) and (3), which are modifications of the gas transfer models of O’Connor and Dobbins (1958) and Negulescu and Rojanski (1969), where (v) is river velocity in m/s and (d) depth in metres.

$$k_1 = 9.301 \times 10^{-3} \left(\frac{v^{0.5}}{d^{1.5}} \right) \quad (2)$$

$$k_2 = 4.87 \times 10^{-4} \left(\frac{v}{d} \right)^{0.85} \quad (3)$$

Although a number of other empirical relationships between velocity, depth and k exist (St John *et al.*, 1984), these two formulations yield values of k that bracket those of most of the other models and thus provide upper and lower estimates of groundwater inflow (Mullinger *et al.*, 2007; Unland *et al.*, 2013). k values for the Gellibrand range between 0.5 and 5 across a range of flows. These are similar to values estimated in other studies of rivers with low gradients and without significant rapids or pool and riffle sequences which can enhance degassing

(Mullinger *et al.*, 2007). Values of k₂ are higher than k₁; therefore, larger groundwater inflows are calculated where k₂ is used in the mass balance.

Groundwater inflows calculated using Equation (1) fluctuate along the river from 0 to 11.1 m³/m/day (Figure 6). Two gaining reaches provide most of the groundwater discharge, separated by a variably losing and gaining section of river. The first gaining reach is between 0 and 7.5 km, with inflows of 0.5 to 1.5 m³/m/day during non-flood campaigns. During the June 2011 flood event, inflows here rise considerably to 5.4 (k₁) – 7.7 (k₂) m³/m/day. A second highly gaining reach at 18 – 22 km then follows, with groundwater inflows that range between 4.3 and 11.1 m³/m/day. Dramatic increases in groundwater inflows are not observed here during flood events.

Between 7.5 and 16.8 km groundwater discharge into the river varies throughout the year. For non-flood events, groundwater fluxes are low (0–1.1 m³/m/day), and depending on the k value chosen, this reach can be interpreted as either gaining or losing. During the June 2011 flood event, the maximum groundwater discharge along this reach increased to 4.7 m³/m/day, with a similar increase (2.7 m³/m/day) seen during the recession of the June 2012 flood.

Cumulative groundwater inflow rates along the river range between 22 079 and 42 526 m³ (k₁) and 29 677 and 54 681 m³ (k₂) in non-flood campaigns; these increase to 69 937 – 106 997 m³/day during the June 2011 flood event. As a proportion of the total river flow at Bunkers Hill (27 km downstream), cumulative groundwater inputs

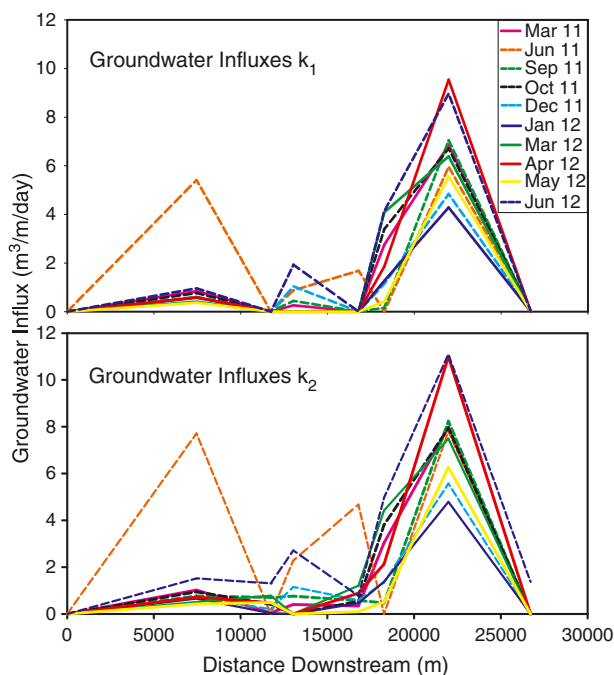


Figure 6. Calculated groundwater inflows downstream using two degassing models (k₁ and k₂)

account for 25 – 46% of river water during non-flood periods, dropping to 8 – 21% in the June 2011 event.

Constraining groundwater inputs using chloride

As groundwater sampled from near river bores generally has higher chloride concentrations (70 – 80 mg/l) than river water (22–49 mg/l), changes in river chloride concentrations (Cl_r) downstream (Figure 3a) can be used to calculate groundwater inflow rates via:

$$I = \frac{(Q \frac{dCl_r}{dx} - wEC_r)}{(Cl_i - Cl_r)} \quad (4)$$

(Cartwright *et al.*, 2011), where Cl_i is the average groundwater chloride concentration in the near-river bores (78 mg/l) and E was again assumed to be 10^{-2} to 10^{-3} m/day (Bureau of Meteorology, 2012).

Groundwater fluxes calculated by the chloride mass balance (Figure 7) are consistent with those calculated by the ^{222}Rn mass balance (Figure 6). Groundwater inflows to the river in non-flood events range between 0 and $11.7 \text{ m}^3/\text{day}$, and areas of high groundwater discharge are consistent with the two dominant gaining reaches at 0–7.5 km and 18–22 km. Between 7.5 and 16.8 km, the stream consists of a number of small reaches which transition between losing and gaining conditions, with groundwater inputs varying between sampling campaigns from 0 to $2.3 \text{ m}^3/\text{day}$. Again, a significant increase in groundwater discharge is seen here during the June 2011 flood event ($5.6 \text{ m}^3/\text{day}$).

Cumulative groundwater inflows of 29 300–51 700 m^3/day occur during non-flood sampling campaigns, with groundwater accounting for 18 – 60% of total river flow at Bunkers Hill (27 km downstream). As with the ^{222}Rn mass balance, the chloride mass balance predicts increased groundwater inflows ($134\,000 \text{ m}^3/\text{day}$) during

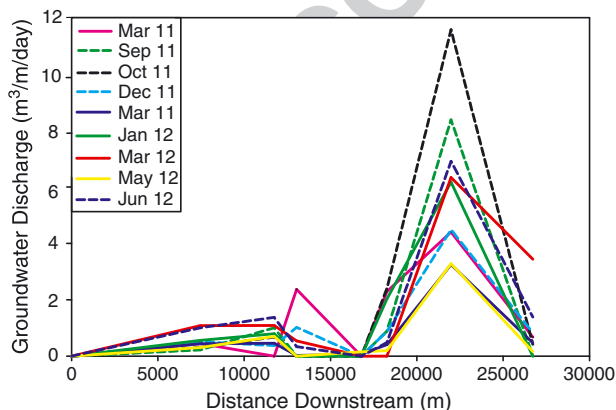


Figure 7. Groundwater discharge calculated via chloride mass balance (June 2011 flood omitted)

the June 2011 flood event. However, the Cl data implies that significant groundwater inflows occur between 18 and 22 km ($31.8 \text{ m}^3/\text{day}$), whereas the ^{222}Rn mass balance indicates significant groundwater discharges between 0 and 7.5 km.

Constraining groundwater inputs using ^3H

Decreases in ^3H downstream coincide with the region between 16.8 and 22 km where ^{222}Rn activities and Cl concentrations are highest. The decreases in river ^3H concentrations downstream can be attributed to the influx of ^3H -free regional groundwater. Total groundwater discharges during March and April 2012 were estimated via Equation (4), using river water ^3H concentrations and a ^3H concentration of 0 TU in the groundwater. Evaporation rates are low and the lack of fractionation of ^2H within the river (Figure 4) implies that there will be negligible in-river ^3H fractionation due to evaporation.

Calculated groundwater discharges using ^3H concentrations are $28\,391 \text{ m}^3/\text{day}$ for March 2012, and $55\,242 \text{ m}^3/\text{day}$ for April 2012. These results correspond well for both months with discharges calculated by ^{222}Rn and Cl (Table I).

Uncertainties in calculated groundwater fluxes

It is important to understand the potential uncertainties in calculated groundwater inflows that arise from hyporheic exchange and uncertainties in the degassing coefficient and groundwater end-member. The flux of water through the hyporheic zone can potentially introduce ^{222}Rn to rivers, where water flowing beneath the streambed accumulates ^{222}Rn from ^{226}Ra in the sediments and returns to the river with increased ^{222}Rn activities. Hyporheic flow may contribute a significant amount of ^{222}Rn in rivers that are losing or have low groundwater inflows, and failure to account for hyporheic flow in rivers with low ^{222}Rn activities may lead to

Table I. Cumulative groundwater discharges for Cl, ^{222}Rn and ^3H calculated for all campaigns

Date	Cumulate groundwater discharge (m^3/day)		
	^{222}Rn	Cl	^3H
03/11	39 900	29 350	–
06/11	88 450	134 000	–
09/11	37 350	38 400	–
10/11	37 175	51 700	–
12/11	28 900	28 650	–
01/12	24 350	18 300	–
03/12	39 500	33 500	28 500
04/12	48 600	53 300	55 250
05/12	26 840	19 140	–
06/12	63 700	47 000	–

overestimates in groundwater inflows. For example, Cook *et al.* (2006) calculated that ^{222}Rn introduced into the Cockburn River, NSW by hyporheic flow resulted in an overestimation of groundwater inflows by 60%.

With high ^{222}Rn activities and groundwater inflow rates (up to $11.7\text{ m}^3/\text{m}/\text{day}$) in the Gellibrand River, the ^{222}Rn mass balance becomes less sensitive to the small relative contribution of ^{222}Rn introduced by hyporheic flow. The river is largely gaining throughout the year and with a consolidated, low hydraulic conductivity clay rich river bed along most of its length hyporheic flux is likely to be of little significance. Chloride concentrations are unaffected by hyporheic processes, and with groundwater inflows calculated using chloride in the majority of campaigns within $\pm 12\%$ of those calculated using ^{222}Rn and ^3H (Figure 8), it appears unlikely that hyporheic exchange has a substantial impact on groundwater discharges estimated via the ^{222}Rn mass balance.

Another potential error in the calculations is the uncertainty in ^{222}Rn reaeration rates (k). The two empirically derived values of k bracket the range of likely values and the resulting range of estimated groundwater inflows takes into account the uncertainty in k . In the variably gaining/losing section of the river between 7.5 and 16.8 km where groundwater inputs are low ($<1\text{ m}^3/\text{m}/\text{day}$), the river may be interpreted as gaining (k_2) or losing (k_1) depending on the value of k applied. However, the groundwater contribution from this area relative to cumulative groundwater inputs along the entire study reach is insignificant due to the dominance of the 16.8–22 km discharge zone. Further to this, it is unlikely losing conditions exist as Cl values increase through the 7.5–16.8 km reach and the potentiometric maps (Figure 1b) also indicate that the river is gaining.

Variations in groundwater ^{222}Rn activities are another uncertainty in studies using tracer mass balances. Systematic spatial variations in groundwater ^{222}Rn activities have been reported in river catchments

(Mullinger *et al.*, 2007, 2009); however, few studies have considered the importance of both spatial and temporal variations in the groundwater end-member. Spatial variation in groundwater ^{222}Rn activities exists in the Gellibrand catchment, likely related to the heterogeneous mineralogy of the sediments. There is, however, no systematic variation with location in the catchment, or with water table fluctuations, such as has been observed in other river catchments (Mullinger *et al.*, 2007).

In the Gellibrand catchment, the ^{222}Rn mass balance is highly sensitive to the chosen value of C_i as groundwater ^{222}Rn activities are only an order of magnitude higher than surface water activities. The relationship between groundwater inflows (I) and the groundwater end-member is asymptotic (Figure 9b); with variation in C_i input into the ^{222}Rn mass balance causing large errors in calculated GW discharge.

Mean, groundwater ^{222}Rn activities for March 2011 of $5296\text{ Bq}/\text{m}^3$ yield discharge estimates between 0 and $8\text{ m}^3/\text{m}/\text{day}$ along the river. Allowing C_i in the ^{222}Rn mass balance to vary by 1σ ($1956\text{ Bq}/\text{m}^3$) produces a range in groundwater inflows from $0\text{--}5.4\text{ m}^3/\text{m}/\text{day}$ to $0\text{--}15.4\text{ m}^3/\text{m}/\text{day}$ (Figure 9a). This results in cumulative groundwater discharge varying from $25\,000$ to $67\,000\text{ m}^3$ (Figure 9b), and river baseflow percentage from 30% ($C_i - 1\sigma$) to 80% ($C_i + 1\sigma$).

Though groundwater bores display significant variations in ^{222}Rn activity throughout the year, temporal variations have a minor impact when constraining the groundwater end-member for the catchment (C_i). When C_i for each sampling campaign is calculated as the average ^{222}Rn activity across all bores, individual bore variations are smoothed with C_i fluctuating over the study period by a maximum of $\pm 1270\text{ Bq}/\text{m}^3$ (Table II). This indicates that in the Gellibrand catchment, constraining temporal variations in groundwater ^{222}Rn is less important than constraining spatial variations in ^{222}Rn across the catchment.

Variations in C_i are also an important factor in the chloride mass balance. Again, there is a large spatial variation in groundwater chloride values across the catchment ($38.6\text{--}123.5\text{ mg}/\text{l}$). A $\pm 10\%$ variation in C_i results in a 5–10% difference in the calculated baseflow component. (The mass balance is more sensitive to underestimations in C_i as the relationship to groundwater discharge as with ^{222}Rn is asymptotic; Figure 9b). Temporal variations in chloride concentrations are also relatively minor in comparison to spatial variability (Table II), remaining stable throughout the sampling campaigns.

In catchments where groundwater ^{222}Rn activities and chloride concentrations are heterogeneous, it is important to ensure a representative groundwater end-member is chosen

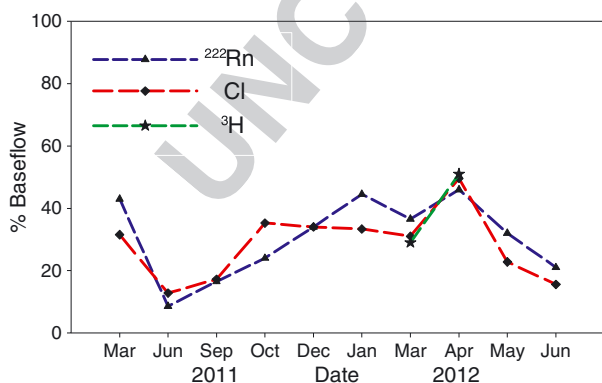


Figure 8. Baseflow as a % of total river discharge calculated for ^{222}Rn , Cl and ^3H over all sampling periods

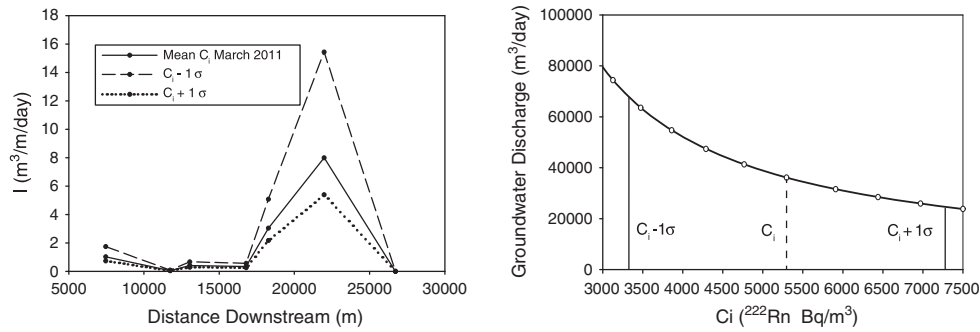


Figure 9. (a). (left) — Importance of variations in the GW ^{222}Rn end-member (C_i) on groundwater discharge (I). 9(b). (right) — The effect of varying C_i on cumulative groundwater influx

Table II. Temporal variations in average groundwater ^{222}Rn activities and C_i concentrations

Date	C_i ^{222}Rn (Bq/m 3)	C_i Cl (mg/l)
30/03/2011	5297	77.3
23/06/2011	5472	76.5
17/01/2012	5871	78.5
06/03/2012	6273	87.7
25/04/2012	5003	78.6
23/05/2012	6220	79.3

for both mass balances; this can only be achieved through sampling of a number of bores throughout the catchment, in particular where no spatial trend can be defined.

Controls on groundwater–surface water interaction in the Gellibrand River

The upland plain of the Gellibrand River is a largely gaining system that receives considerable groundwater inputs. Groundwater contribution to the river system varies with discharge, amounting to 10–20% of total river discharge at Bunkers Hill in higher winter flows (June to September), increasing up to 40–50% in summer months (January to April). This is likely to be related to rainfall patterns where the river becomes increasingly dependent on groundwater contributions in the dry season. The river is deeply incised into the floodplain, with steep banks present on either or both sides of the river. Where shallow water tables intersect the land surface at the base of these banks, this results in the seepage of groundwater into the river.

The majority of groundwater influx occurs in two distinct reaches of the river, in particular a groundwater discharge zone 16.8 – 22 km downstream. Groundwater inflows calculated using ^{222}Rn and Cl suggest that except during flood conditions, between 50 and 90% of the total groundwater discharge in the studied area occurs in this zone. This area corresponds to the region where the Eastern View Formation intersects the river. Total

groundwater contributions to the river calculated by mass balances for the tracers ^3H , Cl and ^{222}Rn are within $\pm 12\%$, suggesting that processes such as degassing and hyporheic exchange are not significant. In the Gellibrand catchment, obtaining a representative groundwater end-member for ^{222}Rn and Cl is shown to be of vital importance for calculating groundwater fluxes using tracer mass balances.

CONCLUSION

A number of studies have used environmental tracers to determine groundwater inflows into rivers, often with considerable variations between fluxes estimated from different tracers (Cartwright *et al.*, 2011). Understanding the factors which limit the use of environmental tracers in constraining groundwater inflow in different environments is integral for their use in groundwater–surface water studies. In this study, groundwater fluxes have been calculated at a high temporal frequency with considerable agreements between estimates made using three different chemical tracers (^3H , ^{222}Rn and Cl). In the Gellibrand River catchment, it is shown that the most important factor in constraining groundwater fluxes using environmental tracers is accurate quantification of ^{222}Rn and Cl groundwater end-members. This can only be achieved by capturing the spatial heterogeneity in groundwater chemistry across river catchments, with failure to do so leading to large errors in calculated groundwater discharge. Temporal variations in groundwater chemistry are shown to be of minor importance. In the Gellibrand catchment, hyporheic exchange and uncertainties in river degassing rates are considered to be of minor importance when calculating groundwater discharge using ^{222}Rn .

ACKNOWLEDGEMENTS

Funding for this research was provided by the National Centre for Groundwater Research and Training (NCGRT)

(program P3). The NCGRT is an Australian Government initiative supported by the Australian Research Council and the National Water Commission. Further funding was provided by the Australian Institute of Nuclear Science and Engineering (AINSE - ALNGRA12028) for ^3H analysis. We would like to thank The Department of Sustainability and Environment (DSE) for help in accessing bores and Malcolm Gardiner for collecting rainfall samples. Analyses were made with the help of Massimo Raveggi and Rachele Pierson (stable isotopes, anions and cations).

REFERENCES

- Aksoy H, Kurt I, Eris E. 2009. Filtered smoothed minima baseflow separation method. *Journal of Hydrology* **372**: 94–101. DOI: 10.1016/j.jhydrol.2009.03.037.
- Arnold JG, Allen PM, Bernhardt G. 1993. A comprehensive surface-groundwater flow model. *Journal of Hydrology* **142**: 47–69. DOI: 10.1016/0022-1694(93)90004-s.
- Banks EW, Simmons CT, Love AJ, Shand P. 2011. Assessing spatial and temporal connectivity between surface water and groundwater in a regional catchment: Implications for regional scale water quantity and quality. *Journal of Hydrology* **404**: 30–49. DOI: 10.1016/j.jhydrol.2011.04.017.
- Boulton AJ, Findlay S, Marmonier P, Stanley EH, Valett HM. 1998. The functional significance of the hyporheic zone in streams and rivers. *Annual Review of Ecological Systems* **29**: 59–81. DOI: 10.1146/annurev.ecolsys.29.1.59.
- Bureau of Meteorology. 2012. Commonwealth of Australia Bureau of Meteorology. <http://www.bom.gov.au>.
- Burnett WC, Dulaiova H. 2006. Radon as a tracer of submarine groundwater discharge into a boat basin in Donnalucata, Sicily. *Continental Shelf Research* **26**: 862–873. DOI: 10.1016/j.csr.2005.12.003
- Burnett WC, Peterson RN, Santos IR, Hicks RW. 2010. Use of automated radon measurements for rapid assessment of groundwater flow into Florida streams. *Journal of Hydrology* **380**: 298–304. DOI: 10.1016/j.jhydrol.2009.11.005.
- Cartwright I, Hofmann H, Sirianos MA, Weaver TR, Simmons CT. 2011. Geochemical and ^{222}Rn constraints on baseflow to the Murray River, Australia, and timescales for the decay of low-salinity groundwater lenses. *Journal of Hydrology* **405**: 333–343. DOI: 10.1016/j.jhydrol.2011.05.030
- Cecil LD, Green JR. 2000. Radon-222. In *Environmental Tracers in Subsurface Hydrology*, Cook PG, Herczeg AL (eds). Kluwer: Boston; 175–194.
- Cendón DI, Larsen JR, Jones BG, Nanson GC, Rickleman D, Hankin SI, Pueyo JJ, Maroulis JC. 2010. Freshwater recharge into a shallow saline groundwater system, Cooper Creek floodplain, Queensland, Australia. *Journal of Hydrology* **382**: 150–163. DOI: 10.1016/j.jhydrol.2010.08.003
- Cook PG. 2012. Estimating groundwater discharge to rivers from river chemistry surveys. *Hydrological Processes*. DOI: 10.1002/hyp.9493.
- Cook PG, Favreau G, Dighton JC, Tickell S. 2003. Determining natural groundwater influx to a tropical river using radon, chlorofluorocarbons and ionic environmental tracers. *Journal of Hydrology* **277**: 74–88. DOI: 10.1016/S0022-1694(03)00087-8
- Cook PG, Lamontagne S, Berhane D, Clark JF. 2006. Quantifying groundwater discharge to Cockburn River, southeastern Australia, using dissolved gas tracers Rn-222 and SF6. *Water Resource Research* **42**: W10411. DOI: 10.1029/2006WR004921
- Coplen TB. 1988. Normalization of oxygen and hydrogen isotope data. *Chemical Geology* **72**: 293–297. DOI: 10.1016/0168-9622(88)90042-5.
- Deforet T, Marmonier P, Rieffel D, Crini N, Giraudoux P, Gilbert D. 2009. Do parafluvial zones have an impact in regulating river pollution? Spatial and temporal dynamics of nutrients, carbon, and bacteria in a large gravel bar of the Doubs River (France). *Hydrobiologia* **623**: 235–250. DOI: 10.1007/s10750-008-9661-0.
- Ellins KK, Roman-Mas A, Lee R. 1990. Using ^{222}Rn to examine groundwater/surface discharge interaction in the Rio Grande de Manati, Puerto Rico. *Journal of Hydrology* **115**: 319–341. DOI: 10.1016/0022-1694(90)90212-G
- Freyer K, Treutler HC, Dehnert J, Nestler W. 1997. Sampling and measurement of radon-222 in water. *Journal of Environmental Radioactivity* **37**: 327–337. DOI: 10.1016/S0265-931X(96)00102-6
- Genereux DP, Hemond HF. 1990. Naturally-occurring Rn-222 as a tracer for streamflow generation—steady-state methodology and field example. *Water Resource Research* **26**: 3065–3075. DOI: 10.1029/WR026i012p03065
- Han DM, Song XF, Currell MJ, Tsujimura M. 2012. Using chlorofluorocarbons (CFCs) and tritium to improve conceptual model of groundwater flow in the South Coast Aquifers of Laizhou Bay, China. *Hydrological Processes* **26**: 3614–3629. DOI: 10.1002/hyp.8450.
- Hancock PJ, Boulton AJ, Humphreys WF. 2005. Aquifers and hyporheic zones: Towards an ecological understanding of groundwater. *Hydrogeology Journal* **13**: 98–111. DOI: 10.1007/s10040-004-0421-6.
- Hatch CE, Fisher AT, Revenaugh JS, Constantz J, Ruehl C. 2006. Quantifying surface water-groundwater interactions using time series analysis of streambed thermal records: Method development. *Water Resources Research* **42**: 14. W10410. DOI: 10.1029/2005wr004787.
- Hofmann H, Gilfedder BS, Cartwright I. 2011. A Novel Method Using a Silicone Diffusion Membrane for Continuous Rn-222 Measurements for the Quantification of Groundwater Discharge to Streams and Rivers. *Environmental Science and Technology* **45**: 8915–8921. DOI: 10.1021/es202683z.
- Kroeger KD, Swarzenski PW, Greenwood, JW, Reich C. 2007. Submarine groundwater discharge to Tampa Bay: Nutrient fluxes and biogeochemistry of the coastal aquifer. *Marine Chemistry*, **104**: 85–97. DOI: 10.1016/j.marchem.2006.10.012
- Larkin RG, Sharp JM. 1992. On the relationship between river-basin geomorphology, aquifer hydraulics and groundwater-flow direction in alluvial aquifers. *Geological Society of America Bulletin* **104**: 1608–1620. DOI: 10.1130/0016-7606(1992)104<1608:otrbrb>2.3.co;2
- Leonard J, Lakey R, Cumming S. 1981. Gellibrand groundwater investigation interim report. *Geological Survey of Victoria*
- Liu YH, Fan NJ, An SQ, Bai XH, Liu FD, Xu Z, Wang ZS, Liu SR. 2008. Characteristics of water isotopes and hydrograph separation during the wet season in the Heishui River, China. *Journal of Hydrology*, **353**: 314–321. DOI: 10.1016/j.jhydrol.2008.02.017.
- Manning AH, Clark JF, Diaz SH, Rademacher LK, Earman S, Plummer LN. 2012. Evolution of groundwater age in a mountain watershed over a period of thirteen years. *Journal of Hydrology* **460–461**: 13–28. DOI: 10.1016/j.jhydrol.2012.06.030.
- McDonnell JJ, McGuire K, Aggarwal P, Beven KJ, Biondi D, Destouni G, Dunn S, James A, Kirchner J, Kraft P, Lyon S, Maloszewski P, Newman B, Pfister L, Rinaldo A, Rodhe A, Sayama T, Seibert J, Solomon K, Soulsby C, Stewart M, Tetzlaff D, Tobin C, Troch P, Weiler M, Western A, Wörman A, Wrede S. 2010. How old is streamwater? Open questions in catchment transit time conceptualization, modelling and analysis. *Hydrological Processes* **24**: 1745–1754. DOI: 10.1002/hyp.7796.
- Morgenstern U, Stewart MK, Stenger R. 2010. Dating of streamwater using tritium in a post-bomb world: continuous variation of mean transit time with streamflow. *Hydrology of Earth System Sciences* **7**: 4731–4760. DOI: 10.5194/hessd-7-4731-2010
- Mullinger NJ, Binley AM, Pates JM, Crook NP. 2007. Radon in Chalk streams: Spatial and temporal variation of groundwater sources in the Pang and Lambourn catchments, UK. *Journal of Hydrology* **339**: 172–182. DOI: 10.1016/j.jhydrol.2007.03.010
- Mullinger NJ, Pates JM, Binley AM, Crook NP. 2009. Controls on the spatial and temporal variability of ^{222}Rn in riparian groundwater in a lowland Chalk catchment. *Journal of Hydrology* **376**: 58–69. DOI: 10.1016/j.jhydrol.2007.03.010
- Mutz M, Rohde A. 2003. Processes of Surface-Subsurface Water Exchange in a Low Energy Sand-Bed Stream. *International Review of Hydrobiology* **88**: 290–303. DOI: 10.1002/iroh.200390026.

- Nathan RJ, McMahon TA, Inst Engineers A. 1990. Evaluation of automated techniques for baseflow and recession analyses. *Water Resources Research* **26**: 1465–1473. DOI: 10.1029/WR026i007p01465
- Negulescu M, Rojanski V. 1969. Recent research to determine reaeration coefficient. *Water Research* **3**: 189–202.
- Neklapilova B. 2008a. Conductivity measurements and large volumes distillation of samples for Tritium analysis. ANSTO internal guideline. Technical Report ENV-I-070-002, ANSTO – Institute for Environmental Research, Australia.
- Neklapilova B. 2008b. Electrolysis and small volume distillation of samples for tritium activity analysis, ANSTO internal guideline. Technical Report ENV-I-070-003, ANSTO – Institute for Environmental Research, Australia.
- O'Connor DJ, Dobbins WE. 1958. Mechanisms of reaeration in natural streams. *Transactions of the American Society of Civil Engineers* **123**: 641–684.
- Oxtobee JPA, Novakowski KS. 2003. Ground water/surface water interaction in a fractured rock aquifer. *Ground Water* **41**: 667–681. DOI: 10.1111/j.1745-6584.2003.tb02405.x.
- Q12** Peterson RN, Santos IR, Burnett WC. 2010. Evaluating groundwater discharge to tidal rivers based on a Rn-222 time-series approach. *Estuarine, Coastal and Shelf Science* **86**: 165–178. DOI: 10.1016/j.eccs.2009.10.022
- Santos IR, Eyre BD. 2011. Radon tracing of groundwater discharge into an Australian estuary surrounded by coastal acid sulphate soils. *Journal of Hydrology* **396**: 246–257. DOI: 10.1016/j.jhydrol.2010.11.013
- Sophocleous M. 2002. Interactions between groundwater and surface water: the state of the science. *Hydrogeology Journal* **10**: 52–67. DOI: 10.1007/s10040-001-0170-8.
- St John JP, Gallagher TW, Paquin PR. 1984. The sensitivity of the dissolved oxygen balance to predictive reaeration equations. In *Gas Transfer at Water Surfaces*, Brutsaert W, Jirka GH (eds). Reidel Publishing Company; 577–588.
- Stellato L, Petrella E, Terrasi F, Belloni P, Belli M, Sansone U, Celico F. 2008. Some limitations in using ^{222}Rn to assess river–groundwater interactions: the case of Castel di Sangro alluvial plain (central Italy). *Hydrogeology Journal* **16**: 701–712. DOI: 10.1007/s10040-007-0263-0
- Stewart MK, Fahey BD. 2010. Runoff generating processes in adjacent tussock grassland and pine plantation catchments as indicated by mean transit time estimation using tritium. *Hydrology and earth system sciences* **14**. DOI: 10.5194/hess-14-1021-2010. **Q13**
- Tetzlaff D, Soulsby C. 2008. Sources of baseflow in larger catchments - Using tracers to develop a holistic understanding of runoff generation. *Journal of Hydrology* **359**: 287–302. DOI: 10.1016/j.jhydrol.2008.07.008.
- Tickell SJ. 1990. Colac and part of Beech Forest. 1:50 000 geological map. Edition 1., Geological Survey of Victoria, Iv, Map
- Unland NP, Cartwright I, Andersen MS, Rau GC, Reed J, Gilfedder BS, Atkinson AP, Hofmann H. 2013. Investigation the spatio-temporal variability in groundwater and surface water interactions: a multi-technique approach. *Hydrology and Earth System Sciences* **17**: 3437–3453. DOI: 10.5194/hess-17-3437-2013
- Victorian Water Resources Data Warehouse. 2012. <http://www.vicwaterdata.net/vicwaterdata/home.aspx>
- Winter TC, Harvey JW, Franke OL, Alley WM. 1998. Groundwater and Surfacewater: A Single Resource. US Geological Survey Circular 1139.

Appendix B
